

The cellular response to different radiation qualities in relation to breast cancer screening and treatment

Julie Depuydt

Thesis submitted in fulfilment of the requirements
for the degree of Doctor in Biomedical Sciences

Department of Basic Medical Sciences
Faculty of Medicine and Health Sciences

2016

Promotor

Prof. dr. Anne Vral

Co-promotor

Prof. dr. Hubert Thierens

Cover

simulation of 4 ^{92}U ions hitting a Be/Au/Si target.
Picture courtesy of P. R. Beukes.

**The cellular response
to different radiation
qualities in relation to
breast cancer screening
and treatment**

Julie Depuydt

22 juni 2016

Ghent University

Ghent University
Faculty of Medicine and Health Sciences
Department of Basic Medical Sciences
Section Histology
Research group Radiation and DNA repair



Supervisors

Prof. dr. Anne Vral
Prof. dr. Hubert Thierens
Prof. dr. Ir. Kathleen Claes

Examination Board

Chairman: Prof. dr. Ir. Carlos De Wagter¹
Prof. dr. Ir. Ans Baeyens¹
dr. Elke Decrock¹
Prof. dr. Alegria Montoro²
Prof. dr. Marc Van Eijkeren¹
Prof. dr. Geert Villeirs¹
Prof. dr. Andrzej Wojcik³

¹ Ghent University, Ghent, Belgium

² Hospital Universitario y Politécnico la Fe, Valencia, Spain

³ Stockholm University, Stockholm, Sweden

Research institute

Ghent University
Faculty of Medicine and Health Sciences
Department of Basic Medical Sciences
De Pintelaan 185 6B3
B-9000 Ghent, Belgium
T +32-9-332 51 35
F +32-9-332 38 23

Aan mijn mannen

Thank you

The writing of this thank you was a bit of a challenge...

How can words be enough to thank you all? How can they express this feeling of gratitude? How can they show that you all deserve hugs and kisses and chocolate?

I procrastinated, I even contemplated ditching it, but I couldn't. So many people deserve a thank you. Besides, so many people only read the thank you...

So without further ado...

To Anne, who is a lion protecting her cubs...

To Leen, who comes in for an early morning chat at the best and worst possible times...

To Eli Peli, who is always generous with kisses and hugs (but not with chocolate)...

To Greet, who is always there in emergencies...

To the guys on the bike, who don't mind my ramblings at 6.30AM...

To Bert, who is actually 'Geachte Prof Thierens' (and always will be)...

To MaxiMini, who only came by a few months ago, but immediately made a huge impression...

To Lore, who lures me away from my desk promising coffee and laughs...

To Andrzej, who always makes me smile (let's hope he keeps that strategy for tonight)...

To Veerle, who taught me the ins and outs of the lab...

To Elke, who probably knows everything about the 12542 ways cells can die...

To Kobus, who invited me to his most wonderful lab in the most wonderful language...

To Alexander, who said most honestly "maar 't is niet erg hoor, dat we weer pizza eten"...

To Stephanie and Filip, who make me sweat on Mondays...

To Mattias, who is the coolest freak in the office (and can even make Senseo-a-la-Julie)...

To Geert, who welcomed me in his brand new building (and I didn't even have to take my shoes off)...

To Ria, who just keeps going, no matter what. Go Ria!

To Stephen and Karen and Lies and Femke, who are the reason you're reading this...

To Paolo, who's important, even if I can't explain why...

To Oude Moeke, who made it...

To my computer, who also made it...

To Charlot, who is my PhD-guru...

To Carlos, who orchestrated this evening perfectly

To Lore and Bert and Thomas, who made sure we're not hangry!...

To Patrick, who is always there...

To Toke, who is always kind and sweet and absolutely Toke...

To Adriaan, who started school the same day I started my PhD. I wonder who learned the most...
To Kim, who didn't mind me firing her...
To Jeroen, who is strangely fond of zebrafish...
To Annelot, who is my perfect counterpart at the lab...
To Daniel, who is always in for a serious chat and sneaks the jokes in when I least expect them...
To Ans, who taught me attention to detail...
To my sisters, who taught me to thank only the VIPs...
To Jesus and Benedicte, who are very VIP...
To Mama and Papa, who are even more VIP...
To Philip, who always says the right thing...
To Alegria, who I wish all the best...
To Lize, who is tough enough to teach them a lesson...
To Stephen and Scott, who introduced me to karaoke...
To Nati, who always has 'some doubts' (but only about MN and dic)...
To Johanna, who only needs half a word and does 200% of what you wanted...
To Elke, who taught me how to handle the LO-guys...
To Sebastián, who taught me to always be happy (except when you want food)...
To Manuel, who is a bit like Sebastián...
To Tinneke, Lynn, Eline, Céline, Abde, Charlotte, Bram, Sophie, Tanguy, Pauwelijn-en-Valerie, Sarah, Indra, Liesbeth and Diego, who kept me young...
To Marc, who taught me to spell (and to whom I apologize)...
To Sarah, who made sure there was a book to read...
To Scott and Bea, who kept me sane (and yet, my nickname is still nutcase *zucht*)...
To Annelies, who magically gave me more time...
To Pamela, who personally kept the glamour in the lab up to standard...
To Heidi, for putting up with my ever changing agenda...
To Kathleen, who knows somebody in every lab...
To Charlot, who has a majestic collection of Nutella-jars...
To Björn and Stefan, who guided me through my initial steps in a lab...
To Anne, who deserves at least two lines...

Thank you!

¹ *hangry*: a contraction of *hungry* and *angry*. A condition to which I am absolutely prone.

Contents

Summary.....	5
Samenvatting.....	7
Acronyms.....	9

PART 1

INTRODUCTION

13

1 Ionizing radiation

15

1.1 What is ionizing radiation.....	15
1.2 Damage by IR.....	15
1.3 LET.....	16
1.4 Relative biological effect or RBE.....	19
1.5 The oxygen enhancement ratio.....	21
1.6 Dose deposition.....	22
1.7 Absorbed dose, equivalent dose and effective dose.....	23
1.8 Radiosensitivity.....	25
1.9 Medical consequences of radiation.....	25
1.10 Low dose irradiation.....	28

2 DNA DSB repair

31

2.1 DNA damage response.....	31
2.2 Cell cycle checkpoint arrest.....	33
2.3 DNA DSB repair pathways.....	35
2.3.1 Non-homologous end joining (NHEJ).....	35
2.3.2 Homologous recombination (HR).....	36
2.3.3 Alternative DNA DSB repair pathways.....	38
2.4 Determinants of DSB repair pathway choice.....	39
2.4.1 Cell cycle phase.....	39
2.4.2 Complexity of the damage.....	39
2.4.3 Chromatin complexity.....	40
2.4.4 Choice of the repair pathway.....	40

2.5 Apoptosis, necrosis, mitotic catastrophe and senescence	41
2.5.1 Apoptosis	42
2.5.2 Necrosis.....	43
2.5.3 Mitotic catastrophe	44
2.5.4 Senescence	44
3 Radiotherapy	47
3.1 Techniques used in radiotherapy.....	47
3.2 Biological fundamentals of radiotherapy.....	48
3.3 Toxic effects following radiotherapy.....	51
4 Breast cancer	53
4.1 Incidence and mortality.....	53
4.1.1 Cancer in general.....	53
4.1.2 Breast cancer	55
4.2 Breast cancer risk factors.....	56
4.2.1 Hormones	56
4.2.2 Lifestyle factors	56
4.2.3 Breast density.....	56
4.2.4 Radiation.....	57
4.2.5 Genetic background.....	57
4.3 Detection and screening of breast cancer.....	60
4.4 Pathology.....	63
4.5 Breast cancer treatment	65
5 Assays to measure the effect of radiation	69
5.1 The γ H2AX foci assay.....	69
5.2 The micronucleus assay.....	71
5.3 Apoptosis assay.....	74
5.4 Crystal violet cell survival assay.....	75
6 Aim of the research	77
7 References	81

PART 2
ORIGINAL RESEARCH **104**

Outline of the research **105**

Article 1 – Induction and disappearance of γ H2AX foci and formation of micronuclei after exposure of human lymphocytes to ^{60}Co γ -rays and p(66)+Be(40) neutrons.....107

Article 2 – The impact of a BRCA1 and BRCA2-mutation on the radiation response induced by gamma-rays and neutrons in MCF-10A cells127

Article 3 – Relative biological effectiveness of mammography X-rays at the level of DNA and chromosomes in lymphocytes151

Article 4 – γ H2AX foci induced by low dose mammography X-rays in breast tissue167

Article 5 – *In vitro* cellular radiosensitivity in relationship to late normal tissue reactions in breast cancer patients: a multi-endpoint case-control study.....183

PART 3
General discussion **210**

1 Biological efficiency of different radiation qualities **211**

1.1 Fast neutrons.....211

 1.1.1 Induction and repair of γ H2AX foci induced by fast neutrons.....212

 1.1.2 Chromosomal aberrations (MN-assay) and cell proliferation (CV cell proliferation assay).....213

1.2 Mammography X-rays.....215

 1.2.1 RBE of mammography X-rays215

 1.2.2 RBE of mammography X-rays after very low dose irradiation218

1.3 Cell cycle dependence of RBE.....221

1.4 Influence of LET on DSB repair pathway choice and cellular radiosensitivity.....223

 1.4.1 Cell cycle and DNA DSB repair225

 1.4.2 Effect of LET in DSB repair deficient cells227

2	Radiosensitivity in relation to breast cancer treatment and diagnostics	231
2.1	Risks of late radiotoxic reactions following radiotherapy for breast cancer.....	231
2.2	Radiosensitivity amongst breast cancer patients.....	232
2.2.1	Prediction of the risks of radiotoxic effects.....	232
2.3	BRCA-radiosensitivity.....	236
2.3.1	Are BRCA mutation carriers radiosensitive?.....	236
2.3.2	BRCA and mammography.....	237
2.3.3	BRCA and radiotherapy.....	239
3	Conclusion	241
4	References	243
	Curriculum	255

Summary

Breast epithelial cells are prone to the development of cancer and radiation is known to be an inducer of cancer. However, irradiation of breast tissue is often used in a useful manner: mammography to detect breast cancer in an early stage or radiotherapy to eradicate breast cancer.

In this thesis, we analyzed the cellular response to radiation in relationship to breast cancer screening and treatment. In a first part, we investigated the biological efficiencies of different radiation qualities in different cell types using different cellular endpoints. In a second part, the individual radiosensitivity was investigated with respect to different clinical endpoints such as normal tissue reactions to radiotherapy and susceptibility to radiation-induced carcinogenesis.

High-LET (linear energy transfer) radiation is used increasingly in radiotherapy due to its high efficiency to induce DNA damage and to kill cancer cells compared to γ -radiation. Furthermore, travelers in space are continuously irradiated with high-LET radiation. Our results obtained with fast neutrons in human peripheral lymphocytes and MCF-10A cells are conform to literature reports regarding the effects of high-LET radiation. While a lower number of radiation-induced DNA DSB (double strand break) was observed for neutron radiation compared to γ -rays until about 4h post-IR, foci repair was slower and more residual foci were present at later time points. Furthermore, neutrons seem to be more effective in inducing micronuclei and inhibiting cell proliferation. These results are important in light of radioprotection in space and to assess the effects of radiotherapy on healthy and cancerous tissue.

In mammography screening doses are low, but there is always the risk to induce DNA damage and this in a large group of asymptomatic women. Irradiation of human lymphocytes with 30kV X-rays resulted in a modest increase in the number of DNA DSB compared to γ -rays, but these DSB were more difficult to repair correctly by the cell and resulted in a more pronounced increase in micronuclei compared to γ -rays. Furthermore, in the 0 to 20 mGy dose-range a hypersensitive response for DSB induction was observed in mammary glandular epithelial cells present in resected breast tissue, probably caused by the bystander effect. This hypersensitive response in the dose range representative for mammography screening, together with the findings obtained with chromosomal aberrations at higher doses might suggest that also in the 0-20mGy dose range more chromosomal aberrations than initially assumed by the linear no threshold (LNT) model will be induced. These findings may have important implications for risk assessment of mammography screening.

Analysis of the relationship between cell cycle phase, LET and radiosensitivity using DSB repair deficient cell lines (MCF-10A cell lines with a knockdown in BRCA1, BRCA2 and Ku70) confirmed that non-homologous end joining (NHEJ) plays a role throughout the whole cell cycle, while homologous recombination (HR) only functions in late S and G2 phase of the cell cycle. Furthermore, the importance of HR in S or G2 phase rises as the complexity of the break increases. This results in relative biological effectiveness (RBE) values for micronucleus (MN) induction which are much higher when cells are irradiated in G1 compared to the S and G2 phase of the cell cycle.

The radiation response is influenced by the clinical radiosensitivity of the individual and the late toxic reaction of some women to radiotherapy limits the dose which can safely be administered. We attempted to identify breast-cancer patients who showed severe late toxic reactions to radiotherapy. In a matched case-control study using human lymphocytes, the *in vitro* clinical radiosensitivity of cases and controls was assessed with four different endpoints related to DNA DSB repair and apoptosis. The results suggest that a patient's intrinsic radiosensitivity is involved in the development of late radiotoxic effects. As the biological mechanisms behind the different symptoms of late toxicity differ, it can be expected that not all clinical manifestations of late radiotoxicity are linked to the same degree to intrinsic radiosensitivity with respect to DNA repair and apoptosis. Of the four radiosensitivity tests applied, the apoptosis assay seems to be most promising in the framework of predicting radiotoxic effects in individual patients.

As BRCA1 and BRCA2 are important proteins in the DNA DSB repair pathways, mutations in the *BRCA* genes could lead to an increased susceptibility to radiation-induced carcinogenesis. The knockdown of BRCA1 and BRCA2 proteins in mammary epithelial cells of about 50%, a condition which is representative for heterozygous mutation carriers, led to a significantly increased radiosensitivity based on MN formation and cell proliferation, which was most pronounced at low doses. The results imply that caution should be taken when administering ionizing radiation to heterozygous *BRCA1* or *BRCA2* mutation carriers.

Samenvatting

Borstepitheelcellen kunnen ontwikkelen tot borstkanker en ioniserende straling is daarvoor een risicofactor. Bestraling van borstweefsel wordt echter ook vaak op een nuttige manier gebruikt, zoals bijvoorbeeld met mammografie om borstkanker in een vroeg stadium te ontdekken of radiotherapie om borstkanker te behandelen.

In deze thesis hebben we de cellulaire respons op straling bestudeerd in relatie tot borstkanker screening en behandeling. In een eerste deel analyseerden we de biologische efficiëntie van verschillende stralingskwaliteiten in verschillende celtypen met verschillende eindpunten. In een tweede deel werd de individuele stralingsgevoeligheid onderzocht in relatie tot verschillende klinische eindpunten zoals de respons van het gezonde weefsel op radiotherapie en de gevoeligheid tot stralingsgeïnduceerde ontwikkeling van kanker.

Hoge LET straling wordt meer en meer gebruikt in radiotherapie door zijn efficiëntie in het induceren van DNA schade en het doden van kankercellen in vergelijking met γ -stralen. Ook worden personen in de lucht- en ruimtevaart continue blootgesteld aan hoge LET (lineaire energie transfer) straling. De resultaten die we verkregen met hoge LET straling in humane lymfocyten en MCF-10A cellen zijn in overeenstemming met wat in de literatuur beschreven wordt voor hoge LET straling. Hoewel een lager aantal stralingsgeïnduceerde DNA DSB (dubbel streng breuken) geteld werd voor bestraling met neutronen in vergelijking met γ -stralen tot ongeveer 4 uur na bestraling, was het herstel van de DSB foci trager en waren er meer persistente foci op latere tijdstippen. Bovendien waren de neutronen efficiënter in het induceren van micronuclei en het inhiberen van cel-proliferatie. Deze resultaten zijn belangrijk in het kader van stralingsprotectie in de ruimte- en luchtvaart en om de effecten van radiotherapie op gezond en aberrant weefsel te kunnen inschatten.

In mammografie screening zijn de dosissen laag, maar er is altijd het risico om DNA schade te induceren, en dit bij een grote groep asymptomatische vrouwen. Bestraling van humane lymfocyten met 30kV X-stralen had in een kleine stijging in het aantal DNA DSB tot gevolg in vergelijking met γ -stralen. Voor de cel is het echter moeilijk om deze DSB correct te herstellen en dit resulteerde in een uitgesproken stijging in het aantal micronuclei in vergelijking met γ -stralen. Bovendien werd in het dosisgebied 0 tot 20 mGy een hypersensitieve respons voor de inductie van DSB geobserveerd in borstepitheelcellen in gedissecteerd borstweefsel, vermoedelijk veroorzaakt door het bystander effect. Deze hypersensitieve respons in een dosisbereik dat representatief is voor mammografie screening in combinatie met onze bevindingen voor chromosomale aberraties bij hogere dosissen, suggereert dat ook in het dosisgebied 0 tot 20 mGy, meer chromosomale aberraties geïnduceerd zullen worden dan initieel aangenomen door het LNT (linear no threshold, lineair zonder drempel) model. Deze observaties kunnen belangrijke implicaties hebben voor de risico-inschatting bij mammografie screening.

Analyse van het verband tussen cel-cyclus, LET en stralingsgevoeligheid in borstepitheel cellijnen die deficiënt zijn in DSB herstel-genen (MCF-10A cellen met een knockdown in BRCA1, BRCA2 en Ku70), bevestigde dat NHEJ (non-homologous end joining, niet homologe verbinding van de DNA-eindes) een rol speelt gedurende de volledige celcyclus en dat HR (homologous recombination, homologe recombinatie) enkel actief is in de late S en G2 fase van de celcyclus. Bovendien stijgt het belang van HR in S en G2 naarmate de complexiteit van de DSB stijgt. Dit resulteert in relatieve biologische efficiëntie (RBE) waarden voor micronucleus-inductie die veel hoger zijn wanneer de cellen bestraald worden in de G1 fase van de celcyclus in vergelijking met de S en G2 fase van de celcyclus.

De stralingsrespons wordt beïnvloed door de klinische stralingsgevoeligheid van het individu en de late toxische reactie van sommige vrouwen op radiotherapie limiteert de dosis die maximaal kan worden toegediend. We deden een poging om borstkankerpatiënten te identificeren die ernstige laat-toxische reacties vertoonden op radiotherapie. In een gepaarde case-controle studie waarbij gebruik werd gemaakt van humane lymfocyten, werd de *in vitro* klinische stralingsgevoeligheid van cases en controles geëvalueerd met vier verschillende eindpunten die gerelateerd zijn aan DNA DSB herstel en apoptose. De resultaten suggereren dat de intrinsieke cellulaire stralingsgevoeligheid van een patiënt betrokken is bij de ontwikkeling van late radiotoxische effecten. Gezien de biologische mechanismen achter de verschillende klinische symptomen verschillen, kan verwacht worden dat niet alle klinische manifestaties van late radiotoxiciteit in dezelfde mate gelinkt zijn aan de intrinsieke radiosensitiviteit gerelateerd met DNA herstel en apoptose. Van de vier testen die gebruikt werden lijkt de apoptose test de meest veelbelovende te zijn om radiotoxische effecten bij individuele patiënten te voorspellen.

Gezien de belangrijke rol van BRCA1 en BRCA2 in de DNA DSB herstel pathway, kunnen *BRCA1* en *BRCA2*-mutaties leiden tot een stijging in gevoeligheid van stralingsgeïnduceerde carcinogenese. De knockdown van BRCA1 en BRCA2 in borstepitheelcellen van ongeveer 50%, een situatie die representatief is voor heterozygote mutatie dragers, leidde tot een significant verhoogde stralingsgevoeligheid, gebaseerd op de vorming van micronuclei en cel-proliferatie en dit was meest uitgesproken voor lage dosissen. Deze resultaten impliceren dat voorzichtigheid geboden is bij het gebruik van straling bij *BRCA1* en *BRCA2* mutatie dragers.

Acronyms

·H	hydrogen radical
·OH	hydroxyl radical
53BP1	p53 Binding protein 1
⁶⁰Co γ-rays	cobalt gamma-rays
7-AAD	7-Aminoactinomycin D

A

ACS	American Cancer Society
AT	Ataxia telangiectasia mutated
ATM	Ataxia telangiectasia mutated
ATR	ATM- and RAD3-related
ATRIP	ATR interacting protein
AUC	area under the curve
AWBUS	automated whole breast ultrasound system

B

Bax	Bcl-2-associated X
BER	Base excision repair
BLM	Bloom's syndrome helicase
BN	binucleated
B-NHEJ	alternative non-homologous end joining
BRCA1	Breast cancer early onset1
BRCA2	Breast cancer early onset2
BRCT	BRCA1 C-terminal
BSA	bovine serum albumin

C

CA	chromosome aberration
caspase	cyclin-dependent aspartate-specific peptidase
Cdc25a	cell division cycle 25a
Cdc45	cell division cycle 45
Cdk	cyclin dependent kinase
CDK2	cyclin dependent kinase 2
CHO	Chinese Hamster Ovarian Cells
COX-2	cyclooxygenase-2
CT	computed tomography
CtIP	CtBP-interacting protein
CV	crystal violet
cyclin-Cdk	cyclin-dependent kinase

D

DAPI	4',6-Diamidino-2-Phenylindole
DDR	DNA damage response
D-loop	displacement loop
DMF	dose modifying factor
DNA	Deoxyribonucleic acid
DNA PK	DNA dependent protein kinase
DNA PKcs	DNA-dependent Protein Kinase catalytic subunit
DNA pol δ	DNA polymerase δ
DSB	double strand break

E

EBV	Epstein Barr Virus
ER+	estrogen receptor positive
EXO1	exonuclease 1

F

FCS	foetal calf serum
FISH	fluorescent in situ hybridisation
FITC	fluorescein Isothiocyanate

G

G1-phase	gap 1 phase
G2-phase	gap 2 phase
GFP	green fluorescent protein
Gy	Gray

H

H2AX	histone subtype H2A isoform X
HE	hematoxylin-eosin
HER2+	human epidermal growth factor 2 receptor positive
HR	homologous recombination
hSSB1	human Single Stranded DNA Binding Protein 1

I

ICRP	International Commission on Radiological Protection
IDC	invasive ductal carcinoma
ILC	invasive lobular carcinoma
IMRT	intensity modulated radiation therapy
IR	ionizing radiation
IRIF	ionizing radiation induced foci

K

KAP-1	KRAB-associated protein 1
kDa	kilo dalton
keV	kilo electronvolt
Ku70	Ku autoantigen 70
Ku80	Ku autoantigen 80
kV	kilo Voltage

L

- LET** linear energy transfer
- LIG4** DNA ligase4
- LNT model** Linear no threshold model
- LSS** lifespan study

M

- MAPK** Mitogen-activated protein kinases
- mdc1** Mediator of DNA damage Checkpoint 1
- MEF** Mouse Embryonic Fibroblast
- MMEJ** microhomology-mediated end-joining
- MN** micronucleus
- M-phase** mitosis phase
- MRI** Magnetic resonance imaging
- MRN complex** Mre11/Rad50/Nbs1 complex
- MTT** 3-(4,5-Dimethylthiazol-2-yl)-2,5-diphenyltetrazolium bromide
- MV** mega voltage

N

- Nbs1** Nijmegen breakage syndrome 1
- NCCN** National Comprehensive Cancer Network
- NER** nucleotide excision repair
- NFKB** nuclear factor kappa-light-chain-enhancer of activated B cells
- NHEJ** non homologous endjoining
- NICE** National Institute for Health and Care Excellence

O

- OER** oxygen enhancement ratio

P

- p(66)+ Be(40)** 66 MeV protons on a Berillium target
- p21** protein encoded by the CDK1NA gene
- p53** tumor protein 53
- PALB2** partner and localizer of BRCA2
- PARP** poly-ADP ribose polymerase
- PFA** paraformaldehyde
- PFGE** pulsed field gel electrophoresis
- pH** measure of the acidity or basicity of a solution
- PHA** Phytohaemagglutinin
- PIK3** Phosphatidylinositol-4,5-bisphosphate 3-kinase
- PIKK** Phosphatidylinositol 3-Kinase like Kinase
- Pol** polymerase
- PR+** progesteron receptor positive

R

- Rb protein** retinoblastoma protein
- RBE** relative biological effectiveness
- RNS** reactive nitrogen species
- ROS** reactive oxygen species
- RPA** replication protein A
- RT** room temperature
- RX** radiography X-rays

S

- SCID** Severe Combined Immuno Deficiency
- SEM** standard error of the mean
- shRNA** short hairpin RNA
- siRNA** short interfering RNA
- SNP** single nucleotide polymorphism
- SOBP** spread out bragg peak
- SPC** second primary cancer
- S-phase** synthesis phase
 - SSA** single strand annealing
 - SSB** single strand break
- ssDNA** single-stranded DNA
- Sv** Sievert

T

- TDLU** terminal duct lobular unit

U

- UNSCEAR** United Nations Scientific Committee on the Effects of Atomic Radiation
- US** ultrasound

W

- WRN** werner syndrome

X

- XLF** XRCC4-like factor
- XRCC** X-ray cross-complementing

Y

- γ H2AX** phosphorylated H2AX



Part 1

Introduction

1 Ionizing radiation

1.1 What is ionizing radiation

Ionizing radiation (IR) consists of electromagnetic waves and/or high energy particles with sufficient energy to eject orbital electrons from atoms and molecules they traverse, thereby ionizing them.

Neutrons, electrons, protons, α -particles and heavy charged ions are different types of particle radiation and can be described by the charge and mass of the particle. Electromagnetic IR has neither mass nor charge and consists of pure energy in the form of photons – wave like particles. X-rays and γ -rays are electromagnetic radiation.

1.2 Damage by IR

Ionizing radiation deposits energy randomly while traversing matter, hereby causing ionizations of atoms and molecules. Direct effects of ionizations occur when radiation deposits part of its energy directly in critical biological target molecules, thereby ionizing a component of this critical target. The indirect effect of ionization occurs when the radiation ionizes a non-critical target and the radicals that are induced by these ionizations in turn subject the critical target to chemical attack (1, 2) (see figure 1.1)

The energy of the ionizing radiation will be deposited in the cell. Since about 80% of the cell consists of water, indirect effects occur primarily through ionization of water molecules. This process is referred to as water radiolysis and leads to the formation of $\text{OH}\cdot$, e_{aq}^- , $\text{H}\cdot$ and H_3O^+ . These ions and free radicals are extremely reactive, and especially the $\text{OH}\cdot$ radical is believed to cause a lot of indirect damage to critical target molecules. The most critical target molecule in the cell, which can be damaged either by indirect or direct ionizations, is the DNA-molecule. There are different categories of radiation damage to the DNA, all of which have a different biological significance (1, 2).

- Base damage: change or loss of a base. While mostly repaired properly, this can lead to mutations in the bases-sequences which can have major consequences to the cell.
- Sugar damage
- Crosslinks: intra- and interstrand DNA-DNA crosslinks and DNA-protein crosslinks. When not properly repaired, this kind of damage may be lethal to the cell.
- DNA single-strand breaks (SSB): breaks in one chain of the DNA molecule. SSB can be efficiently repaired by the cell, with little long-term consequences.
- DNA double strand breaks (DSB): two SSB in opposite strands approximately 10 to 20 base-pairs apart, causing a complete break of the DNA molecule. DNA DSB can be lethal to the cell.
- Complex DNA damage sites: when the density of the ionizations increases (see further), different forms of DNA damage will be clustered in one damage site, which can be highly lethal to the cell.

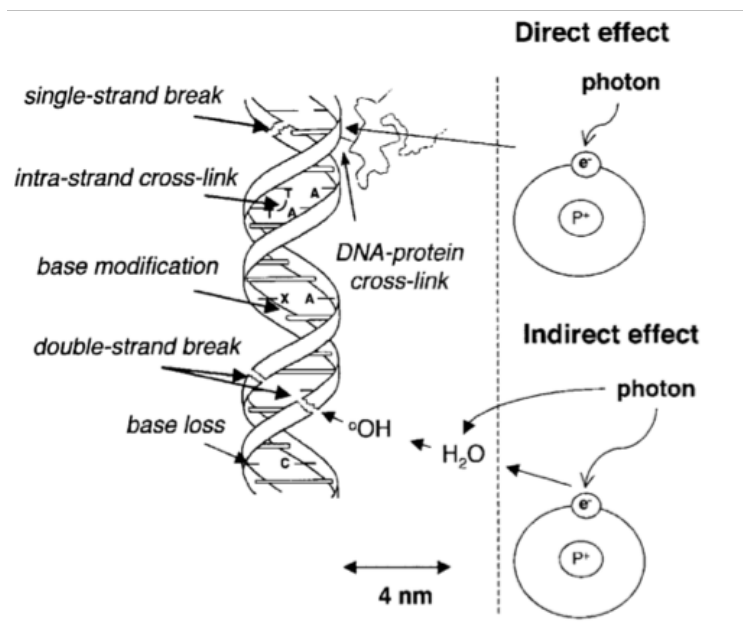


FIGURE 1.1

Schematic representation of direct and indirect radiation-induced DNA lesions. Figure from (1).

1.3 LET

The interactions of radiation with matter are often described in terms of the linear energy transfer (LET). The LET of a particular type of radiation is the average energy deposited along the track of a particle or photon per unit distance and is expressed in $\text{keV}/\mu\text{m}$ (kilo electronvolt/ μm). This ionization density is dependent on several parameters, including the mass, charge and energy of the radiation. On this basis radiation is categorized into two types, low-LET radiation like X-rays, γ -rays and β -particles which have a low average ionization density, and high-LET radiation like neutrons, α -particles and heavy ions, which have a high ionization density (see figure 1.2) (2-4). An inverse relationship exists between the kinetic energy of radiation and the LET (table 1.1) (5).

X-rays and γ -rays have no mass or charge, but through their interaction with the absorbing medium they will eject electrons from atoms by the Photoelectric or Compton effect. These ejected fast electrons, with a low mass and a negative charge, will pass through matter constantly interacting electrostatically with other electrons and in the process lose energy. If the force of the electrostatic interaction is sufficient to remove the electron from its atom, further ionizations occur. As a result, the ionizations are sparse and distant from each other (4). The primary mode of damage to the cell of low-LET radiation will be via indirect ionizations.

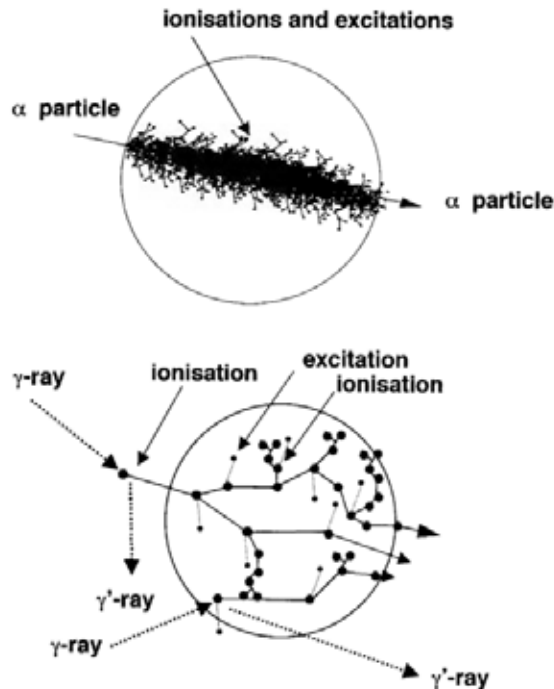


FIGURE 1.2

Schematic representation of the ionizations patterns of high and low-LET radiation. Figure from (1).

Due to its higher mass and/or charge, high-LET radiation has a greater probability to interact with the electrons and atomic nuclei from the absorbing medium. When a particle collides with a heavy nucleus, energy loss can be huge, producing a lot of ionizations in a very short distance (4). Direct ionizations of the DNA molecule are more likely to be caused by high-LET radiation.

Both high and low-LET radiation qualities will induce DSB. Low-LET radiation will produce DSB at the track-ends of low-energy second electrons which will be spread evenly over the cell (see figure 1.2). High-LET radiation will induce DNA DSB along their entire track, but the DSB will be more clustered and as a result they are more complex in nature (see figure 1.2) (6-8). The dose-response curve for DSB induction for both low and high-LET radiation is linear ($Y = c + \alpha D$) over several orders of magnitude (9, 10).

Radiation	LET (keV/ μm)
<i>photons</i>	
^{60}Co (~1.2 MeV)	0.3
3 MeV X-rays	0.3
200 keV X-rays	2.5
30 keV X-rays	4.3
<i>electrons</i>	
1 MeV	0.2
100 keV	0.5
10 keV	2
<i>charged particles</i>	
protons 2 MeV	17
α -particles 2.5MeV	166
α -particles 4 MeV	110
C ions 100 MeV	160
<i>neutrons</i>	
29 MeV p(66)/Be(40)	20
2.5 MeV	15-80

TABLE 1.1

LET values for different types of radiation. Adapted from (5, 11).

When measuring mis- or unrepaired DSB in function of dose, e.g. a dose response curve based on chromosomal aberrations or cell survival, then the difference in ionization density between low and high-LET radiation is reflected in the shape of the dose response curve. Most dose response curves can be described by a linear quadratic function ($Y = c + \alpha D + \beta D^2$ for chromosomal aberrations or $\ln(S) = -\alpha D - \beta D^2$ for cell survival). The linear component results from un- or misrepaired DSB induced by a single-track event, while the quadratic component arises from un- or misrepair of DSB induced by two track events. At low doses of low-LET radiation, the probability of two tracks traversing a target is low and only the linear component will contribute. As the dose increases, the probability of two-track events will also increase. However, as the LET of the radiation increases, the importance of single track events increases as well, and the α -component will become more important. As a result, the curve will become close to linear or linear with increasing LET (figure 1.3) (4, 12).

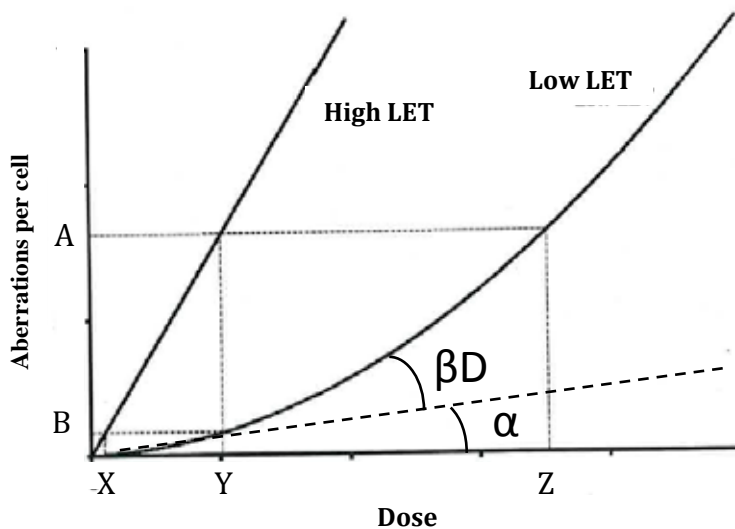


FIGURE 1.3

Schematic representation of the dose response curve for chromosomal aberrations following high and low-LET radiation. Figure adapted from (4).

1.4 Relative biological effect or RBE

Due to the differences in ionization densities between low and high-LET radiation, equal doses of radiations with different LET will cause a different biologic effect. The different effectiveness for inducing a particular biological endpoint by different radiation qualities is represented by the relative biological effect (RBE). The RBE is defined as the ratio of a dose of the reference radiation and the dose to the test radiation that produce the same biological response (1). In figure 1.3 the $RBE_A = Z/Y$ and the $RBE_B = Y/X$.

It is important to note that the RBE for a certain radiation quality is not constant, but varies depending on several factors. In general, when using RBE values to compare the effectiveness of different radiation qualities, is it important to state precisely how a particular RBE measurement was obtained. As stated in the definition, the RBE is dependent on the dose, the endpoint and the reference radiation. Historically 200 kV X-rays were used as reference radiation, nowadays mostly ^{60}Co γ -rays are used (4). An increase in RBE is noted for a decrease in dose (e.g. in figure 1.3

RBE_A is smaller than RBE_B), and changes in RBE are most prominent at low doses (13). End-points that can be considered are e.g. cell survival, chromosomal aberrations and DNA damage induction. Furthermore RBE is influenced by the depth, dose rate, fractionation, cell type used, oxygenation, etc. (13). These factors can influence the level of biological damage differently following exposure to the reference radiation than to the test radiation and as a result influence the RBE of the test radiation.

RBE increases with the LET of a radiation up to an optimum value of approximately $100 \text{ keV}/\mu\text{m}$. At higher LET values, the RBE decreases again due to overkill. A phenomenon where, due to the very high ionization densities, more energy is deposited than needed to kill a cell and the biological effects of the radiation become inefficient (figure 1.4). While recent studies show that there are differences in RBE of different low-LET radiation qualities, for risk calculation all low-LET radiation qualities are considered equally efficient in inducing damage. (1, 14, 15).

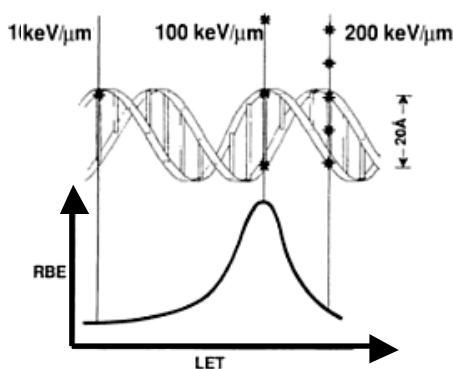


FIGURE 1.4

Dependence of RBE on LET and the phenomenon of overkill by very high-LET radiations. Figure adapted from (13).

1.5 The oxygen enhancement ratio

The radiation damage caused by indirect ionizations of H_2O is dependent on the presence of free oxygen, while this is of less importance for direct ionization. As a result, the cell's oxygen status will greatly affect the response of cells exposed to low-LET radiation while the oxygen status of cells exposed to high-LET radiation has a limited effect (12). The oxygen enhancement ratio (OER) is used to compare the response of cells irradiated in the presence and in the absence of oxygen and is defined as the ratio between the irradiation doses required to produce a biological effect, in the absence and the presence of oxygen respectively (1). The OER of mammalian cells for cell killing ranges from 2.5 to 3 for photons and it decreases with increasing LET. Fast neutron beams exhibit OERs between 1.5 and 1.8, whereas the OER for more densely ionizing α -particles is close to 1 (11) (figure 1.5).

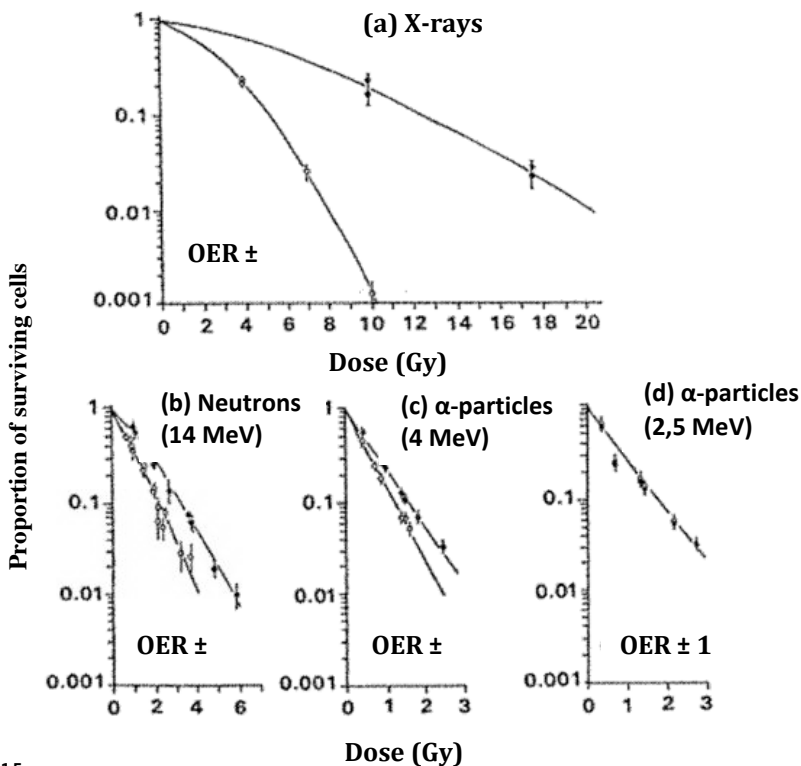


FIGURE 1.5

Survival curves of human kidney cells irradiated under hypoxic and aerobic conditions with different qualities of radiation.

● : radiation under hypoxic conditions; ○ : radiation under aerobic conditions. Figure from (11).

1.6 Dose deposition

The way the radiation beam deposits energy while traveling through mass, the dose distribution, is very different between charged and uncharged particles. With conventional X-rays and γ -rays, the dose absorbed by the tissue increases rapidly and then decreases exponentially with increasing depth (figure 1.5). Heavy charged particles on the other hand, behave very differently. When a charged particle slows down, it loses energy more and more rapidly and reaches a maximum rate of energy loss, called the Bragg peak, just before the particle comes to rest (figure 1.6). The biological effect of such particle will change along with the dose deposition and the Bragg peak will coincide with the highest biological effect. A 195 MeV carbon beam will for example have an RBE of approximately 1.3 in the entrance or plateau region of the depth dose curve, which will rise to approximately 3 in the Bragg peak (16). Due to their mass, heavy charged particles scatter less and their trajectory will be relatively straight. As a consequence a highly precise dose localization is achieved due to limited beam divergence (17). Remark that neutrons, while high-LET, are uncharged particles and their depth-dose characteristics are similar to those of high energy X-rays (12). Protons on the other hand, have a conventional RBE of 1.1 and are considered almost equal to photons, but will deposit most of their energy locally in a Bragg peak (18, 19).

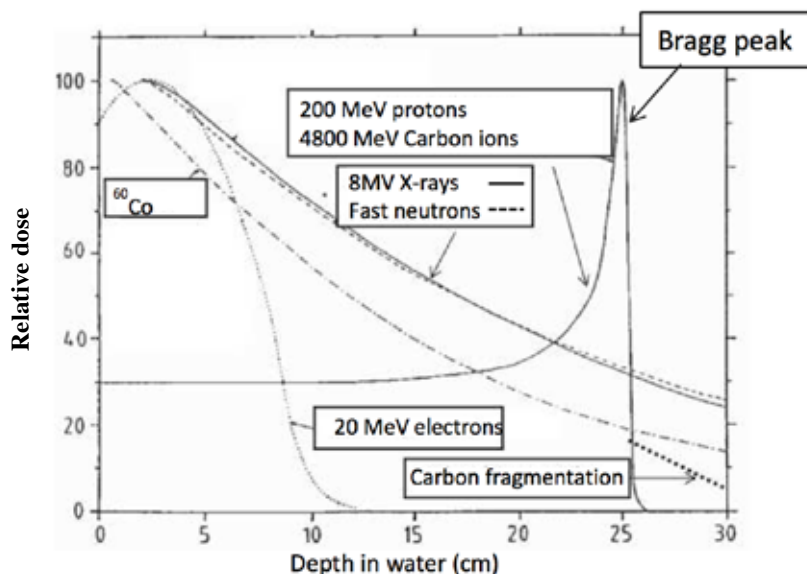


FIGURE 1.6

Depth-dose characteristics for different types of radiation. Figure from (20).

1.7 Absorbed dose, equivalent dose and effective dose

The quantity used to assess radiation exposure is absorbed dose, defined as the amount of energy deposited per unit mass. One joule of energy deposited in a kilogram of matter is referred to as 1 gray (1Gy). While still popular in some countries, the rad is a deprecated unit of absorbed dose and 100 rad equals 1Gy. The absorbed dose does not describe the possible health effects caused by radiation, since it does not take into account the RBE of the radiation and the different radiosensitivities of tissues to radiation.

The equivalent dose takes into account the different biological effects of various types and energies of radiation. H_T is calculated by multiplying the mean absorbed dose deposited in the body or organ T with the radiation weighting factor W_R , which is dependent on the type and energy of the radiation R (see figure 1.7). Examples of W_R are given in table 1.2.

The probability of radiation to induce cancer or genetic effects (stochastic health risks, see further) is dependent of the organ or tissue being irradiated. This is taken into account in the effective dose (E), which converts different radiation doses delivered to specific body parts into an equivalent uniform total body dose that entails the same risk for stochastic effects. The effective dose is the weighted sum of the tissue weighting factors (W_T) with the tissue equivalent doses (see figure 1.7). Examples of W_T are given in table 1.3.

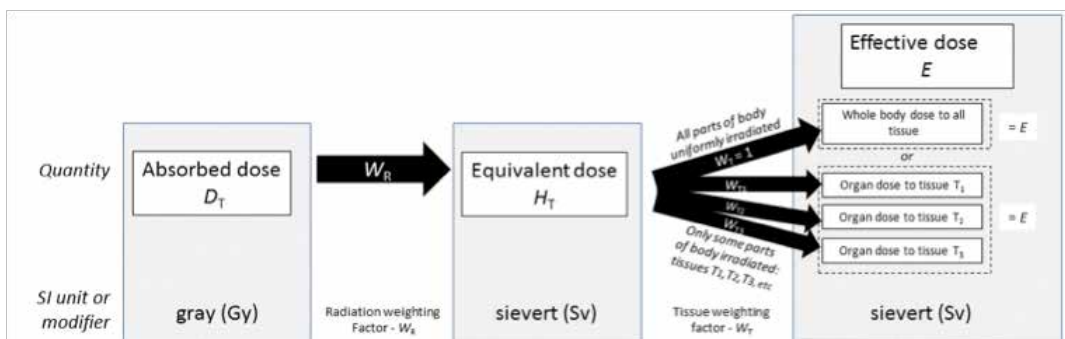


FIGURE 1.7

Overview of absorbed dose, equivalent dose and effective dose. Figure adapted from [21]

radiation	energy	W_R
γ -rays and X-rays		1
neutrons	< 1 MeV	$2.5 + 18.2 * e^{-[\ln(E)]^{2/6}}$
	1 MeV - 50 MeV	$5.0 + 17.0 * e^{-[\ln(2 * E)]^{2/6}}$
	> 50 MeV	$2.5 + 3.25 * e^{-[\ln(0.04 * E)]^{2/6}}$
protons		2
α -particles		20

TABLE 1.2

Examples of radiation weighting factors W_R . Table adapted from (14).

organ	W_T
red bone marrow, colon, lung, stomach, breast	0.12
gonads	0.08
bladder, liver, oesophagus, thyroid	0.04
skin, bone surface, salivary glands, brain	0.01
remainder of the body	0.12
total body	1

TABLE 1.2

Examples of radiation weighting factors W_R . Table adapted from (14).

Both the equivalent dose and the effective dose are expressed in Sievert (Sv). Remark that equivalent dose and effective dose are for use in radiological protection and are not directly measurable. In this thesis, as for all experimental work, the absorbed dose (Gy) has been used as measure for radiation dose.

1.8 Radiosensitivity

Radiosensitivity is a broad term and can be related to cells, tissues and individuals. It is a measure of the degree of response of the cells, tissues or individuals to radiation, with a large response indicating high sensitivity. See table 1.4 for an overview of the use of the term radiosensitivity at different levels (22).

There is a link between the different levels of radiosensitivity. Some tissues are radiosensitive because their cell populations have a high propensity to undergo apoptosis, e.g. salivary glands. Other tissues are more radioresistant because of their structural organization, e.g. if a small part of the lung is destroyed by a high dose of radiation, lung function can be maintained by the remaining healthy tissue. Individuals also vary in radiosensitivity and this can be associated with cellular radiosensitivity and possibly genomic instability. At present, there is only fragmentary understanding of the relationships between the various measures of radiosensitivity (22).

Since the term can be used on different levels, radiosensitivity should always be used in conjunction with a well-defined endpoint. This end-point might be defined clinical, as in the case of normal tissue reactions to radiotherapy or in relationship to specific disease endpoints such as cancer. Alternatively, radiosensitivity can be related to cellular phenomena such as cell killing or the induction of chromosomal damage.

1.9 Medical consequences of radiation

Radiation causes molecular changes and these changes can cause effects at cellular, tissue and organ level. At the individual level, ionizing radiation can cause disease and even death, but the link between the quality of the radiation, the type of exposure, the dose and its effects is not always clear and a lot of parameters play a role. Most evidence for the effects of ionizing radiation comes from epidemiological studies. The lifespan studies (LSS), following the whole-body radiation exposure from the survivors of the atomic bombs in Japan is the most informative and has the most statistical power (e.g. (23-25)). Also data of cohorts of well-defined medically exposed individuals are available (e.g. (26-35)).

Whole organism radiosensitivity	Is measured by assays such as LD50/30, which refers to the radiation dose required to kill 50% of a given population within 30 days of exposure
Normal tissue radiosensitivity or clinical radiosensitivity	generally used in the context of the reaction/damage to non-target tissues as a consequence of radiotherapy for cancer and other conditions. They are asses by clinical evaluation of tissue damage using a variety of scoring schemes. The main tissues of concern include skin (burnin) lung and connective tissue (fibrosis).
Susceptibility to radiation carcinogenesis	refers to differences in susceptibility amongs individuals (or strain of mice) to radiation-induced cancer in specific tissues. It is measured in emidemiological (human) studies or experimental animal carcinogenesis studies. Generally this is considered in terms of yield of tumours (in a specific tissue) per unit absorbed dose.
Tissue radiosensitivity (for cancer)	refers to the difference in sensitivity of individual tissues in organisms to radiation-associated carcinogenesis. Most information for this comes from epidemiological studies and is generally considered in terms of yield of tumours (in specific tissues) per unit absorbed dose. Tissue radiosensitivity can also refer to differences in response to radiotherapy of tissues in terms of their function or structure.
Cellular radiosensitivity	referens to a wide range of phenomena measured at the cellular level where reponses to radiation can vary between individuals or cell types. Endpoints can be cell killing, chromosomal damage, damage/repair to DNA, cell cycle endpoints, apoptosis, etc. It is measured in yield of the endpoint per unit absorbed dose or parameters derived from dose-response relationships.

TABLE 1.4

A summary of the main forms and assays of radiosensitivity in common use. Table adapted from (22).

It is clear that ionizing radiation can induce cellular damage and as a consequence induce disease. The effects of ionizing radiation are categorized into two groups, tissue reactions, formerly known as deterministic effects (36), and stochastic effects (37). Stochastic effects are effects which occur by chance. The probability of occurring but not the severity is regarded as a function of dose without threshold. Stochastic effects result from injury to a single cell, mostly a specific mutation in a single gene or mutations involving loss of DNA. If the damage is not correctly repaired the cell may die or alternatively the cell may survive with DNA mutations that affect cellular behavior. A small fraction of such mutations can contribute to the development of stochastic effects. Cancer and heritable effects are categorized as stochastic effects. The excess lifetime risk of mortality for solid cancers and leukemia are given in table 1.5. The risk of heritable diseases due to exposure is based on animal experiments and is estimated to be 0.54% per Gray (Gy) in the reproductive population (37-40). Tissue reactions, formerly termed deterministic or non-stochastic effects, are effects which only become apparent if a threshold dose is exceeded and the probability and severity of the effect increases with increasing dose. The damage results from the collective injury of a substantial number of cells in the affected tissue. The threshold dose is effect-specific and depends on the individual sensitivity. Acute doses up to 0.5 Gy are believed to produce no tissue effects, although this is under discussion. Examples of tissue effects are cataracts, non-malignant skin damage and impaired fertility (36-38, 41).

Dose (Sv)	Solid cancers (%)	Leukemia (%)
0.1	0.36-0.77	0.03-0.05
1.0	4.3-7.2	0.6-1.0

TABLE 1.5

Excess lifetime risk of mortality (averaged over both sexes). Data from (40).

Upwards from 100 mGy, there is a linear relationship between the dose received and the long term effect of the irradiation (17). The effects of low (<100 mGy) and very low doses (<10 mGy), are less clear. Available epidemiological data do not have sufficient power to assess the radiation risks of low and very low exposure levels (42). However, the inability to quantify these risks does not imply that the risk to the population is negligible. A very small risk, if applied to a large number of healthy individuals, can result in a significant health problem (42).

In vitro studies investigating cellular and genetic effects show the consequences of low and very low doses of ionizing irradiation. After an exposure to just a few mGy, e.g. γ H2AX foci can be demonstrated (10, 43, 44) or changes in transcription level of genes can be detected (45-47). Not only cell effects are present at doses as low as a few mGy, gene expression analysis demonstrated that different gene profiles were highlighted after low and high doses of X-rays in whole blood (48).

However, how these effects translate into low-dose risks, and whether they have detrimental or beneficial effects, is still a matter of debate.

There are different scenarios to extrapolate high dose risks to low doses. The linear no threshold (LNT) model is the golden standard in radiation protection and assumes a linear relationship between dose and risk from 0 Gy upwards (see figure 1.8 curve a). By using the LNT model, the assumption is made that no radiation dose, no matter how small, can be regarded as safe. The LNT model is based on data from epidemiological studies providing a linearly increasing radiation-induced cancer risk from about 100 mGy to 2.5 Gy and extrapolates this linearity to the low and very low dose region. The argument for linear extrapolation considers radiation effects due to autonomous responses of individual cells (17). However, studies show that different mechanisms can play at low and high doses, which can cause us to either under- or overestimate the risks of low doses (42) (see figure 1.8 curves b-e).

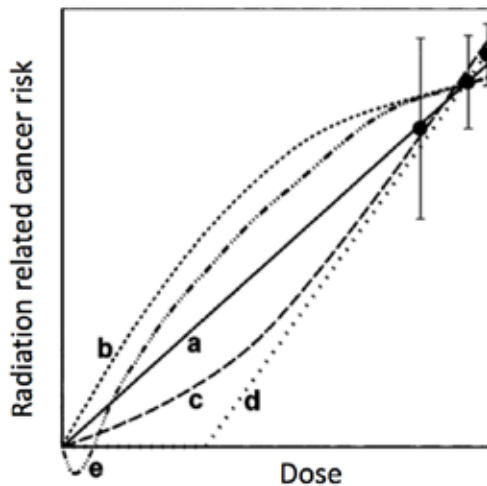


FIGURE 1.8

Schematic representation of different possible extrapolations of measured radiation risks down to very low doses, all of which could, in theory, be considered with higher-dose epidemiological data. curve a: LNT model; curve b: low-dose hypersensitivity; curve c: adaptive response; curve d: threshold hypothesis; curve e: hormesis. Figure from (42).

The observation that ionizing radiation can cause effects in un-irradiated “bystander” cells is called the bystander effect. These un-irradiated cells can be neighboring to the irradiated cells, but also be remote and do not even need to be present at the time of exposure. The bystander effect is predominant at very low doses, down to the mGy level, but stabilizes at higher doses because more cells are directly targeted by the radiation (42, 49, 50). It leads to a steep dose response at very low doses, which saturates at higher doses probably because all relevant cells that can be affected are already affected (51, 52) (See figure 1.6 curve b).

The irradiated cells propagate signaling molecules to neighboring cells via gap-junction mediated intercellular communication and via the release of diffusible factors into the extracellular environment (53-57). Cyclooxygenase-2 (COX-2) seems a crucial modulator of the system (58).

Interestingly, the gene sets which are upregulated after low dose irradiation are inflammatory and immune-related, whereas at high doses the main response is the activation of p53 signaling inducing cell cycle arrest and apoptosis processes. The upregulated chemokines, cytokines, MAPK (mitogen-activated protein kinases) and NF κ B (nuclear factor kappa-light-chain-enhancer of activated B cells) have been proven to play a central role in the bystander effect (48).

The bystander effect can cause low-dose hypersensitivity, which is characterized by a higher than expected biological effectiveness of the radiation at very low doses, while the cells start to exhibit a relative radioresistance at higher doses (59).

Another possible mechanism for low-dose hypersensitivity is the need to pass a certain damage or stress-threshold before efficient repair will take place (60-62) (See figure 1.8 curve b).

While the bystander effect and low-dose hypersensitivity response cause an underestimation of the damage induced by low-dose radiation, other mechanisms could result in an overestimation of the induced damage. The threshold hypothesis implies that below a certain dose there are no radiation health effects (See figure 1.8 curve d). Studies on adaptive response or hormesis (see respectively figure 1.8 curve c and e) claim that irradiating cells with a low priming dose helps them to be “prepared” before being challenged with a higher dose. There are a number of different mechanisms that are thought to be involved in inducing the adaptive response: anti-oxidative stress response by antioxidant molecules, enhanced DNA repair detection and signaling or enhanced repair efficiency and activation of an immune defensive response (63). It is clear that the bystander effect can also be a mechanism for adaptive response. The adaptive, or protective response from the priming dose, can be over a few hours for anti-oxidative stress, up to a few days for DNA repair and up to several months for immune enhancement (64) (See figure 1.8 curve c).

Remark that mechanisms as bystander effect, threshold hypothesis, hypersensitivity and adaptive response are not mutually exclusive. Differences in radiation dose and quality, cell type and cellular environment might trigger a different response to the radiation.

2 DNA DSB repair

2.1 DNA damage response

DNA is constantly damaged by endogenous and exogenous agents. DNA lesions can prevent genomic replication and transcription and if they are not repaired or misrepaired, they can lead to mutations or large-scale genome aberrations that may lead to cell malfunction or cell death. Especially the DNA DSB is considered to be very cytotoxic because their correct repair is intrinsically more difficult than that of other types of DNA damage. Improperly repaired DSB often lead to large chromosomal rearrangements such as deletions, translocations and amplifications, which can lead to tumorigenesis if for example the deleted region encodes a tumor suppressor protein or if an amplified region encodes a protein with oncogenic potential (65). In order to maintain the genomic integrity of the DNA, cells have an elaborate system to counteract the genotoxic stress induced by ionizing radiation, known as the DNA damage response (DDR).

In the DDR pathway the damage is initially detected by “sensor” molecules. The signal is then transferred to “transducer” proteins, that will amplify the signal and recruit “effector” proteins to the damaged site. Subsequently the attracted effector proteins induce cell cycle arrest, DNA damage repair or apoptosis (65) (see figure 2.1).

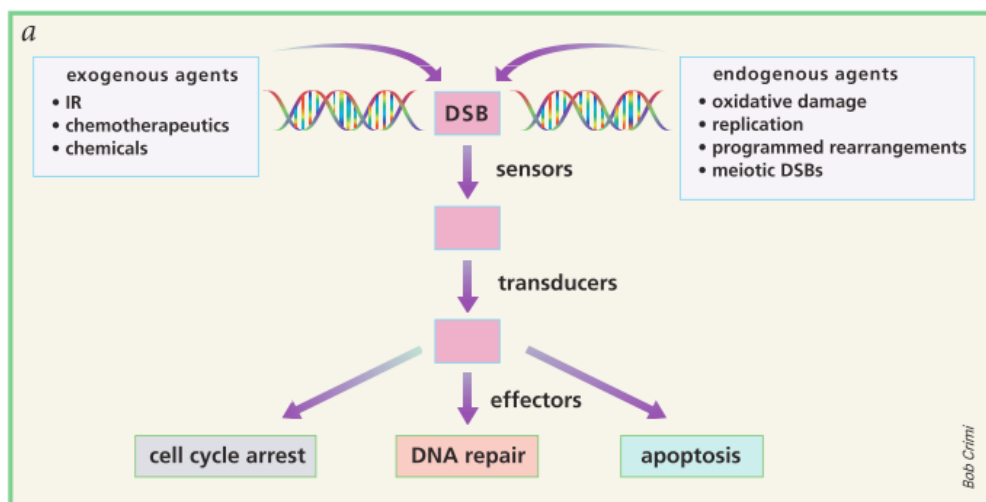


FIGURE 2.1

General organization of the DNA damage response pathway. Figure from (65).

The main sensor protein is always an important member of the PIK3 (phosphatidylinositol-4,5-bisphosphate 3-kinase) kinase family, DNA PKcs (DNA-dependent protein kinase catalytic subunit), ATM (ataxia telangiectasia mutated) or ATR (ATM- and RAD3-related). However, which of these proteins will actually initiate the DDR, is dependent on the origin of the DSB.

There remains controversy about the proteins that initially sense the DNA DSB induced by irradiation and start the signaling cascade. The Mre11/Rad50/Nbs1 (MRN) complex has been ascribed a critical role in detecting the break and recruiting ATM via the C-terminus of Nbs1 (66-68). The ATM kinase is considered a key protein in the DSB response and activation by autophosphorylation at Ser1981 of the kinase results in dissociation of the latent ATM dimers into active monomers (69). Activated ATM monomers have a very strong kinase activity and have been shown to phosphorylate hundreds of monomers, including proteins involved in checkpoint activation and DNA-repair (see figure 2.2) (70, 71).

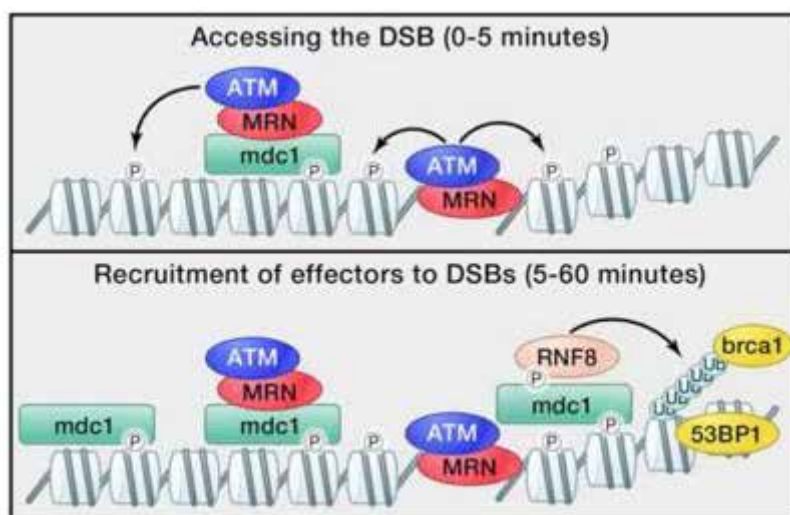


FIGURE 2.2

The initial phases of DSB repair. Figure from (70).

A critical target of ATM in the DDR is the phosphorylation of the C-terminus of the histone variant H2AX (γ H2AX). Phosphorylated γ H2AX creates a binding site for the BRCT (BRCA1 C-terminal) domain of MDC1 (Mediator of DNA damage checkpoint1). Positioning of MDC1 at the DSB creates a binding γ H2AX place for additional DSB-repair proteins, including the MRN-ATM complex. This amplifies the signal, binding of MRN-ATM to MDC1 will phosphorylate more H2AX, creating more binding sites for MDC1 (72-74). 30 Minutes after induction of the break, a plateau is reached with a γ H2AX domain that extends for hundreds of kilobases along the chromatin around the DSB (70) (see top figure 2.2). γ H2AX serves as a docking site for mediator proteins, such as 53BP1 (53 binding protein 1), NBS1 (Nijmegen breakage syndrome 1) and BRCA1 (breast cancer early onset1), which will be phosphorylated by ATM and will transduce the signal to downstream effectors (70) (see bottom figure 2.2).

2.2 Cell cycle checkpoint arrest

To ensure fidelity of DNA replication and chromosome segregation, cell cycle checkpoint arrest ensures the activation of surveillance mechanisms to prevent progression through the cell cycle until critical processes involved in DNA repair have been completed. In response to the initiation of the DDR, proteins involved in the control of the cell cycle checkpoints will also be activated to temporarily stop the transition of the cell through the cell cycle to allow time for repair and to ensure that genetic errors are not transmitted to subsequent generations (75, 76).

The cell cycle has several checkpoints, namely the G₁/S, intra-S-phase, G₂/M and mitotic checkpoints. Checkpoint activation is based on the inhibition of cyclin-dependent kinase (cyclin-Cdk) complexes, which regulate all progression through the cell cycle (see figure 2.3).

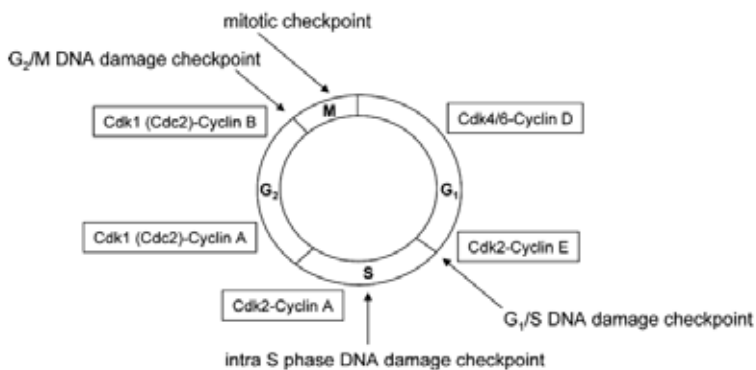


FIGURE 2.3

Control of the cell cycle by cyclins and Cdks and their regulation by cell cycle checkpoints. Figure from (77).

The G1/S checkpoint is induced when DNA damage is detected to prevent replication of DNA of cells that were in G1 at the time of DNA damage to progress into S-phase. The checkpoint is mediated by two distinct signal transduction pathways, the Chk1/Chk2-Cdc25A-Cdk2 pathway and a second pathway centered around p53 (Chk1/Chk2-p53-p21). As a result, the G1-cyclin-Cdk complexes, including cyclin-Cdk2 complexes, are inactive, preventing phosphorylation of the retinoblastoma (Rb) protein. This causes the E2F transcription factor, which is important for the regulation of many genes initiating DNA replication, to remain inactive (see figure 2.4) (77-79).

The intra-S-phase checkpoint is activated to prevent replication of damaged DNA. Downregulation of CDC25A subsequently causes inactivation of the S-phase-promoting Cdk2-cyclinE and prevents loading of Cdc45 on replication origins, hence inhibiting DNA synthesis (79).

The G2/M checkpoint prevents the cells from entering mitosis and transducing DNA damage to daughter cells. This checkpoint is subject to the Chk1/Chk2-Cdc25C-Cdk1 pathway. The arrest is achieved through continued phosphorylation of Cdk1-cyclinB1 kinase, preventing the cell to enter mitosis (see figure 2.4) (77, 79).

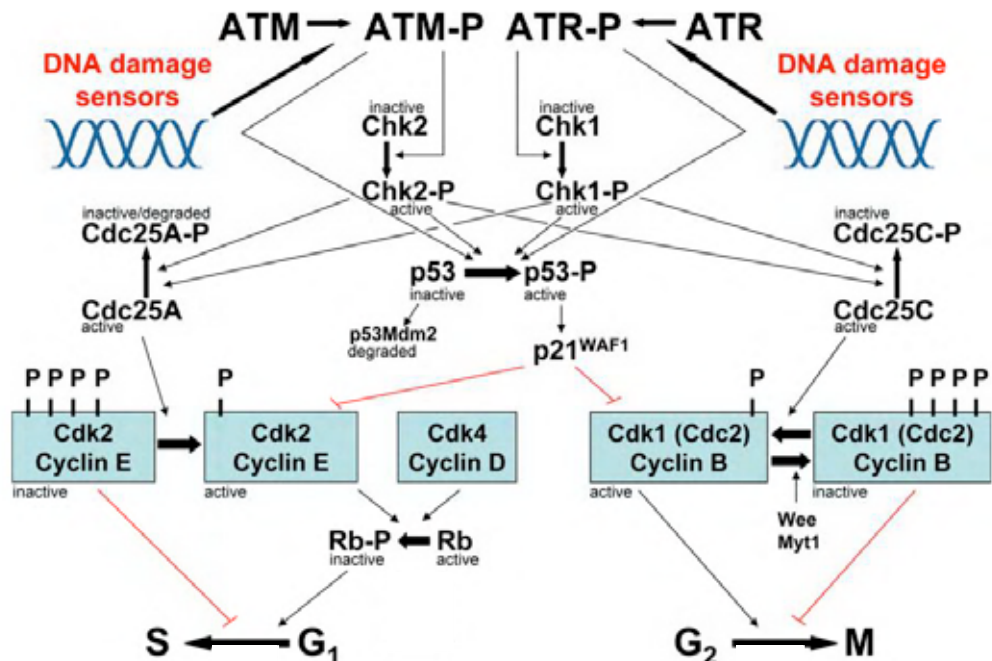


FIGURE 2.4

Overview of the G1/S and G2/M checkpoint regulation pathways following ATM/ATR activation. Figure from (77).

The mitotic or spindle activation checkpoint (SAC) prevents the onset of anaphase until all chromosomes are properly attached to the spindle and ensures that chromosome segregation is correct. Downregulation of CDC20 prevents the activation of the polyubiquitylation activities of the anaphase promoting complex (APC), thereby arresting the cell in metaphase (80).

2.3 DNA DSB repair pathways

DSB are primarily repaired by one of two pathways, non-homologous end joining (NHEJ) or homologous recombination (HR), irrespective of their cause (81). Furthermore a number of back-up pathways exist which can be used under certain conditions or when repair via NHEJ or HR is not possible.

2.3.1 Non-homologous end joining (NHEJ) (see figure 2.5)

Non-homologous end joining is the main DSB repair pathway in mammalian cells and can be used in all phases of the cell cycle (82-84). NHEJ is based on the direct ligation of the two termini of the broken DNA molecule. Ionizing radiation will often induce DSB with nonligatable single stranded ends. For DNA ligation by NHEJ, blunt ends are needed and processing of the single stranded DNA overhangs is in general required prior to ligation. This processing can however result in loss of nucleotides, making this pathway potentially error-prone. DSB repair via the NHEJ pathway takes a few hours to complete.

DNA repair by NHEJ is mainly regulated by actions of DNA-PK and the Ku70/Ku80 heterodimer. Ku is available in abundance and binds with high affinity to DNA termini in a sequence-independent manner. Immediately after induction of a break, Ku will bind to both ends of the broken DNA molecule (85-87). Its binding tethers and protects the DNA termini. Binding of Ku to the DNA recruits the catalytic subunit of DNA PKcs to the DSB site, leading to the formation of the DNA PK holoenzyme (88). DNA PKcs is activated by phosphorylation, mainly via autophosphorylation and potentially by other kinases such as ATM and ATR. The binding of DNA PKcs with both Ku and the DNA termini, enhances greatly its kinase activity, and is thought to be a necessary step in NHEJ repair (89). The activated DNA PKcs facilitates then the recruitment of other repair factors to the DSB site, such as Artemis, the XRCC4/DNA ligase 4 complex and XRCC4-like factor and will expose the termini to the recruited nucleases and polymerases.

Processing of the single-strand overhang to obtain the blunt ends needed for ligation can occur in two ways. The overhang can be resected, which can be done by nucleases such as Artemis (90, 91), Exo1 (exonuclease 1) (81, 92) and WRN (werner syndrome) (81, 93) or a complementary strand can be synthesized using the overhang as template which is done by DNA polymerase μ and λ (71, 94, 95).

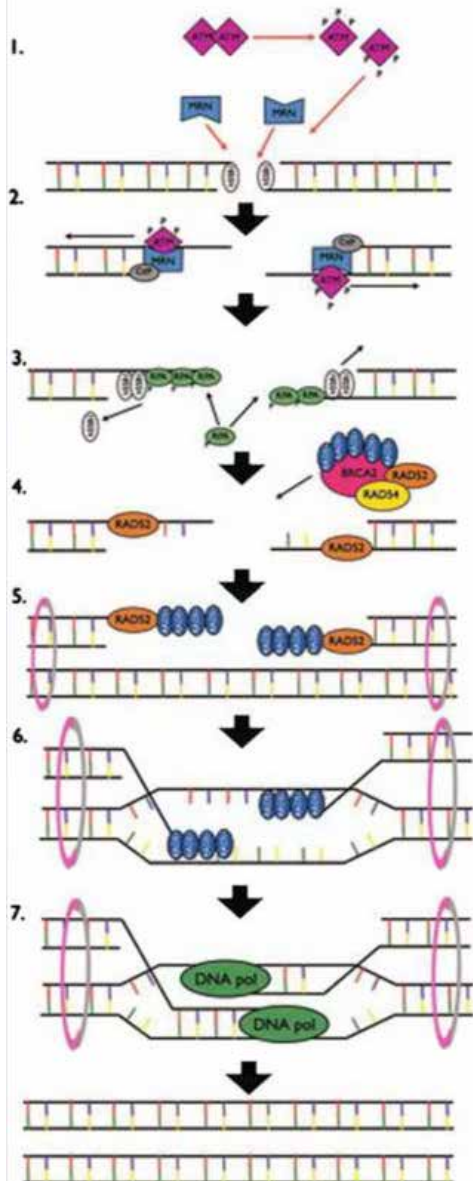
Subsequently, DNA ligase IV, XRCC4 and XLF (XRCC4-like factor) ligate the broken DNA termini to complete repair. XRCC4 has no known enzymatic activity, but will act as a scaffolding protein through which it stabilizes and stimulates the ligase activity of DNA ligase IV (96, 97). XLF is recruited to the break by Ku and stabilized by interactions with the ligase IV/XRCC4 complex. The protein seems to stimulate ligation of non-compatible DNA ends, thereby preventing nucleotide loss during NHEJ (81, 82, 90).

2.3.2 Homologous recombination (HR) (see figure 2.5)

DNA repair by HR uses the undamaged sister chromatid to repair the DSB and is therefore less prone to errors. Consequently HR only plays a role in S and G2 phase of the cell cycle.

The HR pathway is initiated by 5'-end resection at the DSB terminus resulting in 3' single stranded DNA (98, 99). This is facilitated by the endonuclease activity of Mre11 (part of the MRN-complex) and is regulated by CtBP-interacting protein (CtIP) in a ATM and BRCA1 dependent manner (100). Following the formation of long tails of 3' ssDNA, hSSB1 molecules are initially bound to it and then displaced by replication protein A (RPA) to the sites of the DSB (101, 102). The RAD52/BRCA2/RAD51/RAD54 complex is then recruited to the ssDNA by a BRCA1/PALB2 (partner and localizer of BRCA2 (breast cancer early onset2)) complex. This facilitates the replacement of RPA by RAD51, thus stabilizing the filament and catalyzing the invasion (103). To facilitate invasion into the sister chromatid strand, the two chromatids are tethered together by structural maintenance of chromosomes (SMC) proteins 1, 3, 5 and 6 (104). The filaments will search for and invade the homologous template which leads to the formation of a heteroduplex or hybrid DNA referred to as the D-loop (displacement loop) structure. Second end capture of the break by the D-loop results in two four-stranded branched DNA-structures, called Holliday junctions (105). These Holliday junctions are able to undergo branch migration whereby DNA polymerase δ (DNA pol δ) carries out DNA synthesis to restore the missing sequence information using the intact duplex DNA template. Once DNA replication is complete, the Holliday junction is resolved by DNA resolvases through a complex process that remains unclear (106). The entire process takes several hours to complete.

Homologous Recombination



Non-homologous end joining

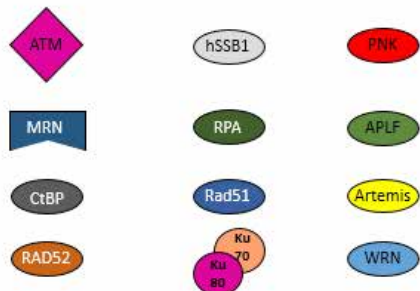
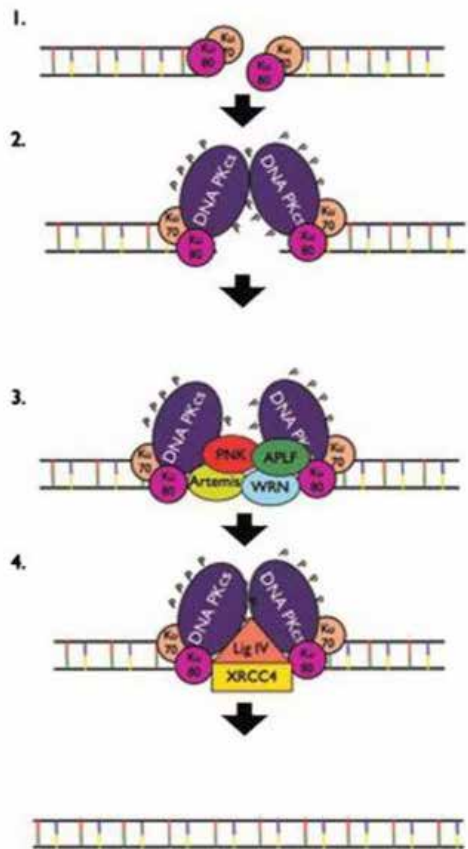


FIGURE 2.5

The two main DNA DSB pathways. HR is represented schematically on the left and NHEJ on the right. Figure adapted from (81).

2.3.3 Alternative DNA DSB repair pathways

Next to NHEJ and HR there are some alternative DNA DSB repair pathways: B-NHEJ, also named alt-NHEJ, Microhomology Mediated End Joining (MMEJ) and Single Strand Annealing (SSA). All three have certain commonalities, but there are also differences between them and it is unclear in how much they are different pathways or variations of a single pathway. B-NHEJ, MMEJ and SSA play an important role as backup pathway for NHEJ in DSB repair in G1 and early S-phase cells. They have slower kinetics than NHEJ, are less faithful than NHEJ and are marked by larger deletions and translocations (107).

These pathways operate independent of the core NHEJ proteins: DNA-PKcs, Ku and Lig4 in complex with XRCC4. Different from NHEJ, these pathways depend on end-resection, initiated by MRN and CtIP (108). POL4, LIG3 are found to be required for MMEJ, while PARP (poly-ADP ribose polymerase) and LIG1 seem to be required for B-NHEJ (see figure 2.6).

For B-NHEJ no homology is needed, while MMEJ relies on homologies of only a few nucleotides and SSA on homologous sequences ranging from 10bp to several kilobases (109).

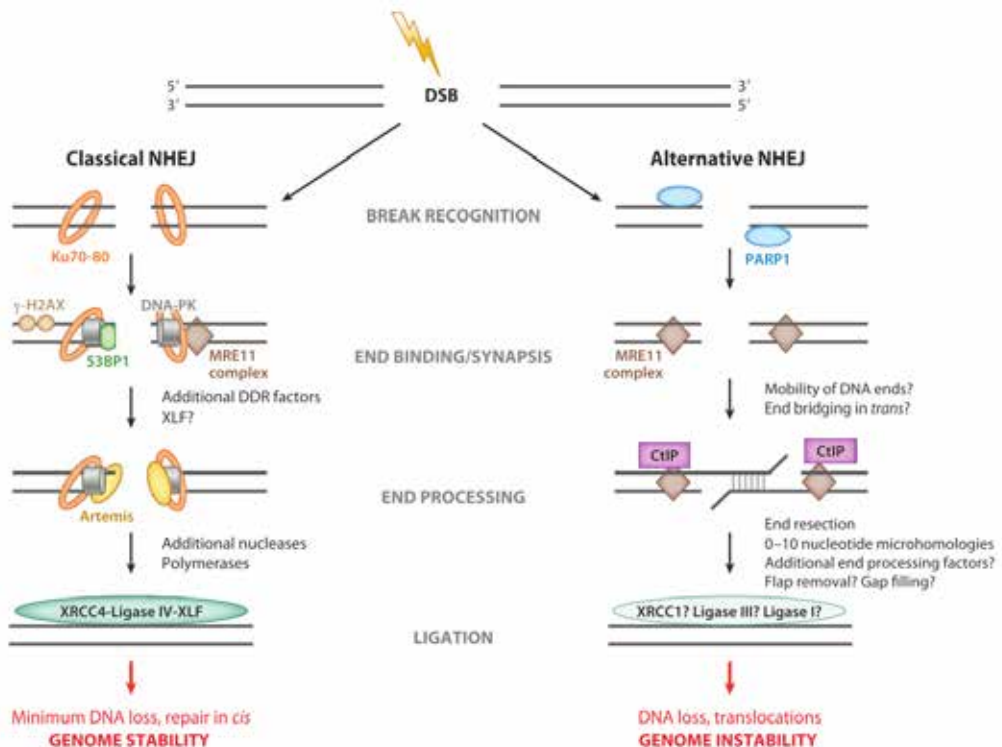


FIGURE 2.6

Comparison between classical NHEJ and alt-NHEJ or B-NHEJ. Figure from (110).

2.4 Determinants of DSB repair pathway choice

Pathway choice is an interplay between different factors such as: phase of the cell cycle, the presence of the sister chromatid, cell type, chromatin complexity and the complexity of the damage induced (81).

2.4.1 Cell cycle phase

Irrespective of the cell cycle, NHEJ is the main DNA DSB repair pathway in most mammalian cells and HR plays a relatively minor role (111). While NHEJ is the main pathway throughout the cell cycle, there is competition with HR and with the alternative pathways. A sister chromatid, which is needed for HR, will only be available in late S and G2 phase of the cell cycle and as such, HR is only available then. B-NHEJ, MMEJ and SSA require no or very small homologies and can be used throughout all phases. Since the different pathways have a different accuracy, the availability and use of a repair-pathway throughout the cell cycle, influences the radiosensitivity of the cell (see figure 2.7).

2.4.2 Complexity of the damage

High-LET radiation, with its dense ionization pattern, will produce more clustered damage and hence complex damaged sites (112-114). These complex damage sites are known to have a slower rate of repair compared to the DSB induced by low-LET radiation (113). Radiation-induced DSB repair is biphasic with a fast component, repairing damage within 2h and a slow component with a half-life of 2-10h (115-117). In mammalian cells, studies have shown that, even though HR has the capacity to function in G2 phase, NHEJ also represents the major DSB repair pathway in G2 (118) and this seems to be the fast component of DSB repair (119, 120). Complex DSB are mainly repaired by the slow component of the DDR (121, 122). CtIP, activated by ATM, is indispensable for the repair of these complex DSB with slow kinetics, both in G1 and G2 phase (17). Thus DSB resection is crucial for repair of complex DNA damage in all cell cycle stages and there seems to be a direct correlation between DSB complexity and the degree of resection. The increased requirement for processing of DNA ends observed for complex DSB, forces the pathway choice towards resection-dependent repair pathways. In G2 this pathway is represented by HR and the importance of HR increases as the LET of the radiation increases (118, 123). Evidence for substantial resection in the G1-phase and lack of HR in this cell cycle stage suggests that MMEJ is a major repair pathway choice for complex DSB in G1-phase, especially for the subset of lesions repaired with slow kinetics. The fact that rejoined DSB arising from ion-induced clustered DNA damage are often characterized by deletions and flanking microhomologies support this notion (124, 125). However, other studies show a dependency on ATM and Artemis, pointing to B-NHEJ (118).

2.4.3 Chromatin complexity

Another important factor that influences the pathway choice is the complex organization of the chromatin. The chromatin structure and nucleosome organization will have a significant influence on the efficient detection and repair of DSB. The DSB-repair machinery must be able to (1) detect DNA damage in different chromatin structures, (2) remodel the local chromatin architecture to provide access to the site of damage, (3) reorganize the nucleosome-DNA template for processing and repair of the damage and (4) restore the local chromatin organization after repair has been completed (70, 126, 127). Recent studies consistently show that the dense packing of nucleosomes and the presence of specific heterochromatin-binding complexes are a significant barrier to repair DSB located in the heterochromatin (70, 128-131). Repair of DSB is significantly slower in heterochromatic regions (121, 132). In response to DSB, the induction of KRAB-associated protein 1 (KAP-1), which functions to maintain the heterochromatin, is phosphorylated by ATM, promoting a general relaxation of the chromatin structure (70). This relaxation of the chromatin will be followed by HR-mediated DSB repair in G2. In G1 and early S-phase, repair by NHEJ is most common after relaxation of the chromatin, however complex breaks in heterochromatin during G1 will be repaired by one of the back-up pathways (133).

2.4.4 Choice of the repair pathway (see figure 2.8)

Following radiation-induced DNA DSB formation, there is competition for binding to the lesion by the Ku/DNA-PK and MRN complex. DNA-PK binds rapidly to all DSB, either because Ku has strong DSB-binding capacity or because it is highly abundant. This will initiate NHEJ, which will make a first attempt to repair the DSB. If rapid rejoining by NHEJ cannot ensue (109) either due to the DNA lesion or chromatin complexity, then DSB repair occurs in an end resection-dependent manner, for which CtIP is indispensable (125). In G2 phase this pathway is HR, while in G1 this is probably MMEJ. If resection cannot ensue, then NHEJ makes a further attempt to repair the DSB and, indeed, can function efficiently. The switch from NHEJ to HR seems to be promoted by BRCA1, which repositions 53BP1 to promote resection (134, 135).

However, resection or possibly a later stage in the progression to HR commits to HR and precludes the possibility of returning to NHEJ usage (121). When HR cannot progress beyond the resection step due to loss of BRCA2, then NHEJ cannot rejoin the DSB. This suggests that excessive resection due to loss of BRCA2 precludes the ability to utilize NHEJ (121).

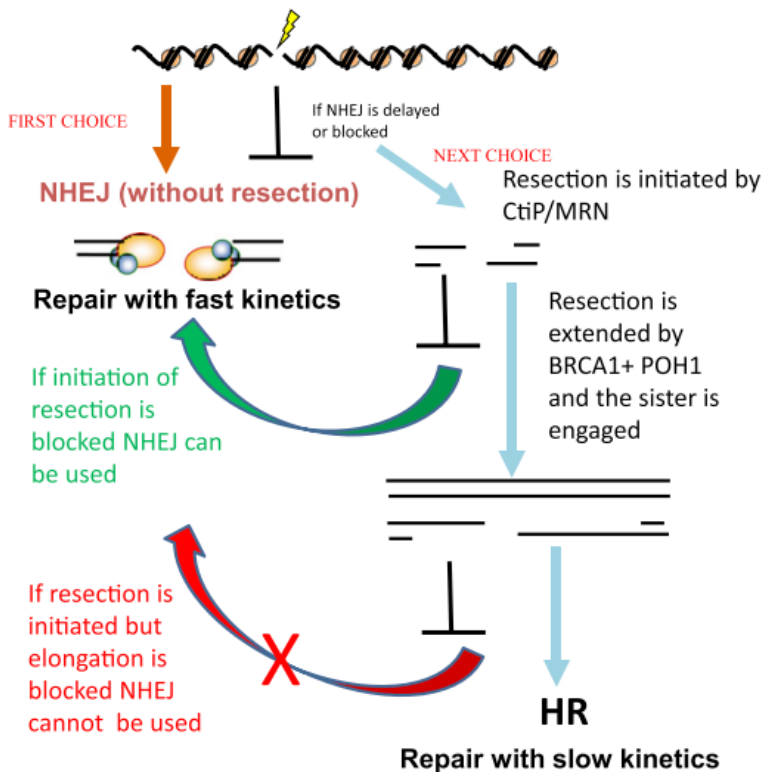


FIGURE 2.8

Decision tree for DNA DSB repair pathway choice. Figure from (109).

2.5 Apoptosis, necrosis, mitotic catastrophe and senescence

In order to prevent transfer of the defective genetic material, cells may activate cell death or senescence, which is an irreversible arrest of cell proliferation, instead of DNA DSB repair pathways. The most important cell death pathways following irradiation are apoptosis, necrosis and mitotic catastrophe.

2.5.1 Apoptosis

Apoptosis, or programmed cell death, represents a regulated suicidal process, that results in the rapid destruction and removal of the cell. Apoptosis is an important process during development and aging and as a homeostatic mechanism to maintain cell populations in tissues. Apoptosis also occurs as a defense mechanism such as in immune reactions or when cells are damaged by e.g. radiation or toxic agents. A wide variety of stimuli and conditions, both physiological and pathological, can trigger apoptosis, however whether or not they actually lead to apoptosis is cell type dependent (136).

Apoptotic cells are characterized by morphological changes like plasma membrane blebbing, chromatin condensation, reduction of cellular volume and finally fragmentation of the cell and nucleus into membrane-enclosed structures, known as apoptotic bodies (137).

The two most important apoptotic-pathways are an extrinsic and an intrinsic pathway, both of which can be regulated at multiple levels and can be activated by radiation (see figure 2.9) (136). Both the intrinsic and extrinsic pathway are characterized by the sequential activation of specific proteases known as caspases (cysteine-dependent, aspartate-specific peptidases) (138). The intrinsic pathway, also called the mitochondrial pathway, is activated more often in response to radiation-induced damage. It is typically initiated by DNA damage, which will lead to activation of p53 and then p21 (139, 140). In response, the balance of pro- and anti-apoptotic proteins is changed, leading to the mitochondrial outer membrane permeabilization (MOMP) which disrupts the mitochondrial function. MOMP releases several potentially lethal proteins from the intermembrane space into the cytoplasm such as e.g. cytochrome c. Cytochrome c will activate and bind with subsequently APAF1 (apoptotic protease activating factor 1) and ATP/dATP ((deoxy)adenosine triphosphate). This conformation, called the apoptosome, will mediate the activation of caspase-9 (138, 141). To activate the extrinsic pathway or death receptor pathway, death-signals from the surrounding environment bind the death-receptors on the membrane, which causes the activation of caspase 8. Both caspase-9 and caspase-8 will go on to activate the cascade of executioner caspases: caspase-3, -6 and -7 via mitochondria dependent and independent mechanisms. This will eventually lead to the formation of apoptotic bodies (138, 141-144).

Induction of apoptosis following radiation can also occur independently of caspases and is then activated by the apoptosis-inducing-factor (AIF). AIF is expressed and compartmentalized into the mitochondria in physiological conditions. After a cellular injury, such as radiation-induced damage, AIF is cleaved and translocated to the nucleus where it interacts with DNA and causes a caspase-independent chromatin condensation and large scale DNA fragmentation (145).

2.5.2 Necrosis

Necrosis has long been regarded as an accidental form of cell death, however more recent evidence shows that some forms of necrosis actively involve defined signaling pathways that contribute to the cell's death. Necrosis can be induced by exposure to various physico-chemical stressors such as ionizing radiation, oxidative stress and calcium overload. Necrosis can be induced very fast, when cells receive a very high dose of ionizing radiation or it can occur delayed following mitotic catastrophe (see further) (146).

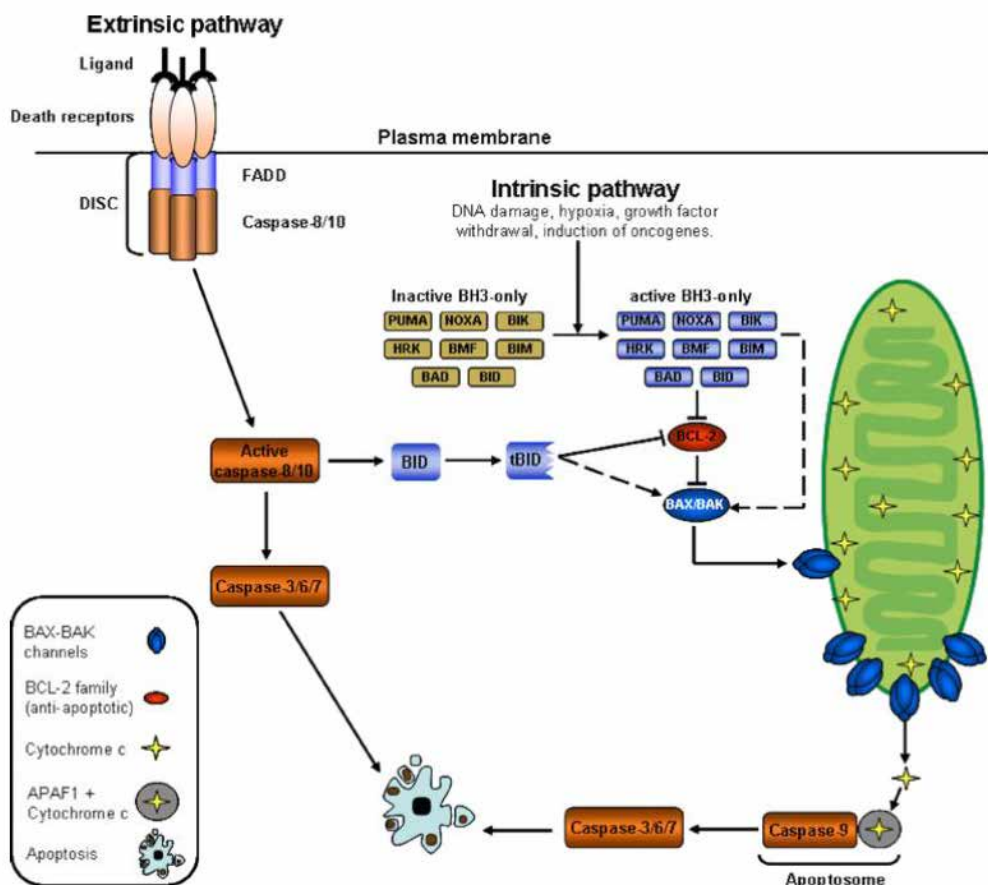


FIGURE 2.9

Overview of the most important pathways radiation-induced apoptotic pathways. Figure from (144).

Necrotic cells are characterized by swelling of the cell and the organelles, formation of intracellular vacuoles and plasma membrane rupture. Unlike apoptosis there is no fragmentation of the DNA. Eventually cell lysis will occur and the intracellular content is spilled, which may induce inflammation (147).

Depending on the initiation-mechanism, different forms of necrosis can be described. TNF (tumor necrosis factor) is the best studied initiator of necrosis, but also pathogens, physico-chemical stress and release of inducers by other necrotic cells may induce necrosis. Most necrotic pathways are dependent on RIPK1 (receptor-interacting protein kinase) and RIPK3 for regulation. Necrosis mostly happens independently of caspases, although some necrotic-like cell-death pathways which involve caspases have been described. Furthermore, caspase-8 seems to negatively regulate TNF-initiated necrosis (147, 148).

2.5.3 Mitotic catastrophe

Mitotic catastrophe is a term used for cell death that occurs during or as a result of an aberrant mitosis. It has been controversial if mitotic catastrophe should be considered a type of cell death or rather an abnormal mitosis leading to cell death executed by apoptosis or necrosis. Consistent for all cell deaths following mitotic catastrophe is that they are delayed, occurring 2 to 6 days following radiation (144, 149, 150).

The two most important mechanisms for induction of mitotic catastrophe is a deficient G2/M checkpoint and hyperamplification of centrosomes, both of which are linked to p53 inactivation (150, 151). As a result, the cell will enter mitosis prematurely where it will be stopped in its progression by the mitotic checkpoint. This delay, which occurs often after radiation, results in caspase activation and subsequent mitochondrial damage and eventually leads to delayed apoptosis in metaphase. However, often cells adapt to the mitotic checkpoint and exit the arrest but fail cytokinesis. These polyploid cells can survive for days and may even proceed to another round of cell division, acquiring an increasing amount of chromosomal aberrations. In the end these polyploid cells will die either by delayed apoptosis, delayed necrosis or induced senescence (144, 149, 152).

2.5.4 Senescence

Senescence is a state of permanent cell cycle arrest, and as such senescence prevents the proliferation of cells that are at risk for tumorigenic transformation. Senescent cells do not divide but remain metabolically active. Replicative senescence is induced by the ageing of the cell, while stress-induced premature senescence can be induced by different stressors like radiation, osmotic

and mechanical stress, heat shock, genotoxic drugs etc. (153-155). However both types are closely related (see figure 2.10).

Cells in both replicative and stress-induced senescence exhibit the same morphological and molecular markers: enlarged and flattened morphology, β -galactosidase activity, an activated DDR and cell cycle arrest machinery (p53, p16, p21) and a senescence-associated secretory phenotype (156, 157).

Induction of a cell into senescence is initiated by activation of ATM. Activated ATM will lead to upregulation of the important downstream target p53, which in turn will trigger the transcription of p21. p21 acts to inhibit cyclin-dependent kinase 2 (CDK2) and blocks functional CDK2/cyclinE complexes, inhibiting the progression of cells from G1 to S-phase of the cell (158-160). The ATM-p53-p21 pathway is active 2 to 4 hours after irradiation (161). Another pathway leading to senescence goes via the p16 protein. Hyperactivation of the oncogenic Ras pathway, upregulates p16. Increased p16 levels inhibit cyclin-dependent kinases 4 and 6 (CDK4 and 6), which are associated with the progression of G1 cells into S-phase (162-164). The p16 pathway is slower and induction of p16 is observed from 5 days after exposure (165, 166).

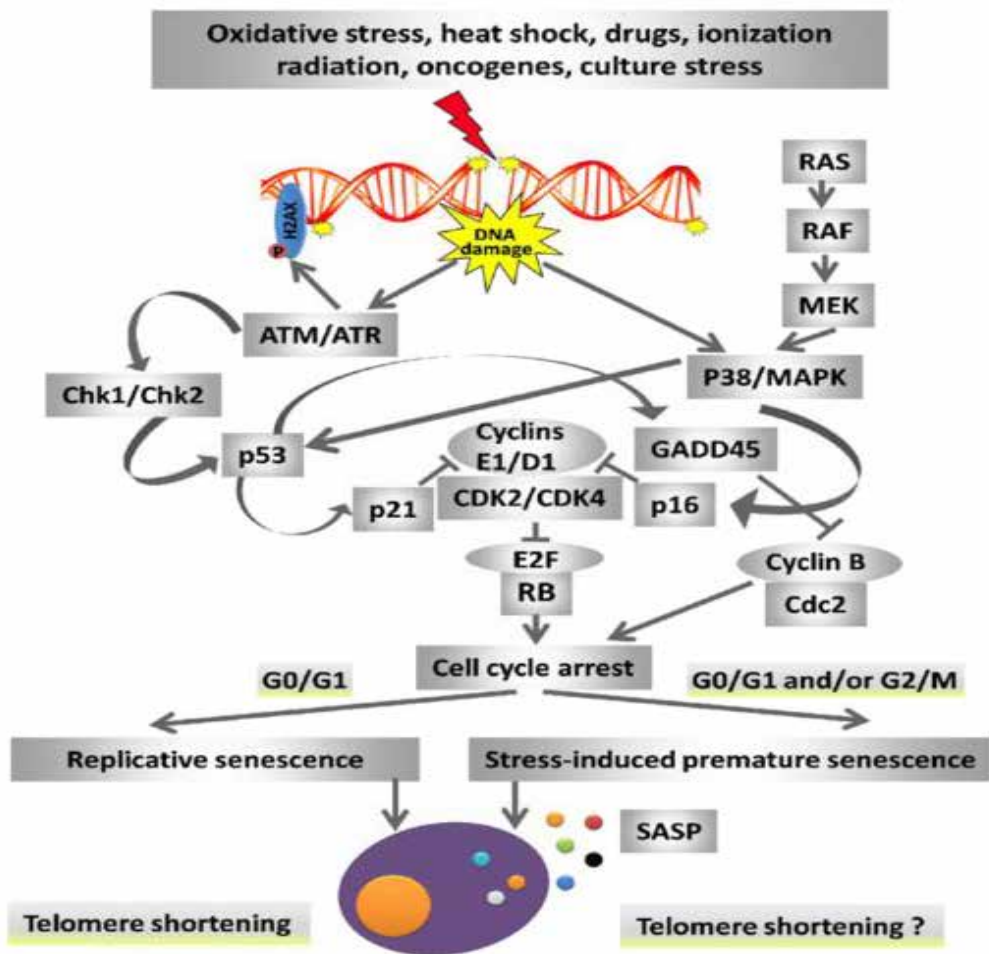


FIGURE 2.9

Major pathways of replicative and stress-induced senescence. Figure adapted from (155)

3 Radiotherapy

Radiotherapy, together with surgery and/or chemotherapy remains one of the cornerstones of cancer treatment. More than half of all cancer-patients are estimated to receive radiotherapy. Radiotherapy aims to long-term control of the tumor or has a palliative role.

3.1 Techniques used in radiotherapy

The two main methods used in radiotherapy are external beam radiation therapy or teletherapy, in which a beam of radiation is directed to the target tissue from outside the body, and brachytherapy, a technique where radioactive sources, such as ^{192}Ir or small ^{60}Co sources, are placed in a body cavity or placed directly in the tissue. For some tumors, such as cancer of the uterine cervix and the prostate, teletherapy and brachytherapy often are used sequentially or even concomitantly (167).

External beam radiation therapy can be delivered with several types of treatment modalities. Linear accelerators producing megavoltage X-rays are today's standard for radiotherapy. ^{60}Co γ -ray sources are mostly used in less developed countries, since they are not so dependent on power and infrastructure and have an exceptionally stable beam output. X-ray machines producing between 50 and 300kVp are used to treat superficial lesions. An increasing number of radiation therapy centers operate cyclotrons or synchrotrons that accelerate beams of protons or heavier charged particles to treat slowly growing, large hypoxic tumors (167).

Radiotherapy often starts with an imaging modality, CT (computed tomography) or MRI (magnetic resonance imaging) often in combination with PET (positron emission tomography) or SPECT (single-photon emission computed tomography) to define the volume of the tumor and the clinical target volume in relationship to the organs at risk. These images together with information about the tumor, lead to the treatment planning (167). Important in the treatment planning is sparing the healthy tissue, the organs at risk in particular, while giving a lethal dose to the clinical target volume. In conventional radiotherapy, the dose given to the healthy tissue is the real limiting factor. However an increase of 10% in dose deposited in the tumor typically gives an increased probability of about 20% of local control of the tumor itself (see figure 3.1) (168).

To deposit those large doses in the tumor while sparing the healthy tissue, different techniques are possible. High energy photon beams are more penetrating than traditional 50-300 kVp energy X-ray beams and have a skin sparing effect. More advanced techniques apply irregular fields using multileaf collimators. These intensity modulation radiation therapy (IMRT) techniques make use of 6 to 10 entrance ports and the intensity of the non-coplanar beams is varied across the ir-

radiation field by means of variable multileaf collimators that are computer controlled (see figure 3.2) (20, 169). Brachytherapy can provide better conservation of healthy tissue since the radiation source is placed within or adjacent to the target tissue and the radiation usually does not have to traverse healthy tissue to reach the target tissue (167). A better dose-deposition to the clinical target volume can be achieved by the use of charged particles. The Bragg peak assures a very precise dose deposition and by modulating the energy of the particles a spread out Bragg peak will be made to cover the complete volume of clinical interest and spare the surrounding tissue and organs (17).

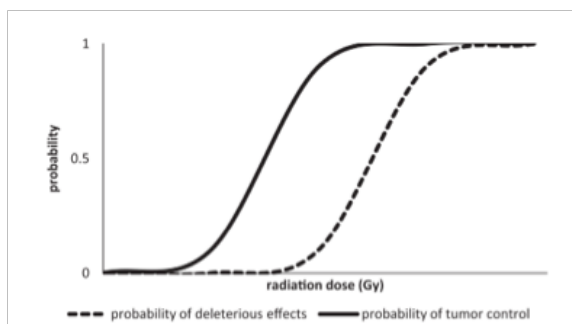


FIGURE 3.1

The probability of tumor control and deleterious effects in the healthy tissue, depends largely on the dose to which both tumor cells and healthy tissue are exposed. Figure from (168).

3.2 Biological fundamentals of radiotherapy

The total prescribed dose in radiotherapy is typically in the range of 40 to 60 Gy, administered in different fractions. The first radiation oncologists realized that giving a smaller daily dose over a period of weeks also resulted in good tumor control with less severe side effects compared to single high-dose treatments (170).

Loss of reproductive ability of the tumor cells caused by DNA DSB is the primary way by which radiation kills cells. Any cell that is incapable of reproducing is by definition considered dead, although it may still be metabolically active for some time. The response of tumors to radiation has therefore been largely characterized in terms of factors that influence the ability of radiation to damage DNA and affect a population of cells in tumors to recover from such damage. In 1975 Withers described the 4 R's, factors that are critical in determining the net effect of radiation therapy on tumors (171). In 1987 a fifth R was added (12, 170, 172, 173):

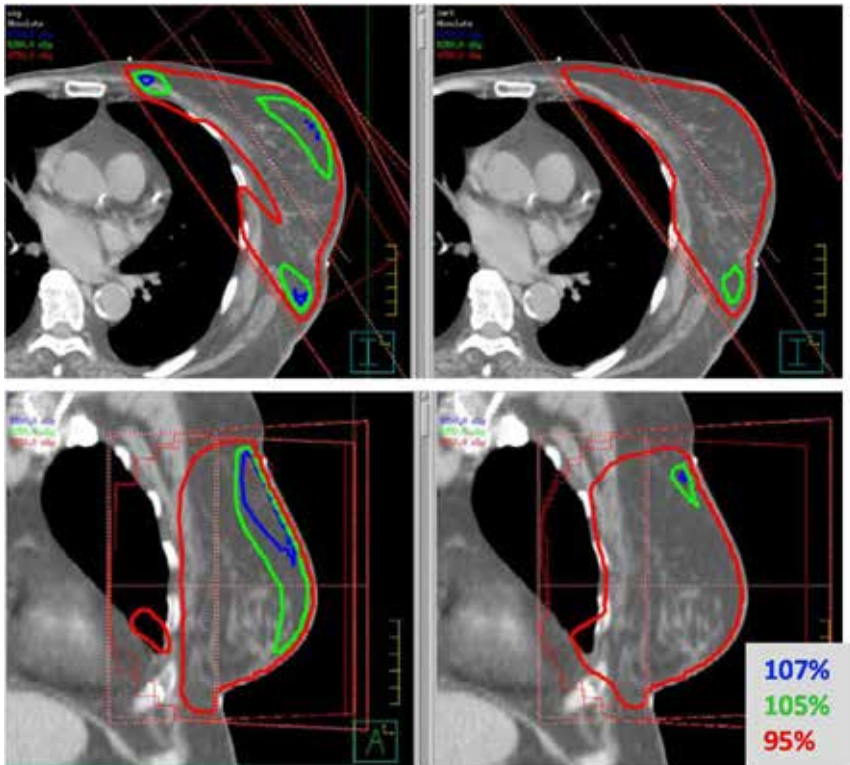


FIGURE 3.2

Dose deposition plan for radiotherapy for a total breast radiation, with at the top a transversal view and at the bottom a sagittal view. The pictures on the left show the dose deposition for conventional radiotherapy using wedges for a better dose homogeneity, the pictures on the right show the dose-deposition for IMRT. The better homogeneity of the dose-deposition using IMRT can immediately be noted. Pictures courtesy of Hurmans C. from the Catharina Hospital in Eindhoven, The Netherlands.

- **Repair.** During a few hours after exposure repair of sublethal cellular damage will occur and cells will recover. This is very important for the healthy tissue surrounding the tumor and happens in the time between the fractions.
- **Repopulation** of tumor cells after radiation. During the 4 to 6 weeks course of radiotherapy, tumor cells that survive the initial fractions may proliferate and thus increase the number of cells which must be killed. This is of course disadvantageous and is an argument against fractionation.

- **Redistribution** of cells within the cell cycle: The cellular sensitivity to radiation is strongly influenced by the position in the cell cycle, with cells in S-phase being the most resistant and cells in late G2 and M the most sensitive (174). Cells in stationary phase also tend to be more radioresistant than cells in active proliferation. The cycling cells that survive the first few fractions, are statistically more likely to be caught later in a sensitive phase and so be killed by a subsequent dose, a process termed cell-cycle re-sensitization.
- **Reoxygenation** of surviving cells. In a tumor, the hypoxic cells will selectively survive the first dose fractions. Thereafter, when their oxygen supply improves, their radiosensitivity will increase. While the process of reoxygenation is not completely understood, different factors seem to play a role.
 - Blood flow through vessels that were temporarily closed have recirculation again
 - In damaged cells respiration will be reduced which increases oxygen diffusion distance
 - Cell death leads to tumor shrinkage and a reduction in intercapillary distances, thus allowing oxygen to reach hypoxic cells.
- **Radiosensitivity** (intrinsic). There are big differences in radiosensitivity between different cell types, whether they are healthy or tumor cells.

Modern radiotherapy protocols are based on manipulating these effects so as to maximize tumor cell kill while avoiding normal tissue toxicities, particularly those arising in late-responding tissues. Treatments generally involve multiple fractions spaced over a period of time. In between the fractions, the healthy tissue will recover from the sublethal damage, while the tumor cells will be sensitized to the damaging effects of later fractions due to reoxygenation and redistribution of the cells over the cell cycle.

Currently the trend in radiotherapy is to use less fractions of a higher dose (hypofractionation). The precise dose-deposition in modern radiotherapy techniques safeguards the healthy tissue, while delivering a markedly higher and more lethal dose to the target volume. This effect seems to be enhanced by the vascular injury sustained by the endothelial cells supplying the cancer tissue with oxygen and nutrients and immunological and bystander effects (18, 172, 175, 176). Furthermore, hypofractionation offers advantages for the patient as well as economic advantages (18). Certain tumors are radioresistant to photons and protons, these are mainly slowly growing tumors for which phenomena as reoxygenation and redistribution are not an important radiosensitizing mechanism. For these tumors, high-LET types of radiation can be advantageous. There are huge differences in intrinsic radiosensitivity between cell types, and these differences are more pronounced for low-LET than high-LET radiation types. If tumor cells are more resistant to X-rays than the critical normal cells, high-LET radiation might reduce this difference in radiosensitivity

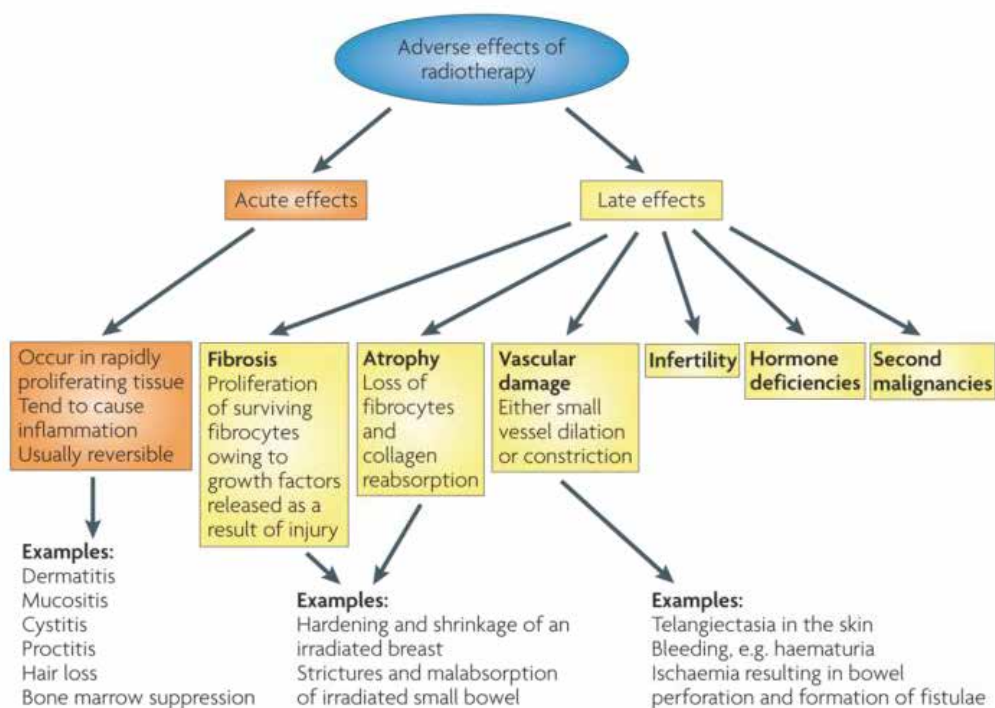
and thus sensitizes the tumor cell population relative to normal tissue. The high RBE of high-LET radiation qualities induces more complex damage, which will be harder to repair by the cells. The differences in radiosensitivity due to cell-cycle position are considerably reduced with high-LET radiation. Furthermore, as human tumors are generally characterized by the presence of hypoxic cell fractions, the role of oxygen in the radiation response of cells may have important implications towards the use of radiotherapy in cancer treatment. Direct ionizations, common for high-LET radiation types, are less sensitive to hypoxic conditions than indirect ionizations (see figure 1.4). Therefore, tumor sites in which hypoxia is a problem, for example some head and neck tumors and prostate cancer, might benefit from high-LET radiotherapy (11, 12, 18, 177-179).

3.3 Toxic effects following radiotherapy

While the dose-deposition in radiotherapy is hugely improved, the healthy tissue still receives a dose, mainly in the entrance and exit channels of the radiation beams, but also where malignant structures invaded the healthy tissue or normal tissues like blood vessels within the tumor. The DNA damage in these tissues can induce early and late toxic effects and lead to systemic disease and cancer (see figure 3.3) (180).

Early or acute toxic effects of radiotherapy occur during or shortly after the radiotherapy and are usually found in tissues with a high proliferative activity. Most acute symptoms, like dermatitis, mucositis and hair loss are the result of radiation-induced DNA damage which causes the cell to lose its ability to proliferate and leads to cell depletion (181). Other acute responses, such as erythema of the skin and increased intracranial pressure in the central nervous system are the effect of an inflammatory response (181). Healing of the inflammation, which is usually complete, is based on proliferation of surviving tissue stem cells within the irradiated volume or migration of stem cells from unirradiated tissue (12, 182).

Late or chronic toxic effects manifest themselves in approximately 5% of the patients, after a latent time of 6 months to many years and are, with a few exceptions, irreversible and progressive (184, 185). Chronic tissue damage is a dose-limiting factor in the treatment of some tumor types and as an increasing number of people are cancer survivors and life expectancy rises, the prevention or reduction of late side effects has become an important issue (186). Late toxic effects present themselves in tissues with a slow turnover. Late toxic effects are an orchestrated, active biological response induced by the early release of cytokines and has the features of wound healing (181, 187). This response is mediated by various cell types, including inflammatory, stromal, endothelial and parenchymal cells actively responding through the release or activation of

**FIGURE 3.3**

Overview of the adverse effects of radiotherapy. Figure from (183).

downstream cytokines and growth factors. The main pathogenic effects occur in the parenchyma of the organs, in the connective tissue and vascular endothelial cells (181). The immune system regularly contributes to the chronic reactions. Chronic toxic effects include e.g. radiation-induced fibrosis, atrophy, vascular damage, neural damage and a range of endocrine and growth-related effects (12, 182, 183). The development of a second primary cancer is also considered a late effect of radiotherapy, with a latency period of 5 years for leukemia and up to 10 years for solid tumors (188, 189). Other factors such as lifestyle (smoking, diet), immune function, hormonal status, genetic variation and concomitant therapy-related elements (e.g. chemotherapy), will also play a role in the development of a second primary cancer. However, the relative risk of developing a second cancer that is associated with specific treatments generally exceeds the risk that is associated with lifestyle factors, including those that might have contributed to the development of the first cancer (188).

4 Breast cancer

4.1 Incidence and mortality (all numbers taken from Globocan (190))

4.1.1 Cancer in general

Cancer is a major illness worldwide. Incidence rates per year worldwide are about 205 and 165 per 100.000 individuals for men and women respectively. There are big differences in incidence across the world, with male incidence rates ranging from 79 per 100.000 in Western Africa to 365 per 100.000 in Australia and New-Zealand, where the high rates of prostate cancer are a significant driver. Female incidence rates have less variation, ranging from 103 per 100.000 in South-Central Asia to 295 per 100.000 in Northern America. There is less regional variability in mortality, with the highest mortality for men in Central and Eastern Europe (173 per 100.000) and the lowest in Western Africa (69 per 100.000). For women the highest mortality rates are in Eastern Africa (111 per 100.000) while the lowest rates are in Central America and South-Central Asia (72 and 65 per 100.000) (see figure 4.1).

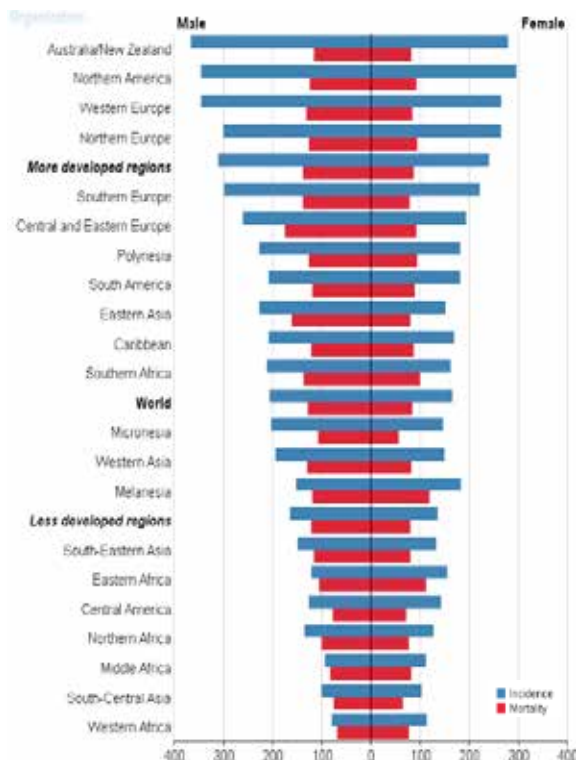


FIGURE 4.1

Overview of cancer incidence and mortality rates throughout the world in 2012. (Figure from (190)).

Worldwide the most prevalent cancer in men is lung cancer (34 per 100.000), closely followed by prostate cancer (30 per 100.000). However, in more developed regions prostate cancer has the highest incidence. The cancer with the highest mortality in men is lung cancer (30 per 100.000). In women breast cancer has the highest incidence rate (43 per 100.000), followed by colorectal, cervix and lung cancer (all three 14 per 100.000). Breast cancer has the highest mortality rate in women (13 per 100.000) worldwide, closely followed by lung cancer (11 per 100.000). Again there are big differences worldwide, however breast, lung, cervix and colorectal cancer are the four cancers with the highest incidence around the world and breast cancer and lung cancer have the highest mortality rates (see figure 4.2).

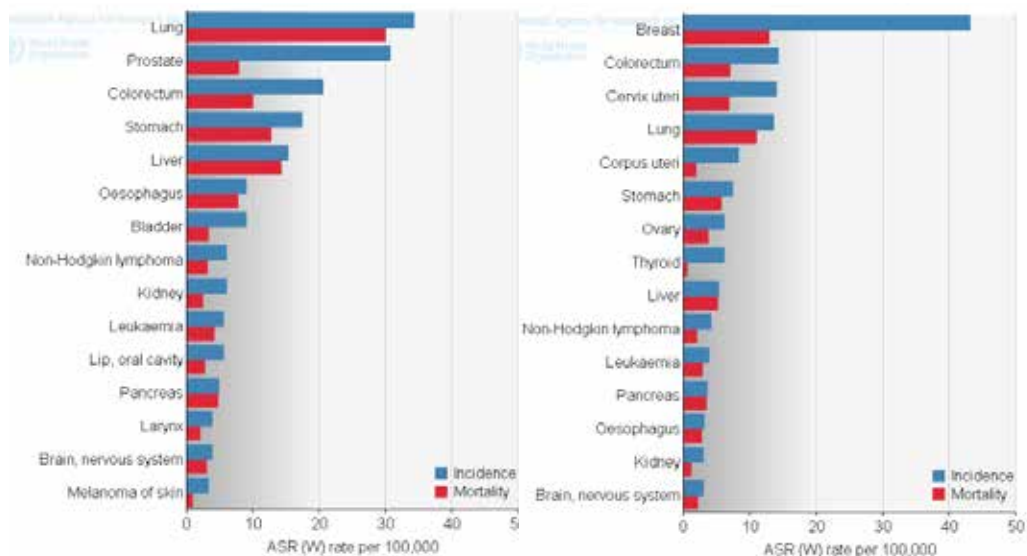


FIGURE 4.2

Incidence and mortality rates of the most prevalent cancers in men (left) and women (right) in 2012. (figure from (190))

4.1.2 Breast cancer

Breast cancer is by far the most common cancer among women, with an estimated 1.67 million new cancer cases diagnosed in 2012. About 25% of all cancers diagnosed in 2012 in women were breast cancers. In more developed regions, incidence rates are highest and range between 85 and 95 per 100.000. In less developed regions the incidence rates are lower and range around 27 per 100.000. Since the late 1980s and early 1990s in developed countries an increase in incidence of breast cancer is observed (191-193).

Over the past 25 years, breast cancer mortality has decreased in North America and several European countries. The more favorable survival of breast cancer in the high-incidence well developed regions of the world, causes the range in mortality rate to be lower across the world, with rates ranging from 6 in Eastern Asia to 20 per 100.000 in Western Africa. The differences in incidence and mortality across the world lead to a survival of about 80% in more developed regions and 40% in less developed regions (191-193).

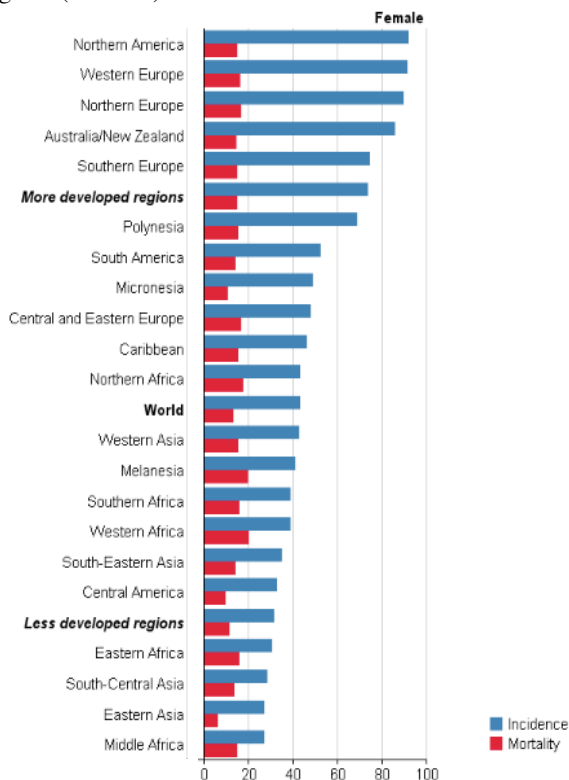


FIGURE 4.3

Incidence and mortality rates of breast cancer throughout the world in 2012. Figure from (190).

4.2 Breast cancer risk factors

4.2.1 Hormones

Exposure to estrogen increases the breast cancer risk, therefore any factor that increases the exposure to these hormones is a potential risk factor.

Reproductive factors associated with increased exposure to endogenous estrogens produced by the ovaries, such as early menarche, late menopause, low parity and late age at first birth are recognized breast cancer risk factors (194-196). Similarly, women exposed to exogenous estrogen, for example through menopausal hormone therapy or oral contraceptives are often at increased risk. New guidelines pointing to the danger of menopausal hormone therapy and the of hormone levels in oral contraceptives led to a decrease in use of exogenous estrogen (197-201).

4.2.2 Lifestyle factors

Lifestyle factors are associated with breast cancer. There is an estimated 10% increased risk per unit of alcohol consumed per day (202) (1 unit equals 10g or 12.5 ml of pure alcohol). Overweight is also associated with breast cancer, but only in postmenopausal women, with a gain of 5kg/m² in body mass index resulting in an 8% increase in risk (202). On the contrary, excess weight is associated with a decrease in risk in premenopausal women. These associations can be explained by hormonal factors: alcohol consumption and postmenopausal obesity are related to higher circulating estrogen levels (203).

Notice that the geographical pattern seen in breast cancer incidence and mortality can largely be explained by reproductive and hormonal factors influencing incidence and by the accessibility to early detection and treatment influencing both incidence related to over-diagnosis and mortality.

4.2.3 Breast density

Breast density reflects the proportion of fibroglandular tissue in the breast as opposed to nondense fatty tissue. High breast density has been shown to be an independent risk factor for increased breast cancer risk and benign breast disease. Comparison of the lowest and the highest breast densities, shows a 4-fold increase in breast cancer risk for the highest breast densities (204-208).

4.2.4 Radiation

Breast exposure to ionizing radiation is associated with an increased risk of breast cancer. Direct evidence comes from studies investigating cancer incidence in the atomic bomb survivors of Hiroshima and Nagasaki and from follow-up studies of patients treated with radiotherapy for hematological malignancies or patients who were intensively monitored by X-ray fluoroscopy e.g. for scoliosis or tuberculosis (23-25, 207, 209-214).

These studies have also shown that some factors described as risk factors for developing breast cancer, also seem to enhance the radiation-induced breast cancer risk: age at irradiation and attained age, age of menarche or the time of first pregnancy, nulliparity, obesity, family history of breast cancer, benign breast disease and genetic factors (215-219). However, most of these factors should be interpreted cautiously as they modify the radiation risk only marginally and reproduction of the results seems challenging (219, 220). Carriers of genetic mutations, like *BRCA1*, *BRCA2* or *ATM*, are suspected to have a higher risk for radiation-induced breast cancer. The evidence for enhanced risk is strongest for *ATM*, but results are still inconclusive (219, 221-223). Age at exposure and attained age seem to have the highest modifying effect on radiation-induced breast-cancer risk. Compared to exposure of young adults (30-40 years) the risk in children appears to be three fold in the atomic bomb lifespan population (23-25). After exposure at young age the risk continues to be elevated throughout the remainder of a woman's life, with the largest excess rates occurring at ages similar to those at which breast cancers are seen in absence of exposure (224). Also dose-time information of the exposure (total dose, dose rate, fractionation, dose per fraction) and radiation quality can modify the risk.

4.2.5 Genetic background

The strongest risk factor for breast cancer development is family history. Up to 15% of the patients diagnosed with invasive breast cancer have at least one first-degree female relative with the disease (225). Individual risk increases with increasing number of relatives affected by breast or ovarian cancer and with decreasing age at which it was diagnosed (225). Twin studies estimate that around 27% of breast cancers are caused by hereditary factors (226, 227). However, only 5 to 10% of breast cancers have a strong inherited component with only 5% being due to high penetrance genes transmitted in an autosomal dominant fashion (228-231). The two most important high penetrance genes are *BRCA1* and *BRCA2* (Breast Cancer susceptibility gene 1 and Breast Cancer susceptibility gene 2). Additional high penetrant genes are *PTEN*, *TP53*, *CDH1* and *STK11* but they are very rare (232, 233). Furthermore, moderate penetrance genes like *ATM*, *CHEK2*, *BRIP1* and *PALB2* (234-237) and low penetrance genes (238) have been identified (see figure 4.4). *BRCA1* was the first high penetrance gene to be discovered in 1990 (228). Pathogenic mutations in

BRCA1 confer a lifetime risk of breast cancer between 60% and 85%, with increased relative risks at younger ages. Type and position of the mutation, genetic modifiers and environmental effects explain the interindividual differences (240, 241). Furthermore, *BRCA1* mutation carriers have an increased risk of ovarian cancer between 40 and 60% (242-247) and may have an increased risk of pancreatic malignancy (248). *BRCA1* mutation carriers are affected by breast or ovarian cancer at substantially younger age and have a breast cancer risk of approximately 3% by the age of 30 (244).

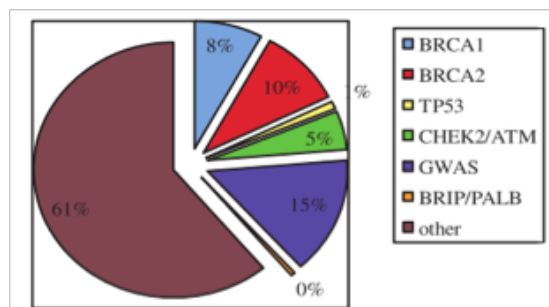


FIGURE 4.4

Proportion of the familial component of breast cancer caused by known genes and low-risk alleles. Figure from (239).

BRCA1 is a large gene with 24 exons located on 17q2.1 and codes for a 220 kiloDalton (kDa) protein. Mutations are found throughout the coding sequence of the gene, with the majority being frameshift mutations resulting in truncated proteins (249). A few founder mutations have been identified, the best known are in the Ashkenazi Jewish population, with 1.2% of the individuals carrying one of the two *BRCA1*-founder mutations (250, 251).

BRCA1 has diverse roles in multiple DNA repair pathways and in checkpoint regulation. It interacts with tumor suppressors, DNA repair proteins and cell cycle regulators through its various functional domains (252, 253). *BRCA1* is directly involved in the very early stages of the HR DNA repair pathway where it binds to the DSB through its association with the abraxas-RAP80 complex. In a next step, it is involved in CtIP-mediated 5' resection of the DSB through its interaction with CtIP and the MRN complex. *BRCA1* also interacts with PALB2 and *BRCA2*, which in turn will attract RAD51 to the DSB (254-257) (see figure 4.5). The role of *BRCA1* in NHEJ and single strand annealing (SSA) is less clear and still under discussion. It is proposed that *BRCA1* removes the NHEJ proteins from the DSB to regulate the choice between HR and NHEJ. *BRCA1*

activates G1/S, S-phase and G2/M checkpoints through complexation with BARD1 (258). The G1/S checkpoint activation goes via phosphorylation of BRCA1 by ATM or ATR and subsequent phosphorylation of p53. The exact mechanism of the BRCA1-BARD1 control of the S-phase and G2/M checkpoint is still not well understood (259-261).

BRCA2, discovered in 1994 (262), is a second high penetrance gene and pathogenic mutations confer a lifetime breast cancer risk between 40 to 85% (243-247, 263-265). There is more variability of risk associated with mutation in *BRCA2*, suggesting that the gene is more modifiable than *BRCA1* (239). The risk of ovarian cancer in *BRCA2* mutation carriers is between 20 and 30% (242-244, 263). Furthermore, women with a pathogenic mutation have an increased risk of cholangiocarcinoma, melanoma, pancreatic and gastric cancers (266). Male carriers of *BRCA2* have a lifetime risk of prostate cancer of 14-20% along with a 10% lifetime risk of male breast cancer (267).

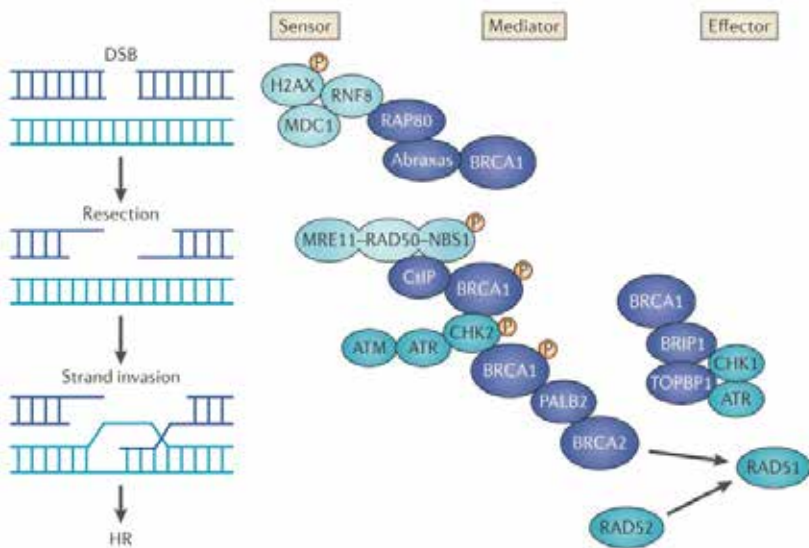


FIGURE 4.5

Overview of the most important functions of BRCA1 and BRCA2 in the DDR pathway. Figure from (268).

BRCA2 is a very large gene with 27 exons, located on 13q12.3 and coding for a 380kDa protein. Mutations occur throughout the gene, as with *BRCA1* the majority being frameshifts. Again a founder mutation in the Ashkenazi Jewish population has been found, with 15% of the population carrying the mutation (250, 251). Homozygous mutations in *BRCA2* have been shown to cause Fanconi Anaemia (*FANCD1*) (269), an autosomal recessive disorder, which is characterized by progressive bone marrow failure, congenital developmental abnormalities and early onset of acute myelogenous leukemia and squamous cell carcinomas of head and neck region (270).

BRCA2 also plays an important function in DSB repair, although the role of *BRCA2* is less broad compared to *BRCA1*. *BRCA2* is recruited to the DSB through interaction via the *BRCA1*-*PALB2* complex and has its main function in facilitating HR through recruitment of *RAD51* to the DSB. It is crucial in HR as it regulates both the strand invasion and the appropriate stabilization/disassembly of the oligomerized *Rad51* (271, 272) (see figure 4.5).

4.3 Detection and screening of breast cancer (see table 4.1)

Detection and treatment of breast cancer in an early stage gives a better prognosis, a better quality of life and a reduction in mortality (273, 274).

Mammography (see figure 4.6 (a)) is the most common detection method for breast cancer. With low energy X-rays, generally 28kVp, the breast tissue is imaged. In standard practice, a cranio-caudal and a mediolateral oblique projections are taken, resulting in breast glandular doses of typically 3-5 mGy per two-view mammography (42, 275-277). The images are analyzed for masses, asymmetries, distortions and micro-calcifications and are compared with previous mammographies for changes which are potentially suspicious. Lesions smaller than 1 cm and not yet palpable can be found with mammography. In many countries, breast cancer screening programs based on periodic mammography exist for women aged between 50 (or 40) and 70 (or 75) years (278). These screening programs have shown to reduce breast cancer mortality (279). However, there are

some limitations to mammography. The sensitivity of mammography is highly variable, ranging from 90% in women with fatty breast parenchyma to 36% in women with dense breasts (280, 281). This can result in false positive screening results and 1.5 to 7% of the women participating in European screening programs are called back for further imaging work-up such as supplementary mammographic views or ultrasound. Of the recalled women, about 20% will receive a biopsy (274, 282-284). Furthermore there is also the concern about the use of ionizing radiation and associated breast dose, which always implies a risk for radiation-induced breast cancer. Although the dose is small, this cannot be neglected in view of the large population size and the repetitive character involved in this type of asymptomatic screening.

The evolution from film-mammography to full field digital mammography already lowered the dose by approximately 22% (276) and further dose reduction can be expected with technological advancements like photon counting (285, 286). Digital breast tomosynthesis is another technical advancement of mammography, where the combination of different mammographic images taken from different angles are combined into a 3D image. Tomosynthesis is designed to overcome the problems of overlapping tissue, and has a higher specificity. However, sensitivity for micro-calcifications is slightly reduced and the dose received is approximately 50% higher than for a conventional mammogram (287, 288).

Ultrasound (see figure 4.6 (c)) is widely available, inexpensive, requires no contrast injection, does not use ionizing radiation and is well tolerated by patients. Hand-held scanning is evolving in two-dimensional automated whole breast ultrasound systems, which aim to standardize the screening examination and produce a consistently high quality examination. Ultrasound in breast cancer screening is sensitive but has a low specificity and is mostly used as an adjunct for mammography or MRI when mammography alone does not give a decisive answer e.g. in patients with high breast density (289, 290).

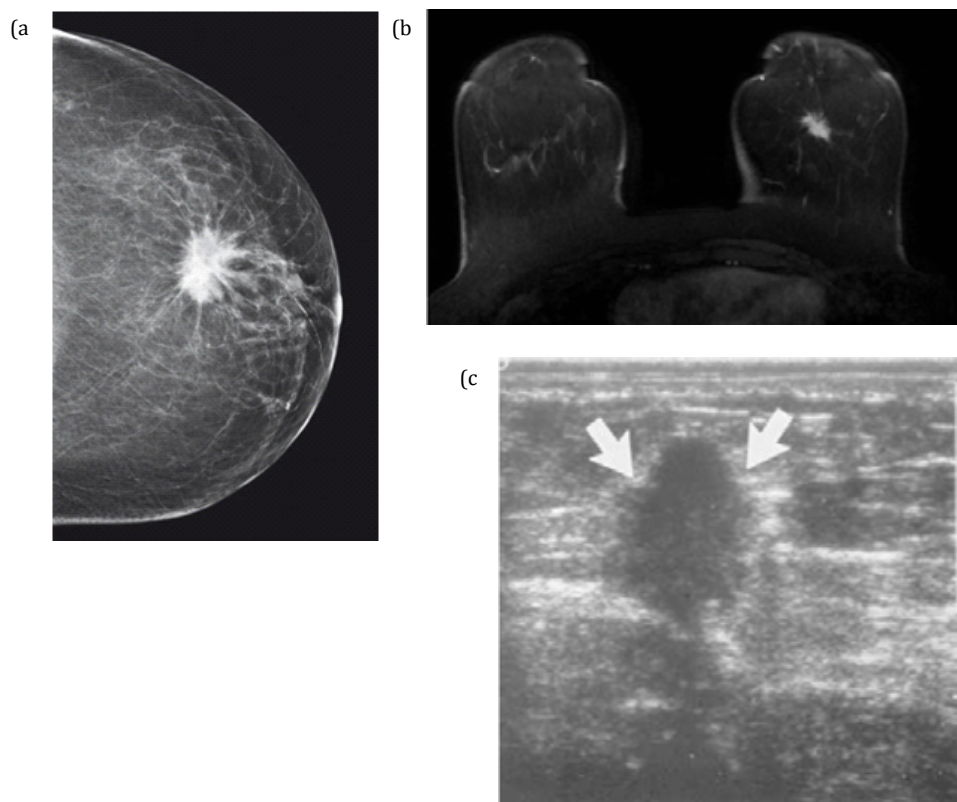


FIGURE 4.6

(a) Mammogram showing an malignant breast tumor. (b) MRI of the breasts. An invasive ductal breast carcinoma is seen in the left breast. (c) Ultrasound of the breast with a mass suspicious for malignancy.

Magnetic Resonance Imaging (MRI) (see figure 4.6 (b)) has superior sensitivity to mammography and ultrasound in the detection of invasive cancer, however it is often criticized for decreased specificity. The sensitivity of MRI can be further increased by the use of contrast MRI, which gives an image of the blood flow. MRI is recommended as an adjunct to mammography in selected patients at high risk for developing breast cancer e.g. patients with a *BRCA1* or *BRCA2* mutation and is also used for evaluating inconclusive mammograms and ultrasounds images and evaluating the response on chemotherapy (291, 292).

Modality	Strengths	Limitations	Screening
Mammography	the standard	variable sensitivity ↑ false positives	yes
photon counting low-dose mammography	approx 40% ↓ in dose	Limited literature	yes
Tomosynthesis	↑ specificity	↑ radiation dose	adjunct
AWBUS	↑ sensitivity	↓ specificity ↑ false positives	adjunct
MRI	↑ sensitivity	↓ specificity ↑ false positives ↑ cost	adjunct

TABLE 4.1

Strengths and limitations of breast imaging modalities.

AWBUS: automated whole breast ultrasound system

MRI: magnetic resonance imaging

Table adapted from (288).

4.4 Pathology

The breasts mammary glands are highly modified apocrine sweat gland. At puberty the female breasts develop under the influence of estrogen and progesterone secreted by the pituitary gland and ovaries. During the first pregnancy, a significant increase in mammary glands is noted, mainly under the influence of estrogen and progesterone, but also prolactin, growth hormone, insulin and adrenal hormones have an influence. After the first pregnancy, the mammary glands are fully developed. Until the menopause, the breasts undergo cyclical changes in activity which is controlled by the hormones of the ovarian cycle. After menopause, the breasts, like the other female reproductive tissues, undergo progressive atrophy and involution (293).

Breast tissue consists mainly of adipose and fibroglandular tissue. The fibroglandular tissue of a breast consists of 15 to 25 independent glandular units called breast lobes. The lobes are separated from each other by moderately dense collagenous septa and are embedded in adipose tissue. Each lobe is drained by a single large duct, the lactiferous duct, which forms a dilatation called the lactiferous sinus just before opening on the surface of the nipple. Within each lobe of the breast, the main duct branches repeatedly to form a number of terminal ducts, each of which leads to a lobule consisting of multiple acini. Each terminal duct and its associated lobule is called a terminal duct-lobular unit. Each terminal duct-lobular unit is surrounded by dense collagenous connective tissue and fat (293) (see figure 4.7).

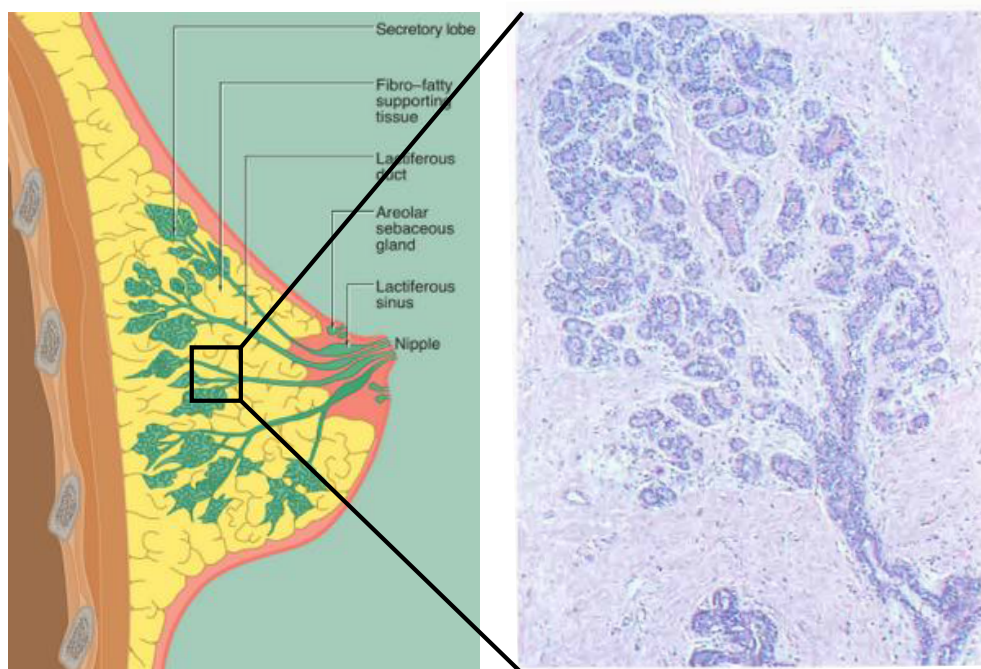


FIGURE 4.7

Normal breast tissue with a terminal duct giving rise to a lobule consisting of multiple acini. Terminal duct together with the lobule form a terminal duct lobular unit (TDLU). The terminal duct lobular unit is surrounded by dense collagenous connective tissue (pink) and fat (white). Picture from (293).

Breast cancer is a heterogeneous disease. Carcinoma in situ of the breast is a pre-cancerous or non-invasive cancerous lesion of the breast and it rarely produces symptoms. Ductal carcinoma in situ (DCIS) is usually detected through screening mammography, while lobular carcinoma in situ is not associated with calcification and is typically an accidental finding in a biopsy performed for another reason (294, 295). DCIS is a non-obligate precursor of invasive breast cancer, and up to 40% of these lesions progress to invasive disease if untreated. Currently it is not possible to predict accurately which DCIS are more likely to progress to invasive carcinoma (296).

Invasive ductal carcinoma (IDC) is by far the most common type of breast cancer, representing 80% of the invasive breast cancer cases, followed by invasive lobular carcinoma (ILC), accounting for 10% of the breast cancers (297, 298). Apart from the different etiology, IDC and ILC are marked by other differences. Patients with ILC are generally 3 years older, and diagnosed in a more advanced stage with tumors which are generally progesterone and estrogen receptor negative (299). ILC seems to be more strongly associated with exposure to female hormones than IDC and as a result it's incidence has varied more than that of IDC depending on environmental and lifestyle factors such as menopausal hormone therapy (300). Genetically, IDC is overrepresented by patients carrying mutations in *BRCA1* and *TP53* (297, 301), while ILC is associated with a mutation in *CDH1*, the diffuse gastric cancer susceptibility gene (300, 302).

Breast tumors are classified according to the histological appearance of the cancer cells. As cancer progresses, the cancer cells lose their differentiation and this is used to grade breast cancer. Three parameters are used to grade breast cancers: mitotic activity, tubule/gland formation and nuclear pleomorphism. Well differentiated cells (low grade) have a better prognosis than poorly differentiated cells (high grade) (303).

TNM-staging is also applied on breast tumors and is based on the size of the tumor (T), whether or not the tumor has spread to the lymph nodes (N) and whether the tumor has metastasized (M). Larger tumor size, nodal spread and metastasis have a higher stage number and a worse prognosis. DCIS and LCIS have a stage 0, while stage 4 cancers are metastatic cancers (303, 304).

4.5 Breast cancer treatment

Treatment of breast cancer generally starts with the surgical removal of the tumor and surrounding tissue. Depending of the size of the tumor, a small part (breast conserving surgery) or the whole breast (mastectomy) can be removed. During the surgery one or more lymph nodes are sampled by sentinel lymph node biopsy to check for invasion of breast cancer cells to the regional lymph nodes.

Radiotherapy is often given after surgery to the region of the tumor bed and the regional lymph nodes (adjuvant radiotherapy). The irradiated volume can be the whole breast or part of the breast surrounding the tumor volume. The majority of breast cancer recurrences occur near the primary tumor site (305-308) and partial breast irradiation has the advantage that it minimizes the dose to the healthy tissue, reducing late effects and it spares the adjacent organs including heart, lungs and ribs (309, 310). IMRT is standard practice, although a good dose-distribution can also be obtained with high energy X-rays in tangential fields and with techniques as irradiation in prone position. Hypofractionated irradiation schemes are now standard, of which the two most important ones are 42.5 Gy in 16 fractions (Canadian Trial) and 39Gy in 13 fractions (START A), possibly followed by a boost to the tumor site of 10 or 16 Gy (311, 312).

Brachytherapy is also used for the treatment of breast cancer. Dose deposition is good, with almost complete sparing of the surrounding tissue. However, with interstitial brachytherapy, fat necrosis and scarring can occur due to the invasive nature of the procedure, while with intercavitary brachytherapy dose homogeneity is difficult when the surgical cavity is irregular and superficial cavities can lead to higher skin doses and increased toxicity. With ^{192}Ir a dose of 34Gy is given in two daily fractions for a period of 5 days.

The role of radiotherapy in decreasing the risk of recurrence and breast cancer death is well established (313-315). Adjuvant radiotherapy given after breast conserving surgery halves the rate of recurrence in the long term and reduces breast cancer related death by one-sixth (316). Additional nodal irradiation in women with node positive breast cancer further reduces the risk of recurrence and increases the overall survival (317).

Adverse side-effects of radiotherapy in breast cancer patients are well described. During or shortly after the course of breast cancer radiotherapy a large portion of the patients will experience radiation dermatitis to a certain degree, leading to poor cosmetic outcomes (318-320). The pathology of late normal tissue reactions in breast cancer patients comprises processes such as pigmentation changes, atrophy, fibrosis and vascular damage (181). Factors associated with an increased risk of late toxic side effects in breast cancer patients can be separated in two general categories. First, radiation therapy related risk factors including the total dose and additional boost, the irradiated volume, the fractionation regimen and the total treatment time (321, 322). Secondly, patient and therapy-related factors may influence the risk and severity of late normal tissue toxicity after breast cancer treatment. Especially breast size increases the risk, but also age, concomitant chemotherapy or hormonal treatment, trauma or surgery in the irradiated site, co-morbidities involving impaired vascularity such as diabetes and hypertension (181, 320, 323).

The induction of second primary cancers (SPC) by radiotherapy for breast cancer treatment is dependent on the same factors as the general late toxic effects. The most common sites of SPC are breast, bone, ovary, lung, thyroid and leukemia (324). Also the development of radiation-induced heart disease has been described after breast cancer irradiation (325). Proton therapy can efficiently spare the heart during the treatment of left-side breast-cancer (326), whereas with X-rays, a large fraction of the heart is generally exposed. Breast cancer is therefore becoming a major application of protontherapy (18, 327-329)

Adjuvant chemotherapy or hormone therapy can be given before or after surgery and in combination with radiotherapy. Which adjuvant therapy will be used is highly dependent on the receptor status of the tumor. Tumors can express receptors for estrogen (ER+), progesterone (PR+) and human epidermal growth factor 2 (HER2+), which can be used for treatment purposes. ER+ and PR+ tumors require estrogen to continue growing, and can be treated(330) by hormone blocking therapy, like tamoxifen, which block the receptors or e.g. aromatase inhibitors which block the production of estrogen (331). Trastuzumab, an anti-HER2 monoclonal antibody is used against HER2+ tumors. Trastuzumab will block the HER2-receptors and prevent growth factors to bind to the receptors and stimulate the cells (332). Triple negative tumors, which have the worst prognosis, are treated with chemotherapy, which destroys fast-growing and/or fast-replicating cells and may cause serious side effects. Often a combination of multiple chemotherapeutic agents are used, depending on different factors such as the stage of the tumor and the health and age of the patient. A standard chemotherapy regimen can e.g. be cytoxan, methotrexate and fluorouracil given 4-weekly for 6 cycles (330).

5 Assays to measure the effect of radiation

Radiation-induced damage can be measured in different ways. Depending on the technique used, the initial DNA damage, the repair kinetics or the cellular outcome can be determined. Throughout this thesis, a number of tests were used: the γ H2AX foci assay, the micronucleus assay, the apoptosis assay and the crystal violet cell proliferation assay.

5.1 The γ H2AX foci assay

The quantification of DNA DSB induction and repair was done in the past with pulsed field gel electrophoresis (PFGE).

More recently the quantification of γ H2AX-foci as a measure for the number of DNA DSB has come into focus (333). The phosphorylation of the histone variant H2AX at the site of the DSB (see chapter 2.1 and figure 5.1), leads to the formation of γ H2AX foci around the break and a quantitative one on one relation between foci and the number of radiation-induced DSB has been found for low-LET radiation, in particular γ -radiation for doses under 1Gy (334). Within minutes after irradiation these foci can be visualized with immunostaining and a maximum is reached 15 to 30 min after exposure (335-338).

The γ H2AX foci assay allows to detect very low doses of a few mGy (10). Furthermore, by analyzing the number of foci at different time-intervals after irradiation, the kinetics of disappearance of the foci and as such the repair of the breaks can be followed. Persistence of repair foci at 24h, 48h or even longer after irradiation can be used as a measure of the repair capacity of the cell. Also foci of other proteins involved in the DDR, such as ATM and 53BP1 show a close correlation to DSB induction and repair and can be visualized with immunostaining (69, 339). To enhance to reliability of the foci-technique and exclude background-foci, a double staining can be done for two DSB-foci proteins, such as γ H2AX and 53BP1 to assess how they co-localize (see figure 5.2) (340).

γ H2AX foci induction will follow a linear dose-response curve, higher doses can however lead to saturation and can cause a flattening of the curve.

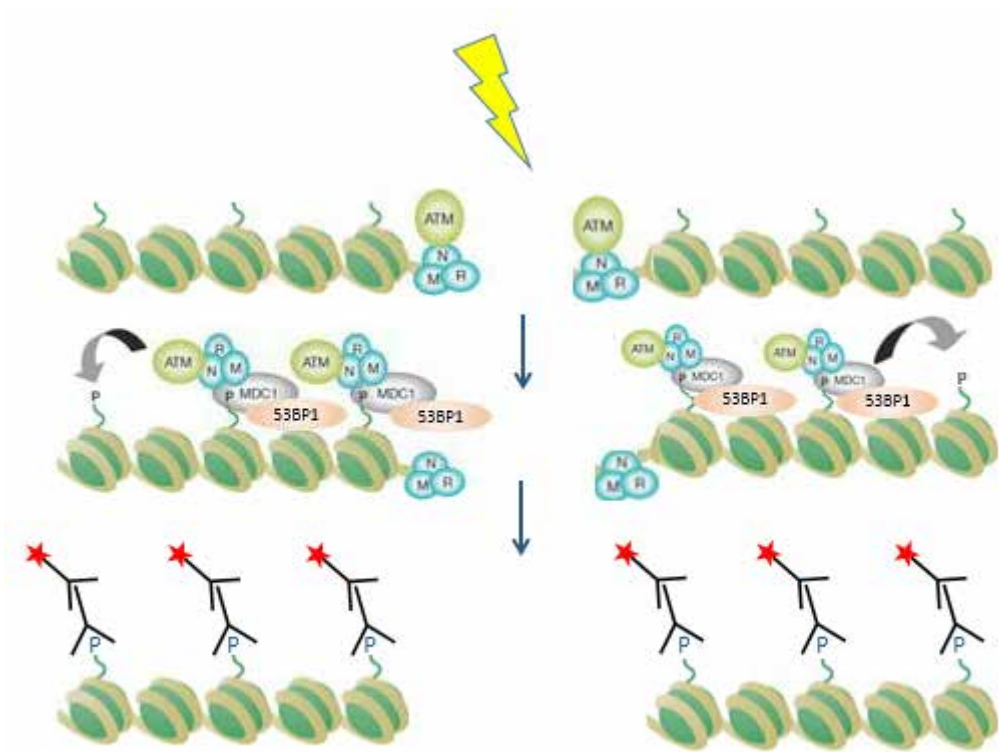


FIGURE 5.1

Schematic overview of the γ H2AX and other repair foci- assay. Ionizing radiation causes a DSB, which triggers the activation of the DNA damage response. The cascade of events results in the phosphorylation of histone variant H2AX in the region around the break (see section 2.1 DNA damage response for more details). γ H2AX, but also e.g. ATM and 53BP1, can be visualized with immunostaining. Figure adapted from [341].

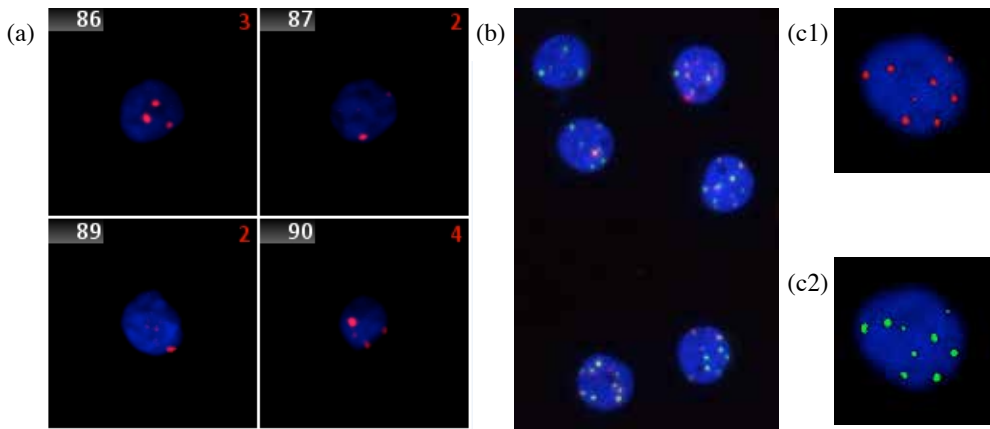


FIGURE 5.2

Repair foci staining. Picture a shows a γ H2AX staining in the nuclei of irradiated lymphocytes. Picture b depicts a γ H2AX and 53BP1 double staining. Picture c shows the same cell stained with a γ H2AX and 53BP1 double staining, the pictures are taken in different fluorescent channels. c1 shows the γ H2AX staining in the TRITC channel, c2 shows the 53BP1 in the FITC channel. Remark the colocalization of both proteins. Figures from our lab.

5.2 The micronucleus assay

By means of cytogenetic analysis, chromosomal aberrations, which are the result of un- or mis-repaired DSB, are scored. Chromosomal aberrations are good biomarkers to assess radiation exposure and radiosensitivity. Examples of cytogenetic techniques used in radiobiology are the dicentric assay, chromosome painting to score stable translocations and the MN assay (cytokinesis-block micronucleus assay).

The MN assay, which is used in this thesis, is based on the analysis of small extranuclear bodies which contain mainly acentric chromosome fragments in binucleated cells. In short, in this assay cells are irradiated and after irradiation cytochalasin B is added to the cell cultures to inhibit cellular division. Mitosis will proceed, but the radiation-induced acentric chromosome fragments, resulting from un- or misrepaired DSB, will not be included in the daughter cells, as the fragments lack a centromere and cannot attach to the spindle fibers. After mitosis a nuclear envelope will form around the new nuclei and around the fragments, which are then called micronuclei (342-344) (figure 5.3 and 5.4).

Radiation-induced MN contain mostly acentric fragment. However, MN can also arise spontaneously and those MN mostly contain whole chromosomes. A high interindividual variation in the number of spontaneous MN will make the assay less sensitive in the low dose range, resulting in a detection limit of approximately 0.2 Gy. A Fluorescent in situ hybridization (FISH) pan-centromere staining can be used to distinguish to a large extent between the radiation-induced and the spontaneous MN (345, 346) and makes the assay more sensitive by lowering the detection limit to 0.05-0.1 Gy (figure 5.4).

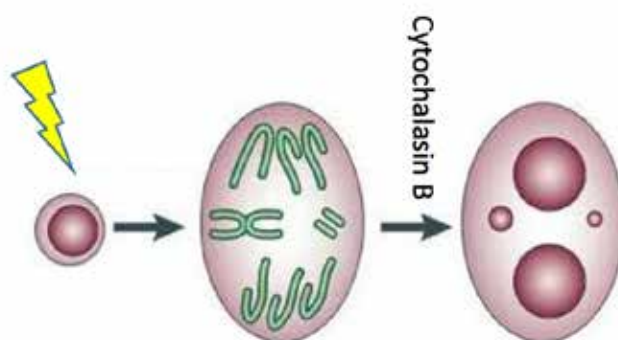


FIGURE 5.3

Schematic overview of the MN assay. Irradiation of the cell will induce chromosomal damage. Both the acentric fragment and the lagging chromosome will lead to the formation of a MN. Cytochalasin B is added to inhibit cellular division. Figure adapted from [343].

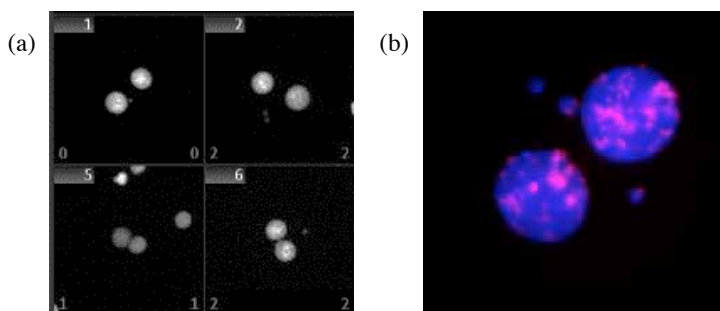


FIGURE 5.4

MN assay on lymphocytes. In picture (a) the cells and MN are stained with DAPI (4',6-diamidino-2-Phenylindole; a nuclear stain). In picture (b), a FISH pan-centromere staining is additionally performed. One MN is centromere-negative and contains an acentric fragment (MN top left), the other two MN have a positive centromere-signal implying they contain whole chromosomes. Figure from our lab.

The MN assay can be done on all cell types that can be stimulated to divide and irradiated cultures will normally contain a mixture of cells in all phases of the cell cycle. Human peripheral blood lymphocytes are often used in the MN-assay for biological dosimetry or in patient studies. Lymphocytes are resting cells in G0 phase of the cell cycle. If the lymphocytes are not stimulated to divide before irradiation but only afterwards, all cells will be irradiated while in G0, which is called the G0 MN assay. In the G2 MN assay, lymphocytes will be first stimulated to divide before they are irradiated and a short incubation time is used after the irradiation. This causes an enrichment of binucleated cells which were irradiated in the G2 phase of the cell cycle (347). The G2 MN +caf assay is an adaptation to the G2 MN assay, where caffeine is added to the irradiated cultures. Caffeine abrogates the G2/M checkpoint (68, 69) and the use of caffeine on G2-cells will allow heavily damaged and yet unrepaired cells, which would otherwise be blocked at the G2/M checkpoint, to progress through mitosis. This allows us to analyze differences in individual repair efficiency independent from differences in individual cell cycle control (70, 71).

The induction of chromosomal aberration typically leads to a dose-response curve which is linear-quadratic in shape and which is defined by an α -component (the linear component) and a β -component (the quadratic component).

In this thesis, ellipses have been constructed to analyze inherent differences in radiosensitivity at the 95% confidence level. The ellipses represent the set of α and β -values that demarcate a 95% confidence interval and are based on the average values and variances. They delimit the covariance between the cellular dose-response parameters which represent the inherent radiosensitivity (α), as well as the capacity to accumulate damage (β). When two ellipses don't overlap, they indicate a significant difference in radiosensitivity at the 95% level (see figure 5.5) (348).

A dose-wise comparison is possible to assess differences in radiosensitivity or in efficiency of radiation-qualities. However, in this thesis, the area under the curve (AUC) was also calculated to assess differences in radiosensitivity based on the whole dose-response curve.

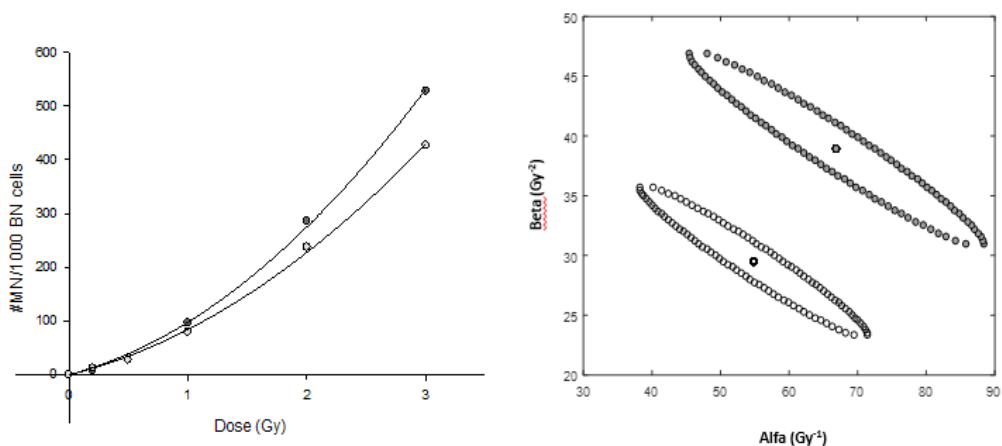


FIGURE 5.5

Example of two the 95% confidence ellipses based on MN dose response curves of two different donors. The ellipses don't overlap, suggesting that the donors are inherently different in radiosensitivity. Figure from our lab.

5.3 Apoptosis assay

Apoptosis or programmed cell death is one of the major cell death pathways activated by IR. Apoptosis will be the result of the DNA damage response when the damage to the DNA is too severe to be repaired. A number of assays can be used to detect apoptosis, such as FLICA staining based on caspase activity (349), TUNEL assay based on detection of DNA fragmentation, Annexin V staining and detection of changes in mitochondrial membrane potential (350, 351).

In this thesis, apoptotic cells were detected with flow cytometry using an Annexin V and 7-aminoactinomycin D (7-AAD) staining. Phosphatidylserine is predominantly located on the cytosolic side of the plasma membrane. One of the first steps in apoptotic cells is the flipflop of phosphatidylserine from the inner side of the membrane to the extracellular side. Annexin V will bind to the extracellular phosphatidylserine and will allow the detection of the early apoptotic cells. 7-AAD is a viability dye, which will be excluded from viable cells during the first phases of apoptosis. In a later stage, loss of membrane integrity will lead to the uptake of 7-AAD and allow for the detection of late apoptotic cells (352).

5.4 Crystal violet cell survival assay

As a consequence of radiation a cell can lose its ability to proliferate, which is known as reproductive failure. The standard assay to determine reproductive failure is the colony formation assay. This assay is based on the ability of individual cells to divide and form macroscopically visible colonies after a few divisions (2, 13).

In this thesis the crystal violet cell survival assay was used. This assay is not based on colony formation but on cell proliferation, and as such is suitable for cells that do not form well-defined colonies (e.g. the MCF-10A cells used in this thesis) (353). In the crystal violet proliferation assay, cells are irradiated and seeded in a low concentration. Cells are incubated for 5 to 10 days, during which time those cells which are still capable of proliferation will divide. After this period, the cells will be fixed and stained with crystal violet. Crystal violet, a basic dye, will bind with cellular components. After washing and bringing the dye in solution again, optic density of the extracted crystal violet can be measured (354, 355). Remark that the crystal violet proliferation assay regularly gives an overestimation of the cell survival rate compared to the colony formation assay, since the measurement of dividing cells can be contaminated a bit by the presence of non-dividing cells. The presence of non-dividing cells may further result in tailing of the survival curves at higher radiation doses (353, 355).

6 Aim of the research

Breast tissue is prone to the development of cancer and radiation is known to be an inducer of cancer. However, irradiation of breast tissue is often used in a useful manner: mammography to detect breast cancer in an early stage or radiotherapy to eradicate breast cancer.

The effectiveness of radiotherapy in cancer treatment is mainly based on the ability of high doses of ionizing radiation to induce DNA damage and kill cancer cells. In diagnostic imaging, the goal is to get a clear image, based on density differences between tissues. Different types of radiation have different properties, mainly determined by the LET, mass and charge of the particles used and can therefore be used with different goals in mind. Low-energy 30 kV X-rays are good in producing good contrast images of the breast. High-LET radiation qualities are used increasingly in radiotherapy due to their high RBE and because particle beams have a good dose deposition. Notwithstanding the dose to the healthy tissue in radiotherapy is kept to a minimum and the important organs are spared as much as possible, the healthy tissue will also receive an amount of radiation. In diagnostic imaging doses are low, although while doing so there is the risk to induce DNA damage. The advantages of using radiation qualities with a higher LET compared to conventional γ -rays or X-rays might come with a cost for the healthy tissue and it is important to know the efficiency of these types of radiation to induce DNA damage.

While breast cancer isn't commonly treated with high-LET radiotherapy, the use of it is rising for a variety of cancer-types. Furthermore, research into the distinct characteristics of high-LET radiation and the differences with low-LET radiation can help to further unravel the DNA damage response pathways activated by radiation-induced DNA DSB.

A **FIRST AIM** of this thesis was to investigate the biological efficiencies of different radiation qualities in different cell types using different cellular endpoints.

We analyzed the efficiency of 30kV X-rays and neutrons to induce DNA DSB (γ H2AX foci assay). Furthermore, we investigated the repair kinetics of the DSB induced by the above mentioned radiation qualities and to what extent an increased number of persistent foci correlated with an

increased number of chromosomal aberrations (micronucleus assay). Finally we analyzed the differences in efficiency of the different radiation qualities to inhibit cell proliferation (crystal violet cell proliferation assay). For these studies peripheral blood lymphocytes from healthy donors, MCF-10A human mammary epithelial cell lines and mammary epithelial cells in dissected breast tissue were used.

Dose is of a different order of magnitude in radiotherapy or diagnostic imaging. Since RBE is function of dose, we analyzed the influences of the above mentioned parameters on RBE in the higher dose range and in the low dose range, with special emphasis on the very low dose range in light of mammography screening.

Cell cycle phase is also a parameter that will influence the RBE. The cell cycle phase will determine which DSB repair pathways can be activated. To investigate the relationship between cell cycle phase, DSB repair pathway and RBE, we constructed DSB repair deficient MCF-10A cell lines. These cell lines were irradiated with neutrons and γ -rays as synchronized G1 cultures and mixed cultures containing cells in G1, S, G2 and M phase of the cell cycle. We analyzed the impact of repair pathway deficiencies and cell cycle on MN-induction after irradiation with both neutrons and γ -rays.

The term radiosensitivity is used to describe many different phenomena such as normal tissue radiosensitivity, susceptibility to radiation carcinogenesis and cellular radiosensitivity. In the first part of this study, we investigated how cellular radiosensitivity, which refers to phenomena such as cell proliferation, chromosomal aberrations and apoptosis, is linked to RBE. The second and third aim of this thesis is dealing with individual radiosensitivity. Individuals vary in radiosensitivity and their 'intrinsic or inherent radiosensitivity' is determined by the genetic background (mutation, single nucleotide polymorphisms (SNP) in repair genes,...). Non-genetic modifying factors, such as smoking, life style but also tissue-volume irradiated, will further influence the individual's response to radiation. A clinical endpoint of individual radiosensitivity is for instance the reaction of normal tissue to radiotherapy, called 'normal tissue radiosensitivity'. This is a re-

sponse from the normal, healthy tissue to radiation, and mostly refers to early or late toxic effects of the healthy tissue following radiotherapy. Different individuals will show different degrees of radiation toxicity, influenced by their inherent radiosensitivity and modifying factors. Another clinical endpoint of individual radiosensitivity is the susceptibility to radiation carcinogenesis. This refers to the susceptibility of an individual to develop radiation-induced cancer in specific tissues.

The health effects of radiation are influenced by a person's inherent radiosensitivity, but are also tissue specific. Different tissues will have different sensitivities to develop radiation-related toxic effects or cancer. Breast tissue is known to be sensitive to radiation and especially the mammary epithelial cells are prone to the development of radiation-induced cancer.

The **SECOND AIM** of this thesis was to investigate if the late toxic normal tissue radiation response of breast cancer patients is related to cellular radiosensitivity. When receiving radiotherapy to treat breast cancer, a small subgroup of women exhibits a late toxic reaction of the healthy tissue to the radiation. This limits the dose which can be safely administered during radiotherapy. Using lymphocytes from breast cancer patients we investigated if biomarkers for cellular radiosensitivity can be used to predict which women will develop late toxic reactions of the healthy tissue.

The **THIRD AIM** of this thesis was to investigate the radiosensitivity of *BRCA1* and *BRCA2* mutation carriers. A long standing discussion is whether or not *BRCA1* and *BRCA2* mutation carriers are more sensitive to develop breast cancer following radiotherapy or mammography. Most studies on this subject are either cohort-studies with often a low power or studies performed on lymphocytes, which are different from breast epithelial cells. To assess the impact of a *BRCA1* or *BRCA2* mutation on radiosensitivity we used mammary epithelial cells (MCF-10A) in which we induced a knockdown of the *BRCA1/2* proteins of approximately 50%, which is comparable with the *BRCA1/2* protein levels in heterozygous mutation carriers. As endpoints we investigated micronucleus formation and cell proliferation.

7 References

1. Pouget JP, Mather SJ, General aspects of the cellular response to low- and high-LET radiation. *European Journal of Nuclear Medicine* 2001; 28, 541-61.
2. laTorre Davis E, *Primer of Medical Radiobiology*. 2 ed. St Louis: Mosby-Year Book; 1989.
3. El-Zein R, Vral A, Etzel CJ, Cytokinesis-blocked micronucleus assay and cancer risk assessment. *Mutagenesis* 2011; 26, 101-06.
4. IAEA, *Cytogenetic Dosimetry: Applications in preparedness for and response to radiation emergencies*: IAEA; 2011.
5. Lehnert S, *Biomolecular action of ionizing radiation*. New York: Taylor & Francis; 2008.
6. Goodhead DT, Initial events in the cellular effects of ionizing-radiations – clustered damage in DNA. *International Journal of Radiation Biology* 1994; 65, 7-17.
7. Goodhead DT, The initial physical damage produced by ionizing radiations. *International Journal of Radiation Biology* 1989; 56, 623-34.
8. Nikjoo H, Uehara S, Wilson WE, Hoshi M, Goodhead DT, Track structure in radiation biology: theory and applications. *International Journal of Radiation Biology* 1998; 73, 355-64.
9. Durante M, Bedford JS, Chen DJ, Conrad S, Cornforth MN, Natarajan AT, et al., From DNA damage to chromosome aberrations: Joining the break. *Mutation Research-Genetic Toxicology and Environmental Mutagenesis* 2013; 756, 5-13.
10. Rothkamm K, Lobrich M, Evidence for a lack of DNA double-strand break repair in human cells exposed to very low x-ray doses. *Proceedings of the National Academy of Sciences of the United States of America* 2003; 100, 5057-62.
11. Wambersie A, Hendry J, Gueulette J, Gahbauer R, Potter D, Gregoire V, Radiobiological rationale and patient selection for high-LET radiation in cancer therapy. *Radiother Oncol* 2004; 73, S1-S14.
12. Joiner MC, van der Kogel A, *Basic Clinical Radiobiology*. 4 ed. UK: Hodder Arnold; 2009.
13. Hall E, Giaccia AJ, *Radiobiology for the radiologist*. 6 ed. Philadelphia: Lippincott Williams & Wilkins; 2006.
14. ICRP, The 2007 recommendations of the International Commission on Radiological Protection. ICRP Publication 103. *Annals of the ICRP* 2007; 37.
15. Hunter N, Muirhead CR, Review of relative biological effectiveness dependence on linear energy transfer for low-LET radiations. *J Radiol Prot* 2009; 29, 5-21.
16. Rong Y, Welsh J, *Basics of Particle Therapy II Biologic and Dosimetric Aspects of Clinical Hadron Therapy*. *American Journal of Clinical Oncology-Cancer Clinical Trials* 2010; 33, 646-49.
17. Averbeck D, Does scientific evidence support a change from the LNT model for low-dose radiation risk extrapolation? *Health Phys* 2009; 97, 493-504.
18. Durante M, New challenges in high-energy particle radiobiology. *British Journal of Radiology* 2014; 87, 14.
19. Carabe A, Espana S, Grassberger C, Paganetti H, Clinical consequences of relative biological effectiveness variations in proton radiotherapy of the prostate, brain and liver. *Physics in Medicine and Biology* 2013; 58, 2103-17.
20. Amaldi U, Kraft G, Hadrontherapy: cancer treatment with proton and carbon beams. In: Lemoigne Y, Caner A editors. *Radiotherapy and Brachytherapy*. 2009.
21. Wikipedia – Equivalent dose, https://en.wikipedia.org/wiki/Equivalent_dose.
22. PHE, Human Radiosensitivity. Report of the independent Advisory group on Ionising Radiation. 2013.
23. Land CE, Studies of cancer and radiation-dose among atomic-bomb survivors – The example of breast-cancer. *Jama-Journal of the American Medical Association* 1995; 274, 402-07.

24. Land CE, Tokunaga M, Koyama K, Soda M, Preston DL, Nishimori I, et al., Incidence of female breast cancer among atomic bomb survivors, Hiroshima and Nagasaki, 1950-1990. *Radiation Research* 2003; 160, 707-17.
25. McGregor H, Land CE, Choi K, Tokuoka S, Liu PI, Wakabayashi T, Breast cancer incidence among atomic bomb survivors, Hiroshima and Nagasaki 1950-1969. *Journal of the National Cancer Institute* 1977; 59, 799-811.
26. Sun LM, Lin CL, Liang JA, Huang WS, Kao CH, Radiotherapy did not increase thyroid cancer risk among women with breast cancer: A nationwide population-based cohort study. *Int J Cancer* 2015; 137, 2896-903.
27. Radivoyevitch T, Sachs RK, Gale RP, Smith MR, Hill BT, Ionizing radiation exposures in treatments of solid neoplasms are not associated with subsequent increased risks of chronic lymphocytic leukemia. *Leuk Res* 2016; 43, 9-12.
28. Huang WY, Muo CH, Lin CY, Jen YM, Yang MH, Lin JC, et al., Paediatric head CT scan and subsequent risk of malignancy and benign brain tumour: a nation-wide population-based cohort study. *British Journal of Cancer* 2014; 110, 2354-60.
29. Hauptmann M, Fossa SD, Stovall M, van Leeuwen FE, Johannesen TB, Rajaraman P, et al., Increased stomach cancer risk following radiotherapy for testicular cancer. *British Journal of Cancer* 2015; 112, 44-51.
30. Groves ML, Zadnik PL, Kaloostian P, Sui J, Goodwin CR, Wolinsky JP, et al., Epidemiologic, functional, and oncologic outcome analysis of spinal sarcomas treated surgically at a single institution over 10 years. *Spine Journal* 2015; 15, 110-14.
31. Farioli A, Violante FS, Mattioli S, Curti S, Kriebel D, Risk of mesothelioma following external beam radiotherapy for prostate cancer: a cohort analysis of SEER database. *Cancer Causes & Control* 2013; 24, 1535-45.
32. Daniel CL, Kohler CL, Stratton KL, Oeffinger KC, Leisenring WM, Waterbor JW, et al., Predictors of colorectal cancer surveillance among survivors of childhood cancer treated with radiation: A report from the Childhood Cancer Survivor Study. *Cancer* 2015; 121, 1856-63.
33. Borrás C, Bares JP, Rudder D, Amer A, Millan F, Abuchaibe O, Clinical effects in a cohort of cancer patients overexposed during external beam pelvic radiotherapy. *International Journal of Radiation Oncology Biology Physics* 2004; 59, 538-50.
34. Barton SE, Najita JS, Ginsburg ES, Leisenring WM, Stovall M, Weathers RE, et al., Infertility, infertility treatment, and achievement of pregnancy in female survivors of childhood cancer: a report from the Childhood Cancer Survivor Study cohort. *Lancet Oncology* 2013; 14, 873-81.
35. Allodji RS, Diallo I, El-Fayech C, Kahlouche A, Dumas A, Schwartz B, et al., Association of Radiation Dose to the Eyes With the Risk for Cataract After Nonretinoblastoma Solid Cancers in Childhood. *JAMA Ophthalmol* 2016; 134, 390-97.
36. ICRP, ICRP Statement on Tissue Reactions / Early and Late Effects of Radiation in Normal Tissues and Organs – Threshold Doses for Tissue Reactions in a Radiation Protection Context. ICRP publication 118. *Annals of the ICRP* 2012; 41.
37. Hamada N, Fujimichi Y, Classification of radiation effects for dose limitation purposes: history, current situation and future prospects. *Journal of Radiation Research* 2014; 55, 629-40.
38. ICRP, Recommendations of the International Commission on Radiological Protection. ICRP publication 26. *Recommendations of the ICRP* 1977.
39. ICRP, Nonstochastic effects of ionizing radiation. ICRP publication 41. *Annals of the ICRP* 1984; 14.
40. UNSCEAR, Report of the United Nations Scientific Committee on the Effects of Atomic Radiation 2010. *UNSCEAR 2010 Report* 2010.
41. Hammer GP, Scheidemann-Wesp U, Samkange-Zeeb F, Wicke H, Neriishi K, Blettner M,

- Occupational exposure to low doses of ionizing radiation and cataract development: a systematic literature review and perspectives on future studies. *Radiation and Environmental Biophysics* 2013; 52, 303-19.
42. Brenner DJ, Doll R, Goodhead DT, Hall EJ, Land CE, Little JB, et al., Cancer risks attributable to low doses of ionizing radiation: Assessing what we really know. *Proceedings of the National Academy of Sciences of the United States of America* 2003; 100, 13761-66.
 43. Bakkenist CJ, Kastan MB, Initiating cellular stress responses. *Cell* 2004; 118, 9-17.
 44. Grudzenski S, Raths A, Conrad S, Rube CE, Lohrich M, Inducible response required for repair of low-dose radiation damage in human fibroblasts. *Proceedings of the National Academy of Sciences of the United States of America* 2010; 107, 14205-10.
 45. Amundson SA, Lee RA, Koch-Paiz CA, Bittner ML, Meltzer P, Trent JM, et al., Differential responses of stress genes to low dose-rate gamma irradiation. *Molecular Cancer Research* 2003; 1, 445-52.
 46. Franco N, Lamartine J, Frouin V, Le Minter P, Petal C, Leplat JJ, et al., Low-dose exposure to gamma rays induces specific gene regulations in normal human keratinocytes. *Radiation Research* 2005; 163, 623-35.
 47. Yang F, Stenoien DL, Strittmatter EF, Wang JH, Ding LH, Lipton MS, et al., Phosphoproteome profiling of human skin fibroblast cells in response to low- and high-dose irradiation. *Journal of Proteome Research* 2006; 5, 1252-60.
 48. El-Saghire H, Thierens H, Monsieurs P, Michaux A, Vandevoorde C, Baatout S, Gene set enrichment analysis highlights different gene expression profiles in whole blood samples X-irradiated with low and high doses. *International Journal of Radiation Biology* 2013; 89, 628-38.
 49. Nagasawa H, Little JB, Induction of sister chromatid exchanges by extremely low doses of alpha-particles. *Cancer Research* 1992; 52, 6394-96.
 50. Belyakov OV, Malcolmson AM, Folkard M, Prise KM, Michael BD, Direct evidence for a bystander effect of ionizing radiation in primary human fibroblasts. *British Journal of Cancer* 2001; 84, 674-79.
 51. Ballarini F, Biaggi M, Ottolenghi A, Sapora O, Cellular communication and bystander effects: a critical review for modelling low-dose radiation action. *Mutation Research-Fundamental and Molecular Mechanisms of Mutagenesis* 2002; 501, 1-12.
 52. Seymour CB, Mothersill C, Relative contribution of bystander and targeted cell killing to the low-dose region of the radiation dose-response curve. *Radiation Research* 2000; 153, 508-11.
 53. Azzam EI, de Toledo SM, Little JB, Stress signaling from irradiated to non-irradiated cells. *Curr Cancer Drug Targets* 2004; 4, 53-64.
 54. Azzam EI, de Toledo SM, Little JB, Direct evidence for the participation of gap junction-mediated intercellular communication in the transmission of damage signals from alpha-particle irradiated to nonirradiated cells. *Proceedings of the National Academy of Sciences of the United States of America* 2001; 98, 473-78.
 55. Hanot M, Hoarau J, Carriere M, Angulo JF, Khodja H, Membrane-dependent bystander effect contributes to amplification of the response to alpha-particle irradiation in targeted and nontargeted cells. *International Journal of Radiation Oncology Biology Physics* 2009; 75, 1247-53.
 56. Mothersill C, Seymour C, Radiation-induced bystander effects: Past history and future directions. *Radiation Research* 2001; 155, 759-67.
 57. Zhou HN, Suzuki M, Geard CR, Hei TK, Effects of irradiated medium with or without cells on bystander cell responses. *Mutation Research-Fundamental and Molecular Mechanisms of Mutagenesis* 2002; 499, 135-41.

58. Zhao Y, de Toledo SM, Hu G, Hei TK, Azzam EI, Connexins and cyclooxygenase-2 crosstalk in the expression of radiation-induced bystander effects. *British Journal of Cancer* 2014; 111, 125-31.
59. Marples B, Cann NE, Mitchell CR, Johnston PJ, Joiner MC, Evidence for the involvement of DNA-dependent protein kinase in the phenomena of low dose hyper-radiosensitivity and increased radioresistance. *International Journal of Radiation Biology* 2002; 78, 1139-47.
60. Joiner MC, Marples B, Lambin P, Short SC, Turesson I, Low-dose hypersensitivity: Current status and possible mechanisms. *International Journal of Radiation Oncology Biology Physics* 2001; 49, 379-89.
61. Marples B, Collis SJ, Low-dose hyper-radiosensitivity: Past, present, and future. *International Journal of Radiation Oncology Biology Physics* 2008; 70, 1310-18.
62. Short SC, Woodcock M, Marples B, Joiner MC, Effects of cell cycle phase on low-dose hyper-radiosensitivity. *International Journal of Radiation Biology* 2003; 79, 99-105.
63. Klammer H, Kadhim M, Iliakis G, Evidence of an Adaptive Response Targeting DNA Non-homologous End Joining and Its Transmission to Bystander Cells. *Cancer Research* 2010; 70, 8498-506.
64. Wall BF, Kendall GM, Edwards AA, Boliffler S, Muirhead CR, Meara JR, What are the risks from medical X-rays and other low dose radiation? *British Journal of Radiology* 2006; 79, 285-94.
65. Khanna KK, Jackson SP, DNA double-strand breaks: signaling, repair and the cancer connection. *Nature Genet* 2001; 27, 247-54.
66. Difilippantonio S, Celeste A, Fernandez-Capetillo O, Chen HT, San Martin BR, Van Laethem F, et al., Role of Nbs1 in the activation of the Atm kinase revealed in humanized mouse models. *Nature Cell Biology* 2005; 7, 675-U56.
67. Lee JH, Paull TT, ATM activation by DNA double-strand breaks through the Mre11-Rad50-Nbs1 complex. *Science* 2005; 308, 551-54.
68. Lee JH, Paull TT, Direct activation of the ATM protein kinase by the Mre11/Rad50/Nbs1 complex. *Science* 2004; 304, 93-96.
69. Bakkenist CJ, Kastan MB, DNA damage activates ATM through intermolecular autophosphorylation and dimer dissociation. *Nature* 2003; 421, 499-506.
70. Price BD, D'Andrea AD, Chromatin Remodeling at DNA Double-Strand Breaks. *Cell* 2013; 152, 1344-54.
71. Matsuoka S, Ballif BA, Smogorzewska A, McDonald ER, Hurov KE, Luo J, et al., ATM and ATR substrate analysis reveals extensive protein networks responsive to DNA damage. *Science* 2007; 316, 1160-66.
72. Lou ZK, Minter-Dykhouse K, Franco S, Gostissa M, Rivera MA, Celeste A, et al., MDC1 maintains genomic stability by participating in the amplification of ATM-dependent DNA damage signals. *Mol Cell* 2006; 21, 187-200.
73. Stucki M, Clapperton JA, Mohammad D, Yaffe MB, Smerdon SJ, Jackson SP, MDC1 directly binds phosphorylated histone H2AX to regulate cellular responses to DNA double-strand breaks. *Cell* 2005; 123, 1213-26.
74. Lee MS, Edwards RA, Thede GL, Glover JNM, Structure of the BRCT repeat domain of MDC1 and its specificity for the free COOH-terminal end of the gamma-H2AX histone tail. *Journal of Biological Chemistry* 2005; 280, 32053-56.
75. Xu B, Kim ST, Lim DS, Kastan MB, Two molecularly distinct G(2)/M checkpoints are induced by ionizing irradiation. *Molecular and Cellular Biology* 2002; 22, 1049-59.
76. Senderowicz AM, Sausville EA, Preclinical and clinical development of cyclin-dependent kinase modulators. *Journal of the National Cancer Institute* 2000; 92, 376-87.
77. Poehlmann A, Roessner A, Importance of DNA damage checkpoints in the pathogenesis of

- human cancers. *Pathology Research and Practice* 2010; 206, 591-601.
78. Yaneva M, Kowalewski T, Lieber MR, Interaction of DNA-dependent protein kinase with DNA and with Ku: biochemical and atomic-force microscopy studies. *Embo Journal* 1997; 16, 5098-112.
 79. Shimada M, Nakanishi M, DNA damage checkpoints and cancer. *Journal of Molecular Histology* 2006; 37, 253-60.
 80. Stukenberg PT, Burke DJ, Connecting the microtubule attachment status of each kinetochore to cell cycle arrest through the spindle assembly checkpoint. *Chromosoma* 2015; 124, 463-80.
 81. Kavanagh JN, Redmond KM, Schettino G, Prise KM, DNA Double Strand Break Repair: A Radiation Perspective. *Antioxidants & Redox Signaling* 2013; 18, 2458-72.
 82. Lieber MR, The Mechanism of Double-Strand DNA Break Repair by the Nonhomologous DNA End-Joining Pathway. In: Kornberg RD, Raetz CRH, Rothman JE, Thorner JW editors. *Annual Review of Biochemistry*, Vol 79. *Place Annual Reviews: Annual Reviews*; 2010.
 83. Wang C, Lees-Miller SP, Detection and Repair of Ionizing Radiation-Induced DNA Double Strand Breaks: New Developments in Nonhomologous End Joining. *International Journal of Radiation Oncology Biology Physics* 2013; 86, 440-49.
 84. Santivasi WL, Xia F, Ionizing Radiation-Induced DNA Damage, Response, and Repair. *Antioxidants & Redox Signaling* 2014; 21, 251-59.
 85. Walker JR, Corpina RA, Goldberg J, Structure of the Ku heterodimer bound to DNA and its implications for double-strand break repair. *Nature* 2001; 412, 607-14.
 86. Kim JS, Krasieva TB, Kurumizaka H, Chen DJ, Taylor AMR, Yokomori K, Independent and sequential recruitment of NHEJ and HR factors to DNA damage sites in mammalian cells. *Journal of Cell Biology* 2005; 170, 341-47.
 87. Kurimasa A, Kumano S, Boubnov NV, Story MD, Tung CS, Peterson SR, et al., Requirement for the kinase activity of human DNA-dependent protein kinase catalytic subunit in DNA strand break rejoining. *Molecular and Cellular Biology* 1999; 19, 3877-84.
 88. Singleton BK, Torres-Arzuayus MI, Rottinghaus ST, Taccioli GE, Jeggo PA, The C terminus of Ku80 activates the DNA-dependent protein kinase catalytic subunit. *Molecular and Cellular Biology* 1999; 19, 3267-77.
 89. Chan DW, Chen BPC, Prithivirajasingh S, Kurimasa A, Story MD, Qin J, et al., Autophosphorylation of the DNA-dependent protein kinase catalytic subunit is required for rejoining of DNA double-strand breaks. *Genes & Development* 2002; 16, 2333-38.
 90. Mahaney BL, Meek K, Lees-Miller SP, Repair of ionizing radiation-induced DNA double-strand breaks by non-homologous end-joining. *Biochemical Journal* 2009; 417, 639-50.
 91. Weterings E, Verkaik NS, Keijzers G, Florea BI, Wang SY, Ortega LG, et al., The Ku80 Carboxy Terminus Stimulates Joining and Artemis-Mediated Processing of DNA Ends. *Molecular and Cellular Biology* 2009; 29, 1134-42.
 92. Bahmed K, Seth A, Nitiss KC, Nitiss JL, End-processing during non-homologous end-joining: a role for exonuclease 1. *Nucleic Acids Research* 2011; 39, 970-78.
 93. Kusumoto R, Dawut L, Marchetti C, Lee JW, Vindigni A, Ramsden D, et al., Werner protein cooperates with the XRCC4-DNA ligase IV complex in end-processing. *Biochemistry* 2008; 47, 7548-56.
 94. McElhinny SAN, Havener JM, Garcia-Diaz M, Juarez R, Bebenek K, Kee BL, et al., A gradient of template dependence defines distinct biological roles for family X polymerases in nonhomologous end joining. *Mol Cell* 2005; 19, 357-66.
 95. Ramsden DA, Asagoshi K, DNA polymerases in nonhomologous end joining: Are there any benefits to standing out from the crowd? *Environmental and Molecular Mutagenesis* 2012; 53, 741-51.

96. Junop MS, Modesti M, Guarne A, Ghirlando R, Gellert M, Yang W, Crystal structure of the Xrcc4 DNA repair protein and implications for end joining. *Embo Journal* 2000; 19, 5962-70.
97. Grawunder U, Zimmer D, Lieber MR, DNA ligase IV binds to XRCC4 via a motif located between rather than within its BRCT domains. *Current Biology* 1998; 8, 873-76.
98. Jazayeri A, Falck J, Lukas C, Bartek J, Smith GCM, Lukas J, et al., ATM- and cell cycle-dependent regulation of ATR in response to DNA double-strand breaks. *Nature Cell Biology* 2006; 8, 37-U13.
99. Yuan JS, Chen JJ, MRE11-RAD50-NBS1 Complex Dictates DNA Repair Independent of H2AX. *Journal of Biological Chemistry* 2010; 285, 1097-104.
100. Sartori AA, Lukas C, Coates J, Mistrik M, Fu S, Bartek J, et al., Human CtIP promotes DNA end resection. *Nature* 2007; 450, 509-U6.
101. Richard DJ, Savage K, Bolderson E, Cubeddu L, So S, Ghita M, et al., hSSB1 rapidly binds at the sites of DNA double-strand breaks and is required for the efficient recruitment of the MRN complex. *Nucleic Acids Research* 2011; 39, 1692-702.
102. Zou Y, Liu YY, Wu XM, Shell SM, Functions of human replication protein A (RPA): From DNA replication to DNA damage and stress responses. *Journal of Cellular Physiology* 2006; 208, 267-73.
103. Masson JY, Tarsounas MC, Stasiak AZ, Stasiak A, Shah R, McIlwraith MJ, et al., Identification and purification of two distinct complexes containing the five RAD51 paralogs. *Genes & Development* 2001; 15, 3296-307.
104. Fujioka Y, Kimata Y, Nomaguchi K, Watanabe K, Kohno K, Identification of a novel non-structural maintenance of chromosomes (SMC) component of the SMC5-SMC6 complex involved in DNA repair. *Journal of Biological Chemistry* 2002; 277, 21585-91.
105. Moynahan ME, Jasin M, Mitotic homologous recombination maintains genomic stability and suppresses tumorigenesis. *Nature Reviews Molecular Cell Biology* 2010; 11, 196-207.
106. Ip SCY, Rass U, Blanco MG, Flynn HR, Skehel JM, West SC, Identification of Holliday junction resolvases from humans and yeast. *Nature* 2008; 456, 357-U39.
107. Simsek D, Brunet E, Wong SYW, Katyal S, Gao Y, McKinnon PJ, et al., DNA Ligase III Promotes Alternative Nonhomologous End-Joining during Chromosomal Translocation Formation. *Plos Genetics* 2011; 7, 11.
108. Symington LS, Gautier J, Double-Strand Break End Resection and Repair Pathway Choice. In: Bassler BL, Lichten M, Schupbach G editors. *Annual Review Genetics*, Vol 45. *Place Annual Reviews: Annual Reviews*; 2011.
109. Kakarougkas A, Jeggo PA, IDNA DSB repair pathway choice: an orchestrated handover mechanism. *British Journal of Radiology* 2014; 87, 8.
110. Deriano L, Roth DB, Modernizing the Nonhomologous End-Joining Repertoire: Alternative and Classical NHEJ Share the Stage. In: Bassler BL, Lichten M, Schupbach G editors. *Annual Review of Genetics*, Vol 47. *Place Annual Reviews: Annual Reviews*; 2013.
111. Shrivastav M, De Haro LP, Nickoloff JA, Regulation of DNA double-strand break repair pathway choice. *Cell Res* 2008; 18, 134-47.
112. Antonelli F, Campa A, Esposito G, Giardullo P, Belli M, Dini V, et al., Induction and Repair of DNA DSB as Revealed by H2AX Phosphorylation Foci in Human Fibroblasts Exposed to Low- and High-LET Radiation: Relationship with Early and Delayed Reproductive Cell Death. *Radiation Research* 2015; 183, 417-31.
113. Moore S, Stanley FKT, Goodarzi AA, The repair of environmentally relevant DNA double

- strand breaks caused by high linear energy transfer irradiation – No simple task. *DNA Repair* 2014; 17, 64-73.
114. Loucas BD, Cornforth MN, The LET Dependence of Unrepaired Chromosome Damage in Human Cells: A Break Too Far? *Radiation Research* 2013; 179, 393-405.
 115. Jeggo PA, Geuting V, Lobrich M, The role of homologous recombination in radiation-induced double-strand break repair. *Radiother Oncol* 2011; 101, 7-12.
 116. Lobrich M, Rydberg B, Cooper PK, Repair of x-ray-induced DNA double-strand breaks in specific Not I restriction fragments in human fibroblasts: Joining of correct and incorrect ends. *Proceedings of the National Academy of Sciences of the United States of America* 1995; 92, 12050-54.
 117. Wu W, Wang M, Wu W, Singh SK, Mussfeldt T, Iliakis G, Repair of radiation induced DNA double strand breaks by backup NHEJ is enhanced in G2. *DNA Repair* 2008; 7, 329-38.
 118. Beucher A, Birraux J, Tchouandong L, Barton O, Shibata A, Conrad S, et al., ATM and Artemis promote homologous recombination of radiation-induced DNA double-strand breaks in G2. *Embo Journal* 2009; 28, 3413-27.
 119. Iliakis G, Backup pathways of NHEJ in cells of higher eukaryotes: Cell cycle dependence. *Radiother Oncol* 2009; 92, 310-15.
 120. Iliakis G, Wang H, Perrault AR, Boecker W, Rosidi B, Windhofer F, et al., Mechanisms of DNA double strand break repair and chromosome aberration formation. *Cytogenetic and Genome Research* 2004; 104, 14-20.
 121. Shibata A, Conrad S, Birraux J, Geuting V, Barton O, Ismail A, et al., Factors determining DNA double-strand break repair pathway choice in G2 phase. *Embo Journal* 2011; 30, 1079-92.
 122. Tommasino F, Friedrich T, Scholz U, Taucher-Scholz G, Durante M, Scholz M, A DNA Double-Strand Break Kinetic Rejoining Model Based on the Local Effect Model. *Radiation Research* 2013; 180, 524-38.
 123. Riballo E, Kuhne M, Rief N, Doherty A, Smith GCM, Recio MJ, et al., A pathway of double-strand break rejoining dependent upon ATM, artemis, and proteins locating to gamma-H2AX foci. *Mol Cell* 2004; 16, 715-24.
 124. Singleton BK, Griffin CS, Thacker J, Clustered DNA damage leads to complex genetic changes in irradiated human cells. *Cancer Research* 2002; 62, 6263-69.
 125. Averbek NB, Ringel O, Herrlitz M, Jakob B, Durante M, Taucher-Scholz G, DNA end resection is needed for the repair of complex lesions in G1-phase human cells. *Cell Cycle* 2014; 13, 2509-16.
 126. Smerdon MJ, DNA repair and the role of chromatin structure. *Current Opinion in Cell Biology* 1991; 3, 422-28.
 127. Soria G, Polo SE, Almouzni G, Prime, Repair, Restore: The Active Role of Chromatin in the DNA Damage Response. *Mol Cell* 2012; 46, 722-34.
 128. Chiolo I, Minoda A, Colmenares SU, Polyzos A, Costes SV, Karpen GH, Double-Strand Breaks in Heterochromatin Move Outside of a Dynamic HP1a Domain to Complete Recom-

- binational Repair. *Cell* 2011; 144, 732-44.
129. Goodarzi AA, Kurka T, Jeggo PA, KAP-1 phosphorylation regulates CHD3 nucleosome remodeling during the DNA double-strand break response. *Nature Structural & Molecular Biology* 2011; 18, 831-U112.
 130. Goodarzi AA, Noon AT, Deckbar D, Ziv Y, Shiloh Y, Lobrich M, et al., ATM signaling facilitates repair of DNA double-strand breaks associated with heterochromatin. *Mol Cell* 2008; 31, 167-77.
 131. Ayoub N, Jeyasekharan AD, Bernal JA, Venkitaraman AR, HP1-beta mobilization promotes chromatin changes that initiate the DNA damage response. *Nature* 2008; 453, 682-U14.
 132. Zafar F, Seidler SB, Kronenberg A, Schild D, Wiese C, Homologous Recombination Contributes to the Repair of DNA Double-Strand Breaks Induced by High-Energy Iron Ions. *Radiation Research* 2010; 173, 27-39.
 133. Taleei R, Nikjoo H, Biochemical DSB-repair model for mammalian cells in G1 and early S phases of the cell cycle. *Mutation Research-Genetic Toxicology and Environmental Mutagenesis* 2013; 756, 206-12.
 134. Zimmerman M, de Lange T, 53BP1: pro choice in DNA repair. *Trends Cell Biol* 2014; 24, 108-17.
 135. Bouwman P, Aly A, Escandell JM, Pieterse M, Bartkova J, van der Gulden H, et al., 53BP1 loss rescues BRCA1 deficiency and is associated with triple-negative and BRCA-mutated breast cancers. *Nature Structural & Molecular Biology* 2010; 17, 688-U56.
 136. Elmore S, Apoptosis: A review of programmed cell death. *Toxicologic Pathology* 2007; 35, 495-516.
 137. Kroemer G, Galluzzi L, Vandenabeele P, Abrams J, Alnemri ES, Baehrecke EH, et al., Classification of cell death: recommendations of the Nomenclature Committee on Cell Death 2009. *Cell Death and Differentiation* 2009; 16, 3-11.
 138. Savitskaya MA, Onishchenko GE, Mechanisms of apoptosis. *Biochemistry-Moscow* 2015; 80, 1393-405.
 139. Mavragani IV, Laskaratou DA, Frey B, Candeias SM, Gaipl US, Lumniczky K, et al., Key mechanisms involved in ionizing radiation-induced systemic effects. A current review. *Toxicology Research* 2016; 5, 12-33.
 140. Xiong SB, Mu TY, Wang GW, Jiang XJ, Mitochondria-mediated apoptosis in mammals. *Protein & Cell* 2014; 5, 737-49.
 141. Fridman JS, Lowe SW, Control of apoptosis by p53. *Oncogene* 2003; 22, 9030-40.
 142. Brentnall M, Rodriguez-Menocal L, De Guevara RL, Cepero E, Boise LH, Caspase-9, caspase-3 and caspase-7 have distinct roles during intrinsic apoptosis. *Bmc Cell Biology* 2013; 14, 9.
 143. Porter AG, Janicke RU, Emerging roles of caspase-3 in apoptosis. *Cell Death and Differentiation* 1999; 6, 99-104.
 144. Eriksson D, Stigbrand T, Radiation-induced cell death mechanisms. *Tumor Biol* 2010; 31, 363-72.

145. Sun HW, Yang SN, Li JH, Zhang YJ, Gao DS, Zhao ST, Caspase-independent cell death mediated by apoptosis-inducing factor (AIF) nuclear translocation is involved in ionizing radiation induced HepG2 cell death. *Biochemical and Biophysical Research Communications* 2016; 472, 137-43.
146. Roninson IB, Broude EV, Chang BD, If not apoptosis, then what? – Treatment-induced senescence and mitotic catastrophe in tumor cells. *Drug Resistance Updates* 2001; 4, 303-13.
147. Vanlangenakker N, Vanden Berghe T, Vandenabeele P, Many stimuli pull the necrotic trigger, an overview. *Cell Death and Differentiation* 2012; 19, 75-86.
148. Proskuryakov SY, Gabai VL, Konoplyannikov AG, Necrosis is an active and controlled form of programmed cell death. *Biochemistry-Moscow* 2002; 67, 387-408.
149. Castedo M, Perfettini JL, Roumier T, Valent A, Raslova H, Yakushijin K, et al., Mitotic catastrophe constitutes a special case of apoptosis whose suppression entails aneuploidy. *Oncogene* 2004; 23, 4362-70.
150. Eriksson D, Blomberg J, Lindgren T, Lofroth PO, Johansson L, Riklund K, et al., Iodine-131 Induces Mitotic Catastrophes and Activates Apoptotic Pathways in HeLa Hep2 Cells. *Cancer Biother Radiopharm* 2008; 23, 541-49.
151. Ianzini F, Bertoldo A, Kosmacek EA, Phillips SL, Mackey MA, Lack of p53 function promotes radiation-induced mitotic catastrophe in mouse embryonic fibroblast cells. *Cancer Cell Int* 2006; 6, 8.
152. Ruth AC, Roninson IB, Effects of the multidrug transporter P-glycoprotein on cellular responses to ionizing radiation. *Cancer Research* 2000; 60, 2576-78.
153. Ben-Porath I, Weinberg RA, When cells get stressed: an integrative view of cellular senescence. *Journal of Clinical Investigation* 2004; 113, 8-13.
154. Cmielova J, Havelek R, Soukup T, Jiroutova A, Visek B, Suchanek J, et al., Gamma radiation induces senescence in human adult mesenchymal stem cells from bone marrow and periodontal ligaments. *International Journal of Radiation Biology* 2012; 88, 393-404.
155. Fridlyanskaya I, Alekseenko L, Nikolsky N, Senescence as a general cellular response to stress: A mini-review. *Experimental Gerontology* 2015; 72, 124-28.
156. Dimri GP, Lee XH, Basile G, Acosta M, Scott C, Roskelley C, et al., A biomarker that identifies senescent human cells in culture and in aging skin in vivo. *Proceedings of the National Academy of Sciences of the United States of America* 1995; 92, 9363-67.
157. Coppe JP, Desprez PY, Krtolica A, Campisi J, The Senescence-Associated Secretory Phenotype: The Dark Side of Tumor Suppression. *Annu Rev Pathol-Mech Dis. Place Annual Reviews: Annual Reviews*; 2010.
158. Caspari T, Checkpoints: How to activate p53. *Current Biology* 2000; 10, R315-R17.
159. Fournier C, Wiese C, Taucher-Scholz G, Accumulation of the cell cycle regulators TP53 and CDKN1A (p21) in human fibroblasts after exposure to low- and high-LET radiation. *Radiation Research* 2004; 161, 675-84.
160. Dulic V, Kaufmann WK, Wilson SJ, Tlsty TD, Lees E, Harper JW, et al., p53-dependent inhibition of cyclin-dependent kinase-activities in human fibroblasts during radiation-induced

- G1 arrest. *Cell* 1994; 76, 1013-23.
161. Ghosh JC, Izumida Y, Suzuki K, Kodama S, Watanabe M, Dose-dependent biphasic accumulation of TP53 protein in normal human embryo cells after X irradiation. *Radiation Research* 2000; 153, 305-11.
 162. Lou ZK, Chen JJ, Cellular senescence and DNA repair. *Experimental Cell Research* 2006; 312, 2641-46.
 163. Parry D, Bates S, Mann DJ, Peters G, Lack of cyclin D-CDK complexes in RB-negative cells correlates with high-levels of P16(INK4/MTS1) tumor-suppressor gene-product. *Embo Journal* 1995; 14, 503-11.
 164. Ohtani N, Zebede Z, Huot TJG, Stinson JA, Sugimoto M, Ohashi Y, et al., Opposing effects of Ets and Id proteins on p16(INK4a) expression during cellular senescence. *Nature* 2001; 409, 1067-70.
 165. Suzuki K, Mori I, Nakayama Y, Miyakoda M, Kodama S, Watanabe M, Radiation-induced senescence-like growth arrest requires TP53 function but not telomere shortening. *Radiation Research* 2001; 155, 248-53.
 166. Suzuki M, Boothman DA, Stress-induced premature senescence (SIPS) – Influence of SIPS on radiotherapy. *Journal of Radiation Research* 2008; 49, 105-12.
 167. UNSCEAR, Sources and effects of ionizing radiation. New York: United Nations; 2008.
 168. Drooger JC, Hooning MJ, Seynaeve CM, Baaijens MHA, Obdeijn IM, Sleijfer S, et al., Diagnostic and therapeutic ionizing radiation and the risk of a first and second primary breast cancer, with special attention for BRCA1 and BRCA2 mutation carriers: A critical review of the literature. *Cancer Treatment Reviews* 2015; 41, 187-96.
 169. Amaldi U, Kraft G, European developments in radiotherapy with beams of large radiobiological effectiveness. *Journal of Radiation Research* 2007; 48, A27-A41.
 170. Mayles P, Nahum A, Rosenwald JC, Handbook of radiotherapy physics. New York: Taylor & Francis; 2007.
 171. Withers HR, The four R's of radiotherapy. *Advances in radiobiology* 1975; 5, 241-71.
 172. Brown JM, Carlson DJ, Brenner DJ, The Tumor Radiobiology of SRS and SBRT: Are More Than the 5 Rs Involved? *International Journal of Radiation Oncology Biology Physics* 2014; 88, 254-62.
 173. Steel GG, McMillan TJ, Peacock JH, The 5Rs of radiobiology. *International Journal of Radiation Biology* 1989; 56, 1045-48.
 174. Sinclair WK, Morton RA, X-ray sensitivity during cell generation cycle of cultured chinese hamster cells. *Radiation Research* 1966; 29, 450-&.
 175. Prasanna A, Ahmed MM, Mohiuddin M, Coleman CN, Exploiting sensitization windows of opportunity in hyper and hypo-fractionated radiation therapy. *Journal of Thoracic Disease* 2014; 6, 287-302.
 176. Fuks Z, Kolesnick R, Engaging the vascular component of the tumor response. *Cancer Cell* 2005; 8, 89-91.
 177. Okayasu R, Repair of DNA damage induced by accelerated heavy ionsuA mini review. *Int J*

- Cancer 2012; 130, 991-1000.
178. Amaldi U, Kraft G, Radiotherapy with beams of carbon ions. Reports on Progress in Physics 2005; 68, 1861-82.
 179. Jones DTL, Wambersie A, Radiation therapy with fast neutrons: A review. Nuclear Instruments & Methods in Physics Research Section a-Accelerators Spectrometers Detectors and Associated Equipment 2007; 580, 522-25.
 180. Alsner J, Andreassen CN, Overgaard J, Genetic markers for prediction of normal tissue toxicity after radiotherapy. Seminars in radiation oncology 2008; 18, 126-35.
 181. Stone HB, Coleman CN, Anscher MS, McBride WH, Effects of radiation on normal tissue: consequences and mechanisms. Lancet Oncol 2003; 4, 529-36.
 182. Bentzen SM, Preventing or reducing late side effects of radiation therapy: radiobiology meets molecular pathology. Nat Rev Cancer 2006; 6, 702-13.
 183. Barnett GC, West CML, Dunning AM, Elliott RM, Coles CE, Pharoah PDP, et al., Normal tissue reactions to radiotherapy: towards tailoring treatment dose by genotype. Nat Rev Cancer 2009; 9, 134-42.
 184. Bentzen SM, Thames HD, Overgaard M, Latent-time estimation for late cutaneous and subcutaneous radiation reactions in a single-follup-up clinical study. Radiother Oncol 1989; 15, 267-74.
 185. Dubray B, Delanian S, Lefaix JL, Late effects of mammary radiotherapy on skin and subcutaneous tissues. Cancer Radiother 1997; 1, 744-52.
 186. Peters LJ, Radiation therapy tolerance limits. For one or for all?--Janeway Lecture. Cancer 1996; 77, 2379-85.
 187. Barcellos-Hoff MH, How do tissues respond to damage at the cellular level? The role of cytokines in irradiated tissues. Radiation Research 1998; 150, S109-S20.
 188. Allan JM, Lois BT, Mechanisms of therapy-related carcinogenesis. Nat Rev Cancer 2005; 5, 943-55.
 189. Boice JD, Cancer following irradiation in childhood and adolescence. Medical and Pediatric Oncology 1996, 29-34.
 190. Globocan, <http://globocan.iarc.fr/Default.aspx>.
 191. Althuis MD, Dozier JM, Anderson WF, Devesa SS, Brinton LA, Global trends in breast cancer incidence and mortality 1973-1997. International Journal of Epidemiology 2005; 34, 405-12.
 192. Parkin DM, Fernandez LMG, Use of statistics to assess the global burden of breast cancer. Breast Journal 2006; 12, S70-S80.
 193. Jemal A, Center MM, DeSantis C, Ward EM, Global Patterns of Cancer Incidence and Mortality Rates and Trends. Cancer Epidemiology Biomarkers & Prevention 2010; 19, 1893-907.
 194. Beral V, Bull D, Doll R, Peto R, Reeves G, La Vecchia C, et al., Breast cancer and breastfeeding: collaborative reanalysis of individual data from 47 epidemiological studies in 30 countries, including 50 302 women with breast cancer and 96 973 women without the disease.

- Lancet 2002; 360, 187-95.
195. Beral V, Bull D, Pirie K, Reeves G, Peto R, Skegg D, et al., Menarche, menopause, and breast cancer risk: individual participant meta-analysis, including 118 964 women with breast cancer from 117 epidemiological studies. *Lancet Oncology* 2012; 13, 1141-51.
 196. Clavel-Chapelon F, Gerber M, Reproductive factors and breast cancer risk. Do they differ according to age at diagnosis ? *Breast Cancer Research and Treatment* 2002; 72, 107-15.
 197. Hilakivi-Clarke L, de Assis S, Warri A, Exposures to Synthetic Estrogens at Different Times During the Life, and Their Effect on Breast Cancer Risk. *Journal of Mammary Gland Biology and Neoplasia* 2013; 18, 25-42.
 198. Rossouw JE, Anderson GL, Prentice RL, LaCroix AZ, Kooperberg C, Stefanick ML, et al., Risks and benefits of estrogen plus progestin in healthy postmenopausal women – Principal results from the Women’s Health Initiative randomized controlled trial. *Jama-Journal of the American Medical Association* 2002; 288, 321-33.
 199. Beral V, Bull D, Doll R, Key T, Peto R, Reeves G, et al., Breast cancer and hormone replacement therapy: collaborative reanalysis of data from 51 epidemiological studies of 52,705 women with breast cancer and 108,411 women without breast cancer. *Lancet* 1997; 350, 1047-59.
 200. Calle EE, Heath CW, MiracleMcMahill HL, Coates RJ, Liff JM, Franceschi S, et al., Breast cancer and hormonal contraceptives: Collaborative reanalysis of individual data on 53297 women with breast cancer and 100239 women without breast cancer from 54 epidemiological studies. *Lancet* 1996; 347, 1713-27.
 201. Zhu H, Lei X, Feng J, Wang Y, Oral contraceptive use and risk of breast cancer: A meta-analysis of prospective cohort studies. *European Journal of Contraception and Reproductive Health Care* 2012; 17, 402-14.
 202. Research WCRFAIfC, Food, Nutrition, Physical Activity, and the prevention of Cancer: a Global Perspective. Washington DC; 2007.
 203. Travis RC, Key TJ, Oestrogen exposure and breast cancer risk. *Breast Cancer Research* 2003; 5, 239-47.
 204. McCormack VA, Silva IDS, Breast density and parenchymal patterns as markers of breast cancer risk: A meta-analysis. *Cancer Epidemiology Biomarkers & Prevention* 2006; 15, 1159-69.
 205. Boyd NF, Dite GS, Stone J, Gunasekara A, English DR, McCredie MRE, et al., Heritability of mammographic density, a risk factor for breast cancer. *New England Journal of Medicine* 2002; 347, 886-94.
 206. Boyd NF, Guo H, Martin LJ, Sun LM, Stone J, Fishell E, et al., Mammographic density and the risk and detection of breast cancer. *New England Journal of Medicine* 2007; 356, 227-36.
 207. Boyd NF, Martin LJ, Bronskill M, Yaffe MJ, Duric N, Minkin S, Breast Tissue Composition and Susceptibility to Breast Cancer. *Journal of the National Cancer Institute* 2010; 102, 1224-37.
 208. Melnikow J, Fenton JJ, Whitlock EP, Miglioretti DL, Weyrich MS, Thompson JH, et al.,

- Supplemental Screening for Breast Cancer in Women With Dense Breasts: A Systematic Review for the US Preventive Services Task Force. *Annals of Internal Medicine* 2016; 164, 268-+.
209. Wanebo CK, Johnson KG, Sato K, Thorslund TW. Breast cancer after exposure to atomic bombings of Hiroshima and Nagasaki. *New England Journal of Medicine* 1968; 279, 667-72.
 210. Boice JD, Harvey EB, Blettner M, Stovall M, Flannery JT. Cancer in the contralateral breast after radiotherapy for breast-cancer. *New England Journal of Medicine* 1992; 326, 781-85.
 211. Boice JD, Preston D, Davis FG, Monson RR. Frequent chest-X-ray fluoroscopy and breast-cancer incidence among tuberculosis patients in Massachusetts. *Radiation Research* 1991; 125, 214-22.
 212. Howe GR, McLaughlin J. Breast cancer mortality between 1950 and 1987 after exposure to fractionated moderate-dose-rate ionizing radiation in the Canadian Fluoroscopy Cohort Study and a comparison with breast cancer mortality in the Atomic Bomb Survivors Study. *Radiation Research* 1996; 145, 694-707.
 213. Hancock SL, Tucker MA, Hoppe RT. Breast-cancer after treatment of Hodgkin's disease. *Journal of the National Cancer Institute* 1993; 85, 25-31.
 214. Doody MM, Lonstein JE, Stovall M, Hacker DG, Luckyanov N, Land CE, et al., Breast cancer mortality after diagnostic radiography – Findings from the US Scoliosis Cohort Study. *Spine* 2000; 25, 2052-63.
 215. Brooks JD, Boice JD, Stovall M, Reiner AS, Bernstein L, John EM, et al., Reproductive Status at First Diagnosis Influences Risk of Radiation-Induced Second Primary Contralateral Breast Cancer in the WECARE Study. *International Journal of Radiation Oncology Biology Physics* 2012; 84, 917-24.
 216. Ronckers CM, Doody MM, Lonstein JE, Stovall M, Land CE. Multiple diagnostic x-rays for spine deformities and risk of breast cancer. *Cancer Epidemiology Biomarkers & Prevention* 2008; 17, 605-13.
 217. Shore RE, Woodard ED, Hempelmann LH, Pasternack BS. Synergism between radiation and other risk-factors for breast-cancer. *Preventive Medicine* 1980; 9, 815-22.
 218. van Leeuwen FE, Klokman WJ, Stovall M, Dahler EC, van't Veer MB, Noordijk EM, et al., Roles of radiation dose, chemotherapy, and hormonal factors in breast cancer following Hodgkin's disease. *Journal of the National Cancer Institute* 2003; 95, 971-80.
 219. UNSCEAR, Sources, Effects and Risks of ionizing radiation. . In: Radiation UNSCotEoA editor.; 2013.
 220. Hill DA, Gilbert E, Dores GM, Gospodarowicz M, van Leeuwen FE, Holowaty E, et al., Breast cancer risk following radiotherapy for Hodgkin lymphoma: modification by other risk factors. *Blood* 2005; 106, 3358-65.
 221. Bernstein JL, Haile RW, Stovall M, Grp WSC. Radiotherapy risks recurrence in ATM-mutated breast cancer patients. *Pharmacogenomics* 2010; 11, 673-73.
 222. Bernstein JL, Thomas DC, Shore RE, Robson M, Boice JD, Stovall M, et al., Contralateral breast cancer after radiotherapy among BRCA1 and BRCA2 mutation carriers: A WECARE

- Study Report. *Eur J Cancer* 2013; 49, 2979-85.
223. Broeks A, Braaf LM, Huseinovic A, Nooijen A, Urbanus J, Hogervorst FBL, et al., Identification of women with an increased risk of developing radiation-induced breast cancer: a case only study. *Breast Cancer Research* 2007; 9, 9.
224. Preston DL, Mattsson A, Holmberg E, Shore R, Hildreth NG, Boice JD, Radiation effects on breast cancer risk: A pooled analysis of eight cohorts. *Radiation Research* 2002; 158, 220-35.
225. Beral V, Bull D, Doll R, Peto R, Reeves G, Collaborative Group on Hormonal Factors in Breast C, Familial breast cancer: collaborative reanalysis of individual data from 52 epidemiological studies including 58 209 women with breast cancer and 101 986 women without the disease. *Lancet* 2001; 358, 1389-99.
226. Lichtenstein P, Holm NV, Verkasalo PK, Iliadou A, Kaprio J, Koskenvuo M, et al., Environmental and heritable factors in the causation of cancer – Analyses of cohorts of twins from Sweden, Denmark, and Finland. *New England Journal of Medicine* 2000; 343, 78-85.
227. Peto J, Mack TM, High constant incidence in twins and other relatives of women with breast cancer. *Nature Genet* 2000; 26, 411-14.
228. Claus EB, Risch N, Thompson WD, Genetic-analysis of breast-cancer in the cancer and steroid-hormone study. *Am J Hum Genet* 1991; 48, 232-42.
229. Newman B, Austin MA, Lee M, King MC, Inheritance of human-breast cancer – Evidence for autosomal dominant transmission in high-risk families. *Proceedings of the National Academy of Sciences of the United States of America* 1988; 85, 3044-48.
230. Hall JM, Lee MK, Newman B, Morrow JE, Anderson LA, Huey B, et al., Linkage of early-onset familial breast-cancer to chromosome-17Q21. *Science* 1990; 250, 1684-89.
231. Miki Y, Swensen J, Shattuckeids D, Futreal PA, Harshman K, Tavtigian S, et al., A strong candidate for the breast and ovarian cancer susceptibility gene BRCA1. *Science* 1994; 266, 66-71.
232. Economopoulou P, Dimitriadis G, Psyri A, Beyond BRCA: New hereditary breast cancer susceptibility genes. *Cancer Treatment Reviews* 2015; 41, 1-8.
233. Shiovitz S, Korde LA, Genetics of breast cancer: a topic in evolution. *Annals of Oncology* 2015; 26, 1291-99.
234. Renwick A, Thompson D, Seal S, Kelly P, Chagtai T, Ahmed M, et al., ATM mutations that cause ataxia-telangiectasia are breast cancer susceptibility alleles. *Nature Genet* 2006; 38, 873-75.
235. Rahman N, Seal S, Thompson D, Kelly P, Renwick A, Elliott A, et al., PALB2, which encodes a BRCA2-interacting protein, is a breast cancer susceptibility gene. *Nature Genet* 2007; 39, 165-67.
236. Seal S, Thompson D, Renwick A, Elliott A, Kelly P, Barfoot R, et al., Truncating mutations in the Fanconi anemia J gene BRIP1 are low-penetrance breast cancer susceptibility alleles. *Nature Genet* 2006; 38, 1239-41.
237. Stratton MR, Rahman N, The emerging landscape of breast cancer susceptibility. *Nature Genet* 2008; 40, 17-22.

238. Turnbull C, Ahmed S, Morrison J, Pernet D, Renwick A, Maranian M, et al., Genome-wide association study identifies five new breast cancer susceptibility loci. *Nature Genet* 2010; 42, 504-U47.
239. Lalloo F, Evans DG, Familial Breast Cancer. *Clinical Genetics* 2012; 82, 105-14.
240. Couch FJ, Nathanson KL, Offit K, Two Decades After BRCA: Setting Paradigms in Personalized Cancer Care and Prevention. *Science* 2014; 343, 1466-70.
241. Rebbeck TR, Mitra N, Wan F, Sinilnikova OM, Healey S, McGuffog L, et al., Association of Type and Location of BRCA1 and BRCA2 Mutations With Risk of Breast and Ovarian Cancer. *Jama-Journal of the American Medical Association* 2015; 313, 1347-61.
242. Couch FJ, Wang XS, McGuffog L, Lee A, Olswold C, Kuchenbaecker KB, et al., Genome-Wide Association Study in BRCA1 Mutation Carriers Identifies Novel Loci Associated with Breast and Ovarian Cancer Risk. *Plos Genetics* 2013; 9, 21.
243. Gaudet MM, Kuchenbaecker KB, Vijai J, Klein RJ, Kirchoff T, McGuffog L, et al., Identification of a BRCA2-Specific Modifier Locus at 6p24 Related to Breast Cancer Risk. *Plos Genetics* 2013; 9, 15.
244. Evans DG, Shenton A, Woodward E, Lalloo F, Howell A, Maher ER, Penetrance estimates for BRCA1 and BRCA2 based on genetic testing in a Clinical Cancer Genetics service setting: Risks of breast/ovarian cancer quoted should reflect the cancer burden in the family. *BMC Cancer* 2008; 8, 9.
245. Ford D, Easton DF, Stratton M, Narod S, Goldgar D, Devilee P, et al., Genetic heterogeneity and penetrance analysis of the BRCA1 and BRCA2 genes in breast cancer families. *Am J Hum Genet* 1998; 62, 676-89.
246. Chen SN, Iversen ES, Friebel T, Finkelstein D, Weber BL, Eisen A, et al., Characterization of BRCA1 and BRCA2 mutations in a large United States sample. *Journal of Clinical Oncology* 2006; 24, 863-71.
247. Antoniou A, Pharoah PDP, Narod S, Risch HA, Eyfjord JE, Hopper JL, et al., Average risks of breast and ovarian cancer associated with BRCA1 or BRCA2 mutations detected in case series unselected for family history: A combined analysis of 22 studies. *Am J Hum Genet* 2003; 72, 1117-30.
248. Thompson D, Easton DF, Breast Canc Linkage C, Cancer incidence in BRCA1 mutation carriers. *Journal of the National Cancer Institute* 2002; 94, 1358-65.
249. Hogervorst FBL, Nederlof PM, Gille JJP, McElgunn CJ, Grippeling M, Pruntel R, et al., Large genomic deletions and duplications in the BRCA1 gene identified by a novel quantitative method. *Cancer Research* 2003; 63, 1449-53.
250. Oddoux C, Struwing JP, Clayton CM, Neuhausen S, Brody LC, Kaback M, et al., The carrier frequency of the BRCA2 6174delT mutation among Ashkenazi Jewish individuals is approximately 1%. *Nature Genet* 1996; 14, 188-90.
251. Roa BB, Boyd AA, Volcik K, Richards CS, Ashkenazi Jewish population frequencies for common mutations in BRCA1 and BRCA2. *Nature Genet* 1996; 14, 185-87.
252. Huen MSY, Sy SMH, Chen JJ, BRCA1 and its toolbox for the maintenance of genome integ-

- rity. *Nature Reviews Molecular Cell Biology* 2010; 11, 138-48.
253. Deng CX, Brodie SG, Roles of BRCA1 and its interacting proteins. *Bioessays* 2000; 22, 728-37.
254. Yun MH, Hiom K, CtIP-BRCA1 modulates the choice of DNA double-strand-break repair pathway throughout the cell cycle. *Nature* 2009; 459, 460-U184.
255. Wang B, Matsuoka S, Ballif BA, Zhang D, Smogorzewska A, Gygi SP, et al., Abraxas and RAP80 form a BRCA1 protein complex required for the DNA damage response. *Science* 2007; 316, 1194-98.
256. Kim H, Chen JJ, Yu XH, Ubiquitin-binding protein RAP80 mediates BRCA1-dependent DNA damage response. *Science* 2007; 316, 1202-05.
257. Kim H, Huang J, Chen JJ, CCDC98 is a BRCA1-BRCT domain-binding protein involved in the DNA damage response. *Nature Structural & Molecular Biology* 2007; 14, 710-15.
258. Bunting SF, Callen E, Wong N, Chen HT, Polato F, Gunn A, et al., 53BP1 Inhibits Homologous Recombination in Brca1-Deficient Cells by Blocking Resection of DNA Breaks. *Cell* 2010; 141, 243-54.
259. Fabbro M, Savage K, Hobson K, Deans AJ, Powell SN, McArthur GA, et al., BRCA1-BARD1 complexes are required for p53(Ser-15) phosphorylation and a G(1)/S arrest following ionizing radiation-induced DNA damage. *Journal of Biological Chemistry* 2004; 279, 31251-58.
260. Siliciano JD, Canman CE, Taya Y, Sakaguchi K, Appella E, Kastan MB, DNA damage induces phosphorylation of the amino terminus of p53. *Genes & Development* 1997; 11, 3471-81.
261. Xu B, Kim ST, Kastan MB, Involvement of Brca1 in S-phase and G(2)-phase checkpoints after ionizing irradiation. *Molecular and Cellular Biology* 2001; 21, 3445-50.
262. Wooster R, Neuhausen SL, Mangion J, Quirk Y, Ford D, Collins N, et al., Localizaion of breast-cancer susceptibility gene, BRCA2, to chromosome 13Q12-13. *Science* 1994; 265, 2088-90.
263. Chen SN, Parmigiani G, Meta-analysis of BRCA1 and BRCA2 penetrance. *Journal of Clinical Oncology* 2007; 25, 1329-33.
264. Lalloo F, Varley J, Ellis D, Moran A, O'Dair L, Pharoah P, et al., Prediction of pathogenic mutations in patients with early-onset breast cancer by family history. *Lancet* 2003; 361, 1101-02.
265. Peto J, Collins N, Barfoot R, Seal S, Warren W, Rahman N, et al., Prevalence of BRCA1 and BRCA2 gene mutations in patients with early-onset breast cancer. *Journal of the National Cancer Institute* 1999; 91, 943-49.
266. van Asperen CJ, Brohet RM, Meijers-Heijboer EJ, Hoogerbrugge N, Verhoef S, Vasen HFA, et al., Cancer risks in BRCA2 families: estimates for sites other than breast and ovary. *Journal of Medical Genetics* 2005; 42, 711-19.
267. Basham VM, Lipscombe JM, Ward JM, Gayther SA, Ponder BAJ, Easton DF, et al., BRCA1 and BRCA2 mutations in a population-based study of male breast cancer. *Breast Cancer*

- Research 2002; 4, 5.
268. Roy R, Chun J, Powell SN, BRCA1 and BRCA2: different roles in a common pathway of genome protection. *Nat Rev Cancer* 2012; 12, 68-78.
 269. Reid S, Renwick A, Seal S, Baskcomb L, Barfoot R, Jayatilake H, et al., Biallelic BRCA2 mutations are associated with multiple malignancies in childhood including familial Wilms tumour. *Journal of Medical Genetics* 2005; 42, 147-51.
 270. Kitao H, Takata M, Fanconi anemia: a disorder defective in the DNA damage response. *International Journal of Hematology* 2011; 93, 417-24.
 271. Moynahan ME, Pierce AJ, Jasin M, BRCA2 is required for homology-directed repair of chromosomal breaks. *Mol Cell* 2001; 7, 263-72.
 272. Yuan SSF, Lee SY, Chen G, Song MH, Tomlinson GE, Lee E, BRCA2 is required for ionizing radiation-induced assembly of rad51 complex in vivo. *Cancer Research* 1999; 59, 3547-51.
 273. Puliti D, Zappa M, Breast cancer screening: are we seeing the benefit? *Bmc Medicine* 2012; 10, 4.
 274. Feig SA, Auditing and benchmarks in screening and diagnostic mammography. *Radiol Clin N Am* 2007; 45, 791-+.
 275. Klein R, Aichinger H, Dierker J, Jansen JTM, JoiteBarfuss S, Sabel M, et al., Determination of average glandular dose with modern mammography units for two large groups of patients. *Physics in Medicine and Biology* 1997; 42, 651-71.
 276. Hendrick RE, Pisano ED, Averbukh A, Moran C, Berns EA, Yaffe MJ, et al., Comparison of Acquisition Parameters and Breast Dose in Digital Mammography and Screen-Film Mammography in the American College of Radiology Imaging Network Digital Mammographic Imaging Screening Trial. *American Journal of Roentgenology* 2010; 194, 362-69.
 277. Hendrick RE, Radiation Doses and Cancer Risks from Breast Imaging Studies. *Radiology* 2010; 257, 246-53.
 278. Altobelli E, Lattanzi A, Breast cancer in European Union: An update of screening programmes as of March 2014 (Review). *International Journal of Oncology* 2014; 45, 1785-92.
 279. Kuhl CK, Kuhn W, Schild H, Management of women at high risk for breast cancer: New imaging beyond mammography. *Breast* 2005; 14, 480-86.
 280. Kolb TM, Lichy J, Newhouse JH, Comparison of the performance of screening mammography, physical examination, and breast US and evaluation of factors that influence them: An analysis of 27,825 patient evaluations. *Radiology* 2002; 225, 165-75.
 281. Mandelson MT, Oestreicher N, Porter PL, White D, Finder CA, Taplin SH, et al., Breast density as a predictor of mammographic detection: Comparison of interval- and screen-detected cancers. *Journal of the National Cancer Institute* 2000; 92, 1081-87.
 282. Paci E, Broeders M, Hofvind S, Puliti D, Duffy SW, Grp EW, European Breast Cancer Service Screening Outcomes: A First Balance Sheet of the Benefits and Harms. *Cancer Epidemiology Biomarkers & Prevention* 2014; 23, 1159-63.
 283. Campari C, Rossi PG, Mori CA, Ravaioli S, Nitrosi A, Vacondio R, et al., Impact of the In-

- roduction of Digital Mammography in an Organized Screening Program on the Recall and Detection Rate. *J Digit Imaging* 2016; 29, 235-42.
284. Jacobsen KK, Abraham L, Buist DSM, Hubbard RA, O'Meara ES, Sprague BL, et al., Comparison of cumulative false-positive risk of screening mammography in the United States and Denmark. *Cancer Epidemiology* 2015; 39, 656-63.
285. Aslund M, Cederstrom B, Lundqvist M, Danielsson M, Scatter rejection in multislit digital mammography. *Medical Physics* 2006; 33, 933-40.
286. Cole EB, Toledano AY, Lundqvist M, Pisano ED, Comparison of Radiologist Performance with Photon-Counting Full-Field Digital Mammography to Conventional Full-Field Digital Mammography. *Academic Radiology* 2012; 19, 916-22.
287. Skaane P, Bandos AI, Gullien R, Eben EB, Ekseth U, Haakenaasen U, et al., Comparison of Digital Mammography Alone and Digital Mammography Plus Tomosynthesis in a Population-based Screening Program. *Radiology* 2013; 267, 47-56.
288. Drukteinis JS, Mooney BP, Flowers CI, Gatenby RA, Beyond Mammography: New Frontiers in Breast Cancer Screening. *American Journal of Medicine* 2013; 126, 472-79.
289. Kelly KM, Dean J, Comulada WS, Lee SJ, Breast cancer detection using automated whole breast ultrasound and mammography in radiographically dense breasts. *European Radiology* 2010; 20, 734-42.
290. Kelly KM, Richwald GA, Automated Whole-Breast Ultrasound: Advancing the Performance of Breast Cancer Screening. *Seminars in Ultrasound Ct and Mri* 2011; 32, 273-80.
291. Berg WA, Zhang Z, Lehrer D, Jong RA, Pisano ED, Barr RG, et al., Detection of Breast Cancer With Addition of Annual Screening Ultrasound or a Single Screening MRI to Mammography in Women With Elevated Breast Cancer Risk. *Jama-Journal of the American Medical Association* 2012; 307, 1394-404.
292. Saslow D, Boetes C, Burke W, Harms S, Leach MO, Lehman CD, et al., American Cancer Society guidelines for breast screening with MRI as an adjunct to mammography. *Ca-a Cancer Journal for Clinicians* 2007; 57, 75-89.
293. young B, Heath JW, Wheather's Functional Histology. 4 ed. Edinburgh: Harcourt Publishers; 2000.
294. Sinn HP, Kreipe H, A Brief Overview of the WHO Classification of Breast Tumors, 4th Edition, Focusing on Issues and Updates from the 3rd Edition. *Breast Care* 2013; 8, 149-54.
295. Welch HG, Woloshin S, Schwartz LM, The sea of uncertainty surrounding ductal carcinoma in situ – The price of screening mammography. *Journal of the National Cancer Institute* 2008; 100, 228-29.
296. Cowell CF, Weigelt B, Sakr RA, Ng CKY, Hicks J, King TA, et al., Progression from ductal carcinoma in situ to invasive breast cancer: Revisited. *Molecular Oncology* 2013; 7, 859-69.
297. Li CI, Anderson BO, Daling JR, Moe RE, Trends in incidence rates of invasive lobular and ductal breast carcinoma. *Jama-Journal of the American Medical Association* 2003; 289, 1421-24.
298. Li CI, Daling JR, Changes in breast cancer incidence rates in the united states by histologic

- subtype and race/ethnicity, 1995 to 2004. *Cancer Epidemiology Biomarkers & Prevention* 2007; 16, 2773-80.
299. Li CI, Uribe DJ, Daling JR, Clinical characteristics of different histologic types of breast cancer. *British Journal of Cancer* 2005; 93, 1046-52.
 300. Dossus L, Benusiglio PR, Lobular breast cancer: incidence and genetic and non-genetic risk factors. *Breast Cancer Research* 2015; 17, 8.
 301. Mavaddat N, Barrowdale D, Andrulis IL, Domchek SM, Eccles D, Nevanlinna H, et al., Pathology of Breast and Ovarian Cancers among BRCA1 and BRCA2 Mutation Carriers: Results from the Consortium of Investigators of Modifiers of BRCA1/2 (CIMBA). *Cancer Epidemiology Biomarkers & Prevention* 2012; 21, 134-47.
 302. Rakha EA, Patel A, Powe D, Benhasouna A, Green AR, Lambros MB, et al., Clinical and Biological Significance of E-cadherin Protein Expression in Invasive Lobular Carcinoma of the Breast. *American Journal of Surgical Pathology* 2010; 34, 1472-79.
 303. Gannon LM, Cotter MB, Quinn CM, The classification of invasive carcinoma of the breast. *Expert Review of Anticancer Therapy* 2013; 13, 941-54.
 304. Howlader N, Chen VW, Ries LAG, Loch MM, Lee R, DeSantis C, et al., Overview of Breast Cancer Collaborative Stage Data Items-Their Definitions, Quality, Usage, and Clinical Implications: A Review of SEER Data for 2004-2010. *Cancer* 2014; 120, 3771-80.
 305. Fowble B, Solin LJ, Schultz DJ, Rubenstein J, Goodman RL, Breast recurrence following conservative surgery and radiation – patterns of failure, prognosis and pathological findings from mastectomy specimen with implications for treatment. *International Journal of Radiation Oncology Biology Physics* 1990; 19, 833-42.
 306. Kurtz JM, Amalric R, Brandone H, Ayme Y, Jacquemier J, Pietra JC, et al., Local recurrence after breast-conserving surgery and radiotherapy – frequency, time course and prognosis. *Cancer* 1989; 63, 1912-17.
 307. Smith TE, Lee D, Turner BC, Carter D, Haffty BG, True recurrence vs. new primary ipsilateral breast tumor relapse: An analysis of clinical and pathologic differences and their implications in natural history, prognoses, and therapeutic management. *International Journal of Radiation Oncology Biology Physics* 2000; 48, 1281-89.
 308. Fisher ER, Anderson S, Redmond C, Fisher B, Ipsilateral breast-tumor recurrence and survival following lumpectomy and irradiation – pathological findings from NSABP protocol B-06. *Seminars in Surgical Oncology* 1992; 8, 161-66.
 309. Holland R, Veling SHJ, Mravunac M, Hendriks J, Histologic multifocality of T1S, T1-2 breast carcinomas – implications for clinical trials of breast-conserving surgery. *Cancer* 1985; 56, 979-90.
 310. Vaidya JS, Vyas JJ, Chinoy RF, Merchant N, Sharma OP, Mitra I, Multicentricity of breast cancer: Whole-organ analysis and clinical implications. *British Journal of Cancer* 1996; 74, 820-24.
 311. Bentzen SM, Agrawal RK, Aird EGA, Barrett JM, Barrett-Lee PJ, Bliss JM, et al., The UK Standardisation of Breast Radiotherapy (START) Trial B of radiotherapy hypofractionation

- for treatment of early breast cancer: a randomised trial. *Lancet* 2008; 371, 1098-107.
312. Bentzen SM, Agrawal RK, Aird EGA, Barrett JM, Barrett-Lee PJ, Bliss JM, et al., The UK Standardisation of Breast Radiotherapy (START) Trial A of radiotherapy hypofractionation for treatment of early breast cancer: A randomised trial. *Lancet Oncology* 2008; 9, 331-41.
313. Ragaz J, Jackson SM, Le N, Plenderleith IH, Spinelli JJ, Basco VE, et al., Adjuvant radiotherapy and chemotherapy in node-positive premenopausal women with breast cancer. *New England Journal of Medicine* 1997; 337, 956-62.
314. Ragaz J, Olivotto IA, Spinelli JJ, Phillips N, Jackson SM, Wilson KS, et al., Locoregional radiation therapy in patients with high-risk breast cancer receiving adjuvant chemotherapy: 20-year results of the British Columbia randomized trial. *Jnci-Journal of the National Cancer Institute* 2005; 97, 116-26.
315. Vallis KA, Tannock IF, Postoperative radiotherapy for breast cancer: Growing evidence for an impact on survival. *Jnci-Journal of the National Cancer Institute* 2004; 96, 88-89.
316. EBCTCG, Effect of radiotherapy after breast-conserving surgery on 10-year recurrence and 15-year breast cancer death: meta-analysis of individual patient data for 10801 women in 17 randomized trials. *Lancet* 2011; 378, 1707-60.
317. Whelan TJ, Olivotto I, Ackerman I, Chapman JW, Chua B, Nabid A, et al., NCIC-CTG MA. 20: An intergroup trial of regional nodal irradiation in early breast cancer. *Journal of Clinical Oncology* 2011; 29, 1.
318. Feight D, Baney T, Bruce S, McQuestion M, Putting Evidence Into Practice: Evidence-Based Interventions for Radiation Dermatitis. *Clinical Journal of Oncology Nursing* 2011; 15, 481-92.
319. Waljee JF, Hu ES, Ubel PA, Smith DM, Newman LA, Alderman AK, Effect of esthetic outcome after breast-conserving surgery on psychosocial functioning and quality of life. *Journal of clinical oncology : official journal of the American Society of Clinical Oncology* 2008; 26, 3331-7.
320. De Langhe S, Mulliez T, Veldeman L, Remouchamps V, van Greveling A, Gilsoul M, et al., Factors modifying the risk for developing acute skin toxicity after whole-breast intensity modulated radiotherapy. *BMC Cancer* 2014; 14, 9.
321. Bentzen SM, Constine LS, Deasy JO, Eisbruch A, Jackson A, Marks LB, et al., Quantitative analysis of normal tissue effects in the clinic (Quantec): an introduction to the scientific issues. *International Journal of Radiation Oncology Biology Physics* 2010; 76, S3-S9.
322. Deantonio L, Gambaro G, Beldi D, Masini L, Tunesi S, Magnani C, et al., Hypofractionated radiotherapy after conservative surgery for breast cancer: analysis of acute and late toxicity. *Radiation Oncology* 2010; 5, 7.
323. Barnett GC, Wilkinson JS, Moody AM, Wilson CB, Twyman N, Wishart GC, et al., The Cambridge Breast Intensity-modulated Radiotherapy Trial: Patient- and Treatment-related Factors that Influence Late Toxicity. *Clin Oncol* 2011; 23, 662-73.
324. Marcu LG, Santos A, Bezak E, Risk of second primary cancer after breast cancer treatment. *European Journal of Cancer Care* 2014; 23, 51-64.

325. Rosen EM, Day R, Singh VK, New approaches to radiation protection. *Frontiers in Oncology* 2015; 4, 15.
326. Wang X, Zhang X, Li X, Amos RA, Shaitelman SF, Hoffman K, et al., Accelerated partial-breast irradiation using intensity-modulated proton radiotherapy: do uncertainties outweigh potential benefits? *British Journal of Radiology* 2013; 86, 12.
327. Bush DA, Slater JD, Garberoglio C, Do S, Lum S, Slater JM, Partial Breast Irradiation Delivered With Proton Beam: Results of a Phase II Trial. *Clinical Breast Cancer* 2011; 11, 241-45.
328. Chang JH, Lee NK, Kim JY, Kim YJ, Moon SH, Kim TH, et al., Phase II trial of proton beam accelerated partial breast irradiation in breast cancer. *Radiother Oncol* 2013; 108, 209-14.
329. MacDonald SM, Patel SA, Hickey S, Specht M, Isakoff SJ, Gadd M, et al., Proton Therapy for Breast Cancer After Mastectomy: Early Outcomes of a Prospective Clinical Trial. *International Journal of Radiation Oncology Biology Physics* 2013; 86, 484-90.
330. O'Shaughnessy J, Osborne C, Pippen JE, Yoffe M, Patt D, Rocha C, et al., Iniparib plus Chemotherapy in Metastatic Triple-Negative Breast Cancer. *New England Journal of Medicine* 2011; 364, 205-14.
331. Dowsett M, Forbes JF, Bradley R, Ingle J, Aihara T, Bliss J, et al., Aromatase inhibitors versus tamoxifen in early breast cancer: patient-level meta-analysis of the randomised trials. *Lancet* 2015; 386, 1341-52.
332. Hicks DG, Kulkarni S, Trastuzumab as adjuvant therapy for early breast cancer – The importance of accurate human epidermal growth factor receptor 2 testing. *Archives of Pathology & Laboratory Medicine* 2008; 132, 1008-15.
333. Rogakou EP, Pilch DR, Orr AH, Ivanova VS, Bonner WM, DNA double-stranded breaks induce histone H2AX phosphorylation on serine 139. *Journal of Biological Chemistry* 1998; 273, 5858-68.
334. Horn S, Barnard S, Rothkamm K, Gamma-H2AX-Based Dose Estimation for Whole and Partial Body Radiation Exposure. *Plos One* 2011; 6, 8.
335. Leatherbarrow EL, Harper JV, Cucinotta FA, O'Neill P, Induction and quantification of gamma-H2AX foci following low and high LET-irradiation. *International Journal of Radiation Biology* 2006; 82, 111-18.
336. Olive PL, Banath JP, Phosphorylation of histone H2AX as a measure of radiosensitivity. *International Journal of Radiation Oncology Biology Physics* 2004; 58, 331-35.
337. Vandersickel V, Depuydt J, Van Bockstaele B, Perletti G, Philippe J, Thierens H, et al., Early Increase of Radiation-induced gamma H2AX Foci in a Human Ku70/80 Knockdown Cell Line Characterized by an Enhanced Radiosensitivity. *Journal of Radiation Research* 2010; 51, 633-41.
338. Antonelli F, Belli M, Cuttone G, Dini V, Esposito G, Simone G, et al., Induction and repair of DNA double-strand breaks in human cells: Dephosphorylation of histone H2AX and its inhibition by calyculin A. *Radiation Research* 2005; 164, 514-17.
339. Schultz LB, Chehab NH, Malikzay A, Halazonetis TD, p53 Binding protein 1 (53BP1) is an early participant in the cellular response to DNA double-strand breaks. *Journal of Cell*

- Biology 2000; 151, 1381-90.
340. Horn S, Barnard S, Brady D, Prise KM, Rothkamm K, Combined analysis of gamma-H2AX /53BP1 foci and caspase activation in lymphocyte subsets detects recent and more remote radiation exposures. *Radiat Res* 2013; 180, 603-9.
 341. West AG, van Attikum H, Chromatin at the crossroads – Meeting on signalling to chromatin epigenetics. *Embo Reports* 2006; 7, 1206-10.
 342. Fenech M, The in vitro micronucleus technique. *Mutation Research-Fundamental and Molecular Mechanisms of Mutagenesis* 2000; 455, 81-95.
 343. Fenech M, Cytokinesis-block micronucleus cytochrome assay. *Nature Protocols* 2007; 2, 1084-104.
 344. Fenech M, The cytokinesis-block micronucleus technique and its application to genotoxicity studies in human populations. *Environmental Health Perspectives* 1993; 101, 101-07.
 345. Baeyens A, Swanson R, Herd O, Ainsbury E, Mabhengi T, Willem P, et al., A semi-automated micronucleus-centromere assay to assess low-dose radiation exposure in human lymphocytes. *International Journal of Radiation Biology* 2011; 87, 923-31.
 346. Vral A, Thierens H, deRidder L, In vitro micronucleus-centromere assay to detect radiation-damage induced by low doses in human lymphocytes. *International Journal of Radiation Biology* 1997; 71, 61-68.
 347. Claes K, Depuydt J, Taylor AMR, Last JI, Baert A, Schietecatte P, et al., Variant Ataxia Telangiectasia: Clinical and Molecular Findings and Evaluation of Radiosensitive Phenotypes in a Patient and Relatives. *Neuromol Med* 2013; 15, 447-57.
 348. Sokal RR, Rohlf FJ, *Biometry: the principles and practice of statistics in biological research*. 4th ed: W. H. Freeman and Company; 2012.
 349. Chua MLK, Horn S, Somaiah N, Davies S, Gothard L, A'Hern R, et al., DNA double-strand break repair and induction of apoptosis in ex vivo irradiated blood lymphocytes in relation to late normal tissue reactions following breast radiotherapy. *Radiation and Environmental Biophysics* 2014; 53, 355-64.
 350. Martinez MM, Reif RD, Pappas D, Detection of apoptosis: A review of conventional and novel techniques. *Analytical Methods* 2010; 2, 996-1004.
 351. Sgonc R, Gruber J, Apoptosis detection: An overview. *Experimental Gerontology* 1998; 33, 525-33.
 352. Demchenko AP, Beyond annexin V: fluorescence response of cellular membranes to apoptosis. *Cytotechnology* 2013; 65, 157-72.
 353. Vandersickel V, Slabbert J, Thierens H, Vral A, Comparison of the colony formation and crystal violet cell proliferation assays to determine cellular radiosensitivity in a repair-deficient MCF10A cell line. *Radiation Measurements* 2011; 46, 72-75.
 354. Slabbert J, Theron T, Serafin A, Jones DTL, Böhm L, Schmitt G, Radiosensitivity variations in human tumor cell lines exposed in vitro to p(66)/Be neutrons or ⁶⁰Co γ-rays. *Strahlenther Onkol* 1996; 172, 567-72.
 355. Cross P, Marshall E, Baguley B, Finlay G, Matthews J, Wilson W, Proliferative assays for the assessment of radiosensitivity of tumor cell lines using 96-well microcultures. *Radiation oncology Investigations* 1994; 1, 261-69.



Part 2

Original research

Outline of the research

Article 1

Induction and disappearance of gamma H2AX foci and formation of micronuclei after exposure of human lymphocytes to Co-60 gamma-rays and p(66) + Be(40) neutrons

Vandersickel V, Beukes P, Van Bockstaele B, Depuydt J, Vral A, Slabbert J.

International Journal of Radiation Biology 2014; 90, 149-58.

The induction of γ H2AX foci and the formation of micronuclei were analyzed in human lymphocytes from 10 healthy donors after exposure to γ -rays and neutrons with doses ranging between 0 and 4 Gy. Also the kinetics of foci-disappearance were followed up to 24h after a dose of 0.5Gy of neutrons and γ -rays in a single donor. We observed a lower number of radiation-induced DNA DSB (γ H2AX foci) for neutron radiation compared to γ -rays until about 4h post-IR, however, foci repair was slower and more residual foci were present at later time points. Furthermore, micronucleus yields following neutron exposure were consistently higher compared to micronucleus yields following γ -ray exposure.

Article 2

The impact of a BRCA1 and BRCA2-mutation on the radiation response induced by gamma rays and neutrons in MCF10-A cells.

Depuydt J, Beukes PR, Baert A, Verstraete B, Van Heetvelde M, Vandersickel V, Thierens H, Slabbert J.P., Vral A.

Submitted to: International Journal of Radiation Biology

Downregulation of BRCA1, BRCA2 and Ku70 proteins in human mammary epithelial MCF-10A cell was obtained using RNA interference transduction. Mock transduced (CONBRCA and CON-Ku70) and knockdown (BRCA1i, BRCA2i and Ku70i) MCF-10A cell were irradiated as mixed cell cultures (G1, S, G2 and M) and as synchronized G1 cultures with γ -rays and fast neutrons. Cellular and chromosomal radiosensitivity was measured with the crystal violet (CV) cell proliferation assay and the micronucleus (MN) assay, respectively. We found that neutrons were more efficient in inducing MN and inhibiting cell proliferation. Furthermore, the BRCA1i, BRCA2i and Ku70i cell lines were characterized by an increased radiosensitivity which is dependent on LET, dose and cell cycle.

Article 3

Relative biological effectiveness of mammography X-rays at the level of DNA and chromosomes in lymphocytes.

Depuydt J, Baert A, Vandersickel V, Thierens H, Vral A.

International Journal of Radiation Biology 2013; 89, 532-38.

The induction of γ H2AX foci and the formation of micronuclei were analyzed in human lymphocytes from 5 healthy donors after exposure to γ -rays and 30kV X-rays with doses ranging between 0 and 2 Gy. We found that 30kV X-rays are slightly more efficient in inducing γ H2AX foci. Micronucleus yields following 30kV exposure were consistently higher compared to micronucleus yields following γ -ray exposure and a low-dose RBE value between 3 and 4 was determined.

Article 4

Relative biological effectiveness of mammography X-rays in breast tissue

Depuydt J, Viaene T, Blondeel P, Roche N, Thierens H, Vral A.

Article in preparation for Radiation Research

The induction of γ H2AX foci in mammary epithelial cells in breast tissue from healthy donors was analyzed after irradiation with 30kV X-rays and γ -rays. The dose response curve following 30kV X-ray irradiation was biphasic, showing a hypersensitive response in the 0 to 20 mGy region, probably caused by the bystander effect. The RBE in the 20-500 mGy dose range was 1 and the RBE in the 0-40 mGy dose range was 3.7.

Article 5

***In vitro* cellular radiosensitivity in relationship to late normal tissue reactions in breast cancer patients: a multi-endpoint case-control study**

Vandevoorde C*, Depuydt J*, Veldeman L, De Neve W, Sebastia N, Wieme G, Baert A, De Lange S, Philippe J, Vral A, Thierens H.

* These authors contributed equally to this work

Submitted to: International Journal of Radiation Biology

The radiosensitivity of 12 cases exhibiting late toxic effects following radiotherapy and 12 matched controls who showed no or minimal effects was assessed with four cellular assays using lymphocytes from the patients: radiation-induced late apoptosis (8Gy, 48h), residual γ H2AX foci (4Gy, 24h), G0 and G2 MN assay. A significant difference was observed between cases and controls for all endpoints, with the apoptosis-assay being the most promising assay. Our results suggest that patient's intrinsic radiosensitivity is involved in the development of late normal tissue reactions after radiotherapy.

Article 1

Induction and disappearance of γ H2AX foci and formation of micronuclei after exposure of human lymphocytes to ^{60}Co γ -rays and p(66)+Be(40) neutrons

Veerle Vandersickel^a, Philip Beukes^a, Bram Van Bockstaele^b, Julie Depuydt^c, Anne Vralc and Jacobus Slabberta.

a NRF iThemba LABS (Laboratory for Accelerated Based Sciences), PO box 722, 7129 Somerset West, South Africa and Department of Medical Imaging and Clinical Oncology, University of Stellenbosch, South Africa

b Department of Experimental-Clinical and Health Psychology, Ghent University, Henri Dunantlaan 2, 9000 Gent, Belgium

c Department of Basic Medical Sciences, Ghent University, De Pintelaan 185, 9000 Gent, Belgium

International Journal of Radiation Biology 2014; 90, 149-58

Abstract

Purpose: To investigate both the formation of micronuclei (MN) and the induction and subsequent loss of phosphorylated histone H2AX foci (γ H2AX foci) after *in vitro* exposure of human lymphocytes to either ^{60}Co γ -rays or p(66)+Be(40) neutrons.

Materials and methods: MN dose response (DR) curves were obtained by exposing isolated lymphocytes of 10 different donors to doses ranging from 0 to 4 Gy γ -rays or 0 to 2 Gy neutrons. Also, γ H2AX foci DR curves were obtained following exposure to doses ranging from 0 to 0.5 Gy of either γ -rays or neutrons. Foci kinetics for lymphocytes for a single donor exposed to 0.5 Gy γ -rays or neutrons were studied up to 24 hours post-irradiation.

Results: Micronuclei yields following neutron exposure were consistently higher compared to that from ^{60}Co γ -rays. All MN yields were over-dispersed compared to a Poisson distribution. Over-dispersion was higher after neutron irradiation for all doses > 0.1 Gy. Up to 4 hours post-irradiation lower yields of neutron-induced γ H2AX foci were observed. Between 4 and 24 hours the numbers of foci from neutrons were consistently higher than that from γ -rays. The half-life of foci disappearance is only marginally longer for neutrons compared to that from γ -rays. Foci formations were more likely to be over-dispersed for neutron irradiations.

Conclusion: Although neutrons are more effective to induce MN, the absolute number of induced γ H2AX foci are less at first compared to γ -rays. With time neutron-induced foci are more persistent. These findings are helpful for using γ H2AX foci in biodosimetry and to understand the repair of neutron-induced cellular damage.

Introduction

Exposure of cells to ionizing radiation (IR) induces different types of DNA damage, of which double-strand breaks (DSB) are considered the most genotoxic. As it is important to maintain the genomic integrity of DNA, eukaryotic cells developed a complex network of signalling and effector pathways to reconstitute these DSB as accurately as possible to their original pre-irradiated state. This sophisticated and highly coordinated network is referred to as the DNA damage response. In this response, the induc-

tion of a DSB will lead to the activation of sensor molecules that detect the damage and transduce this signal to different downstream effector pathways. The latter include pathways that lead to cell cycle arrest and repair of the break or cell death if the damage is irreparable (Khanna and Jackson 2001). Under normal circumstances induction of a DSB immediately results in the activation of a phosphatidylinositol-3-OH-kinase-like kinase member, the Ataxia Telangiectasia Mutated (ATM) protein (Stucki and Jackson 2006). Within minutes fol-

lowing exposure to ionizing radiation ATM's kinase activity leads to the phosphorylation of the H2AX histone protein, a variant of the nucleosomal H2A histone core protein, at the site of the DSB. This phosphorylation of the H2AX protein, referred to as γ H2AX, rapidly spreads over an extensive region surrounding the DSB leading to the formation of so called γ H2AX foci (Rogakou et al. 1998, 1999). With the use of an appropriate phospho-specific antibody these foci can be easily detected and visualized. Of all IR-induced DNA lesions, only DNA DSB induce H2AX phosphorylation. Due to the close relationship between the number of γ H2AX foci and the number of radiation-induced DNA DSB (Rogakou et al. 1998, Sedelnikova et al. 2002, Rothkamm and Löbrich 2003), formation of γ H2AX foci have been exploited as being a sensitive and quantitative marker of radiation-induced DNA DSB (Kinner et al. 2008). Besides H2AX, ATM phosphorylates and activates numerous other damage response proteins (Cann and Hicks 2007). Initiation of ATM dependent and independent damage response pathways (Jeggo and Löbrich 2006, Jeggo and Lavin 2009) results in the activation of repair pathways and restoration of the break. Despite the attempt of this cellular machinery to properly repair the break, some breaks escape accurate repair and erroneously rejoining of free DNA DSB ends occurs. When breaks are not repaired or misrepaired, this can lead to the formation chromosomal aberrations (including micronuclei), which, depending on their nature can cause cell death (Olive 1998) or underlie tumorigenesis (Pierce et al. 2001,

Rothkamm and Löbrich 2002).

To investigate and describe differential biological effects of different radiation qualities, analysis of cell death (cell survival) and formation of chromosomal aberrations are used widely. It is well known that the effectiveness of inducing cell death and producing chromosomal aberrations depends on the ionization density of the radiation beam. Radiation types with a high-linear energy transfer (LET) are more effective than sparsely ionizing radiation in inducing cell lethality and chromosomal aberrations for a given absorbed dose.

To describe this increased efficiency of high-LET radiation types compared to low-LET beams when using these biological endpoints, the relative biological effectiveness (RBE) is specified. Since it is generally acknowledged that induction of DSB can lead to both phenomena, understanding and identifying the underlying mechanisms resulting in RBE differences frequently involves the study of induction and loss (i.e. repair/rejoining kinetics) of DSB (eg, Leatherbarrow et al. 2006).

Before the discovery of H2AX phosphorylation, physical methods such as neutral sucrose density gradient centrifugation, neutral filter elution, gel electrophoresis techniques including pulsed field gel electrophoresis (PFGE) – were standard methods used to investigate DSB induction and repair/rejoining kinetics (Prise et al. 1998, 2001, Kinner et al. 2008). Because these assays require high doses of radiation to assess rejoining kinetics, analysis of γ H2AX foci at clinical relevant doses is now frequently applied to monitor DSB induction

and repair (Rothkamm and Löbrich 2003, Kinner et al. 2008).

When investigating the use of new particle beams like carbon ions in radiotherapy as well as estimating the health risk during long-term space flights, knowledge of the biological effects and their underlying mechanisms of actions for different radiation qualities are very important. In addition, in the field of biological dosimetry there is an urgent need for more information about the effects of different radiation types on the induction and loss of γ H2AX foci in human lymphocytes (Rothkamm and Horn 2009).

To address this need, the induction and loss of DSB as well as chromosomal damage resulting from unrepaired or misrepaired DSB were investigated in this study. This after exposure of human lymphocytes *in vitro* to either ^{60}Co γ -rays or p(66)+Be(40) neutrons.

Analysis of induction and loss of DSB was done by applying the γ H2AX foci assay. Chromosomal damage was assessed using the MN assay because radiation-induced micronuclei contain mainly acentric chromosome fragments that are unstable aberrations resulting from unrepaired or misrepaired DSB (Vral et al. 2011, Depuydt et al. 2013, Fenech 2011, Boei et al. 2000).

The radiobiological properties of the p(66)+Be(40) clinical neutron beam (mean energy 29 MeV) used in this study are different from that of lower neutron energy sources – e.g. d(14)/Be (mean energy 5.5 MeV) that have been used previously to analyze the induction of micronuclei (Slabbert et al. 2000, 2010; Vral et al. 1994).

Materials and Methods

Study design

Blood samples of 10 healthy donors aged between 29 and 60, both males (7) and females (3) were used for this study. This work was conducted with ethical approval by the Health Research Ethics Committee of the University of Stellenbosch, South Africa (Ethics Reference #: S12/04/091). Informed consent was obtained from each donor before the start of the study. Blood samples were collected by venipuncture in lithium-heparin coated tubes. Peripheral blood lymphocytes were separated from whole blood using low density gradient centrifugation. Separated lymphocytes were diluted in Roswell Park Memorial Institute (RPMI) medium (Life Technologies, Johannesburg, Gauteng, South Africa) supplemented with 10% fetal calf serum (FCS) (Life Technologies) and the final cell concentration was adjusted according to the assay used.

This study was divided in two parts. In a first set of experiments, dose response (DR) data were generated for both the induction of γ H2AX foci and the formation of MN, using isolated lymphocytes from 10 donors. To reduce experimental / intra-donor variability, both dose response curves for γ H2AX foci and MN were obtained from the same pool of isolated lymphocytes.

In a second part of the study, repair kinetic (RK) experiments were conducted to analyze induction and disappearance of γ H2AX foci. These experiments were done using lymphocyte samples obtained on two occasions from a single donor.

Irradiation experiments

Lymphocyte suspensions were kept at 37°C in a waterbath prior to irradiation. The suspension cultures were irradiated at room temperature with either ⁶⁰Co γ -rays or a clinical neutron beam.

Lymphocyte suspensions were exposed to ⁶⁰Co γ -rays using a teletherapy unit (Theratron 780). Cell suspensions were placed on a 0.5 cm thick Perspex table to ensure dose build-up and a 10 cm thick 30 x 30 cm Perspex block was placed on top of the cells to provide backscatter. A source to surface distance (SSD) of 75 cm applies using a 30 x 30 cm field. A vertical beam pointing upwards was used with a dose rate of 0.5 Gy/min to cell suspensions. The latter was measured using a Nuclear Enterprises (NE) farmer-type 0.6 cc ionization chamber and electrometer.

Lymphocyte suspensions were exposed to a clinical neutron beam which is produced by the reaction of 66 MeV protons on a Beryllium target: $p(66)+Be(40)$. The neutrons used in this study have an average energy of 29 MeV and a mean LET of about 20 keV/ μ m (Slabbert et al. 1989). Neutron exposures were performed using a vertical beam directed downwards. Test tubes containing cell suspensions were positioned on a 15 cm-thick backscatter block of Perspex and irradiated in a 29 x 29 cm field. A 20 mm thick sheet of polyethylene was used as build-up material. Under these conditions the γ -ray component in the beam is 6.9 % and the total neutron dose rate to the samples was 0.4 Gy/min. The dose rate was determined by using a 0.5 cm³ tissue equivalent ionization chamber. Neutron

dose conformations at the irradiated position were done as part of the routine quality control measures used for daily radiation therapy.

Micronucleus assay

For the micronucleus assay, 1 million cells were diluted in 2 ml of RPMI for each treatment sample. Duplicate cultures were exposed to doses ranging from 0 to 4 Gy of γ -rays or 0 to 2 Gy of neutrons. After irradiations, phytohaemagglutinin (PHA, M form, 20 μ g/ml final concentration; Life Technologies) was added to stimulate the growth of T-lymphocytes. Twenty four hours after placing cultures in a humidified 5% CO₂ incubator at 37°C, cytochalasin B (6 μ g/ml final concentration; Sigma-Aldrich, Aston Manor, Gauteng, South Africa) was added to the cultures to block cytokinesis. After harvesting cells 72h post-IR (for details see Depuydt et al. 2013), concentrated cell suspensions were dropped on clean slides and stained with Vectashield® containing 4',6-diamidino-2-phenylindole (DAPI) (Vectorlab, Clubview, Gauteng, South Africa). For each culture, slides were prepared in duplicate. Slides were then scanned automatically using the MSearch software module of the Metafer 4 scanning system (MetaSystems, Altlussheim, Germany) as described by Willems et al. (2010). Using pre-defined cell classifiers consisting of parameters that precisely describe the appearance of the nuclei of binucleated (BN) cells, the MSearch module allows automated detection and visualization of BN cells with or without MN. After completion of the automated image acquisition, an overview of the selected BN

cells is available in an image gallery. For each slide, where possible, 1000 BN cells were analysed for the appearance of MN by inspecting those displayed in the image gallery. In total between 13936 and 32480 BN cells were analysed per dose point for the 10 donors used in the study.

γ H2AX foci assay

For the γ H2AX foci assay, 0.8 million lymphocytes were diluted in 2 ml of RPMI medium for each treated sample. For the dose response experiments, 2 ml cultures were irradiated with different doses ranging from 0 to 0.5 Gy of γ -rays or p(66)+Be(40) neutrons. For the repair kinetics experiments, cultures were irradiated with a dose of 0.5 Gy. After irradiation, cell cultures were incubated at 37°C to allow foci formation. For the dose response experiments, cultures were stopped 30 min post-irradiation by placing the cultures in ice water. For the repair kinetics experiments, cells were put on ice at different time points post-irradiation (2 min, 15 min, 30 min, 1h, 2h, 4h, 8h, 16h, 24h). After 15 min on ice, 250 μ l of each cell suspension was centrifuged onto poly-L-Lysine coated slides (VWR, Leuven, Belgium). For both the DR and RK experiments, 2 slides were prepared for each measurement. Cells were then fixed and incubated with anti- γ H2AX (Biolegend, Clubview, Gauteng, South Africa) followed by rabbit anti-mouse tetramethyl rhodamine isothiocyanate (RAM-TRITC; Dako, Honeydew, Gauteng, South Africa) antibodies as described by Depuydt et al. (2013). Finally, slides were scanned automatically using the MetaCyte

software module of the Metafer 4 scanning system as described by Vandersickel et al. (2010a). Briefly, automated image acquisition is done by first capturing the DAPI images using a well-defined cell selection classifier and subsequently capturing TRITC signals in the selected nuclei. All TRITC signals were acquired as a z-stack with a total of 10 focal planes and a step size of 0.35 μ m between planes. The combined DAPI-TRITC images are simultaneously stored and displayed in the image gallery. For each slide, ~2000 lymphocytes were captured. After coding of the slides, 100 randomly distributed nuclei on each slide were analyzed manually for the presence of γ H2AX foci by visual inspection of the image gallery.

Data analysis

MN frequencies (Y) for ^{60}Co γ -rays (γ) as a function of dose (D) were best fitted to a linear quadratic model, with α , the coefficient of the linear term and β the coefficient of the quadratic term

$$Y_{\gamma} = c_{\gamma} + \alpha_{\gamma}D_{\gamma} + \beta_{\gamma}D_{\gamma}^2$$

The coefficient of the constant term c_{γ} is the background micronuclei frequency.

MN frequencies (Y) for neutrons (n) as a function of dose (D) were best fitted to a linear function,

$$Y_n = c_n + \alpha_n D_n$$

To compare the effectiveness of different radiation qualities, the RBE values were calculated.

The RBE is given by the ratio of the γ -ray dose (D_γ) to the neutron dose (D_n) to obtain an equal level of biological effect (iso-effect). Because of the different shapes of the dose response curves for the different radiation qualities, no single RBE value for neutrons with respect to γ -rays, covering the whole dose range, can be given. Therefore isoeffect RBE values have been calculated for different doses by solving

$$c_\gamma + \alpha_\gamma D_\gamma + \beta_\gamma D_\gamma^2 = c_n + \alpha_n D_n$$

for D_γ and substituting the result in the RBE expression (iso-effect RBE = D_γ/D_n) (Vral et al. 1994). This yields

$$\text{RBE}_{\text{MN}} = \frac{-\alpha_\gamma + \sqrt{\alpha_\gamma^2 + 4\alpha_n \beta_\gamma D_n}}{2\beta_\gamma D_n}$$

Foci frequencies (Y) as a function of dose (D) were best fitted for both radiation qualities to a linear quadratic model,

$$Y = c + \alpha D + \beta D^2$$

Isoeffect RBE values have been calculated for different doses by solving

$$c_\gamma + \alpha_\gamma D_\gamma + \beta_\gamma D_\gamma^2 = c_n + \alpha_n D_n + \beta_n D_n^2$$

for D_γ . Substituting the result in the RBE expression then yields (Vandersickel et al. 2010b),

$$\text{RBE}_{\text{foci}} = \frac{-\alpha_\gamma + \sqrt{\alpha_\gamma^2 + 4\beta_\gamma(\alpha_n D_n + \beta_n D_n^2)}}{2\beta_\gamma D_n}$$

Dose response and repair kinetic data were plotted using Graphpad Prism 4 software. The same software was used for linear and non-linear regression analysis. Analysis of the frequency distribution of MN and γ H2AX foci following exposure to the different radiation qualities was done by calculating the relative variance using Dose Estimate (Ainsbury and Lloyd, 2010). Statistical analysis of the data was performed using Statistical Package For Social Sciences (SPSS) software. Repeated measures Analysis of Variances (ANOVA) and paired samples t-tests were used to analyse statistical significant differences in MN or foci numbers and distributions between the different radiation qualities.

Results

Dose response experiments

Micronuclei formation

A repeated measures ANOVA was performed to analyze the influences of both Dose and Radiation Quality on MN formation. The significant main effect of Dose, $F(6, 4) = 79.53$, $p < .001$, showed that MN gradually increase with dose. This is so for both radiation qualities (Table I, figure 1). The main effect of Radiation Quality was also found to be significant, $F(1, 9) = 89.85$, $p < .001$, illustrating that the number of MN for the same absorbed dose was higher after neutron irradiation than after γ -irradiation. The interaction between Dose and Radiation Quality was also significant, $F(6, 4) = 47.26$, $p < .001$, indicating that

the dose dependent increase in the formation of MN is different for the different radiation qualities. Regression analysis further showed that the mean number of MN as a function of γ -ray dose follows a linear quadratic response. By contrast the shape of the MN dose response curve following neutron irradiation is linear (figure 1). The coefficients for the best regression analysis for the respective data are listed in Table II. No significant differences were found between the spontaneous number of MN observed in the sham-irradiated cell samples for γ -ray treatments and neutron irradiations ($t(9) < 1$, $p = .57$). Thus the c coefficient used in subsequent fits of dose-response data is the mean of all spontaneous MN values. RBE values calculated at levels of iso-effect using the respective dose-response parameters, range between 3.6 and 1.6 for neutron doses of 0.05 Gy and 2 Gy respectively (Table III). Next, paired samples t-tests were done to determine the threshold doses at which the

two radiation qualities induce MN. In the dose range studied, a dose of 0.05 Gy of either γ -rays or neutrons yields MN significantly higher than background readings – $t(9) = 3.08$, $p < .05$ for γ -rays and $t(9) = 12.47$, $p < 0.001$ for neutrons.

To compare the distribution of MN in cells irradiated with γ -rays or neutrons, the dispersion index (i.e. ratio of variance to the mean) was calculated for each dose (Table I, figure 2A). When the ratio of the variance (σ^2) to the mean (μ) = 1, MN follow a Poisson distribution. If the ratio $\sigma^2/\mu > 1$, MN are overdispersed compared to that expected for a Poisson distribution. If the ratio $\sigma^2/\mu < 1$, MN are underdispersed. To determine whether the mean dispersion indices per dose point are different from unity, one sample t-tests were used. These showed that dispersion indices for all γ -ray and neutron doses were significantly higher than 1 (all $t > 2.95$, all $p < .05$ for γ -rays, all $t > 3.43$, all $p < .01$ for neutrons).

Table I. Dose response data for MN following exposure to γ -rays or neutrons. All data represent the mean values obtained for 10 different donors.

Dose (Gy)	$^{60}\text{Co } \gamma\text{-rays}$				$p(66)+\text{Be}(40)$ neutrons			
	Mean No of MN/1000 BN	SEM	σ^2/μ		Mean No of MN/1000 BN	SEM	σ^2/μ	
0	10.1	1.7	1.19	> 1	9.2	1.2	1.09	> 1
0.05	12.4	1.9	1.16	> 1	19	1.2	1.16	> 1
0.1	12.7	1.5	1.12	> 1	29.1	2.6	1.20	> 1
0.2	17.6	1.6	1.11	> 1	48	3.2	1.23	> 1
0.5	35.5	2.1	1.06	> 1	104.4	5.8	1.20	> 1
1	79.9	3.7	1.11	> 1	232.5	13.8	1.25	> 1
2	232.8	15.4	1.12	> 1	425.6	37.6	1.31	> 1
4	637.5	60.3	1.36	> 1	/	/	/	/

TABLE I

Dose response data for MN following exposure to γ -rays or neutrons. All data represent the mean values obtained for 10 different donors.

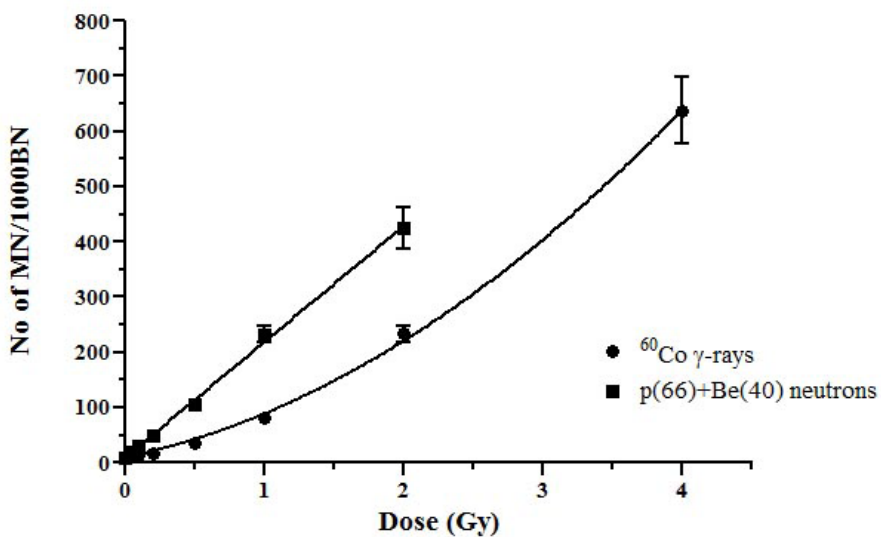


FIGURE 1

Dose response curves for MN in human lymphocytes following exposure to ^{60}Co γ -rays or p(66)+Be(40) neutrons. Each data point represents the mean number of MN (\pm SEM) for 10 different donors.

radiation type	endpoint	α	β	c^*
^{60}Co γ -rays	MN	54.1 ± 16.3	25.9 ± 4.6	9.6 ± 1
p(66) +Be(40) neutrons		209.8 ± 6.4	/	9.6 ± 1
^{60}Co γ -rays	γH2AX	22.5 ± 1	-11.5 ± 2.1	0.4 ± 0.068
p(66) +Be(40) neutrons	foci	15.7 ± 0.9	-7.3 ± 2	0.4 ± 0.068

TABLE II

Best-fit values for coefficients of dose response curves for MN and γH2AX foci following exposure to graded doses of ^{60}Co γ -rays or p(66)+Be(40) neutrons.

* c -values represent the mean spontaneous number of MN/1000 BN cells or foci/cell resp. Dn neutron dose

D_n	RBE	
	MN	Foci
0.01	/	0.70
0.025	/	0.69
0.05	3.57	0.69
0.1	3.34	0.69
0.2	3.01	0.68
0.5	2.45	0.64
1	1.99	/
2	1.56	/

TABLE III

RBE values calculated at levels of iso-effects using MN or foci dose-response parameters D_n neutron dose

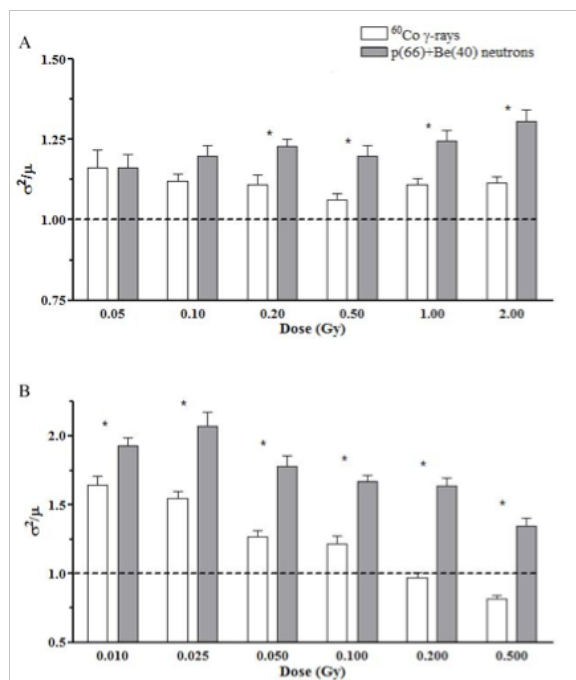


FIGURE 2

Schematic representation of the mean values of the dispersion indices. Each data point represents the mean dispersion index \pm SEM for MN (A) or γH2AX foci (B) counted in lymphocytes of 10 different donors. * σ^2/μ values are significantly higher for neutrons compared to γ -rays.

A repeated measures ANOVA was then used to compare the dispersion indices noted for the different radiation qualities used in the study. This analysis showed a significant main effect for Radiation Quality, $F(1, 8) = 16.52$, $p < .001$. Therefore, on average a higher degree of overdispersion is noted for neutrons compared to γ -rays. Neither the effect of Dose, $F(6, 3) = 4.15$, $p = .14$, nor the interaction between Dose and Radiation Quality is significant – $F(6, 3) = 2.44$, $p = .25$. Paired samples t-tests showed that overdispersion was significantly higher for neutrons compared to γ -rays for doses of 0.2, 0.5, 1 and 2 Gy – all $t > 3.55$, all $p < .01$. Overdispersion did not differ between neutrons and γ -rays for doses 0, 0.05, and 0.1Gy – all $t < 2.26$, all $p > .05$.

γ H2AX foci formation

A repeated measures ANOVA was performed for γ H2AX foci formation for data obtained from 10 donors. This analysis showed a significant main effect of Dose, $F(6, 4) = 244.123$, $p < .001$. This main effect indicates that γ H2AX foci gradually increase with increasing dose (Table IV, figure 3). A significant main effect

of Radiation Quality, $F(1, 9) = 92.70$, $p < .001$, was also noted illustrating that foci formation after γ -irradiation was higher than after neutron irradiation. Both main effects were subsumed under a significant interaction between Dose and Radiation Quality, $F(6, 4) = 6.41$, $p < .05$, indicating that the dose dependent increase in the formation of foci is different for the different radiation qualities (figure 3). Regression analysis showed that the mean number of foci/cell after exposure to graded doses of either radiation qualities was best fitted to a second order polynomial equation. (Figure 3, Table II). The c coefficient represents the mean spontaneous value of all sham-irradiated samples. This as no significant difference ($t < 1$, $p = .66$) was found between the spontaneous number of foci scored in sham-irradiated samples for γ -rays and neutron experiments. Calculated RBE values range between 0.70 and 0.64 for a neutron dose of 0.01 Gy and 0.5 Gy respectively (Table III). Using a paired samples t-test, a threshold detection dose of 0.01 Gy could be determined for γ -rays ($t(9) = 6.22$, $p < .001$). The same threshold dose was determined for neutrons ($t(9) = 3.31$, $p < .01$).

Dose (Gy)	$^{60}\text{Co } \gamma\text{-rays}$				$p(66) + \text{Be}(40)$ neutrons			
	Mean No of foci/cell	SEM	σ^2/μ		Mean No of foci/cell	SEM	σ^2/μ	
0	0.45	0.12	1.85	> 1	0.41	0.08	1.8	> 1
0.01	0.89	0.08	1.64	> 1	0.62	0.06	1.93	> 1
0.025	1.26	0.11	1.55	> 1	0.98	0.13	2.07	> 1
0.05	1.70	0.09	1.27	> 1	1.26	0.11	1.78	> 1
0.1	2.60	0.12	1.22	> 1	1.89	0.11	1.67	> 1
0.2	4.32	0.13	0.97	= 1	3.24	0.15	1.64	> 1
0.5	8.84	0.26	0.82	< 1	6.44	0.27	1.35	> 1

TABLE IV

Dose response data for γ H2AX foci following exposure to γ -rays or neutrons. All data represent the mean values obtained for 10 different donors.

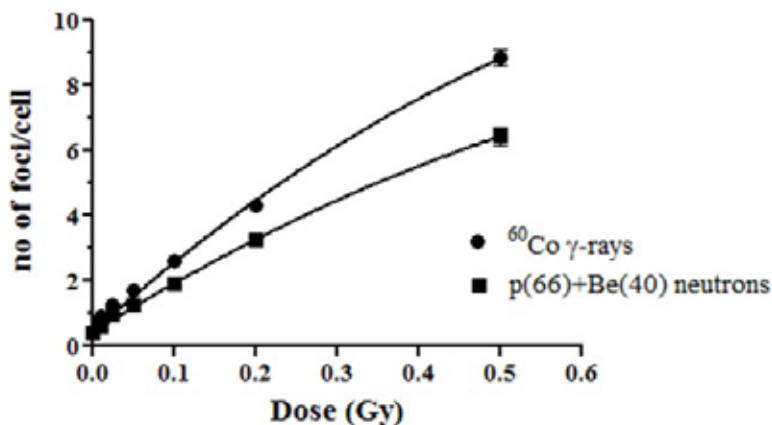


FIGURE 3

Dose response curves for the mean number of γH2AX foci/cell for lymphocytes exposed to ^{60}Co γ -rays and p(66)+Be(40) neutrons. Each data point represents the mean number of foci \pm SEM of lymphocytes obtained from 10 different donors.

Calculation of dispersion indices shows that foci frequencies were overdispersed for all neutron doses (all $t > 6.20$, all $p < .001$). Following γ -irradiations, foci frequencies were overdispersed for the lower doses up to 0.1 Gy (all $t > 4.02$, all $p < .005$). For a dose of 0.2 Gy, foci frequencies followed a Poisson distribution as the σ^2/μ did not differ from $1 - t(9) < 1$, $p = .42$. Underdispersion was noted for the highest γ -ray dose of 0.5 Gy used in the study ($t(9) = 6.77$, $p < .001$) (figure 2B).

Repeated measures ANOVA were used to compare the dispersion indices of γH2AX foci formation following γ -ray and neutron exposures. This analysis shows a significant main effect for Radiation Quality, $F(1, 9) = 138.36$, $p < 0.001$ and Dose, $F(6, 4) = 35.61$, $p < 0.05$. These main effects were subsumed under a significant interaction, $F(6, 4) = 8.35$, $p < 0.05$, indicating a difference in dispersion between gamma and neutron irradiations. Paired sample t-tests showed

that the dispersion of foci was higher for neutrons compared to γ -rays for all doses (all $t > 3.27$, all $p < .05$). No differences in dispersion indices could be detected for repeated sham-irradiated samples $t < 1$, $p = .76$ (Table IV).

Repair kinetics of γH2AX foci

Foci formation at different time points post-irradiation were studied following the exposure of isolated lymphocytes of a single donor to either γ -rays or neutrons (figure 4A). The maximum number of foci/cell was reached at 30 minutes post-irradiation. This for both γ -rays (mean value of 9.21 ± 0.38) and neutrons (mean value of 7.06 ± 0.08). After 30 minutes, the number of foci decreased gradually for both radiation qualities. Foci induced by neutrons disappeared slower than those induced by γ -rays. Eight hours post-irradiation the foci frequencies for neutron irradiated samples exceeded that of γ -rays.

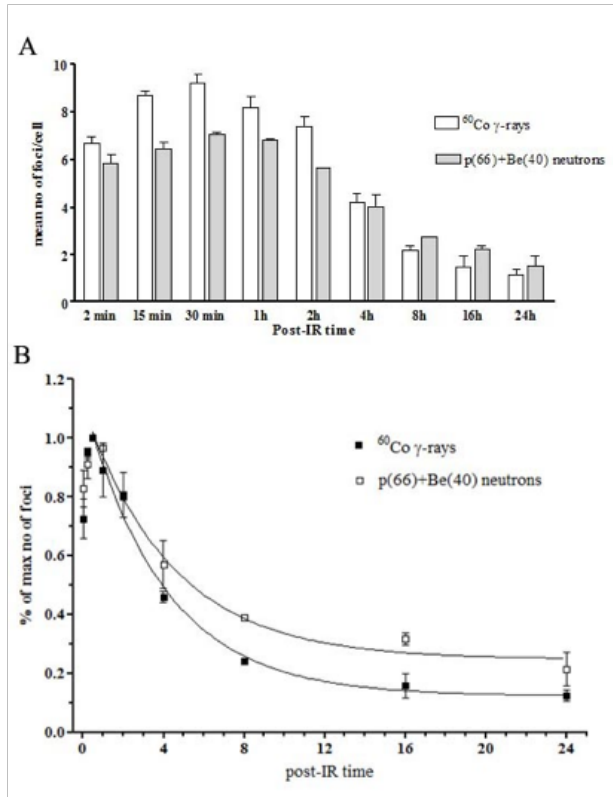


FIGURE 4

The number of γH2AX foci as a function of time for isolated lymphocytes exposed to 0.5 Gy of neutrons or 0.5 Gy of γ -rays. Data points represent the mean number of foci/cell \pm SEM of 2 independent experiments. In figure 4B foci numbers were normalized to the maximum number of foci induced 30 minutes post-irradiation and fitted to an equation for one-phase exponential decay.

To better compare the results of the different radiation qualities, the foci numbers were normalized to that assessed at 30 minutes (figure 4B). Differences in the relative number of foci/cell are noted at different time points post-irradiation. At 4 hours post-irradiation and beyond the number of remaining foci is higher after neutron irradiation compared to γ -irradiation. Although DSB repair kinetics have been described by a second order exponential decay (Horn et al. 2011, Iliakis et al. 2004), the data

were best fitted to a one-phase exponential decay equation ($Y = (Y_0 - \text{Plateau}) * \exp(-K*X) + \text{Plateau}$, with K the rate constant; Graphpad Prism Software). From this analysis a repair half-life of 2.8 hours (95% confidence interval (CI): 2.1 to 4.1h) is estimated for γ -rays. For neutrons a repair half life of 3.0 hours (95% CI: 2.3 to 4.4h) is calculated. The estimated plateau values were 0.12 (95% CI: 0.043 to 0.20) and 0.25 (95% CI: 0.18 to 0.32) for γ -rays and neutrons respectively.

Discussion

Understanding the mechanisms underlying the biological effects observed for different radiation qualities is very important in the field of radiotherapy, biological dosimetry and risk estimation during long-term space flights. Differences in induction and repair of DSB are considered fundamental in the outcome of biological effects noted after irradiations with different radiation qualities. Therefore, we investigated micronucleus formation and the induction and disappearance of γ H2AX foci after *in vitro* exposures of human lymphocytes to either ^{60}Co γ -rays or p(66)+Be(40) neutrons.

As expected, analysis of MN dose response data shows that the yield of MN induced by high energy neutrons was higher compared to ^{60}Co γ -rays. RBE values calculated from the fitted parameters range between 3.6 and 1.6 for neutron doses of 0.05 Gy and 2 Gy respectively. Data obtained in this study using an automated image analysis system for MN scoring are consistent with micronuclei data obtained by manual scoring in T-lymphocytes exposed to the same p(66)+Be(40) neutron beam (Slabbert et al. 2010). The higher RBE values show that neutrons are indeed more effective than γ -rays in inducing MN in human lymphocytes and relatively more so at lower doses. A mean dose limiting maximum RBE (RBE_m) value of 3.9 can be calculated from the data and this is in agreement with that noted by Slabbert et al. (2010). It is also consistent with higher RBE_m reported for a lower energy 5.5 MeV neutron beam (Vral et al. 1994).

In biological dosimetry the distribution analysis of chromosomal aberrations is important because treatment modalities of different ionization densities are expected to produce different distributions of chromosomal damage (International Atomic Energy Agency (IAEA) 2011). This is indeed the case for dicentrics, where irradiation with low-LET X- or γ -rays produces a spreading that follows a Poisson distribution (Edwards et al. 1979). By contrast, irradiations with neutrons or other high-LET radiation types results in overdispersion (IAEA 2011). In this study MN frequency distributions in the affected cell populations show to be overdispersed compared to a Poisson distribution after irradiation with either neutrons or γ -rays. Although the formation of MN does not display the same distribution patterns as dicentrics for low-LET radiation, the observation that MN are overdispersed even for low-LET radiation is generally reported (Vral et al. 1994, IAEA 2011). In this study we did however observe that overdispersion indices were significantly higher after neutron exposure compared to γ -irradiations for all doses > 0.1 Gy. This observation is also in line with previous studies (Vral et al. 1994 and references herein) and indicates that to a certain extent MN frequency distributions do reflect differences in ionization densities of different radiation qualities.

To further investigate the underlying mechanism of MN formation, the induction of γ H2AX foci, was simultaneously analysed. Lower yields of foci were observed after neutron irradiation and this was seen repeatedly in cell samples analysed from different donors.

RBE values ranging between 0.70 for low dose irradiation to 0.64 for higher doses were calculated from the dose response data. This implies that high energy neutrons used in radiotherapy are less effective in inducing γ H2AX foci compared to γ -rays. Furthermore the range of RBE values obtained for foci induction (i.e. 0.70 – 0.64) was much narrower compared to that for MN formation (i.e. 3.57 – 1.56). Since photons and neutrons – as well as other high-LET radiation types – are reported to induce a higher or at least a comparable number of DSB (RBE \geq 1) (Britten et al. 2001), the RBE value $<$ 1, found in our study was at first unexpected. However, differences in methodology may explain this discrepancy. It has indeed been shown that results obtained by PFGE – based on separation of DNA fragments with different sizes, cannot be directly compared with results obtained by γ H2AX foci analysis – based on the analysis of cellular responses to the induction of damage. Close inspection of literature data on foci induction after high-LET radiation revealed variable results. For instance, Franken et al. (2011) observed RBE values of about unity after exposure of human lung carcinoma cell lines to α -particles (130 keV/ μ m) or γ -rays. By contrast, Costes et al. (2006) detected fewer foci after exposure of human foreskin fibroblasts to nitrogen ions (130 keV/ μ m) compared to X-rays (i.e. RBE $<$ 1). Similar findings were made by Asaithamby et al. (2008) who reported lower maximum numbers of foci after exposure of human skin fibroblasts to either iron ions (150 and 236 keV/ μ m), silicon ions (44 keV/ μ m), oxygen ions (14 keV/

μ m) compared to γ -rays. Okumura et al. (2013) further detected similar numbers of p53 binding protein 1(53BP1) foci, known to colocalize with γ H2AX foci (Lassman et al. 2010), after exposing hamster ovary cells to a mixed neutron beam and γ -rays (i.e. RBE about 1). Importantly, to date no studies have been reported on the yield of γ H2AX foci after exposure of human lymphocytes to high energy neutrons. The lower than unity RBE values for γ H2AX foci noted in this and other studies can however in part be explained when considering the biological basis of the formation of radiation-induced foci. Manifestation of γ H2AX foci can be the outcome of different scenarios occurring at the level of the formation of DSB, or at the level of foci formation, or a combination thereof. Since energy depositions of high-LET radiation are more clustered along the particle tracks, this can result in the induction of more closely spaced DSB. On the one hand, several data suggest that multiple DSB are very likely to cluster into common repair centres. These individual repair centres then appear as a single focus but may contain more than one DSB (Neumaier et al. 2012). A single focus may thus not represent the actual number of radiation-induced DSB. Support for this idea also comes from the observation that none of the DSB marker proteins, including γ H2AX foci, examined by Jakob et al. represented the total number of expected DSB after heavy ion irradiation (Jakob et al. 2003, 2009). On the other hand, it is also possible that each DSB does result in the formation of a focus, despite the occurrence of several DSB in close proximity. Aten et al.

(2004) analysed the track morphology after exposure of HeLa cells to α -particles at different time points post-IR. These results suggested that clusters of foci can indeed form as a result of relocation of the H2AX foci along high energy density tracks. Therefore, it is possible that closely spaced individual foci cluster together and consequently make clear discrimination of individual foci difficult (Rübe et al. 2011). Otherwise, discrimination of closely spaced and/or overlapping foci can also be limited by the optical resolution of the microscope system and lead to an underestimation of actual foci numbers (Okumura et al. 2013).

Regardless of which hypothesis applies to our observations, it is clear that the probability of clustering of either DSBs or foci is higher when cells are exposed to high-LET radiation compared to low-LET radiation qualities. The same argument applies when using progressively higher doses of either radiation modalities. Indeed, in this study, foci numbers counted for both radiation qualities were best fitted to a second order function instead of a linear function. This deviation from linearity indicates that foci levels saturate at higher dose levels and supports the argument that clustering of DSB and/or foci occurs (Horn et al. 2011). Further support for the idea that clustering occurs resides in the distribution of foci. Foci distributions show a decreasing tendency for overdispersion with increasing dose and this after both gamma and neutron irradiation. Since the number of DSB per cell increases as the dose increases, the likelihood of 2 foci coalescing and combining into 1 also increases.

When further comparing foci distributions between the two radiation qualities, we observed that overdispersion of foci was higher for all neutron doses compared to γ -rays. This indicates that physical differences in the energy deposition patterns for the neutrons and γ -rays seem to be reflected in the distribution of foci in irradiated cells.

Further differences in foci formation between neutrons and γ -rays are noted when analysing repair kinetic data. After neutron irradiation, lower absolute foci numbers are apparent for time slots 2 minutes up to 2 hours. In addition, more variation in foci induction and loss for γ -rays is clear during the first 2h after irradiation. At 4 hours, foci numbers for the same dose of neutrons and γ -rays are about the same (figure 4A). At 8, 16 and 24 hours after irradiation, the number of foci remain higher after neutron irradiation compared to γ -irradiation resulting in RBE values greater than 1. Normalizing foci yields to the maximum number of foci noted at 30 minutes after radiation, demonstrates less disappearance of neutron-induced foci compared to these induced by γ -rays. Assuming that foci disappearance reflects DSB repair/rejoining, our results are in agreement with the observation that the extent of repair of DSB induced by neutrons or high-LET radiation is less than that induced by low-LET radiation (for a review, see Britten et al. 2001). Notwithstanding the above, the half-life of foci disappearance is only marginally longer for neutrons than that for gammas and not significantly different on the 95% confidence level. A possible explanation for more persistent foci following

neutron exposure can be the consequence of the more clustered energy depositions that form along the particle tracks of high-LET radiation. This can not only cause the production of more closely spaced breaks/lesions, but also an increase in break/lesion complexity. Indeed, the rejoining of DSB and the extent of unrejoined damage has been correlated to the complexity of the break (Pastwa et al. 2003). On the other hand, Costes et al. (2010) hypothesized that the increasing probability of clustering of closely spaced DSB in one focus with high-LET radiation results in slower repair kinetics as multiple DSB residing in one focus take longer to repair than one DSB in one focus.

Nevertheless, a slower disappearance of DSB has been associated with an increase in misrejoining events and thus the formation of chromosome aberrations – such as dicentrics – as there is more time for exchange between the ends of free DNA DSB. Formation of dicentric chromosomes are accompanied by the formation of acentric fragments which are detected as MN in binucleated cells. Therefore, slower disappearance of γ H2AX foci supports the higher MN yields observed after neutron irradiation. It should however be kept in mind that higher MN yields may not only be related to a slower disappearance of DSB, but may also be related to the induction of more closely spaced DSB. Indeed, the production of multiple breaks in close proximity may well facilitate exchange formations since the probability of breaks rejoining incorrectly increases with the coincidence of multiple breaks (Rothkamm and Löbrich 2002).

In summary, this study investigated the formation of micronuclei and the induction and loss of γ H2AX foci after *in vitro* exposure of human lymphocytes to either ^{60}Co γ -rays and high-LET p(66)+Be(40) neutrons. Despite neutrons being more effective in inducing MN compared to γ -rays, less γ H2AX foci were observed for high-LET radiation between 2 minutes and about 4h post-IR. Differences in the extent of foci loss for radiation modalities with different ionization densities were also observed.

These results have important implications towards the use of the γ H2AX foci assay in biodosimetry. Both the observations that different radiation qualities yield (a) different numbers of foci per unit dose (see also Depuydt et al. 2013, Beels et al. 2010) and (b) differences in foci disappearance necessitate the establishment of distinctive dose-effect curves at different time points as previously suggested by Horn et al. (2011). In addition, to apply foci formation in neutron biodosimetry additional readings at different time points post- irradiation are desired to detect qualitative differences in foci formations from different ionization densities. More precisely, additional studies using γ H2AX foci should attempt to detect different overdispersions for low-LET partial body exposures than that for high-LET radiation (Rothkamm 2007, 2009, Horn et al. 2011). Also, besides describing the distribution patterns of foci with respect to radiation quality and uniformity, qualitative analysis of foci size and intensity may prove useful (Costes et al. 2006, Whalen et al. 2008). Finally, considering that patients are treated daily, the higher number of foci noted for

neutrons at 24 hours post treatment has consequences for high-LET particle radiotherapy. The neutron source used in this study has an ionization density similar to that of modern carbon ion beams used in radiotherapy (Gueulette et al. 2010). Also, the extensive repair seen in this study for neutron damage during the first 8 hour post-irradiation suggests that double fraction treatments with high-LET particle therapy beams should not be attempted during this time. More studies with tissue types resulting in late radiation damage/effects should be conducted to further understand the implications of inter-fraction treatment times.

Acknowledgements

The authors would like to thank all volunteers who donated the blood samples.

Declaration of interest

The authors report no conflicts of interest.

The work was supported by a University Development Cooperation ‘VLIR Own Initiative Programme’ between Belgium and South Africa (ZEIN 2005PR309, ZEIN2011PR387) and the National Research Foundation of South Africa.

References

- Asaithamby A, Uematsu N, Chatterjee A, Story MD, Burma S, Chen DJ. 2008. Repair of HZE-particle-induced DNA double-strand breaks in normal human fibroblasts. *Radiation Research* 169: 437-446.
- Aten JA, Stap J, Krawczyk PM, van Oven CH, Hoebe RA, Essers J, Kanaar R. 2004. Dynamics of DNA double-strand breaks revealed by clustering of damaged chromosome domains. *Science* 303: 92-95.
- Beels L, Werbroutck J, Thierens H. Dose response and repair kinetics of gamma-H2AX foci induced by in vitro irradiation of whole blood and T-lymphocytes with X- and gamma-radiation. 2010. *International Journal of Radiation Biology* 86: 760-768.
- Boei J, Vermeulen S, Natarajan AT. 2000. Analysis of radiation-induced chromosomal aberrations using telomeric and centromeric PNA probes. *International Journal of Radiation Biology* 76: 163 – 167.
- Britten RA, Peters LJ, Murray D. 2001. Biological factors influencing the RBE of neutrons: implications for their past, present and future use in radiotherapy. *Radiation Research* 156: 125-135.
- Cann KL, Hicks GG. 2007. Regulation of the cellular DNA double-strand break response. *Biochemistry and Cell Biology* 85: 663-674.
- Costes SV, Boissière A, Ravani S, Romano R, Parvin B, Barcellos-Hoff MH. 2006. Imaging features that discriminate between foci induced by high- and low-LET radiation in human fibroblasts. *Radiation Research* 165: 505-515.
- Costes SV, Chiolo I, Pluth JM, Barcellos-Hoff MH, Jakob B. 2010. Spatiotemporal characterization of ionizing radiation induced DNA damage foci and their relation to chromatin organization. *Mutation Research* 704: 78-87.
- Depuydt J, Baert A, Vandersickel V, Thierens H, Vral A. 2013. Relative biological effectiveness of mammography X-rays at the level of DNA and chromosomes in lymphocytes. *International Journal of Radiation Biology* 89: 532-538.
- Du G, Drexler GA, Friedland W, Greubel C, Hable V, Krücken R, Kugler A, Tonelli L, Friedl AA, Dollinger G. 2011. Spatial dynam-

- ics of DNA damage response protein foci along the ion trajectory of high-LET particles. *Radiation Research* 176: 706-715.
- Edwards AA, Lloyd DC, Purrot RJ. 1979. Radiation induced chromosome aberrations and the Poisson distribution. *Radiation and Environmental Biophysics* 16: 89-100.
- Fenech M. 2007. Cytokinesis-block micronucleus cytochrome assay. *Nature Protocols* 2: 1084-1104.
- Fenech M, Kirsch-Volders M, Natarajan AT, Surrallés J, Crott JW, Parry J, Norppa H, Eastmond DA, Tucker JD, Thomas P. 2011. Molecular mechanisms of micronucleus, nucleoplasmic bridge and nuclear bud formation in mammalian and human cells. *Mutagenesis* 26: 125-132.
- Franken NA, ten Cate R, Krawczyk PM, Stap J, Haveman J, Aten J, Barendsen GW. 2011. Comparison of RBE values of high-LET α -particles for the induction of DNA-DSBs, chromosome aberrations and cell reproductive death. *Radiation Oncology* 6: 64.
- Gueulette J, Slabbert J, Biscchoff P, Denis J, Wambersie A, Jones D. 2010. Fast neutrons: inexpensive and reliable tool to investigate high-LET particle radiobiology. *Radiation Measurements* 45: 1414-1416.
- Horn S, Barnard S, Rothkamm K. 2011. Gamma-H2AX-based dose estimation for whole and partial body radiation exposure. *PLoS One*. 6: e25113.
- Iliakis G, Wang H, Perrault AR, Boecker W, Rosidi B, Windhofer F, Wu W, Guan J, Terzoudi G, Pantelias G. 2004. Mechanisms of DNA double strand break repair and chromosome aberration formation. *Cytogenet Genome Res* 104: 14-20.
- International Atomic Energy Agency (IAEA). 2011. *Cytogenetic dosimetry: Applications in preparedness for and response to radiation emergencies*. Technical report series. IAEA: Vienna.
- Jackson SP. 2009. The DNA-damage response: new molecular insights and new approaches to cancer therapy. *Biochemical Society Transactions* 37: 483-494.
- Jakob B, Scholz M, Taucher-Scholz G. 2003. Biological imaging of heavy charged-particle tracks. *Radiation Research* 159: 676-684.
- Jakob B, Splinter J, Taucher-Scholz G. 2009. Positional stability of damaged chromatin domains along radiation tracks in mammalian cells. *Radiation Research* 171: 405-418.
- Jeggo P, Löbrich M. 2006. Radiation-induced DNA damage responses. *Radiation Protection Dosimetry* 122: 124-127.
- Jeggo P, Lavin MF. 2009. Cellular radiosensitivity: how much better do we understand it? *International Journal of Radiation Biology* 85: 1061-1081.
- Khanna KK, Jackson SP. 2001. DNA double-strand breaks: signaling, repair and the cancer connection. *Nature Genetics* 27: 247-254.
- Kinner A, Wu W, Staudt C, Iliakis G. 2008. γ -H2AX in recognition and signaling of DNA double-strand breaks in the context of chromatin. *Nucleic Acids Research* 36: 5678-5694.
- Lassmann M, Hänscheid H, Gassen D, Biko J, Meineke V, Reiners C, Scherthan H. 2010. In vivo formation of gamma-H2AX and 53BP1 DNA repair foci in blood cells after radioiodine therapy of differentiated thyroid cancer. *Journal of Nuclear Medicine* 51: 1318-1325.
- Leatherbarrow EL, Harper JV, Cucinotta FA, O'Neill P. 2006. Induction and quantification of gamma-H2AX foci following low and high LET-irradiation. *International Journal of Radiation Biology* 82: 111-118.
- Neumaier T, Swenson J, Pham C, Polyzos A, Lo AT, Yang P, Dyball J, Asaithamby A, Chen DJ, Bissell MJ, Thalhammer S, Costes SV. 2012. Evidence for formation of DNA repair centers and dose-response nonlinearity in human cells. *Proceedings of the National Academy of Sciences of the U S A* 109: 443-448.
- Okumura K, Kinashi Y, Kubota Y, Kitajima E, Okayasu R, Ono K, Takahashi S. 2013. Relative biological effects of neutron mixed-beam irradiation for boron neutron capture ther-

apy on cell survival and DNA double-strand breaks in cultured mammalian cells. *Journal of Radiation Research* 54: 70-75.

Olive PL. 1998. The role of DNA single- and double-strand breaks in cell killing by ionizing radiation. *Radiation Research* 150: S42-51.

Pastwa E, Neumann RD, Mezhevaya K, Winters TA. 2003. Repair of radiation-induced DNA double-strand breaks is dependent upon radiation quality and the structural complexity of double-strand breaks. *Radiation Research* 159: 251-261.

Pierce AJ, Stark JM, Araujo FD, Moynahan ME, Berwick M, Jasin M. 2001. Double-strand breaks and tumorigenesis. *Trends in Cell Biology* 11: S52-59.

Pouget JP, Mather SJ. 2001. General aspects of the cellular response to low- and high-LET radiation. *European Journal of Nuclear Medicine and Molecular imaging* 28: 541-561.

Prise KM, Ahnström G, Belli M, Carlsson J, Frankenberg D, Kiefer J, Löbrich M, Michael BD, Nygren J, Simone G, Stenerlöw B. 1998. A review of dsb induction data for varying quality radiations. *International Journal of Radiation Biology* 74: 173-184.

Article 2

The impact of a BRCA1 and BRCA2-mutation on the radiation response induced by gamma-rays and neutrons in MCF-10A cells

J. Depuydt¹, Vandersickel V.¹, Beukes P.R.², Baert A.¹, Verstraete B.³, Van Heetvelde M.³, Thierens H.¹, Slabbert J.P.² and A. Vral¹.

1 Ghent University, Department of Basic Medical Sciences, Gent, Belgium

2 NRF iThemba LABS, Somerset West, South Africa

3 Ghent University Hospital, Center for Medical Genetics, Gent, Belgium

Submitted to International Journal of Radiation Biology

Abstract

Purpose: BRCA1 and BRCA2 play an important role in DNA double strand break (DSB) repair: BRCA2 in homologous recombination (HR) and BRCA1 in non-homologous end-joining (NHEJ) and HR. The radiosensitivity of BRCA1 and BRCA2 mutation carriers is a long standing question and can have implications for the treatment and screening procedures of BRCA1 and BRCA2 mutation carriers. In this study we investigated the impact of the knockdown of the BRCA1 and BRCA2 proteins in a spontaneous immortalized non-tumorigenic human mammary epithelial cell line (MCF-10A) on HR and NHEJ after *in vitro* exposure to ionizing radiation.

Methods: Downregulation of BRCA1, BRCA2 and Ku70 proteins in MCF-10A cell was obtained using RNA interference (RNAi) transduction. Mock transduced and knockdown (BRCA1i, BRCA2i and Ku70i) MCF-10A cells were irradiated as mixed cell cultures (G1, S, G2 and M) and as synchronized G1 cultures with ^{60}Co γ -rays and fast neutrons. Cellular and chromosomal radiosensitivity was measured with the crystal violet (CV) cell proliferation assay and the micronucleus (MN) assay, respectively.

Results: We observed an increased radiosensitivity in BRCA1i and Ku70i cells in both G1 cell cultures and mixed cell cultures, which was most pronounced at low doses. For BRCA2i cells, the radiosensitivity was only increased in the mixed cell cultures. Relative biological effectiveness (RBE) values were comparable or slightly lower for the knockdown cell lines compared to the mock transduced control cell lines.

Conclusion: BRCA1i and BRCA2i cell lines are characterized by an increased radiosensitivity, which is dependent on LET, dose and cell cycle. Our results imply that caution should be taken when administering ionizing radiation to heterozygous mutation carriers.

Introduction

The advantages of the use of ionizing radiation for diagnostic imaging as well as for therapeutic purposes are well described (1-3). However, there is also no doubt that breast exposure to ionizing radiation is associated with an increased risk of breast cancer. Evidence for this can be found in epidemiological studies on atomic bomb survivors of Hiroshima and Nagasaki, in follow-up studies of patients treated with radiotherapy for hematological malignan-

cies and in studies performed on patients intensively monitored by x-rays e.g. for scoliosis or tuberculosis (4-11).

Several of studies have highlighted a number of individual factors that modify the radiation-induced (RI) breast-cancer risk. Factors suggested to enhance the RI breast cancer risk in the literature are: age at irradiation and attained age, age of menarche or the time of first pregnancy, nulliparity, obesity, family history of breast cancer, benign breast diseases and ge-

netic factors (12-16). However, some of these factors modify the radiation risk only marginally and reproduction of the results seems challenging (16, 17).

Carriers of mutations in genes like *BRCA1*, *BRCA2* or *ATM*, are suspected to have a higher risk for radiation-induced breast cancer. The evidence for enhanced risk is stronger for *ATM* mutation carriers, though the evidence is not univocal (16, 18-20).

Age at exposure and attained age seem to have the highest modifying effect on radiation-induced breast-cancer risk. Compared to exposure of young adults (30-40 years) the risk in children appears to be three fold in the Hiroshima lifespan study population (5, 21). After exposure at young age the risk continues to be elevated throughout the remainder of a woman's life, with the largest excess rates occurring at ages similar to those at which breast cancers are seen in the absence of exposure (22). Dose-time exposure parameters (total dose, dose rate, fractionation, dose per fraction) and radiation quality can also modify the risk. The beam quality has been widely discussed in the case of mammography X-rays, which have a much lower energy than conventional X-rays (23-25). The importance of radiation quality on breast cancer risk is even more pronounced with the use of e.g. neutrons, protons or carbon ions in radiotherapy (26-28). The relative biological effectiveness (RBE) of a radiation quality for a specific cell type or tissue is not only determined by the linear energy transfer (LET) of the radiation used, but is also dependent on several other factors, like the phase of the cell

cycle, the inherent radiosensitivity linked to genetic mutations and the oxidation of the tissue. The main target of radiation in the cell is the DNA. Radiation induces the formation of inter- and intra-strand crosslinks, damage at the level of single bases, single-strand breaks and double strand breaks (DSB), the latter being considered the most lethal form of DNA damage (29). A cell has different pathways to repair DNA DSBs, the major being non-homologous end joining (NHEJ) and homologous recombination (HR) (30, 31). NHEJ ligates the break ends without the need for a homologous template and is therefore prone to errors. It is available during the whole cell cycle and is considered the main pathway for repair of radiation-induced DSB in mammalian cells. DNA repair by HR on the contrary is more accurate because it uses the undamaged sister chromatid sequence to repair the DSBs. Consequently HR is only active in the S and G2 phase of the cell cycle. According to recent literature, only the more complex DSB in the S or G2 phase will be repaired by HR (32-36). In the DNA damage response, not only repair proteins are activated but also proteins involved in the control of the cell cycle checkpoints (37, 38).

The DNA damage response pathways involve many proteins amongst which are the two major breast cancer predisposition genes *BRCA1* and *BRCA2*, whose functions are extensively reviewed by Roy et al (39). *BRCA1* is involved in the very early stages of the HR DNA repair pathway and seems to play a role in NHEJ and single strand annealing as well. *BRCA2* has its main function in facilitating HR. The crucial

role of BRCA1 and BRCA2 in DNA DSB repair suggest a higher sensitivity to ionizing radiation when those proteins are not fully functional or lacking, as DNA DSB will be repaired less efficiently. DSB can be transformed into chromosomal aberrations during cell division and subsequently can cause cell death or trigger tumorigenesis (40-42).

Patient studies are mostly focused on the association between the medical radiation burden and the occurrence or recurrence of breast cancer in persons with and without a *BRCA1* or *BRCA2* mutation. Results are inconclusive, partly because of the big variation in doses, radiation qualities, age and irradiated tissue. Some studies find an increased sensitivity to radiation in *BRCA1/2* mutation carriers (43-45), often closely linked to age at the time of exposure, while other studies don't (46-49). To overcome the difficulties of *in vivo* studies, *in vitro* experiments investigating the radiosensitivity of lymphocytes, fibroblasts or EBV cell lines (Epstein Barr virus immortalized cell lines) derived from patients with and without a *BRCA1* or *BRCA2* mutation have been performed. These studies lead again to contradictory results, with some studies pointing to an increased sensitivity (50-52), and others not (52, 53). Human mammary epithelial cells are however different from lymphocytes or fibroblasts both in cell characteristics and cellular environment and therefore their response to ionizing radiation may be different to the latter. In this study we investigated the impact of BRCA2 knockdown on HR and BRCA1 knockdown on HR and NHEJ after exposure *in vitro*

to ionizing radiation. Since it would be very interesting to compare this with the expression-impact of a protein solely playing a role in NHEJ, we also investigated the impact of Ku70 expression (54, 55) after exposure to ionizing radiation. We obtained a downregulation of the BRCA1, BRCA2 and Ku70 proteins in a spontaneous immortalized non-tumorigenic human mammary epithelial cell line (MCF-10A) using RNA interference (RNAi) transduction. Protein levels of about 50%, which corresponds to the situation present in heterozygote mutation carriers, were obtained. Cellular and chromosomal radiosensitivity was measured with the crystal violet (CV) cell proliferation assay and the micronucleus (MN) assay, respectively. Since BRCA1, BRCA2 and Ku70 have different functions in the DNA damage response pathway depending on the nature of the DSB and the cell cycle phase, mock transduced and knockdown MCF-10A cells were irradiated as mixed (G1, S, G2, M) cultures and as synchronized G1 cultures with 2 different radiation qualities: ^{60}Co γ -rays or p(66)+Be(40) neutrons.

Material and methods

Cell lines

MCF-10A cells were cultured as monolayer in DMEM/F12-ham (Invitrogen, Belgium) supplemented with 5% fetal calf serum (Invitrogen), antibiotics and growth factors (10 $\mu\text{g}/\text{ml}$ insulin (Sigma, Belgium); 0.5 $\mu\text{g}/\text{ml}$ hydrocortisone (Sigma); 20 ng/ml epidermal growth factor (Tebu-bio, Belgium); 50 U/ml penicillin

and 50 μ g/ml streptomycin (Invitrogen)) as described by Debnath et al (56).

The knockdown BRCA1 and BRCA2 cell lines (hence forward called BRCA1i and BRCA2i) together with their mock-transduced control cell line (CON_{BRCA}), were kindly provided to us by the VIB (Laboratory for Mechanism of Cell Transformation, KULeuven, Belgium). To generate repair deficient MCF-10A cell lines, MCF-10A cells were transduced with lentiviral particles harboring DNA sequences encoding for short hairpin RNA specific for BRCA1 or BRCA2 RNA interference. Lentiviruses were constructed using pLKO.1-puro vectors. The sequence used for BRCA1 was CCCTAAGTTTCACTTCTCTAAA and TACAATGTACACATGTAA-CAC for BRCA2. Together with the RNAi sequences, resistance to puromycin was built into the vector. Transduction was done by adding 1 μ g/ml DNA, TurboFect (1.5 μ l/ml) and polybrene (1 μ l/ml) to a 30% confluent culture of MCF-10A cells. Two days after transduction puromycin (2 μ g/ml) was added to the medium, cells were grown in medium containing puromycin during 15 days to obtain stably transduced cell lines.

The knockdown Ku70 cell line and its control were used previously by Vandersickel et al (54) and an elaborate description about their construction can be found there. Cells infected with lentiviral particles generated with the pLVTHM/shKu70/GFP vector are labeled Ku70i, cells infected with lentiviral particles generated with the empty pLVTHM/GFP control vector are called CON_{Ku70}. Stable knockdown of the protein expression of the silenced genes was evaluated by western blot analysis.

Determination of the cell cycle distribution at the moment of irradiation was done by flow cytometry. Cells were harvested, resuspended in 0.5ml PBS and fixed by slowly adding 3 ml of 95% EtOH. Before analysis, cells were washed and resuspended in hypotonic DNA staining solution (0.1% tri sodium citrate, 0.3% Triton, 0.01% propidium iodide and 0.002% ribonuclease A, dissolved in water). Cells were incubated for 30min at 4°C before being analyzed by flow cytometry.

Western blot

For the western blots, protein was extracted from each cell line with TE lysis buffer (0.1M Tris; 50mM EDTA; 1% NP-40; 1% protease inhibitor (Sigma P8340)). 50 μ g of protein together with LDS sample buffer (ThermoScientific NP0008; 25%) and dithiothreitol (DDT; Sigma Aldrich 43816; 10%) were loaded on a 3-8% tris-acetate gel. Gels were run for 5h at 25mA in tris-acetate running buffer complemented with 2.5% anti-oxidant. PVDF membrane was pretreated with methanol and proteins were transferred to it in tris-glycine transfer buffer with 10% methanol (17h; 30V; 4°C).

After one hour of blocking (3% BSA, 5% dried milk powder, 0.1% tween in tris buffered saline (TBS)), the membrane was incubated (overnight, 4°C) with the primary antibodies (mouse mAb α -BRCA2 (Millipore OP-95; diluted 1/500); rabbit pAb α -BRCA1 (sc-642; diluted 1/1000); mouse mAb α -actinine (sc-17829; diluted 1/30000)), followed by washing and incubation with hrp-conjugated secondary antibodies (1.5h, 20°C) (BRCA1: GAR-hrp

(Perbio 34160; diluted 1/1000); BRCA2 and actinin: RAM-hrp (ThermoScientific 31450; diluted 1/1000)). Visualisation was done using chemoluminescence (ThermoScientific 34076) and detection was done with the Chemidoc-it imaging system (UVP) and Software Vision Works. Protein concentration was determined based on band intensity, using ImageJ software (ImageJ 1.48v).

Sample preparation

Three days before each experiment, the BRCA1i, BRCA2i and CON_{BRCA} cells were grown for 48h in medium containing puromycin (2 μ h/ml). The Ku70i and CON_{Ku70} cells were checked for their GFP-fluorescence.

Experiments performed on synchronized G1 cultures

For the experiments on synchronized G1 cells (hence forward called G1 cultures), cells were seeded three days prior to irradiation and let grown to confluence in order to establish a population of G1 cells. Just before irradiation, these confluent cells were trypsinized and seeded in a concentration of 300.000 cells per well in 6-well plates for the MN-assay and in 24-well plates for the CV cell proliferation assay (2500 cells per well). Approximately 2h after seeding, the cells were attached to the plate and the cultures were irradiated.

Experiments performed on mixed cultures

For the experiments on mixed cultures, sub-confluent cultures of exponentially dividing cells were needed at the moment of irradiation.

For the MN assay cells were trypsinized and seeded in 6-well plates (200.000 cells per well) 1 day prior irradiation. For the CV cell proliferation assay exponentially growing cultures were trypsinized and seeded in 24-well plates at a concentration of 2500 cells per well 2h prior to irradiation.

All MN-assays were done in duplicate and the proliferations assays in quadruplicate. Each experiment was repeated three times.

Irradiations

All cells were irradiated with a ⁶⁰Co γ -source or a clinical neutron beam. Doses from 0.2 up to 6 Gy were given and in each experiment sham-irradiated cultures were included. The ⁶⁰Co γ -rays were produced at a dose rate of 0.5Gy per minute by a teletherapy unit (Theratron 780). Samples were irradiated under charged particle equilibrium conditions, achieved by placing a 0.5 cm thick Perspex table which served as build-up and a 10 cm thick Perspex block for backscatter. The neutron beam was produced by the reaction of 66 MeV protons on a beryllium target producing (p66)+Be(40) neutrons. A 20mm thick sheet of polyethylene was used for dose build-up and a 15cm thick block of Perspex as backscatter. The γ -ray component in the beam was 6.9% and the total neutron dose rate to the samples was 0.4 Gy/min. The neutrons produced by this beam have a mean energy of 29MeV and a mean LET of 20keV/ μ m (57).

Micronucleus (MN) Assay

Chromosomal damage was assessed with the

MN assay. Immediately after irradiation cytochalasin B (2.25 μ g/ml; Sigma) was added to block cytokinesis. The irradiated cells were kept at 37°C in a humidified 5% CO₂ atmosphere incubator for 16h (mixed cultures) or 48h (G1 cultures). After incubation, the cells were harvested by trypsinization, followed by a cold hypotonic shock with 0.075 M KCl and followed by overnight fixation in 3/1/4 methanol/acetic acid/ringer solution (ringer: 9g NaCl, 0.42g KCl and 0.24g CaCl₂ in 1l water). Subsequently, the cells were fixed three times in 3/1 methanol/acetic acid. For further analysis, a suspension of cells was dropped on clean slides and stained with DAPI Vectashield (Lab Consult). Slides were scanned with the MSearch software module of the Metafer 4 scanning system (MetaSystems), using a Zeiss Imager.Z2 microscope (Zeiss) and a CoolCube1 camera (MetaSystems). The MSearch software allows automated detection of binucleated cells and scoring of MN. Two slides per culture were automatically scanned and analyzed with a 10X magnification. The scanned images with the BN cells were coded and the MN score of all BN cells detected by MSearch were checked manually. Per slide approximately 400 BN cells were scored.

Crystal violet (CV) cell proliferation assay

While the clonogenic assay is considered the golden standard to evaluate the *in vitro* response of cells to ionizing radiation, it is not suited for MCF-10A cells due to their inability to form well defined colonies. In a previous study, we showed that the CV cell proliferation

assay provides a useful alternative (58, 59). The same protocol was used here.

In short, after irradiation cells were incubated at 37°C and 5% CO₂ for approximately 4 days until the sham irradiated plates nearly reached confluence. Cells were then fixed for 10 min in a solution of buffered formalin (3.7%), washed with PBS (pH 7.3) and stained with a 0.01% crystal violet solution. After removing excess stain, the stain was overnight dissolved in 1 ml of 10 sodium dodecyl sulfate (SDS). The optical density of the dissolved stain was measured with a spectrophotometer at 590 nm.

Analysis

For the analysis of the MN data, a dose response curve was determined for each condition assuming a linear-quadratic model ($Y = c + \alpha D + \beta D^2$). When no quadratic component was found, a linear response model was used ($Y = c + \alpha D$).

Cell survival was analyzed by fitting log cell surviving fractions (S) as a function of radiation dose (D) to a linear-quadratic model ($\log_e(S) = -\alpha D - \beta D^2$). When no quadratic component was found, a linear model was used ($\log_e(S) = -\alpha D$).

To evaluate the effect of knocking down the repair proteins on the radiation response, the dose modifying factor (DMF) is calculated. The DMF quantifies the radiation response of the knockdown cell line compared to the response of the control cell line. When dose response curves are linear-quadratic in shape the DMF is dose-dependent and can be calculated for different dose points by using the following formula:

$$DMF = \frac{-\alpha_{control} + \sqrt{\alpha_{control}^2 + 4\beta_{control}(\alpha_{knockdown}D + \beta_{knockdown}D^2)}}{2\beta_{control}D}$$

The DMF increases as the dose decreases and reaches its maximum when the dose reaches zero. This DMF_M is calculated with the following formula: $DMF_M = \frac{\alpha_{knockdown}}{\alpha_{control}}$. In the analysis the DMF is calculated for a dose of 2 Gy (DMF_{2Gy}) and the DMF_M is calculated. The 2Gy dose-point was chosen because of its relevance for radiotherapy as often fractions of 2Gy are given, while the DMF_M is important in the frame of low-dose irradiations, like those used in diagnostics.

Whenever the dose response curves are linear in shape for both the control cell line and the knockdown cell line, the DMF becomes dose-independent and equal to DMF_M .

To compare the effects of the different radiation qualities (γ -rays versus neutrons), the relative biological effect (RBE) of neutrons beam compared to γ -rays is calculated. When the dose-response curves are linear-quadratic, the RBE is dose-dependent and can be calculated using the following formula:

$$RBE = \frac{-\alpha_n + \sqrt{\alpha_n^2 + 4\beta_n(\alpha_n D + \beta_n D^2)}}{2\beta_\gamma D}$$

An increase in RBE is noted as the dose decreases. The maximal RBE (RBE_M) is reached when the dose approaches zero and is calculated as follows: $RBE_M = \frac{\alpha_n}{\alpha_\gamma}$. In this study the RBE has been calculated at a dose of 2Gy (RBE_{2Gy}) and the RBE_M has been calculated.

When the dose response curves are linear in shape for both neutron-irradiation and ^{60}Co γ -irradiation, the RBE becomes dose-independent and equal to RBE_M .

Statistical analysis was done using a Student t-test or Mann-Whitney Rank Sum Test, whichever was appropriate depending on the normal distribution of the data. When a pairwise analysis was done, a two sided paired t-test or Wilcoxon Signed Rank Test was used, again depending on the normal distribution of the data.

Results

Western blot

Western blot showed a knockdown of the BRCA1 protein of 70% in the BRCA1i cells and 51% for the BRCA2 protein in the BRCA2i cells. The Ku70 protein has a knockdown of 43% in the Ku70i cells (fig 1).

Cell cycle

At the moment of irradiation the distribution of the cells over the cell cycle was determined for each cell line. For the G1-cultures, 86 ± 4 % of the cells were in G1 after synchronization, 7 ± 2 % in S and 7 ± 2 % in G2. The mixed cultures had 37 ± 4 % of the cells in G1, 25 ± 8 % in G2 and 39 ± 10 % in S phase of the cell cycle.

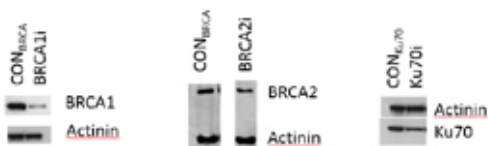


FIGURE 1

Western blot of MCF-10A cells after lentiviral transduction of shRNA for BRCA1, BRCA2 and Ku70 silencing (BRCA1i, BRCA2i and Ku70i) together with their control cell lines (CONBRCA and CONKu70). Actinin was used as a protein loading control.

Micronucleus assay

No significant difference in the radiation response was observed between the two mock-transduced cell lines (CON_{BRCA} and CON_{Ku70}) ($p = 0.24$). The MN dose response curves of both cell lines are depicted in figure 2a.

The spontaneous MN yield (MN/1000 BN cells) \pm SEM for CON_{BRCA} , BRCA1i, BRCA2i, CON_{Ku70} and Ku70i were 28.1 ± 2.5 ; 31.7 ± 4.2 , 26.0 ± 1.7 ; 30.4 ± 2.9 and 39 ± 3.6 respectively. There was no significant difference between the two control cell lines ($p=0.56$), between the BRCA1/2i cell lines and the CON_{BRCA} ($p=0.47$ and $p=0.52$) and between the Ku70i cell line and the CON_{Ku70} ($p=0.07$). For further cal-

culations the number of spontaneous MN was subtracted from the number of MN obtained in the irradiated samples in order to obtain the radiation-induced number of MN.

After γ -irradiation of the knockdown cell lines the radiation-induced MN yields displayed a linear-quadratic response, while for neutrons a linear response was observed. The α and β values are listed in table 1. The BRCA1i cell line didn't recover after irradiation of the cells in the G1 phase of the cell cycle and gave a very low number of BN cells. This behavior was observed in the 3 repeated experiments and no MN results are available for the G1 cultures of the BRCA1i cell line. All dose-response curves are depicted in figure 2 b-d.

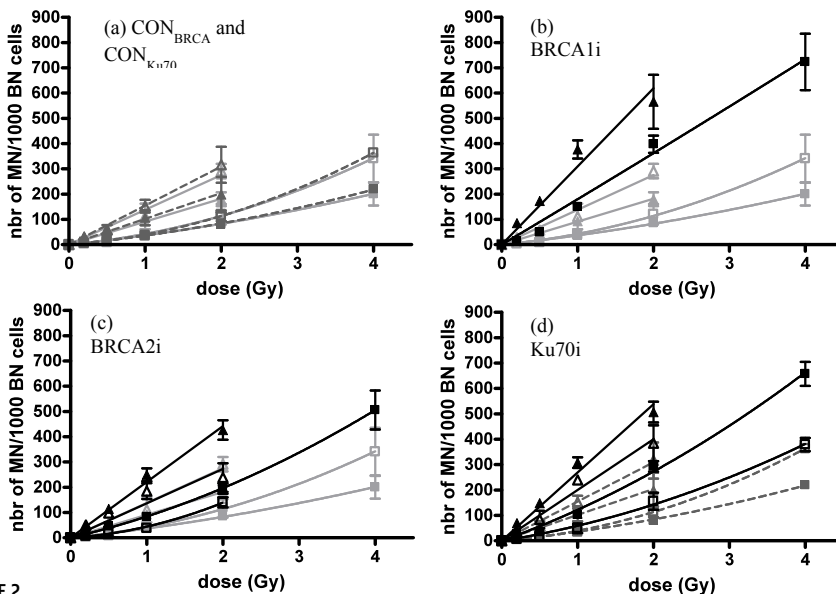


FIGURE 2

MN dose response curves for γ -rays and neutrons of the different cell lines. (a) CON_{Ku70} (dark grey, dashed line) and CON_{BRCA} (light grey, full line) (b) BRCA1i (c) BRCA2i (d) Ku70i. The light grey curves in b and c represent the MN dose response curves of CON_{BRCA} , the dark grey curves in d are the MN dose response curves of CON_{Ku70} . The black curves are the MN dose response curves of the knock down cell lines. ■: gamma irradiation of the mixed cultures; ▲: neutron irradiation of the mixed cultures; □: gamma irradiation of the synchronized G1 cultures; △: neutron irradiation of the synchronized G1 cultures

The DMF quantifies the effect of the knock-down of the repair protein on the radiation-induced MN response. In table 2 the DMF with the 95% confidence limits are given for all cell lines for the 2 Gy dose point (DMF_{2Gy}) and when the dose reaches zero (DMF_M). The 2Gy dose-point (DMF_{2Gy} ; relevant dose for radiotherapy) and when the dose reaches zero (D_{MFM} ; relevant for diagnostic imaging). Due to the absence of a β -component in the MN dose response curve for neutron irradiation, the DMF is dose-independent and there is no difference between

the D_{MFM} and the DMF_{2Gy} . The overview of the DMFs in table 2 shows that all knockdown cell lines were more sensitive than the control cell lines ($DMF > 1$), with the exception of BRCA2i cells synchronized in G1 ($DMF \approx 1$). The effect of the knockdown of the repair proteins was more pronounced when the mixed cultures were irradiated ($DMF_{mix} > DMF_{G1}$). The absence of BN cells when G1 cultures of BRCA1i cells were irradiated and the high DMF_{mix} point to a high radiosensitivity of BRCA1 defective cells. Table 3 lists the RBEs with the 95% confi-

		mixed cultures		G1 cultures	
		gamma	neutron	gamma	neutron
CON _{BRCA}	MN - α	32.3 \pm 3.5	90.8 \pm 5.0	28.1 \pm 17.7	137.7 \pm 9.7
	MN - β	4.5 \pm 1.1		14.4 \pm 4.9	
	CV - α	0.067 \pm 0.011	0.152 \pm 0.026	0.070 \pm 0.025	0.176 \pm 0.084
	CV - β	0.009 \pm 0.002	0.012 \pm 0.005	0.023 \pm 0.007	0.017 \pm 0.016
BRCA1i	MN - α	178.5 \pm 13.0	309.4 \pm 21.4		
	MN - β	1.2 \pm 3.6			
	CV - α	0.309 \pm 0.007	0.500 \pm 0.014	0.461 \pm 0.020	0.582 \pm 0.048
	CV - β				
BRCA2i	MN - α	70.3 \pm 12.8	221.1 \pm 9.2	19.0 \pm 12.4	136.2 \pm 13.9
	MN - β	14.0 \pm 3.6		25.3 \pm 6.9	
	CV - α	0.130 \pm 0.010	0.246 \pm 0.004	0.140 \pm 0.055	0.281 \pm 0.020
	CV - β	0.005 \pm 0.002		0.017 \pm 0.011	
CON _{Ku70}	MN - α	29.7 \pm 3.3	102.0 \pm 6.4	22.3 \pm 4.8	154.8 \pm 8.0
	MN - β	6.2 \pm 1.0		17.2 \pm 1.4	
	CV - α	0.079 \pm 0.010	0.195 \pm 0.022	0.063 \pm 0.042	0.155 \pm 0.073
	CV - β	0.008 \pm 0.002	0.006 \pm 0.005	0.026 \pm 0.008	0.021 \pm 0.014
Ku70i	MN - α	107.0 \pm 6.1	269.0 \pm 10.1	47.2 \pm 9.3	199.9 \pm 13.4
	MN - β	14.7 \pm 1.8		12.0 \pm 2.6	
	CV - α	0.207 \pm 0.021	0.352 \pm 0.007	0.325 \pm 0.065	0.446 \pm 0.030
	CV - β	0.012 \pm 0.006		0.006 \pm 0.018	

TABLE 1

Overview of the α and β values \pm SEM of MN dose response curves and crystal violet cell survival curves for all cell lines and irradiation conditions.

dence limits for all cell lines at 2 Gy (RBE_{2Gy} , radiotherapy relevant dose) and when the dose reaches zero (RBE_M ; relevant in diagnostics). For all cell lines neutron irradiation was more effective in inducing MN than γ -irradiation ($RBE > 1$), with higher RBE values when G1 cultures were irradiated compared to mixed cultures ($RBE_{G1} > RBE_{mix}$). The lowest RBE values were found in the BRCA1i cells.

Crystal violet cell proliferation assay (CV)

No significant difference in CV cell survival was observed between the two control cell lines (CON_{BRCA} and CON_{Ku70}) ($p=0.14$). The cell survival curves of CON_{BRCA} and CON_{Ku70} after irradiation of mixed cultures and G1 cultures with γ -rays and neutrons are depicted in figure 3a. The CV cell survival curves of the knockdown cell lines together with their control cell lines

are shown in figure 3 b-d. They followed a linear-quadratic response, except for BRCA1i (γ and neutron irradiation) and BRCA2i and Ku70i (neutron irradiation), where there was a linear response. It is apparent that the shoulder of the cell survival curves, which is a measure of repair capability, was reduced for all knockdown cell lines compared to their controls related to a lower or absent β -value. A less efficient repair also resulted in an increased failure of the knockdown cell lines to continue to proliferate at higher doses. Due to the presence of non-proliferating cells, tailing could be observed for Ku70i and BRCA1i (above 3 or 4Gy). For these cell lines the higher dose points have been omitted for the regression, the points itself are however plotted on the graph. The α and β values of the survival curves are listed in table 1.

		mixed cultures				G1 cultures				
		DMF_M		DMF_{2Gy}		DMF_M		DMF_{2Gy}		
MN assay	BRCA1i	gamma	5.52	[4.62-6.64]	3.04	[2.51-3.72]				
		neutron	3.41	[3.01-8.56]	3.41	[3.01-8.56]				
	BRCA2i	gamma	2.17	[1.60-2.88]	1.97	[1.49-2.56]	0.67	[0.14-3.02]	1.14	[0.62-1.99]
		neutron	2.44	[2.21-2.69]	2.44	[2.21-2.69]	0.99	[0.83-1.17]	0.99	[0.83-1.17]
	Ku70i	gamma	3.61	[3.61-4.29]	2.33	[2.04-2.69]	2.12	[1.40-3.24]	1.15	[0.93-1.40]
		neutron	2.64	[2.39-2.82]	2.64	[2.39-2.82]	1.29	[1.45-1.15]	1.29	[1.45-1.15]
CV assay	BRCA1i	gamma	4.60	[3.88-5.59]	2.70	[2.37-3.14]	6.62	[4.65-10.82]	2.51	[2.04-3.27]
		neutron	3.29	[2.73-4.08]	2.41	[1.99-3.10]	3.32	[2.06-6.89]	2.29	[1.49-6.07]
	BRCA2i	gamma	1.90	[1.53-2.47]	1.50	[1.22-1.86]	2.01	[0.89-4.39]	1.33	[0.71-2.20]
		neutron	1.62	[1.36-1.99]	1.34	[1.12-1.70]	1.60	[1.01-3.29]	1.28	[0.83-3.08]
	Ku70i	gamma	2.63	[2.11-3.30]	2.06	[1.65-2.57]	5.15	[0.53-7.89]	2.01	[0.46-3.37]
		neutron	1.80	[1.59-2.06]	1.64	[1.40-2.00]	2.89	[0.46-7.76]	1.91	[0.46-5.64]

TABLE 2

Overview of the DMF_{2Gy} [95% LCL – 95% UCL] and DMF_M [95% LCL – 95% UCL] for the MN assay and the crystal violet assay for all cell lines and radiation qualities.

		mixed cultures				G1 cultures			
		RBE _M		RBE _{2Gy}		RBE _M		RBE _{2Gy}	
MN assay	CON _{BRCA}	2.81	[2.39-3.32]	1.85	[1.60-2.19]	4.90	[2.80-14.18]	1.75	[1.32-2.53]
	BRCA1i	1.73	[1.50-2.00]	1.69	[1.40-2.00]				
	BRCA2i	3.15	[2.55-4.01]	1.82	[1.54-2.22]	7.19	[3.9-22.77]	1.47	[1.16-1.94]
	CON _{Ku70}	3.44	[2.90-4.11]	1.91	[1.68-2.20]	6.94	[5.41-9.32]	1.82	[1.66-2.01]
	Ku70i	2.51	[2.29-2.77]	1.71	[1.57-1.87]	4.24	[3.30-5.63]	2.06	[1.74-2.50]
CV assay	CON _{BRCA}	2.26	[1.62-3.15]	1.78	[1.31-2.36]	2.52	[0.96-5.84]	1.51	[0.69-2.60]
	BRCA1i	1.62	[1.54-1.70]	1.62	[1.54-1.70]	1.26	[1.11-1.43]	1.26	[1.11-1.43]
	BRCA2i	1.90	[1.73-2.10]	1.60	[1.51-1.90]	2.00	[1.34-3.54]	1.50	[1.03-2.58]
	CON _{Ku70}	2.49	[1.68-2.64]	1.90	[1.51-2.38]	2.45	[0.47-7.15]	1.43	[0.12-5.03]
	Ku70i	1.70	[1.52-1.93]	1.50	[1.26-1.73]	1.40	[1.07-1.83]	1.30	[0.96-1.83]

TABLE 3

Overview of the RBE_{2Gy} [95%LCL-95%UCL] and the RBE_M [95%LCL-95%UCL] for the MN assay and the crystal violet assay for all cell lines and radiation qualities.

In table 2 an overview can be found of the DMFs, which quantify the effect of knockdown of the repair proteins on radiation-induced cell survival, with the 95% confidence limits of all cell lines at 2Gy (DMF_{2Gy}; relevant dose for radiotherapy) and when the dose reaches zero (DMF_M; relevant for radiodiagnostics). Due to the presence of a quadratic component in the survival curves of the control-cell lines for both γ and neutron irradiation, all DMFs were dose dependent. The radiosensitizing effect of the knockdown could be observed to different extents in all cell lines (DMF>1). The difference between the DMFs in the mixed cultures and the DMFs in the G1 cultures was limited,

with the exception of Ku70i, which had higher DMF_M in the G1 cultures than in the mixed cultures (DMF_{M,G1} > DMF_{M,mix}).

In table 3, an overview is given of all RBEs (RBE_{2Gy} and RBE_M). In the BRCA1i cell line, the RBE was dose-independent due to the absence of a β -component in the cell survival curves and there was no difference between the RBE_M and the RBE_{2Gy}. For all cell lines neutrons were more effective in reducing cell proliferation/increasing cell death compared to γ -rays (RBE >1). The impact of RBE was relatively constant over all cell lines and dose points, with the exception of the BRCA1i cells which had a lower RBE.

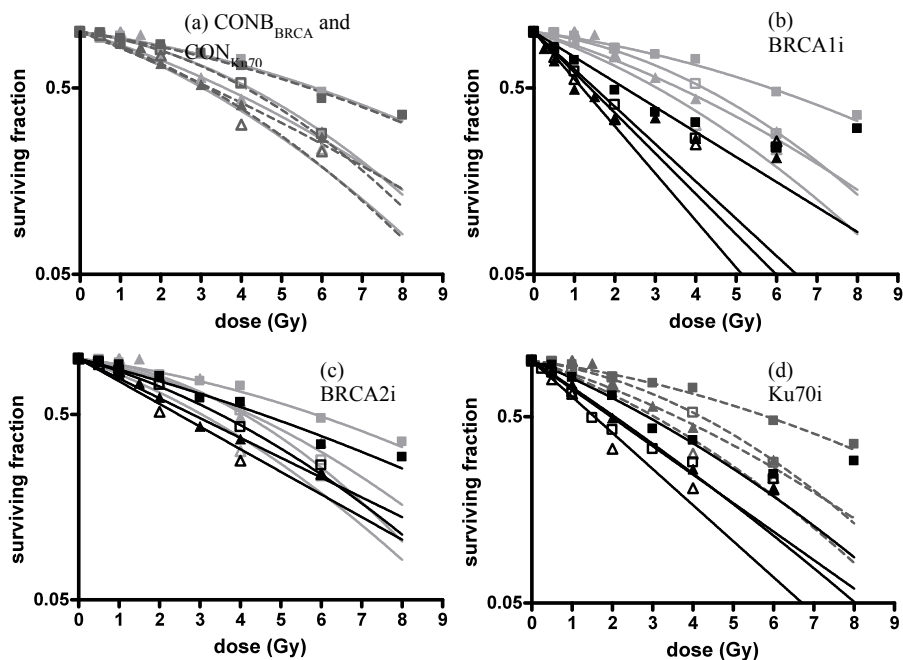


FIGURE 3

CV cell survival curves for γ -rays and neutrons of the different cell lines. (a) CONKu70 (dark grey, dashed line) and CONBRCA (light grey, full line) (b) BRCA1i (c) BRCA2i (d) Ku70i. The light grey curves in b and c are the survival curves of CONBRCA, the dark grey curves in d are the survival curves of CONKu70. The black curves are the survival curves of the knock down cell lines. ■: gamma irradiation of the mixed cultures; ▲: neutron irradiation of the mixed cultures; □: gamma irradiation of the synchronized G1 cultures; △: neutron irradiation of the synchronized G1 cultures.

Discussion

Whether or not *BRCA1* and *BRCA2* mutation carriers are more sensitive to ionizing radiation and how this is influenced by LET or cell cycle stage is an important matter, due to its implications in radiotherapy, radiodiagnostics and mammography breast screening. *BRCA1* homozygous mutations are embryonically lethal

and no homozygous *BRCA1* mutation carriers have been described in any species. A group of Fanconi Anemia (FA) patients have been found to carry a homozygous mutation in *BRCA2* (FA patients with mutation in *FANCD1*). While there is still controversy about radiosensitivity of FA patients, there is a consensus about the fact that they are clinically radiosensitive when

exposed to radiotherapy for cancer treatment or in the conditioning regimen for hematopoietic stem cell transplantation (60-64). *In vivo* studies or *in vitro* experiments performed on lymphocytes or fibroblasts of heterozygous mutation carriers of *BRCA1* or *BRCA2* don't seem to give a clear answer on whether *BRCA1* and *BRCA2* mutation carriers are more sensitive to ionizing radiation. As stated in the introduction, due to small populations and the many variables involved, *in vivo* studies often lack the power to ultimately demonstrate a connection between the presence of *BRCA1* or *BRCA2* mutations and increased radiosensitivity (65). Lymphocytes or fibroblasts derived from heterozygous mutation carriers, which are mostly used in *in vitro* studies, are different from breast epithelial cells and their inherent radiosensitivity could be different. From *in vitro* functional studies we got a good insight in the roles of *BRCA1* and *BRCA2* in DNA repair, which clearly suggest the possibility of a high sensitivity to ionizing radiation. However, these studies seldom investigated the impact of *BRCA1/2*-expression specific to ionizing irradiation and again often the results seem to be inconclusive or contradictory (66-68).

The MCF-10A cell-line used in this study consisted of spontaneously immortalized but non-transformed human breast epithelial cells, and is very suitable to investigate the intrinsic sensitivity of mammary epithelial cells to different irradiation conditions. A 70% knockdown of *BRCA1* and a 51% knockdown of *BRCA2*, allowed to mimic the condition present in the mammary epithelial cells of heterozygous

mutation carriers, thus allowing to investigate the effect of lowered functional *BRCA1* and *BRCA2* proteins levels on radiosensitivity and breast cancer development. The main results obtained in this study with the *BRCA1i*, *BRCA2i* and *Ku70i* mammary epithelial cell lines point to an increase in radiosensitivity following *BRCA1*, *BRCA2* and *Ku70* knock-down.

Depending on the nature of the DSB and the cell cycle phase, the DNA damage response pathway functions differently. *BRCA1*, *BRCA2* and *Ku70* have different functions in the DSB repair pathway, and the radiation response of the knockdown cell lines could be influenced by cell cycle phase and the radiation quality. We investigated the radiation response in the knockdown and control cell lines after irradiation of G1 synchronized or mixed cell cultures exposed to a low-LET γ -source or a high-LET neutron source.

With the MN assay we found neutron-RBE values in the control cell lines (CON_{BRCA}/CON_{Ku70}) cell line of 1.85/1.91 and 1.75/1.82 ($RBE_{2Gy:mix}$ and $RBE_{2Gy;G1}$) rising to an RBE_M of 2.81/3.44 and 4.90/6.94 ($RBE_{M:mix}$ and $RBE_{M;G1}$). Using the same CON_{Ku70} cell line and the same neutron beam, Vandersickel *et al* (55) found an $RBE_{MN;2Gy}$ in mixed cultures of 2.16 and an $RBE_{CV;2Gy}$ in mixed cultures of 2.07, which compares well to our $RBE_{2Gy:mix}$ values of 1.91 (MN assay) and 1.90 (CV assay).

Vral *et al* reported an $RBE_{M;MN}$ of 7.6 in G0 lymphocytes irradiated with 5 MeV neutrons (69). Our reported RBE_M -values were lower, which can be due to the higher energy of the

neutrons used in this study (29 MeV), which is in agreement with the energy dependence of the radiation weighting factor (70). The difference can also be attributed to differences in inherent radiosensitivity between lymphocytes and MCF-10A cells. The same 29 MeV beam was used by Slabbert *et al* (71) and by Vandersickel *et al* (72) on unstimulated G0 lymphocytes from different donors, resulting in RBE_M values between 1.8 and 8. The RBE_M of 4.9 obtained in synchronized G1 MCF10-A cell cultures lies in this range.

The results of the CV cell proliferation assay are in agreement with the results of the MN assay. However, the DMF and RBE values obtained with the CV cell proliferation assay are generally lower than those obtained with the MN assay. Presumably this is because the MN assay focuses specifically on chromosomal aberrations, which are the result of misrepaired or non-repaired DNA DSB, while the crystal violet proliferation assay gives a more general picture of the cell's sensitivity to ionizing radiation.

BRCA2 has an important function in HR, a DSB repair pathway which is only active in the S and G2 phases of the cell cycle. The BRCA2i cell line used in this study showed no increased MN formation compared to its control cell line when synchronized G1 cultures were irradiated ($DMF_{2Gy,y}=1.14$; $DMF_{2Gy,n}=0.99$), but showed increased sensitivity when mixed cultures were irradiated ($DMF_{2Gy,y}=1.97$; $DMF_{2Gy,n}=2.44$). These observations are in line with the prominent role of BRCA2 in HR, as in the G1 cultures approximately 87% of the cells were in

G1 phase in which HR is not active. In mixed cultures, where approximately 65% of the cells were in S or G2, HR can be activated in response to DSB. The results obtained with the CV cell proliferation assay are less straightforward, with a $DMF_{2Gy,y}$ of 1.5 and $DMF_{2Gy,n}$ 1.34 in mixed cell cultures and a $DMF_{2Gy,y}$ of 1.33 and $DMF_{2Gy,n}$ 1.28 in synchronized G1 cell cultures (table 2).

Studies have shown that the NHEJ pathway remains the primary option for DSB repair in all phases of the cell cycle, and that cells switch to HR as a function of chromatin condensation and complexity of the break. More complex breaks, like those produced by higher LET radiation qualities (e.g. neutrons), will typically be repaired by HR (32, 73-76). Therefore the effects of the down regulation of the BRCA2 repair protein could be expected to be more pronounced after neutron-irradiation. Takahashi *et al* demonstrated that this is not the case for a HR-deficient mouse embryonic fibroblast (MEF) cell line, which had approximately the same LET-RBE relationship as the control cell line (77). Similarly, in our study we found that the efficiency of neutrons versus γ -rays to introduce MN and cell death is not clearly altered in cells defective in BRCA2 compared to the control cell line, as comparable RBE values were obtained (table 3)

BRCA1 is involved in HR, but also has a role in detection and signalization of DSB in NHEJ, in single strand annealing (SSA) and in cell cycle control. The results obtained in this study seem to confirm the broader role of BRCA1 in DSB repair since the BRCA1i cell line showed

a higher sensitivity to ionizing radiation, compared to the control cell line and this in both G1 and mixed cultures.

After irradiation of BRCA1i G1 cultures, the number of binucleated cells dropped quickly in a dose-dependent fashion, making it impossible to set up a MN dose-response curve. With the CV cell proliferation assay, data could only be collected for the lower dose points (up to 3Gy), due to a marked reduction in cell proliferation at higher dose points. The BRCA1i survival curve obtained for γ irradiations was characterized by the absence of a shoulder, indicating a strongly reduced repair capacity of the BRCA1i cells (78), which resulted in a dose-related failure of the BRCA1i cells to continue to proliferate. This is in agreement with the low number of binucleated cells obtained in the MN assay. Such strong inhibition of cell proliferation was not observed in the Ku70 and BRCA2 knockdown cell lines. This may point to the fact that BRCA1 depletion seriously affects the repair of radiation-induced DSB in G1, by which the damaged cells are irreversibly blocked in G1 and will probably undergo cell death by apoptosis or senescence (54, 79). However, the high radiosensitivity of the BRCA1i cell line can also be caused by the knockdown of 70% of the BRCA1 protein compared to only 51% and 43% of the BRCA2 and Ku70 proteins respectively.

After irradiation of the BRCA1i mixed cell cultures, cell proliferation was less affected and a MN dose-response curve could be obtained. BRCA1i mixed cultures were found to be highly radiosensitive compared to CON_{BRCA},

with DMF_{MN} values exceeding 3. The reduction in cell proliferation at higher dose points in the CV cell proliferation assay and the high DMF_{CV} values in the range of 2.4-4.6 showed a marked increase in radiosensitivity of BRCA1i cells compared to CON_{BRCA} cells in the mixed cultures. It is clear that the knockdown of BRCA1 affects the radiosensitivity of the cells severely, especially in the low-dose region. The effect was more pronounced than upon depletion of BRCA2, presumably because depletion of BRCA1 does not only affects HR, but also affects NHEJ and SSA (80-82). However, no absolute comparison is possible as the extent of the BRCA1 and BRCA2 knockdowns are different.

The difference in efficiency of both radiation qualities used in this study was less pronounced for BRCA1i cells compared to all other cell lines. Although RBE values higher than 1 were observed in BRCA1i cells, they were lower than those observed in the control and other knockdown cell lines and this effect is more pronounced in the low-dose regions. This has been described previously for MEF cells being deficient in both NHEJ and HR (77).

In the present study we also compared the knockdown of BRCA1 and BRCA2 with the knockdown of another DNA repair protein, Ku70, involved in NHEJ (54, 55). Vandersickel et al also used the KU70i cell line, demonstrating an increase in radiosensitivity. DMFs and RBEs obtained by Vandersickel et al are comparable with our results (55). From table 2 and 3 it can be observed that the radiation response obtained in the BRCA1i cells was sim-

ilar or more pronounced than the response of the Ku70i cells. Increased radiosensitivity was obtained for both mixed and G1 cultures. Although the effect is smaller than the one shown by the BRCA1i cells, the RBE values obtained in the Ku70i cell line were lower than those of the CON_{Ku70} . This can be explained by the fact that this cell line is deficient in NHEJ and proficient in HR, as reported by other researchers (77, 83, 84). However, again no absolute comparison is possible as the extent of the knock-downs are different.

Although both NHEJ and HR play an important role in the repair of radiation-induced DSB, it is still a matter of debate which pathway is used as backup for the repair of radiation-induced DSB in cells carrying inactivating mutations genes involved in NHEJ or HR. BRCA2-defective cells are deficient in HR and proficient in NHEJ. However, BRCA2 only plays a role in HR after DNA end-resection, and it has been shown that switching back to NHEJ after this stage is impossible (32, 66). In BRCA2 deficient cells, SSA has been proposed as a back-up repair pathway (81, 85, 86). BRCA1i cells are deficient in both HR and NHEJ and also need a back-up pathway. Studies have shown the involvement of BRCA1 in SSA, ruling SSA out as back-up pathway (82, 87, 88). Most probably an annealing-dependent pathway like Microhomology Mediated End-Joining may be activated (33, 65, 75, 76, 89, 90).

In conclusion, our study shows increased radiosensitivity of human mammary epithelial cells containing a 70% knockdown for BRCA1 and a 51% knockdown for BRCA2. This reduced

protein level is comparable with the BRCA1 and BRCA2 levels in heterozygous mutation carriers. Our results may imply that caution should be taken when administering ionizing radiation to heterozygous BRCA1 or BRCA2 mutation carriers. When comparing neutrons and γ -rays there seems to be no significant differences in RBE values, as the knockdown cell lines showed similar (BRCA2i) or slightly lower (BRCA1i and Ku70i) RBE values compared to their controls. The increased radiosensitivity observed in the BRCA1 and BRCA2 knock-down cell lines is most pronounced at low doses. Radiosensitivity is increased in both G1 and mixed cultures of BRCA1i and Ku70i cells, but only in mixed cultures of BRCA2i cells. This is in accordance with the different functions of BRCA1, BRCA2 and Ku70. The dependence of the radiation response of the repair deficient cell lines on LET, dose and cell cycle might have implications in radiotherapy and diagnostic screening. However, further research must clarify the practical consequences and possible advantages of the different response of BRCA1 and BRCA2 mutation carriers to ionizing radiation. Which back-up pathways are used in cells defective in BRCA1 and BRCA2, and how a cell will switch from one DSB repair pathway to another is not yet elucidated, but alternative NHEJ pathways such as MMEJ and SSA may be involved.

Acknowledgements

We thank professor Gianpaolo Perletti for his useful comments on the manuscript. The

work was supported by a University Development Cooperation ‘VLIR Own Initiative Programme’ between Belgium and South Africa (ZEIN2011PR387).

Declaration of interest

The authors report no conflicts of interest.

References

1. EBCTCG, Effect of radiotherapy after breast-conserving surgery on 10-year recurrence and 15-year breast cancer death: meta-analysis of individual patient data for 10801 women in 17 randomized trials. *Lancet* 2011; 378, 1707-60.
2. EBCTCG, Effect of radiotherapy after mastectomy and axillary surgery on 10-year recurrence and 20-year breast cancer mortality: meta-analysis of individual patient data for 8135 women in 22 randomised trials. *Lancet* 2014; 383, 2127-35.
3. Yaffe MJ, Mainprize JG, Risk of Radiation-induced Breast Cancer from Mammographic Screening. *Radiology* 2011; 258, 98-105.
4. Wanebo CK, Johnson KG, Sato K, Thorslun.Tw, Breast cancer after exposure to atomic bombings of Hiroshima and Nagasaki. *New England Journal of Medicine* 1968; 279, 667-&.
5. Land CE, Tokunaga M, Koyama K, Soda M, Preston DL, Nishimori I, et al., Incidence of female breast cancer among atomic bomb survivors, Hiroshima and Nagasaki, 1950-1990. *Radiation Research* 2003; 160, 707-17.
6. Boyd NF, Martin LJ, Bronskill M, Yaffe MJ, Duric N, Minkin S, Breast Tissue Composition and Susceptibility to Breast Cancer. *Journal of the National Cancer Institute* 2010; 102, 1224-37.
7. Boice JD, Harvey EB, Blettner M, Stovall M, Flannery JT, CANCER IN THE CONTRALATERAL BREAST AFTER RADIOTHERAPY FOR BREAST-CANCER. *New England Journal of Medicine* 1992; 326, 781-85.
8. Boice JD, Preston D, Davis FG, Monson RR, Frequent chest-X-ray fluoroscopy and breast-cancer incidence among tuberculosis patients in Massachusetts. *Radiation Research* 1991; 125, 214-22.
9. Howe GR, McLaughlin J, Breast cancer mortality between 1950 and 1987 after exposure to fractionated moderate-dose-rate ionizing radiation in the Canadian Fluoroscopy Cohort Study and a comparison with breast cancer mortality in the Atomic Bomb Survivors Study. *Radiation Research* 1996; 145, 694-707.
10. Hancock SL, Tucker MA, Hoppe RT, Breast-cancer after treatment of Hodgkins-disease. *Journal of the National Cancer Institute* 1993; 85, 25-31.
11. Doody MM, Lonstein JE, Stovall M, Hacker DG, Luckyanov N, Land CE, et al., Breast cancer mortality after diagnostic radiography – Findings from the US Scoliosis Cohort Study. *Spine* 2000; 25, 2052-63.
12. Brooks JD, Boice JD, Stovall M, Reiner AS, Bernstein L, John EM, et al., Reproductive Status at First Diagnosis Influences Risk of Radiation-Induced Second Primary Contralateral Breast Cancer in the WECARE Study. *International Journal of Radiation Oncology Biology Physics* 2012; 84, 917-24.
13. Ronckers CM, Doody MM, Lonstein JE, Stovall M, Land CE, Multiple diagnostic x-rays for spine deformities and risk of breast cancer. *Cancer Epidemiology Biomarkers & Prevention* 2008; 17, 605-13.
14. Shore RE, Woodard ED, Hempelmann

- LH, Pasternack BS, Synergism between radiation and other risk-factors for breast-cancer. *Preventive Medicine* 1980; 9, 815-22.
15. van Leeuwen FE, Klokman WJ, Stovall M, Dahler EC, van't Veer MB, Noordijk EM, et al., Roles of radiation dose, chemotherapy, and hormonal factors in breast cancer following Hodgkin's disease. *Journal of the National Cancer Institute* 2003; 95, 971-80.
 16. UNSCEAR, Sources, Effects and Risks of ionizing radiation. . In: Radiation UNSCotEoA editor.; 2013.
 17. Hill DA, Gilbert E, Dores GM, Gospodarowicz M, van Leeuwen FE, Holowaty E, et al., Breast cancer risk following radiotherapy for Hodgkin lymphoma: modification by other risk factors. *Blood* 2005; 106, 3358-65.
 18. Bernstein JL, Haile RW, Stovall M, Grp WSC, Radiotherapy risks recurrence in ATM-mutated breast cancer patients. *Pharmacogenomics* 2010; 11, 673-73.
 19. Bernstein JL, Thomas DC, Shore RE, Robson M, Boice JD, Stovall M, et al., Contralateral breast cancer after radiotherapy among BRCA1 and BRCA2 mutation carriers: A WECARE Study Report. *Eur J Cancer* 2013; 49, 2979-85.
 20. Broeks A, Braaf LM, Huseinovic A, Nooijen A, Urbanus J, Hogervorst FBL, et al., Identification of women with an increased risk of developing radiation-induced breast cancer: a case only study. *Breast Cancer Research* 2007; 9, 9.
 21. Tokunaga M, Land CE, Tokuoka S, Nishimori I, Soda M, Akiba S, Incidence of female breast-cancer among atomic-bomb survivors, 1950-1985. *Radiation Research* 1994; 138, 209-23.
 22. Preston DL, Mattsson A, Holmberg E, Shore R, Hildreth NG, Boice JD, Radiation effects on breast cancer risk: A pooled analysis of eight cohorts. *Radiation Research* 2002; 158, 220-35.
 23. Depuydt J, Baert A, Vandersickel V, Thierens H, Vral A, Relative biological effectiveness of mammography X-rays at the level of DNA and chromosomes in lymphocytes. *International Journal of Radiation Biology* 2013; 89, 532-38.
 24. Heyes GJ, Mill AJ, Charles MW, Mammography-oncogenecity at low doses. *J Radiol Prot* 2009; 29, A123-A32.
 25. Heyes GJ, Mill AJ, Charles MW, Enhanced biological effectiveness of low energy X-rays and implications for the UK breast screening programme – Reply. *British Journal of Radiology* 2006; 79, 855-57.
 26. Jones DTL, Wambersie A, Radiation therapy with fast neutrons: A review. *Nuclear Instruments & Methods in Physics Research Section a-Accelerators Spectrometers Detectors and Associated Equipment* 2007; 580, 522-25.
 27. Amaldi U, Kraft G, Radiotherapy with beams of carbon ions. *Reports on Progress in Physics* 2005; 68, 1861-82.
 28. Valuckas KP, Atkocius V, Kuzmickiene I, Aleknavicius E, Liukpetryte S, Ostapenko V, Second malignancies following conventional or combined Cf-252 neutron brachytherapy with external beam radiotherapy for breast cancer. *Journal of Radiation Research* 2013; 54, 872-79.
 29. Travis E, *Primer of Medical Radiobiology*. 2 ed: Mosby; 1984.
 30. Khanna KK, Jackson SP, DNA double-strand breaks: signaling, repair and the cancer connection. *Nature Genet* 2001; 27, 247-54.
 31. Jackson SP, Sensing and repairing DNA double-strand breaks – Commentary. *Carcinogenesis* 2002; 23, 687-96.
 32. Kakaroukas A, Jeggo PA, IDNA DSB repair pathway choice: an orchestrated handover mechanism. *British Journal of Radiology* 2014; 87, 8.

33. Shibata A, Conrad S, Birraux J, Geuting V, Barton O, Ismail A, et al., Factors determining DNA double-strand break repair pathway choice in G2 phase. *Embo Journal* 2011; 30, 1079-92.
34. Rothkamm K, Kruger I, Thompson LH, Lobrich M, Pathways of DNA double-strand break repair during the mammalian cell cycle. *Molecular and Cellular Biology* 2003; 23, 5706-15.
35. Wyman C, Kanaar R, Homologous recombination: Down to the wire. *Current Biology* 2004; 14, R629-R31.
36. Hefferin ML, Tomkinson AE, Mechanism of DNA double-strand break repair by non-homologous end joining. *DNA Repair* 2005; 4, 639-48.
37. Xu B, Kim ST, Lim DS, Kastan MB, Two molecularly distinct G(2)/M checkpoints are induced by ionizing irradiation. *Molecular and Cellular Biology* 2002; 22, 1049-59.
38. Senderowicz AM, Sausville EA, Preclinical and clinical development of cyclin-dependent kinase modulators. *Journal of the National Cancer Institute* 2000; 92, 376-87.
39. Roy R, Chun J, Powell SN, BRCA1 and BRCA2: different roles in a common pathway of genome protection. *Nat Rev Cancer* 2012; 12, 68-78.
40. Olive PL, The role of DNA single- and double-strand breaks in cell killing by ionizing radiation. *Radiation Research* 1998; 150, S42-S51.
41. Rothkamm K, Lobrich M, Misrepair of radiation-induced DNA double-strand breaks and its relevance for tumorigenesis and cancer treatment (Review). *International Journal of Oncology* 2002; 21, 433-40.
42. Pierce AJ, Stark JM, Araujo FD, Moynahan ME, Berwick M, Jasin M, Double-strand breaks and tumorigenesis. *Trends Cell Biol* 2001; 11, S52-S59.
43. Pijpe A, Andrieu N, Easton DF, Kesminiene A, Cardis E, Nogues C, et al., Exposure to diagnostic radiation and risk of breast cancer among carriers of BRCA1/2 mutations: retrospective cohort study (GENE-RAD-RISK). *British Medical Journal* 2012; 345.
44. Andrieu N, Easton DF, Chang-Claude J, Rookus MA, Brohet R, Cardis E, et al., Effect of chest x-rays on the risk of breast cancer among BRCA1/2 mutation carriers in the International BRCA1/2 Carrier Cohort Study: A report from the EMBRACE, GENEPSO, GEO-HEBON, and IBCCS Collaborators' Group. *Journal of Clinical Oncology* 2006; 24, 3361-66.
45. Gronwald J, Pijpe A, Byrski T, Huzarski T, Stawicka M, Cybulski C, et al., Early radiation exposures and BRCA1-associated breast cancer in young women from Poland. *Breast Cancer Research and Treatment* 2008; 112, 581-84.
46. Goldfrank D, Chuai S, Bernstein JL, Cajal TR, Lee JB, Alonso MC, et al., Effect of mammography on breast cancer risk in women with mutations in BRCA1 or BRCA2. *Cancer Epidemiology Biomarkers & Prevention* 2006; 15, 2311-13.
47. Narod SA, Lubinski J, Ghadirian P, Screening mammography and risk of breast cancer in BRCA1 and BRCA2 mutation carriers: a case-control study (vol 7, pg 402, 2006). *Lancet Oncology* 2006; 7, 453-53.
48. Drooger JC, Hooning MJ, Seynaeve CM, Baaijens MHA, Obdeijn IM, Sleijfer S, et al., Diagnostic and therapeutic ionizing radiation and the risk of a first and second primary breast cancer, with special attention for BRCA1 and BRCA2 mutation carriers: A critical review of the literature. *Cancer Treatment Reviews* 2015; 41, 187-96.
49. Bernier J, Poortmans P, Clinical relevance of normal and tumour cell radiosensitivity

- in BRCA1/BRCA2 mutation carriers: A review. *The breast* 2015; 24, 100-06.
50. Buchholz TA, Wu XF, Hussain A, Tucker SL, Mills GB, Haffty B, et al., Evidence of haplotype insufficiency in human cells containing a germline mutation in BRCA1 or BRCA2. *Int J Cancer* 2002; 97, 557-61.
 51. Foray N, Randrianarison V, Marot D, Pericaudet M, Lenoir G, Feunteun J, Gamma-rays-induced death of human cells carrying mutations of BRCA1 or BRCA2. *Oncogene* 1999; 18, 7334-42.
 52. Frankenberg-Schwager M, Gregus A, Chromosomal instability induced by mammography X-rays in primary human fibroblasts from BRCA1 and BRCA2 mutation carriers. *International Journal of Radiation Biology* 2012; 88, 846-57.
 53. Baeyens A, Thierens H, Claes K, Poppe B, De Ridder L, Vral A, Chromosomal radiosensitivity in BRCA1 and BRCA2 mutation carriers. *International Journal of Radiation Biology* 2004; 80, 745-56.
 54. Vandersickel V, Mancini M, Marras E, Willems P, Slabbert J, Philippe J, et al., Lentivirus-mediated RNA interference of Ku70 to enhance radiosensitivity of human mammary epithelial cells. *International Journal of Radiation Biology* 2010; 86, 114-24.
 55. Vandersickel V, Mancini M, Slabbert J, Marras E, Thierens H, Perletti G, et al., The radiosensitizing effect of Ku70/80 knockdown in MCF10A cells irradiated with X-rays and p(66)+Be(40) neutrons. *Radiation Oncology* 2010; 5.
 56. Debnath J, Muthuswamy SK, Brugge JS, Morphogenesis and oncogenesis of MCF-10A mammary epithelial acini grown in three-dimensional basement membrane cultures. *Methods* 2003; 30, 256-68.
 57. Slabbert JP, Binns PJ, Jones HL, Hough JH, A quality assessment of the effects of a hydrogenous filter on a p(66)Be(40) neutron beam. *British Journal of Radiology* 1989; 62, 989-94.
 58. Vandersickel V, Slabbert J, Thierens H, Vral A, Comparison of the colony formation and crystal violet cell proliferation assays to determine cellular radiosensitivity in a repair-deficient MCF10A cell line. *Radiation Measurements* 2011; 46, 72-75.
 59. Slabbert J, Theron T, Serafin A, Jones DTL, Böhm L, Schmitt G, Radiosensitivity variations in human tumor cell lines exposed in vitro to p(66)/Be neutrons or ⁶⁰Co γ -rays. *Strahlenther Onkol* 1996; 172, 567-72.
 60. Gluckman E, Devergie A, Dutreix J, Radiosensitivity in Fanconi anemia – Application to the conditioning regimen for bone-marrow transplantation. *British journal of haematology*; 1989; 54, 431-40.
 61. Macmillan M, Auberbach A, Davies S, Defor T, Gillio A, Giller R, et al., Haematopoietic cell transplantation in patients with Fanconi anaemia using alternate donors: Results of a total body irradiation dose escalation trial. *British journal of haematology*; 2000; 109, 121-29.
 62. Birkeland A, Auberbach A, Sanborn E, Parashar B, Kuhel W, Chandrasekharappa S, et al., Postoperative Clinical Radiosensitivity in Patients With Fanconi Anemia and Head and Neck Squamous Cell Carcinoma. *Archives of otolaryngology-head & neck surgery*; 2011; 139, 930-34.
 63. Kitao H, Takata M, Fanconi anemia: a disorder defective in the DNA damage response. *International Journal of Hematology* 2011; 93, 417-24.
 64. Alter B, Radiosensitivity in Fanconi's anemia patients. *Radiother Oncol* 2002; 62, 345-47.
 65. Kan C, Zhang JR, BRCA1 Mutation: A Predictive Marker for Radiation Therapy? *International Journal of Radiation Oncology Biology Physics* 2015; 93, 281-93.
 66. Lee SA, Baker MD, Analysis of DNA

- repair and recombination responses in mouse cells depleted for Brca2 by SiRNA. *DNA Repair* 2007; 6, 809-17.
67. Yu D, Sekine E, Fujimori A, Ochiya T, Okayasu R, Down regulation of BRCA2 causes radio-sensitization of human tumor cells in vitro and in vivo. *Cancer Science* 2008; 99, 810-15.
 68. Patel KJ, Yu V, Lee HS, Corcoran A, Thistlethwaite FC, Evans MJ, et al., Involvement of Brca2 in DNA repair. *Mol Cell* 1998; 1, 347-57.
 69. Vral A, Verhaegen F, Thierens H, Deridder L, Micronuclei induced by fast-neutrons versus Co-60 gamma-rays in human peripheral-blood lymphocytes. *International Journal of Radiation Biology* 1994; 65, 321-28.
 70. ICRP, Relative Biological Effectiveness, Radiation Weighting and Quality Factor. ICRP Publication 92. *Annals of the ICRP* 2003; 33.
 71. Slabbert JP, August L, Vral A, Symons J, The relative biological effectiveness of a high energy neutron beam for micronuclei induction in T-lymphocytes of different individuals. *Radiation Measurements* 2010; 45, 1455-57.
 72. Vandersickel V, Beukes P, Van Bockstaele B, Depuydt J, Vral A, Slabbert J, Induction and disappearance of gamma H2AX foci and formation of micronuclei after exposure of human lymphocytes to Co-60 gamma-rays and p(66) + Be(40) neutrons. *International Journal of Radiation Biology* 2014; 90, 149-58.
 73. Mladenov E, Iliakis G, Induction and repair of DNA double strand breaks: The increasing spectrum of non-homologous end joining pathways. *Mutation Research-Fundamental and Molecular Mechanisms of Mutagenesis* 2011; 711, 61-72.
 74. Mladenov E, Kalev P, Anachkova B, The Complexity of Double-Strand Break Ends is a Factor in the Repair Pathway Choice. *Radiation Research* 2009; 171, 397-404.
 75. Aparicio T, Baer R, Gautier J, DNA double-strand break repair pathway choice and cancer. *DNA Repair* 2014; 19, 169-75.
 76. Durante M, Bedford JS, Chen DJ, Conrad S, Cornforth MN, Natarajan AT, et al., From DNA damage to chromosome aberrations: Joining the break. *Mutation Research-Genetic Toxicology and Environmental Mutagenesis* 2013; 756, 5-13.
 77. Takahashi A, Kubo M, Ma HY, Nakagawa A, Yoshida Y, Isono M, et al., Non-homologous End-Joining Repair Plays a More Important Role than Homologous Recombination Repair in Defining Radiosensitivity after Exposure to High-LET Radiation. *Radiation Research* 2014; 182, 338-44.
 78. Thames HD, Withers HR, Peters LJ, Fletcher GH, Changes in early and late radiation responses with altered dose fractionation – implications for dose-survival relationships. *International Journal of Radiation Oncology Biology Physics* 1982; 8, 219-26.
 79. Jones KR, Elmore LW, Jackson-Cook C, Demasters G, Povirk LF, Holt SE, et al., p53-dependent accelerated senescence induced by ionizing radiation in breast tumour cells. *International Journal of Radiation Biology* 2005; 81, 445-58.
 80. Jiang GC, Plo I, Wang T, Rahman M, Cho JH, Yang E, et al., BRCA1-Ku80 Protein Interaction Enhances End-joining Fidelity of Chromosomal Double-strand Breaks in the G(1) Phase of the Cell Cycle. *Journal of Biological Chemistry* 2013; 288, 8966-76.
 81. Stark JM, Pierce AJ, Oh J, Pastink A, Jasin M, Genetic steps of mammalian homologous repair with distinct mutagenic consequences. *Molecular and Cellular Biology* 2004; 24, 9305-16.

-
82. Zhuang J, Zhang JR, Willers H, Wang H, Chung JH, van Gent DC, et al., Check-point kinase 2-mediated phosphorylation of BRCA1 regulates the fidelity of nonhomologous end-joining. *Cancer Research* 2006; 66, 1401-08.
 83. Moore S, Stanley FKT, Goodarzi AA, The repair of environmentally relevant DNA double strand breaks caused by high linear energy transfer irradiation – No simple task. *DNA Repair* 2014; 17, 64-73.
 84. Okayasu R, Okada M, Okabe A, Noguchi M, Takakura K, Takahashi S, Repair of DNA damage induced by accelerated heavy ions in mammalian cells proficient and deficient in the non-homologous end-joining pathway. *Radiation Research* 2006; 165, 59-67.
 85. Larminat F, Germanier M, Papouli E, Defais M, Deficiency in BRCA2 leads to increase in non-conservative homologous recombination. *Oncogene* 2002; 21, 5188-92.
 86. Tutt A, Bertwistle D, Valentine J, Gabriel A, Swift S, Ross G, et al., Mutation in Brca2 stimulates error-prone homology-directed repair of DNA double-strand breaks occurring between repeated sequences. *Embo Journal* 2001; 20, 4704-16.
 87. Zhong Q, Chen CF, Chen PL, Lee WH, BRCA1 facilitates microhomology-mediated end joining of DNA double strand breaks. *Journal of Biological Chemistry* 2002; 277, 28641-47.
 88. Badie S, Carlos AR, Folio C, Okamoto K, Bouwman P, Jonkers J, et al., BRCA1 and CtIP promote alternative non-homologous end-joining at uncapped telomeres. *Embo Journal* 2015; 34, 410-24.
 89. Averbek NB, Ringel O, Herrlitz M, Jakob B, Durante M, Taucher-Scholz G, DNA end resection is needed for the repair of complex lesions in G1-phase human cells. *Cell Cycle* 2014; 13, 2509-16.
 90. Thompson EG, Fares H, Dixon K, BRCA1 requirement for the fidelity of plasmid DNA double-strand break repair in cultured breast epithelial cells. *Environmental and Molecular Mutagenesis* 2012; 53, 32-43.

Article 3

Relative biological effectiveness of mammography X-rays at the level of DNA and chromosomes in lymphocytes

J. Depuydt, A. Baert, V. Vandersickel, H. Thierens and A. Vral
Department of Basic Medical Sciences, University of Ghent, Belgium

International Journal of Radiation Biology 2013; 89, 532-38.

Abstract

Purpose: In many countries, breast cancer screening programs based on periodic mammography exist, giving a large group of women regularly a small dose of ionizing radiation. In order to assess the benefit/risk ratio of those programs the relative biological effectiveness (RBE) of mammography X-rays needs to be determined.

Materials and Methods: Blood of 5 healthy donors was irradiated *in vitro* with 30kV X-rays and ^{60}Co γ -rays with doses between 5 and 2000mGy. The γH2AX -foci technique was used to quantify the number of DNA double strand breaks (DSB) after irradiation. Chromosomal damage resulting from non- or misrepaired DNA DSB was quantified with the micronucleus (MN)-assay and the sensitivity was improved by counting only centromere negative micronuclei (MNCM-).

Results: The threshold detection dose obtained with the γH2AX -foci test was 10mGy for mammography X-rays compared to 50mGy for γ -rays. With the MN-assay respectively MN-centromere-assay threshold detection doses of 100 respectively 50mGy were obtained for mammography X-rays compared to 200 respectively 100mGy for γ -rays.

An RBE of 1.4 was obtained with the γH2AX -foci assay. With the MN-assays low-dose RBE values between 3 and 4 were determined.

Conclusion: Our results indicate that exposure to mammography X-rays resulted in a modest increase in the induction of DSB compared to γ -rays. However, due to the higher LET nature of mammography X-rays more clustered DNA damage is produced that is more difficult to repair and results in a more pronounced increase in micronucleus formation.

Introduction

Breast cancer is the most prevailing cancer among women and about 1 in 9 women will be confronted with it (1). 23% of cancer cases in women are breast cancers and they are the leading cause of cancer death in females worldwide (2). In many countries an increase in the incidence of breast cancer since the late 1980s and early 1990s is observed. This is likely to be the result from changes in reproductive factors like the increased use of postmenopausal hormone therapy as well as an increased screening

intensity. In contrast, over the past 25 years, breast cancer mortality has been decreasing in North America and several European countries largely as a result of early detection through mammography screening and improved treatment (3-5).

In many countries, breast cancer screening programs based on periodic mammography exist for women aged between 50-70 years to diagnose breast cancer in an early stage. Detection and treatment in an early stage gives a better prognosis and a reduction in mortality. Breast

glandular doses are low and typically 2-4 mGy per two-view mammography (6-8). The use of ionizing radiation always implies a risk for radiation-induced breast cancer and although the dose is small, this cannot be neglected in view of the large population size and the repetitive character involved in this type of asymptomatic screening.

Current radiation risk estimates for low linear energy transfer (LET) radiations are based on epidemiologic datasets observed in populations exposed to X-rays with significantly higher energies than are used in breast cancer screening programs, e.g. a pooled analysis of eight cohorts of women exposed to ionizing radiation varying from 80 kVp X-rays to ^{60}Co and ^{226}Ra γ -rays can be found in Preston (9).

Mammography X-rays are low-energy X-rays with a peak and mean photon energy typically 28-30 kV and 15-20 keV, compared to ^{60}Co γ -rays which have a high energy of approximately 1.25 MeV. As a result, 30 kV X-rays have a denser ionization pattern resulting in a higher LET (LET 4.34 keV/ μm) compared to ^{60}Co γ -rays (LET 0.3 keV/ μm). The impact on the biological effect of the higher LET of low energy X-rays like mammography X-rays compared to ^{60}Co γ -rays is still a matter of debate. The International Commission on Radiological Protection acknowledges that, based on *in vitro* experiments on cells, there seem to be significant differences in relative biological effectiveness RBE in radiation qualities of low-LET radiations, but still recommends the use of an RBE value of 1 for 30 kV X-rays (10).

In breast cancer screening programs based

on mammography X-rays it is important to demonstrate that benefit, arising from reduced mortality due to early diagnosis, exceeds any potential risk arising from future radiation-induced breast cancers. Although there are several ways to assess benefit/risk ratios, a simplified approach is to calculate the breast cancer detection over induction ratio (DIR). These calculations are essentially based on epidemiological data of breast screening programs, breast radiation doses and cancer induction risk factors (10-12). Although such calculation models are subject to a certain degree of statistical uncertainty, they can be used to assess benefit/risk taking into account that the number of breast cancers detected must exceed the number of induced cancers by a significant margin. The magnitude of this margin is still under discussion (11), but for women included in most national screening programs, being over 50 and having a 2-year screening-interval, the DIR is over 100 which seems to be ample (13, 14). Several recent *in vitro* radiobiological studies have reported that if we take into account the reported higher radiobiological efficacy of the low-energy X-rays used for mammography compared to conventional higher kV X-rays or ^{60}Co γ -rays it seems that the risk could be underestimated by a factor of 4 ((15-17) for a review see (18)) which obviously will have a huge impact on the DIR. Since DIR-values are used to justify low doses of low energy radiation exposures to a large asymptomatic population it is necessary to have a correct estimation of the RBE of 30 kV X-rays, since this has an impact on the safe use of mammography.

One of the most important biological endpoints to consider for calculating RBE values related to radiation-induced breast cancer is the damage at the level of the DNA. The most genotoxic radiation-induced lesion is the DNA double strand break (DSB) as information is lost in both strands of the DNA. Although DSB can be repaired by different repair-pathways, some will not or will be misrepaired resulting in chromosome aberrations (eg. dicentrics, translocations, micronuclei) which are good biomarkers for cancer risk assessment (19-22). In this study we investigated the RBE of mammography X-rays at the DNA and chromosomal level in comparison to ^{60}Co γ -rays in peripheral blood lymphocytes (PBL) starting from doses as low as 5 mGy. PBL were chosen as they are easy to obtain and they represent a homogeneous cell population (G0 phase) at the moment of *in vitro* irradiation. Moreover, several studies have shown that the degree of radiation sensitivity of an individual is detectable in cells of a type different from the tissues suffering the adverse effect (23). By using the γH2AX -foci assay we quantified the number of DNA DSB induced by radiation in PBL (24). Chromosomal damage was quantified by means of the *in vitro* micronucleus (MN) assay and the more sensitive micronucleus-centromere assay. Radiation-induced micronuclei in PBL contain mainly acentric chromosome fragments which are unstable chromosome aberrations resulting from unrepaired (terminal deletions) or misrepaired DSB (interstitial deletions, acentric fragments arising from asymmetrical exchanges such as dicentrics and centric rings). By this

the MN assay is an easy, alternative method to study chromosomal damage (18, 25-30). The application of the γH2AX -foci assay and the MN assay gives us on the one hand information about the initial number of radiation-induced DSB and on the other hand information about the residual chromosomal damage that remained after repair took place.

Material and Methods

Irradiations

Per experiment, a blood sample was taken by venipuncture from a healthy donor, divided in small volumes and irradiated at room temperature with mammography X-rays or ^{60}Co γ -rays, with doses ranging from 5 to 2000 mGy. In total, blood samples of 5 different donors were analysed in 10 experimental set-ups (2 experiments per donor, one for each radiation quality). Ethical clearance was received from the commission for medical ethics from the Ghent university hospital. Informed consent, allowing the analysis of the effects of irradiation in PBL, was obtained from each volunteer. All donors stated that, to their knowledge, there is no history of breast cancer in the family. The irradiations with ^{60}Co γ -rays were performed at a dose rate of 0.15 Gy/min in a water bath. Mammography-irradiations were performed with a Siemens Mammomat3 producing a 30 kV Mo/Mo X-ray spectrum at a dose rate of 0.125 Gy/min. A layer of exactly 2mm whole blood was irradiated. Within each experiment sham-irradiated controls were included. After

each irradiation the γ H2AX-foci assay and the MN-assay were applied.

γ H2AX-foci assay

The γ H2AX-foci assay was used to quantify radiation-induced DNA DSB. After irradiation with doses ranging from 5 to 500 mGy the blood was incubated at 37°C for 30 minutes to allow maximal foci formation. This incubation period was followed by cooling the blood in ice water to block DNA repair processes. T-lymphocytes were isolated with the RosetteSep blood separation technique (StemCell Technologies, Grenoble, France). Cells were centrifuged onto poly-L-lysine slides (VWR, Leuven, Belgium), fixed in paraformaldehyde (PFA) 3% during 30 min and kept at 4°C in PFA 0.5% overnight. Slides were washed in Dulbecco's phosphate buffered saline (D-PBS) and permeabilized in D-PBS with 0.2% Triton X-100 (Sigma Aldrich, Bornem, Belgium). Cells were blocked with D-PBS with 1% bovine serum albumin (BSA; Roche, Vilvoorde, Belgium) (3 times 10 minutes). Immunostaining was done by incubating the cells during 1h using a mouse-anti- γ H2AX primary antibody (ImTec Diagnostics, Antwerpen, Belgium) diluted 1/500 in blocking buffer, followed by an incubation with RAM-TRITC secondary antibody (DakoCytomation, Heverlee, Belgium) during 1h diluted 1/1000 in blocking buffer. The cells were washed in D-PBS (3 times 10 minutes) and the nuclei were counterstained with 2% DAPI (Sigma Aldrich) dissolved in Fluoromount Mounting Medium (Sigma Aldrich). Slides were scanned using a Metafer

4 scanning system (MetaSystems, Altussheim, Germany) as described by Vandersickel et al. (31). This system uses a Zeiss Imager.Z2 microscope (Zeiss, Zaventem, Belgium) and the images are captured by a CoolCube1 camera (MetaSystems). The metafer software module of the Metafer allows automated interphase nucleus recognition and cell signal detection and counting. First the nuclei are selected and captured as DAPI images using a well defined cell selection classifier with a 40X magnification. In a second step, the fluorescence filter is changed to TRITC and the TRITC signals are captured in the selected nuclei as a z-stack with a total of 10 focal planes and a step size of 0.35 μ m between planes. Per experimental condition 2 slides were scanned. The scanned images were coded and 100 cells per slide were analyzed manually for the presence of foci. Foci size was not considered as overlapping foci edges resulting in underscoring due to 'foci fusion' is only occurring at higher doses (32).

Micronucleus (MN)-assay

The MN-assay was used to quantify residual chromosome damage resulting from mis- or non-repaired DSB (18, 25-30). After irradiation, blood cultures were set up and T-lymphocytes were stimulated by adding 100 μ l phytohemagglutinin (PHA) (Life Technologies, Gent, Belgium). 24 hours later 6 μ g/ml cytochalasin B (Sigma Aldrich) was added to block cytokinesis. Cells were harvested 70h post irradiation by a cold hypotonic shock with 0.075 M KCl, followed by overnight fixation in 4/1/5 Methanol/acetic acid/ringer solution. Subsequently,

the cells were fixed another three times in 4/1 methanol/acetic acid. Suspension of cells was dropped on clean slides and stained with DAPI Vectashield (Lab Consult, Brussel, Belgium) for further analysis. Slides were scanned with the MSearch software module of the Metafer 4 scanning system (MetaSystems) as described by Willems et al (33), using a Zeiss Imager.Z2 microscope (Zeiss) and a CoolCube1 camera (MetaSystems). The MSearch software allows automated detection of binucleated (BN) cells and automated scoring of MN. 2 slides per culture were automatically scanned with a 10X magnification and analyzed. The scanned gallery-images were coded and all BN cells were checked manually on their MN-score. Per slide approximately 2000 BN cells were scored.

In a population of healthy individuals the background MN frequency is rather high and variable (34), limiting its use for the detection of very low doses. The sensitivity of the MN-assay in the low dose range can however be increased by applying a protocol that allows to distinguish between spontaneously occurring MN harboring whole chromosomes and MN induced by radiation containing only acentric chromosome fragments (35, 36). Therefore fluorescent in situ hybridization (FISH) staining with a pancentromere probe was applied on the MN-slides (dose range 0-500 mGy). A home-tailored probe based on polymerase chain reaction (PCR) technology and labeled by the nick-translation method was used (37). Before hybridization MN slides were dehydrated through consecutive solutions of 70, 90 and 100% ethanol, each for 5 min. 20 μ l of probe

dissolved in 120 μ l hybridization buffer was placed on a slide under a coverslip and denaturation (76°C; 5 min) and hybridization (38°C; 20h) was done using a thermocycler (Thermobrite; Abbott, Wavre, Belgium). Coverslips were removed by soaking in a 2X Sodium Salt Citrate (SSC) solution (room temperature; 1-5 min) and were washed in 0.4X SSC+0.1% tween20 (Sigma Aldrich) (70-72°C; 1min) and 2X SSC (room temperature; 5 min). Slides were mounted in a drop of DAPI Vectashield (Lab Consult). For the analysis, MN were first identified by the MSearch module of the Metafer 4 scanning system (MetaSystems). In a second step the BN cells with MN were selected for Autocapt Analysis. During Autocapt analysis the selected cells are scanned at 40X magnification, first with a DAPI filter to visualize the nuclei and next with a TRITC filter to visualize the pancentromeric probe. The presence of a centromeric signal was checked manually on the two colored images shown on the display and in the image gallery.

Data analysis

For both radiation qualities, the foci-frequencies (Y) as a function of dose (D) were best represented by a linear function.

$$Y = c + \alpha D \quad (1)$$

From this, the RBE for foci (RBE_{foci}), equal to the maximal low-dose RBE (RBE_M), is calculated:

$$RBE_{foci} = \frac{\alpha_{30kV}}{\alpha_Y} \quad (2)$$

The MN-frequencies (Y) as a function of dose (D) were best represented by a linear-quadratic model:

$$Y = c + \alpha D + \beta D^2 \quad (3)$$

From this fit, the RBE for MN (RBE_{MN}), which is function of the dose, is calculated by the following formula (38, 39):

$$RBE_{MN} = \frac{-\alpha_\gamma + \sqrt{\alpha_\gamma^2 + 4\beta_\gamma(\alpha_{30kV}D + \beta_{30kV}D^2)}}{2\beta_\gamma D} \quad (4)$$

The micronucleus dispersion index (σ^2/μ), evaluating the distribution of micronuclei compared to the Poisson distribution, was calculated using Dose Estimate (40).

A Wilcoxon test was used to determine the differences in the dose response data for foci, MN and MN without centromeric signal (MNCM-)

between 30 kV X-rays and ^{60}Co γ -rays. All other statistics were done using the two-sided paired t-test.

Results

Applying the γH2AX foci-assay resulted in an average number of background foci of 0.43 ± 0.29 for ^{60}Co γ -rays and 0.33 ± 0.28 for mammography X-rays. A significantly higher number of radiation-induced foci was found after irradiation with mammography X-rays compared to ^{60}Co γ -rays ($p \leq 0.001$; Wilcoxon-test). For both radiation-qualities, a linear dose-response curve was best fitted through the data (figure1). The α -values are listed in Table I. From these linear regressions an RBE-value of 1.36 was calculated (Table II).

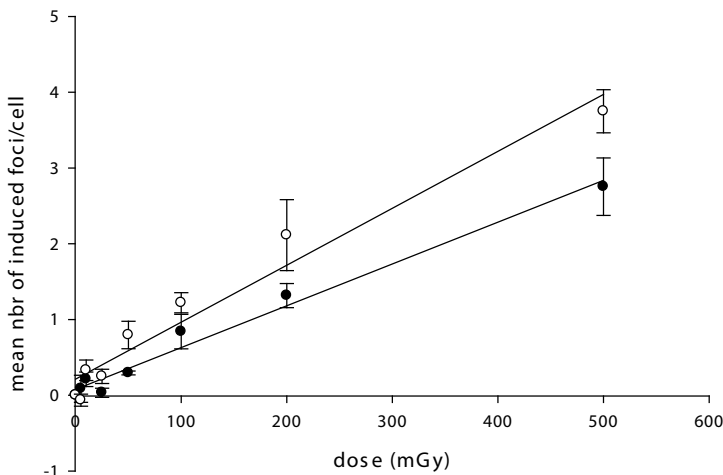


FIGURE 1

Dose-response curves for the mean number of radiation-induced γH2AX -foci per cell for ^{60}Co γ -rays (●) and 30 kV X-rays (○). Error bars indicate the standard error of the mean (SEM) for 5 independent experiments.

For the MN-assay, the average number of background MN was 18 ± 7 for ^{60}Co γ -rays and 15 ± 6 for mammography X-rays. Linear-quadratic dose-response curves were best fitted through the data. In figure 2 the MN dose-response curves are shown and the α and β values are listed in table I. A significantly higher number of radiation-induced MN is seen after irradiation with mammography X-rays compared

to ^{60}Co γ -rays ($p \leq 0.001$; Wilcoxon-test). MN dispersion indices were lying between 1.084 ± 0.019 and 1.164 ± 0.018 for ^{60}Co γ -rays and 1.094 ± 0.021 and 1.165 ± 0.021 for mammography X-rays, indicating a slight overdispersion as would be expected (38). No significant differences in MN dispersion were observed between the two radiation qualities.

	foci		MN		MN _{NCM} -	
	30 kV	^{60}Co	30 kV	^{60}Co	30 kV	^{60}Co
α	0.0075	0.0052	0.090	0.004	0.066	0.015
β	-	-	4.706E-05	4.297E-05	6.453E-05	4.349E-05
c	0.0785	0.2136	-0.816	0.220	-0.043	0.375

TABLE I

a, b and c values of the linear (γH2AX ; figure 1) and linear-quadratic (MN assays; figure 2 and 3) curve fittings.

dose (mGy)	RBE_{foci}		RBE_{MN}		$\text{RBE}_{\text{MN}_{\text{NCM}}}$	
	mean	[95%LCL - 95%UCL]	mean	[95%LCL - 95%UCL]	mean	[95%LCL - 95%UCL]
10			-	-	-	-
25			7.50	[1.82 - 15.40]	3.57	[2.3 - 5.52]
50	1.36	[0.96 - 1.98]	5.67	[1.68 - 10.53]	3.16	[2.12 - 4.59]
100			4.24	[1.51 - 7.30]	2.70	[1.98 - 3.73]
200			3.17	[1.35 - 5.13]	2.27	[1.64 - 3.02]
500			2.20	[1.19 - 3.31]	1.81	[1.32 - 2.34]
1000	-	-	1.74	[1.11 - 2.45]	-	-
2000	-	-	1.44	[1.06 - 1.89]	-	-

TABLE II

RBE-values of mammography X-rays relative to ^{60}Co γ -rays for the γH2AX -foci and the micronucleus data. The numbers between brackets give the 95% upper and lower confidence limit of the RBE.

Dose-response curves for MNCM- are given in figure 3. The results are in line with the results of the standard MN-assay and a significantly higher number of MNCM- was found after irradiation with mammography X-rays compared to ^{60}Co γ -rays ($p \leq 0.001$; Wilcoxon-test). Also here a linear-quadratic curve was best fitted through the data points and the α and β values are listed in Table I. RBE values, calculated according to formula (4) are given in Table II for both MN and

MNCM- assays.

For each radiation quality and biological endpoint studied the threshold detection doses, leading to a significant increase in DNA-damage compared to sham-irradiated controls at the 95% confidence level, were determined and the values are given in Table III.

To better understand the correlation between foci and MN, the radiation-induced foci were plotted against the radiation-induced MN for 30kV X-rays and ^{60}Co γ -rays in figure 4.

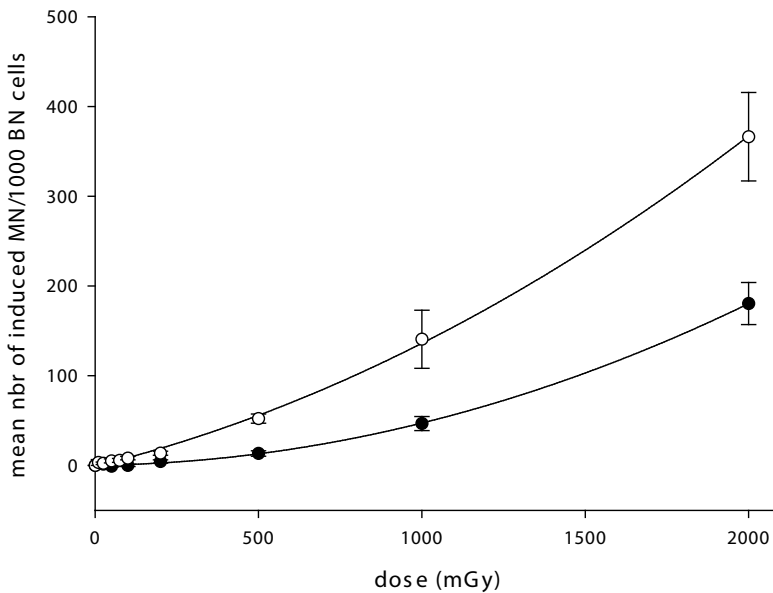


FIGURE 2

Dose-response curves for the mean number of radiation-induced MN per 1000 BN cells for ^{60}Co γ -rays (●) and 30 kV X-rays (○). The dose-response curves are fitted using a weighted linear-quadratic regression. Error bars indicate the standard error of the mean (SEM) for 5 independent experiments.

Discussion

During one mammographic screening session the average dose delivered to the breast glandular tissue is typically 2 – 4mGy (two-view mammography) and screening will be repeated ten times in a two year screening program. In most RBE studies higher doses have been used to study the damaging nature of mammography X-rays and these results are then extrapolated to the low-dose range.

In the present study we used actual mammography-equipment for the irradiations and focused on the low-dose range using two different bio-

logical endpoints. The γ H2AX-assay, used to quantify the number of radiation-induced DSB, is a very sensitive assay that allows the study of low dose effects (41). As a second endpoint for studying RBE, micronuclei, representing residual chromosomal damage, were used. As the presence of high and variably spontaneous MN yields hinders low dose effect estimation, MN slides were stained with a pancentromere probe to discriminate between radiation-induced MN (MNCM-) and spontaneous MN (MNCM+) (33, 35, 37).

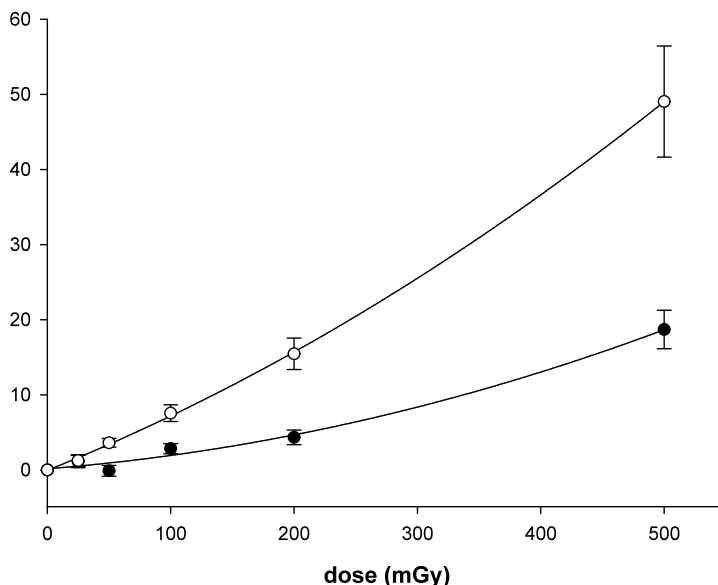


FIGURE 3

Dose response curves of the mean number of radiation-induced centromere negative MN per 1000 BN cells for ^{60}Co γ -rays (●) and 30 kV X-rays (○). Dose-response curves are best fitted through the data using weighted linear-quadratic regression. Error bars indicate the standard error of the mean (SEM) for 5 independent experiments.

The dose-response curves obtained for γ H2AX-foci formation (figure 1) show that for each dose point a higher number of foci (\approx DSB) was obtained after irradiation with 30 kV X-rays compared to ^{60}Co γ -rays. This finding is in line with the physical characteristics of 30 kV

ported by Kühne after irradiation of primary skin fibroblasts with doses between 16 and 64 Gy and analysis by specialized pulsed field gel electrophoresis (PFGE) (44). In the study of Colin et al. (2011), DSB induction by 28 kVp X-rays in exact conditions of mammog-

assay	Dose (mGy)	
	^{60}Co	30 kV
γ H2AX	50	10
MN	200	100
MNCM-	100	50

TABLE III

Threshold detection doses obtained with the γ H2AX foci assay and MN assays for 30 kV X-rays and ^{60}Co γ -rays.

X-rays. 30 kV X-rays indeed produce ionization tracks more dense compared to ^{60}Co γ -rays, by which the chance of one ionization track producing two or more single strand breaks in close proximity leading to a double strand break is higher compared to ^{60}Co γ -rays (42). This higher efficiency of 30 kV X-rays to induce DSB is reflected in RBE values higher than 1 (Table II) and in a lower threshold detection dose (Table III). A dose of 10 mGy can be detected after irradiation with 30 kV X-rays, while for ^{60}Co γ -rays the low dose detection limit is 50 mGy. This dose detection threshold of 50 mGy for ^{60}Co γ -rays was also found by Beels et al. (43). Literature studies reporting on the RBE of mammography X-rays with the induction of DNA DSB as biological endpoint are scarce. The RBE of 1.36 found in our study corresponds with the RBE of 1.15 ± 0.05 re-

raphy irradiation procedures was investigated in primary mammary epithelial cell cultures. By means of the γ H2AX-foci assay they could demonstrate a significant dose effect after exposure to a single dose of 4mGy and a repeated 2+2 mGy dose simulating a two-view mammography (45). The lower dose detection threshold of 4 mGy found by Colin et al. compared to the 10mGy found in our study for mammography X-rays in lymphocytes can be due to differences in the γ H2AX-foci protocol or may point to a higher sensitivity of mammary epithelial cells compared to lymphocytes. In comparison with our DSB-results, the radiation quality effect of 30 kV X-rays compared to ^{60}Co γ -rays was much stronger for chromosomal damage represented by the MN or MNCM- numbers (figure 2) and this for all dose points. This higher efficiency translates

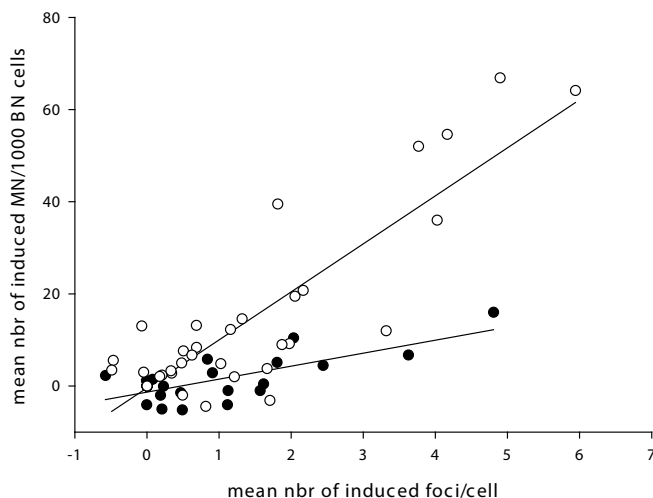


FIGURE 4

Radiation-induced MN as a function of radiation-induced γ H2AX-foci for 30 kV X-rays (○) and ^{60}Co γ -rays (●).

in a lower threshold detection doses for 30 kV X-rays compared to ^{60}Co γ -rays (50 mGy versus 100 mGy (MNCM-) and 100 mGy versus 200 mGy (MN)) (Table III) and meaningful RBE-values between 3 and 4 taking the threshold detection doses for mammography X-rays as limiting dose point (Table II).

Different studies investigating the RBE of low energy X-rays by means of cytogenetic assays have been published, but comparison is difficult due to differences in the physical characteristics and energies (25-50 kV) of the X-rays, the reference radiation quality, the cell type and cytogenetic assay used. Using 200 kV X-rays as reference radiation, RBE_M values vary from 1.2 to 1.7 with MN or dicentric as endpoint (46-48); RBE_M values ranging between 2

and 6 were found for MN or dicentric when ^{60}Co γ -rays were used as reference (49, 50).

The higher RBE values obtained in our study for mammography X-rays compared to ^{60}Co γ -rays with the γ H2AX-assay and the MN-assay clearly point to the higher efficiency of this type of photon radiation to induce DNA damage. Figure 4 demonstrates that the same number of induced foci results in more induced MN after irradiation with 30 kV X-rays compared to ^{60}Co γ -rays. This is also reflected in higher RBE values for MN and implies that mammography X-rays not only induce more DSB compared to ^{60}Co γ -rays but also that DSB arising from 30 kV X-rays are more difficult to repair, probably because they are more complex. These results are in line with the results of Kühne et al.

who analyzed misrejoining using specialized PFGE after irradiation of primary human skin fibroblast with doses ranging between 16 and 80 Gy and found that DSB produced by 29 kV X-rays are misrejoined more frequently than those induced by ^{60}Co γ -rays (44). Mestres et al. investigated the complexity of radiation-induced chromosomal-breakages by FISH after irradiation of whole blood with doses ranging between 2 and 6 Gy. They came to the conclusion that exposure to 30 kVp X-rays resulted in a 1.6 time increase in incomplete and complex aberrations observed compared to 80 and 120 kVp X-rays, which would suggest that the original DNA damage induced by 30 kVp X-rays is more difficult to repair (51). Although in both studies much higher doses were used, it seems that the higher efficiency of 30 kV X-rays to produce more complex breaks also applies to the lower dose area.

Conclusion

With the MN assay, a good biomarker assay for estimating cancer risk, a low dose RBE value of at least 3 was obtained for mammography X-rays. These results confirm recent literature data regarding a higher RBE for mammography X-rays and indicate that the currently used DIR values based on an RBE of 1 (10) are too high. Although *in vitro* radiobiological experiments using lymphocytes cannot be used directly as a basis for reviewing breast cancer screening programs, our results may assist those who design screening programs for groups of younger women.

Acknowledgements

The authors are grateful to the volunteers who donated the blood samples.

Declaration of interest

The authors report no conflicts of interest. The work was supported by a University Development Cooperation 'VLIR Own Initiative Programme' between Belgium and South Africa (ZEIN 2005PR309, ZEIN2011PR387).

References

1. Ferlay J, Autier P, Boniol M, Heanue M, Colombet M, Boyle P, Estimates of the cancer incidence and mortality in Europe in 2006. *Annals of Oncology* 2007; 18, 581-92.
2. Jemal A, Bray F, Center MM, Ferlay J, Ward E, Forman D, Global Cancer Statistics. *Ca-a Cancer Journal for Clinicians* 2011; 61, 69-90.
3. Althuis MD, Dozier JM, Anderson WF, Devesa SS, Brinton LA, Global trends in breast cancer incidence and mortality 1973-1997. *International Journal of Epidemiology* 2005; 34, 405-12.
4. Parkin DM, Fernandez LMG, Use of statistics to assess the global burden of breast cancer. *Breast Journal* 2006; 12, S70-S80.
5. Jemal A, Center MM, DeSantis C, Ward EM, Global Patterns of Cancer Incidence and Mortality Rates and Trends. *Cancer Epidemiology Biomarkers & Prevention* 2010; 19, 1893-907.
6. Klein R, Aichinger H, Dierker J, Jansen JTM, JoiteBarfuss S, Sabel M, et al., Determination of average glandular dose with modern mammography units for two large groups of patients. *Physics in Medi-*

- cine and Biology 1997; 42, 651-71.
7. Brenner DJ, Doll R, Goodhead DT, Hall EJ, Land CE, Little JB, et al., Cancer risks attributable to low doses of ionizing radiation: Assessing what we really know. *Proceedings of the National Academy of Sciences of the United States of America* 2003; 100, 13761-66.
 8. Hendrick RE, Pisano ED, Averbukh A, Moran C, Berns EA, Yaffe MJ, et al., Comparison of Acquisition Parameters and Breast Dose in Digital Mammography and Screen-Film Mammography in the American College of Radiology Imaging Network Digital Mammographic Imaging Screening Trial. *American Journal of Roentgenology* 2010; 194, 362-69.
 9. Preston DL, Mattsson A, Holmberg E, Shore R, Hildreth NG, Boice JD, Radiation effects on breast cancer risk: A pooled analysis of eight cohorts. *Radiation Research* 2002; 158, 220-35.
 10. ICRP, The 2007 recommendations of the International Commission on Radiological Protection. ICRP Publication 103. *Annals of the ICRP* 2007; 37.
 11. Law J, Faulkner K, Cancers detected and induced, and associated risk and benefit, in a breast screening programme. *British Journal of Radiology* 2001; 74, 1121-27.
 12. Law J, Faulkner K, Concerning the relationship between benefit and radiation risk, and cancers detected and induced, in a breast screening programme. *British Journal of Radiology* 2002; 75, 678-84.
 13. Heyes GJ, Mill AJ, Charles MW, Enhanced biological effectiveness of low energy X-rays and implications for the UK breast screening programme. *British Journal of Radiology* 2006; 79, 195-200.
 14. Law J, Faulkner K, Two-view screening and extending the age range: the balance of benefit and risk. *British Journal of Radiology* 2002; 75, 889-94.
 15. Frankenberg D, Kelnhofner K, Bar K, Frankenberg-Schwager M, Enhanced neoplastic transformation by mammography X rays relative to 200 kVp x rays: Indication for a strong dependence on photon energy of the RBE_M for various end points. *Radiation Research* 2002; 157, 99-105.
 16. Goggelmann W, Jacobsen C, Panzer W, Walsh L, Roos H, Schmid E, Re-evaluation of the RBE of 29 kV x-rays (mammography x-rays) relative to 220 kV x-rays using neoplastic transformation of human CGL1-hybrid cells. *Radiation and Environmental Biophysics* 2003; 42, 175-82.
 17. Heyes GJ, Mill AJ, The neoplastic transformation potential of mammography X rays and atomic bomb spectrum radiation. *Radiation Research* 2004; 162, 120-27.
 18. Hunter N, Muirhead CR, Review of relative biological effectiveness dependence on linear energy transfer for low-LET radiations. *J Radiol Prot* 2009; 29, 5-21.
 19. Khanna KK, Jackson SP, DNA double-strand breaks: signaling, repair and the cancer connection. *Nature Genet* 2001; 27, 247-54.
 20. Bonassi S, Znaor A, Ceppi M, Lando C, Chang WP, Holland N, et al., An increased micronucleus frequency in peripheral blood lymphocytes predicts the risk of cancer in humans. *Carcinogenesis* 2007; 28, 625-31.
 21. Bonassi S, Norppa H, Ceppi M, Stromberg U, Vermeulen R, Znaor A, et al., Chromosomal aberration frequency in lymphocytes predicts the risk of cancer: results from a pooled cohort study of 22 358 subjects in 11 countries. *Carcinogenesis* 2008; 29, 1178-83.
 22. El-Zein R, Vral A, Etzel CJ, Cytokinesis-blocked micronucleus assay and cancer risk assessment. *Mutagenesis* 2011; 26, 101-06.
 23. Rieger KE, Hong WJ, Tusher VG, Tang

- J, Tibshirani R, Chu G, Toxicity from radiation therapy associated with abnormal transcriptional responses to DNA damage. *Radiother Oncol* 2004; 72, S29-S29.
24. Rogakou EP, Pilch DR, Orr AH, Ivanova VS, Bonner WM, DNA double-stranded breaks induce histone H2AX phosphorylation on serine 139. *Journal of Biological Chemistry* 1998; 273, 5858-68.
 25. Vral A, Fenech M, Thierens H, The micronucleus assay as a biological dosimeter of in vivo ionising radiation exposure. *Mutagenesis* 2011; 26, 11-17.
 26. Fenech M, Cytokinesis-block micronucleus cytome assay. *Nature Protocols* 2007; 2, 1084-104.
 27. Fenech M, Kirsch-Volders M, Natarajan AT, Surrallés J, Crott JW, Parry J, et al., Molecular mechanisms of micronucleus, nucleoplasmic bridge and nuclear bud formation in mammalian and human cells. *Mutagenesis* 2011; 26, 125-32.
 28. Thomas P, Umegaki K, Fenech M, Nucleoplasmic bridges are a sensitive measure of chromosome rearrangement in the cytokinesis-block micronucleus assay. *Mutagenesis* 2003; 18, 187-94.
 29. Boei J, Vermeulen S, Fomina J, Natarajan AT, Detection of incomplete exchanges and interstitial fragments in X-irradiated human lymphocytes using a telomeric PNA probe. *International Journal of Radiation Biology* 1998; 73, 599-603.
 30. Boei J, Vermeulen S, Natarajan AT, Analysis of radiation-induced chromosomal aberrations using telomeric and centromeric PNA probes. *International Journal of Radiation Biology* 2000; 76, 163-67.
 31. Vandersickel V, Depuydt J, Van Bockstaele B, Perletti G, Philippe J, Thierens H, et al., Early Increase of Radiation-induced gamma H2AX Foci in a Human Ku70/80 Knockdown Cell Line Characterized by an Enhanced Radiosensitivity. *Journal of Radiation Research* 2010; 51, 633-41.
 32. Rothkamm K, Horn S, gamma-H2AX as protein biomarker for radiation exposure. *Annali Dell Istituto Superiore Di Sanita* 2009; 45, 265-71.
 33. Willems P, August L, Slabbert J, Romm H, Oestreicher U, Thierens H, et al., Automated micronucleus (MN) scoring for population triage in case of large scale radiation events. *International Journal of Radiation Biology* 2010; 86, 2-11.
 34. Bonassi S, Fenech M, Lando C, Lin YP, Ceppi M, Chang WP, et al., HUman MicroNucleus Project: International database comparison for results with the cytokinesis-block micronucleus assay in human lymphocytes: I. Effect of laboratory protocol, scoring criteria, and host factors on the frequency of micronuclei. *Environmental and Molecular Mutagenesis* 2001; 37, 31-45.
 35. Vral A, Thierens H, deRidder L, In vitro micronucleus-centromere assay to detect radiation-damage induced by low doses in human lymphocytes. *International Journal of Radiation Biology* 1997; 71, 61-68.
 36. Thierens H, Vral A, Barbe M, Aousalah B, De Ridder L, A cytogenetic study of nuclear power plant workers using the micronucleus-centromere assay. *Mutation Research-Genetic Toxicology and Environmental Mutagenesis* 1999; 445, 105-11.
 37. Baeyens A, Swanson R, Herd O, Ainsbury E, Mabhenghu T, Willem P, et al., A semi-automated micronucleus-centromere assay to assess low-dose radiation exposure in human lymphocytes. *International Journal of Radiation Biology* 2011; 87, 923-31.
 38. Vral A, Verhaegen F, Thierens H, Deridder L, Micronuclei induced by fast-neutrons versus Co-60 gamma-rays in human peripheral-blood lymphocytes. *International Journal of Radiation Biology* 1994; 65, 321-28.

39. Vandersickel V, Mancini M, Slabbert J, Marras E, Thierens H, Perletti G, et al., The radiosensitizing effect of Ku70/80 knockdown in MCF10A cells irradiated with X-rays and p(66)+Be(40) neutrons. *Radiation Oncology* 2010; 5.
40. Ainsbury EA, Lloyd DC, Dose estimation software for radiation biodosimetry. *Health Phys* 2010; 98, 290-95.
41. Rothkamm K, Lohrich M, Evidence for a lack of DNA double-strand break repair in human cells exposed to very low x-ray doses. *Proceedings of the National Academy of Sciences of the United States of America* 2003; 100, 5057-62.
42. Charlton DE, Nikjoo H, Humm JL, Calculation of initial yields of single-strand and double-strand breaks in cell-nuclei from electrons, protons and alpha-particles. *International Journal of Radiation Biology* 1989; 56, 1-19.
43. Beels L, Werbrouck J, Thierens H, Dose response and repair kinetics of gamma-H2AX foci induced by in vitro irradiation of whole blood and T-lymphocytes with X- and gamma-radiation. *International Journal of Radiation Biology* 2010; 86, 760-68.
44. Kuhne M, Urban G, Frankenberg D, Lohrich M, DNA double-strand break misrejoining after exposure of primary human fibroblasts to C-K characteristic X rays, 29 kVp X rays and Co-60 gamma rays. *Radiation Research* 2005; 164, 669-76.
45. Colin C, Devic C, Noel A, Rabilloud M, Zabol MT, Pinet-Isaac S, et al., DNA double-strand breaks induced by mammographic screening procedures in human mammary epithelial cells. *International Journal of Radiation Biology* 2011; 87, 1103-12.
46. Slonina D, Spekl K, Panteleeva A, Brankovic K, Hoinkis C, Dorr W, Induction of micronuclei in human fibroblasts and keratinocytes by 25 kV x-rays. *Radiation and Environmental Biophysics* 2003; 42, 55-61.
47. Lehnert A, Lessmann E, Pawelke J, Dorr W, RBE of 25 kV X-rays for the survival and induction of micronuclei in the human mammary epithelial cell line MCF-12A. *Radiation and Environmental Biophysics* 2006; 45, 253-60.
48. Mestres M, Caballin MR, Barrios L, Ribas M, Barquinero JE, RBE of X rays of different energies: A cytogenetic evaluation by FISH. *Radiation Research* 2008; 170, 93-100.
49. Schmid E, Regulla D, Kramer HM, Harder D, The effect of 29 W X rays on the dose response of chromosome aberrations in human lymphocytes. *Radiation Research* 2002; 158, 771-77.
50. Verhaegen F, Vral A, Sensitivity of micronucleus induction in human-lymphocytes to low-LET radiation qualities – RBE and correlation of RBE and LET. *Radiation Research* 1994; 139, 208-13.
51. Mestres M, Benkhald L, Caballin MR, Barrios L, Ribase M, Barquinero JF, Induction of Incomplete and Complex Chromosome Aberrations by 30 kVp X Rays. *Radiation Research* 2011; 175, 201-07

Article 4

γ H2AX foci induced by low dose mammography X-rays in breast tissue

J. Depuydt¹; T. Viaene¹, P. Blondeel², N. Roche², H. Thierens¹, A. Vral¹

1 Department of Basic Medical Sciences, University of Ghent, Belgium

2 Plastic surgery, Ghent University Hospital, Belgium.

Article in preparation to submit to Radiation Research

Abstract

Purpose: Most studies investigating the RBE of mammography X-rays use blood lymphocytes, primary fibroblasts or cell lines. Breast tissue is however a very specific tissue, which is very sensitive to radiation due to the presence of reproductive hormones like estrogen. In this study we investigated the efficiency of mammography X-rays to induce DSB in the low-dose range (0-500 mGy) in mammary epithelial cells present in freshly resected healthy breast tissue.

Methods: Not cancerous, freshly resected breast tissue was irradiated with mammography X-rays in the dose range 0-500mGy with a special emphasis on the very low doses (0-20mGy). With the yH2AX-foci assay we quantified the number of DNA DSB induced by radiation in the glandular tissue.

Results: Foci-induction by 30kV X-rays followed bi-phasic linear dose-response curve, with the low-dose part (0-40mGy) being 8.7 times steeper than the higher dose part (20-500mGy). This resulted in an RBE of 3.75 in the low-dose range.

Conclusions: Our results indicate the existence of a low-dose hypersensitive response observed for DSB induction in the dose range representative for mammography screening which is probably caused by the bystander effect. This could affect the risk calculations for mammography screening.

Introduction

Breast tissue consists mainly of adipose and fibroglandular tissue. 15 to 25 glandular units consist each of a single large duct which branches repeatedly to form a terminal duct-lobular unit (TDLU). Each TDLU consists of a terminal duct and a lobule consisting of multiple acini. Invasive ductal carcinoma originates in the ducts of the glandular tissue and is by far the most common type of breast cancer, representing 80% of the invasive breast cancers. 10% of the invasive breast cancers are invasive lobular carcinomas.

Breast cancer is the most prevailing cancer among women and about 1 in 9 women in Europe will be confronted with it (1). 23% of

cancer cases in women are breast cancers and they are the leading cause of cancer death in females worldwide (2). In many countries an increase in the incidence of breast cancer since the late 1980s and early 1990s is observed. This is likely to be the result from changes in reproductive factors like the increased use of postmenopausal hormone therapy as well as an increased screening intensity. In contrast, over the past 25 years, breast cancer mortality has been decreasing in North America and several European countries largely as a result of early detection through mammography screening and improved treatment modalities (3-5). In many countries, breast cancer screening programs based on periodic mammography exist

for women aged between 45-50 to 70-75 years to diagnose breast cancer in an early stage (6). Detection and treatment in an early stage gives a better prognosis and a reduction in mortality. Breast glandular doses are low and typically 3-5 mGy per two-view mammography (7-9). The use of ionizing radiation always implies a risk for radiation-induced breast cancer and although the dose is small, this cannot be neglected in view of the large population size and the repetitive character (annual or biannual) involved in this type of asymptomatic screening. Mammography X-rays are low-energy X-rays with a peak and mean photon energy typically 28-30 kV and 15-20 keV respectively. 30 kV X-rays have a more dense ionization pattern resulting in a higher LET (LET 4.34 keV/ μm) compared to high energy photons such as e.g. ^{60}Co γ -rays (LET 0.3 keV/ μm , energy 1.25MeV). The impact on the biological effect of the higher LET of low energy X-rays as mammography X-rays compared to high energy photons is still a matter of debate. The International Commission on Radiological Protection acknowledges that, based on *in vitro* experiments on cells, there seems to be significant differences in relative biological effectiveness (RBE) in radiation qualities of low-LET radiations related to the energy, but still recommends the use of a radiation weighting factor of 1 for 30 kV X-rays (10).

In the high dose range upwards from 100mGy as applied in radiotherapy, there is a linear relationship with the dose received and the long term effects of radiation (11). The effects of low (<100 mGy) and very low doses (<10 mGy), as

applied in medical diagnostics, are less clear. Available epidemiological data do not have sufficient statistical power to assess the radiation risks of the low and very low exposure levels (8). However, the inability to quantify these risks does not imply that the risk to the population is negligible. A very small risk, if applied to a large number of healthy individuals, can result in a significant health problem (8).

In vitro studies investigating cellular and genetic effects can highlight the consequences of low and very low doses of ionizing irradiation. After an exposure to just a few mGy, e.g. γH2AX foci, which are representative for DNA DSB, can be demonstrated (12-14), even in primary breast epithelial cells (15) or changes in transcription level of genes can be detected (16-18). Doses as low as a few mGy have an impact on the cell physiology and gene expression analysis demonstrated that different gene profiles are activated after low and high doses of X-rays in whole blood (19). However, how these effects translate into low-dose risks, and whether they have detrimental or beneficial effects, is still a matter of debate. In radiation protection practice a linear no threshold extrapolation is used (LNT) to calculate the risks at low doses using data from higher doses. However, this is just a working hypothesis which might underestimate or overestimate the effects of low dose radiation (8).

Most data on the low dose effects of mammography X-rays are derived from blood lymphocytes, primary fibroblasts or cell lines. However, breast tissue is a very specific tissue, which is very sensitive to radiation due to the pres-

ence of reproductive hormones like estrogen. Estrogens might be complete carcinogens as estrogens stimulate both estrogen receptor-mediated cell proliferation and induce DNA damage by the formation of genotoxic metabolites such as reactive oxygen species (ROS) (20-23). In this study we investigated the effect of mammography X-rays in the low-dose range (0-500 mGy) in mammary epithelial cells present in freshly resected healthy breast tissue. By using γ H2AX-foci assay we quantified the number of DNA DSB induced by radiation in the glandular tissue (24). To study the RBE ^{60}Co γ -rays were used as reference radiation quality.

Material and methods

Patients, preparation of the breast tissue and irradiations

No cancerous, freshly resected breast tissue was obtained from the department for plastic surgery from the Ghent University Hospital. The tissue specimens were collected during surgery from healthy individuals undergoing a breast reduction or mastectomy related to a high risk genetic profile for breast cancer. Ethical clearance was received from the commission for medical ethics from the Ghent University hospital. Signed informed consent, allowing the analysis of the effects of irradiation on breast tissue, was obtained from each donor. In total 15 breast tissue-samples from a total of 18 were of good quality (see further), 11 from donors without an increased risk for breast cancer, 4 from donors with a high risk profile for breast

cancer of which 3 have a confirmed BRCA1/2 mutation. Donors were on average 41 years old. Immediately after resection, the tissue was processed for irradiation. For this, fat tissue was removed as much as possible and the remaining connective tissue containing the glands was cut in slices between 1.5 and 2mm thick, while kept in physiological solution (Ringer's Solution: 9g NaCl Sigma-Aldrich, Bornem, Belgium; 0.42g CaCl_2 and 0.24g KCl both VWR, Leuven, Belgium; 1l aqua dest., pH 7.2). Once the slices of breast tissue were prepared for irradiation, they were kept in a 5% CO_2 -incubator at 37°C in DMEM/F12-ham medium (Invitrogen, Belgium) supplemented with 5% fetal calf serum (Invitrogen), antibiotics and growth factors (10 $\mu\text{g}/\text{ml}$ insulin (Sigma, Belgium); 0.5 $\mu\text{g}/\text{ml}$ hydrocortisone (Sigma); 20ng/ml epidermal growth factor (Tebu-bio, Belgium); 50 U/ml penicillin and 50 $\mu\text{g}/\text{ml}$ streptomycin (Invitrogen)).

Samples were irradiated with mammography X-rays, with doses ranging from 2 to 500 mGy (doses: 2, 4, 10, 20, 40, 100 and 500 mGy). In addition samples were also irradiated with ^{60}Co γ -rays as reference radiation quality. Mammography-irradiations were performed with a Siemens Mammomat3 producing a 30 kV Mo/Mo X-ray spectrum at a dose rate of 0.125 Gy/min in a warm box at 37°C. A layer of exactly 2mm medium with tissue was irradiated. The irradiations with ^{60}Co γ -rays were performed at a dose rate of 5mGy/min for doses till 40mGy and at 0.6 Gy/min for higher doses in a water bath at 37°C. Within each experiment sham-irradiated controls were included.

Fixation, embedding and haematoxylin-eosin staining

Immediately after the irradiation, the tissue-samples were incubated for exactly 30min at 37°C, the time at which foci-formation is at its maximum. After this time, samples were transferred to cold ringer's solution and kept on ice-water to inhibit repair processes. Subsequently they were transferred to paraformaldehyde (PFA; 4%; VWR) for fixation.

After 24h in PFA the tissue-samples were dehydrated and embedded in paraffin. Tissue sections of 5 μ m were cut with a microtome. Per sample 2 tissue sections were placed on the same slide and multiple slides were made.

The quality of the tissue and the presence of glandular tissue was inspected by performing a haematoxylin-eosin staining. This staining was done automatically using a multipurpose slide staining device (Robot stainer: Microm HMS 740; Walldorf, Germany).

γ H2AX immunostaining

Prior to the γ H2AX immunostaining, tissue sections were deparaffinised and rehydrated using the Robot stainer (Microm HMS 740).

Antigen retrieval was done in sodium citrate buffer (0.2 g citric acid (Merck, Darmstadt, Germany) in 1l aqua dest.; pH6). The tissue sections were brought in the buffer and boiled twice during 5 min using a microwave. After washing of the sections in PBS, they were pre-treated in 3% H₂O₂ (VWR) to inactivate the endogenous peroxidases. Sections were further incubated in blocking serum (BS) (PBS 5 ml, BSA 50mg (Bovine serum albumin; Roche Di-

agnostics, Vilvoorde, Belgium); NRS 0.250 ml (Normal rabbit serum; Dako); Tween 20 (1ml 10% Tween 20 (VWR)) for 30 min to avoid nonspecific binding and to permeabilize the membranes.

Immunostaining was done using a tri-step reaction using consecutively mouse-anti- γ H2AX (primary antibody; Biolegend, Trembodegem, Belgium; 2h, 1/1000 in PBS with 10% BS at room temperature (RT)), biotinylated rabbit-anti-mouse (secondary antibody; Dako, 30min, 1/200 in PBS with 10% BS at RT) and streptavidine-horse radish peroxidase (Dako; 30 min, 1/200 in PBS at RT). Between the steps the tissue-sections were washed in PBS (2x5 min). Next, the sections were incubated with DAB-NiCl₂ (stock solution (ss) DAB: 25mg/1ml AD; ss NiCl₂: 4g/50ml AD; work solution: 200 μ l DAB ss; 50 μ l NiCl₂ ss; 10ml PBS; 5 μ l H₂O₂) during 10 min in the dark to visualize the γ H2AX foci. Slides were washed during 10 min in running tap water before dehydrating and mounting the sections with mounting medium (Thermo Scientific). Slides were sealed with a cover slip.

Foci scoring

γ H2AX-foci scoring was done manually, using a light microscope (Leica LEITZ-DM-RB, Diegem, Belgium) at 63X magnification (Fluotar 63X/1.25 Oil, Leica). Per breast tissue sample and per radiation condition, at least two tissue-sections were counted by two experienced researchers. In each section the number of γ H2AX foci in 100 nuclei was scored, if possible in at least 4 different glandular groups.

Only the epithelial cells from the inner luminal layer were taken into account.

Analysis

For the analysis of the γ H2AX foci data, a dose response curve was fitted for 30 kV X-ray in the dose range (0-20mGy) and the range (20-500mGy) assuming a linear model ($Y=c+\alpha D$). For γ -irradiation, a linear dose-response curve was fitted.

To compare the effects of the different radiation qualities (γ -rays versus 30kV X-rays), the relative biological effect (RBE) of 30kV X-rays compared to γ -rays is calculated using the following formula: $RBE = \alpha_x / \alpha_y$.

Statistical analysis was done using the program SigmaPlot (SigmaPlot for Windows Version 13.0). To compare two groups of data, a Student t-test or a rank sum test was used, depending on the normal distribution of the data.

Results

Hematoxylin-eosin (HE) staining

Inspection of the samples by HE staining (figure 1) revealed that some samples contained cells with an abnormal morphology. In those cases, all tissue samples for that donor were rejected from the study.

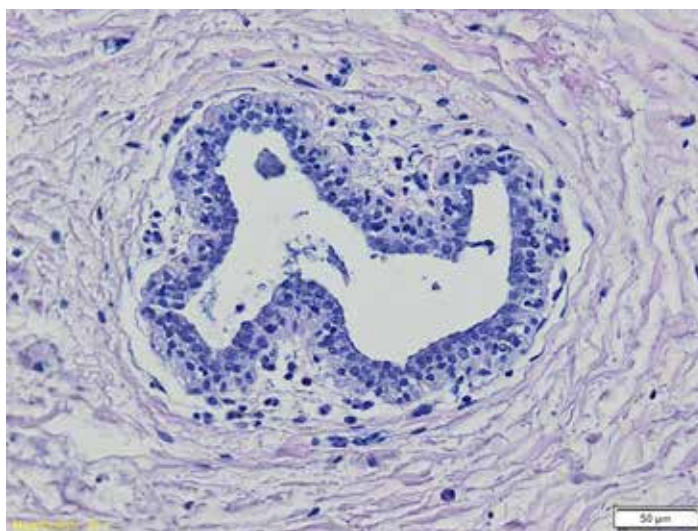


FIGURE 1

Haematoxylin-eosin staining of breast-tissue showing a duct surrounded by connective tissue. Images were taken with a 20X objective. Scale bar 50 μ m.

In a number of tissue sections there was no glandular tissue present. Especially samples taken from elderly individuals tended to contain a very limited amount of glandular tissue. Tissue samples containing less than 100 epithelial cells were discarded. As a result, per patient not all dose points and sham-irradiated controls could be analysed for foci formation.

γ H2AX foci assay

After selection of the good quality samples, immunostaining was consistently good. Examples of the staining are given in figure 2. The use of DAB-NiCl₂ resulted in very distinct black foci and a light background staining of the tissue.

No counterstain was used, since the immunostaining already resulted in sufficient contrast to the tissue and counterstaining tended to darken the nuclei, reducing the ability to distinguish the foci. After selection of the good quality samples, immunostaining was consistently good. Examples of the staining are given in figure 2. The use of DAB-NiCl₂ resulted in very distinct black foci and a light background staining of the tissue. No counterstain was used, since the immunostaining already resulted in sufficient contrast to the tissue and counterstaining tended to darken the nuclei, reducing the ability to distinguish the foci.

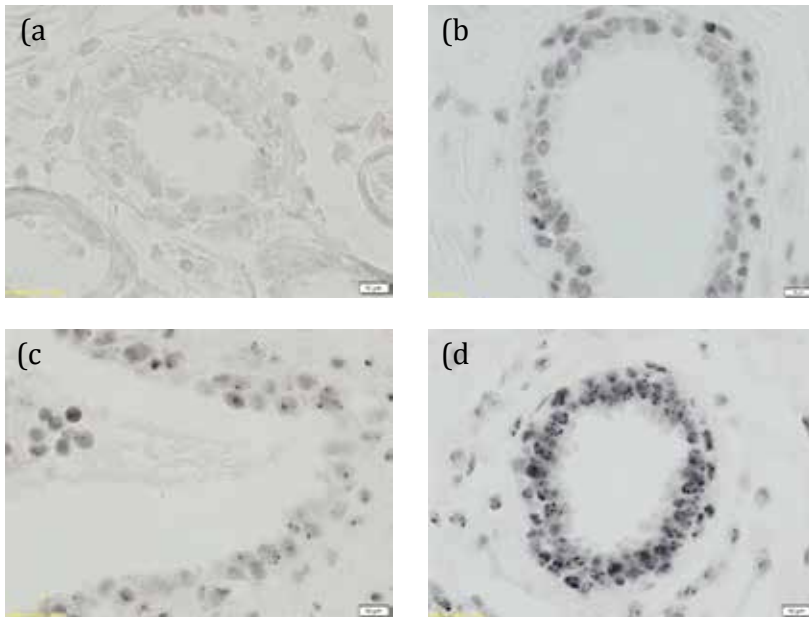


FIGURE 2

γ H2AX immunostaining, images were taken with a 63 X objective. (a) Negative control (no primary antibody); (b) unirradiated sample; (c) sample irradiated with 100 mGy; (d) sample irradiated with 500 mGy. Scale bar 10 μ m.

Background number of foci could be measured in all high-risk donors (4) and in 5 donors with a normal risk profile. No difference in background number of foci could be detected between donors at high risk for breast cancer and donors without an elevated risk (average 0.44 foci per cell \pm 0.15 (SEM)) for high risk patients and 0.36 \pm 0.10 for patients without elevated risk; $p=0.68$). Also for all irradiated samples (2-500mGy), no significant differences between donors with and without elevated risk could be observed.

As no differences were observed between donors with and without elevated risk, the data of all patients was pooled and the average background number of foci in the pooled samples was 0.38 \pm 0.08 (foci per cell \pm SEM). The threshold detection dose, leading to a significant increase in number of foci per cell, was 10mGy after irradiation with 30kV X-rays ($p=0.05$) while this was 20mGy after irradiation with ^{60}Co γ -rays ($p=0.04$).

The dose response curve through the pooled

data for 30 kV X-rays shows a bi-phasic linear course, with the low-dose part (0-40 mGy) being steeper than the higher dose part (20-500 mGy) (figure 3, black dots). The dose response curve for γ -rays follows a linear course (figure 3, red dots). Furthermore a linear regression omitting the dose-points 2-40mGy is given (dashed line), which corresponds to the curve which would be obtained if a linear no threshold model would have been used. In figure 4 a detailed presentation of the dose response curves in the 0-20mGy dose-range with the 95% confidence intervals is given. An overview of the α -values of the linear dose response curves are given in table 1. The slope increased 9-fold between the 0-40mGy dose-range and the 20-500mGy dose-range after 30 kV X-ray irradiation.

Table 1 lists the RBE values with the 95% confidence limits for both the 0-20 and in the 20-500 mGy dose range. In the low dose range (0-40mGy), the 30kV X-rays were more effective in inducing DNA DSB than γ -rays (RBE>1).

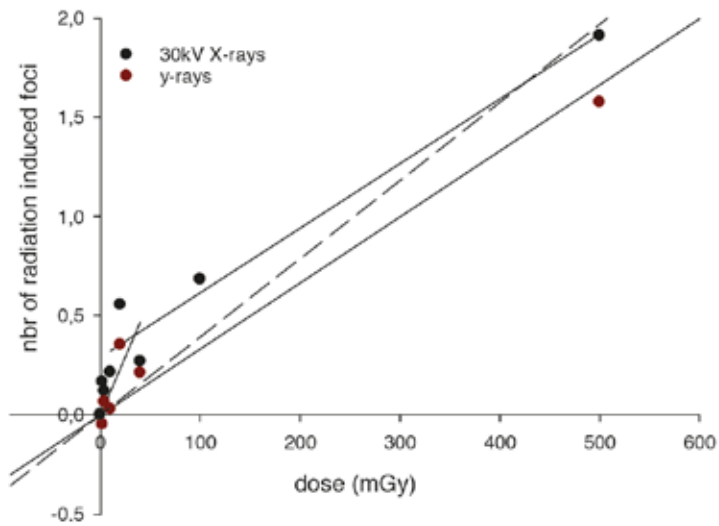


FIGURE 3

Dose response curve for γ H2AX foci-induction after irradiation with γ -rays and 30kV X-rays. The linear regression curves in the high dose range and the low dose range are shown (full lines), together with the regression omitting the 2 to 40mGy dose points for 30kV X-rays (dashed line) (LNT model).

Note that the 100mGy dose points for 30kV X and γ irradiation fall on top of each other, making the dose point for 100mGy 30kV X-ray irradiation invisible.

	0-40mGy	[95%CL]	20-500mGy	[95%CL]	α_L/α_H	[95%CL]
$\alpha_{30kV\ X\text{-rays}}$	0.012	[0.009-0.016]	0.003	[0.003-0.004]	8.710	[6.824-11.237]
$\alpha_{\gamma\text{-rays}}$	0.003	[0.003-0.004]	0.003	[0.003-0.004]	1.000	[0.750-1.333]
	3.750	[2.250-5.710]	1.031	[0.750-1.333]		

TABLE1

overview of α -values in both dose-ranges together with the RBE ($=\alpha_{30kV}/\alpha_{\gamma}$) values in both dose ranges and the ratio of the α -values obtained by the linear regression in the 0-40 and 20-500 mGy dose-range (α_L/α_H).

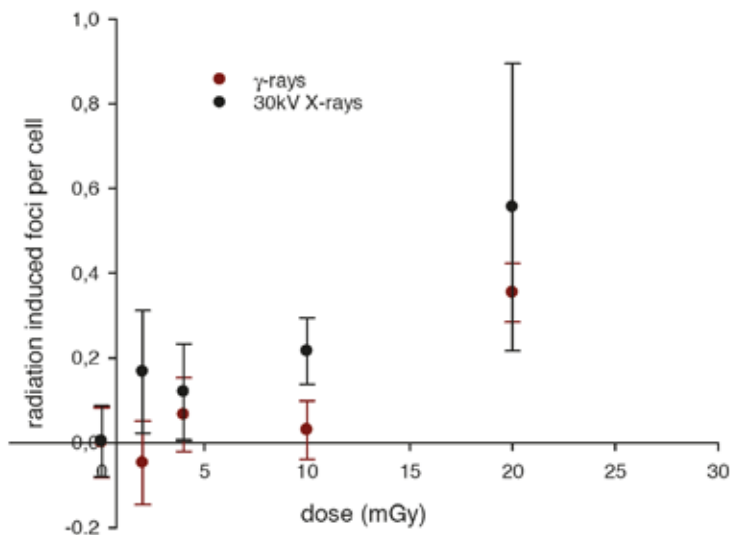


FIGURE 4

Linear dose response curves for γ H2AX induction in the low dose range for γ -rays and 30kV X-rays. Error bars indicate the SEM.

Discussion

A mammography examination consists of 2 views of 2mGy each resulting in a glandular dose of 3-5 mGy. In most screening programs 10 examinations are performed during a screening period of about 20 years, giving a total glandular dose of approximately 40 mGy which may be considered as a relatively low dose. At low doses, phenomena such as hypersensitivity, bystander effect, adaptive response, threshold hypothesis and hormetic response can play a role (8, 11, 25) and extrapolation of radiation-effects from the high-dose range to the low-dose range by the LNT model can lead

to both an underestimation and overestimation of the low-dose effects of radiation.

In this study we wanted to investigate the biological efficacy of mammography X-rays for DNA DSB induction in glandular epithelial cells present in resected breast tissue and *ex vivo* irradiated with very low doses. This setup corresponds as close as possible to the exact physiological conditions of mammography screening.

As our patient population also consisted of 4 patients with an increased risk for breast cancer, we first investigated if a significant difference could be observed between patients with

a high risk for breast cancer and patients without a high risk for breast cancer in number of background γ H2AX foci, or in number of radiation-induced foci at any dose. No significant differences were detected. These results are in contrast with the results of Colin et al who found an increased background number of γ H2AX and an increased radiation-induced number of foci (2 mGy, 4 mGy and fractionated 2+2 mGy) in cell cultures of primary mammary epithelial cells of high-risk patients compared to low-risk patients (15). Since γ H2AX functions upstream of BRCA1 and BRCA2, it is not surprising that no differences are found in γ H2AX induction between donors with and without a BRCA1 or BRCA2 mutation. Analysis of the kinetics of γ H2AX foci, which is closely related to the repair of the DSB, might be better suited to detect deficiencies in DSB-repair.

As no differences were observed the data of all the patients was pooled for further analysis.

Using a γ H2AX foci-assay, a threshold detection dose of 10mGy after irradiation with 30kV X-rays was found. In a previous study using lymphocytes, we also found a significant increase in γ H2AX foci after 10 mGy of 30kV X-rays (26). Other research groups showed a statistical significant increase of DNA DSB in MCF-10A cells after 9 mGy of 30kV X-rays (27) and in cultured primary breast epithelial cells a threshold detection dose of 4 mGy and a fractionated 2+2 mGy was found (15). These results seem to indicate that the threshold detection dose of mammography X-rays for DSB induction is around or below 10 mGy.

Beels et al found a hypersensitive response in

whole blood in pediatric patients exposed *in vivo* to low doses of X-rays for cardiac catheterization (mean dose 6mSv). She later confirmed these results with a study on γ H2AX-induction in whole blood and isolated T-lymphocytes irradiated *in vitro* with X (100kVp) and γ -radiation (28, 29). When whole blood was irradiated with X-rays, a very steep response was noted in the 0-10mGy dose range, which became less steep if doses higher than 20mGy were used. After irradiation with γ -rays, the biphasic effect was still there, but much less pronounced. The effects were also less pronounced when isolated lymphocytes instead of whole blood was used. She concluded that both cellular environment and radiation quality play a role in this hypersensitive response. A strong correlation between cell culture conditions and a low-dose hypersensitive response was also found by Groesser et al (30).

The results obtained in this study are comparable with those of Beels et al. A clear bi-phasic dose response was noted, with a low dose hypersensitive component for 30 kV X-rays. Extrapolation of the dose response from 0 mGy to 100 mGy without taking into account the low-dose points (0-40mGy; dashed line in figure 3), clearly shows that the LNT-model would have resulted in an underestimation of the induced damage.

The different response in the 0 to 20 mGy dose-range versus the 20-500 mGy dose range resulted in different RBE values. An RBE of 1 was obtained in the 20-500mGy range, while an RBE of 3.75 was obtained in the 0-40mGy range.

This low-dose hypersensitivity is probably caused by the bystander effect. The bystander effect is largely propagated by damaged cells which release signaling molecules to neighboring cells via gap-junction mediated intercellular communication and via the release of diffusible factors such as ROS into the extra-cellular milieu (31-35). In our study, 2mm thick slices of breast tissue, including epithelial glandular structures, were irradiated and as such, gap-junction mediated communication between cells in their natural micro-environment is still intact. Also, estrogens, which are highly available in breast tissue, are an important source of ROS.

Mills et al on the other hand, did not find an increased RBE in the low dose range (0-30mGy) for mammography X-rays, on the contrary, she found an RBE value of only 1.1 (27). The difference between our study and the study of Mills could be due to the fact that in the study of Mills MCF-10A cells were grown in monolayer, which could influence gap-junction mediated intercellular communication. Furthermore, the cells were kept at 0°C some time before, during and after the irradiation. From literature it is known that hypothermia is a known radioprotectant and has a protective role against the damaging effects of ROS (36, 37). Moreover, hypothermia could influence cell processes such as cellular communication.

Overall, it seems that the bystander effect might induce a hypersensitive response in breast tissue and that this response is dependent on radiation quality, cell and tissue culture conditions and on temperature.

In conclusion, our results indicate the existence of a hypersensitive response in the mammary epithelial cells of breast tissue in the low-dose region induced by mammography X-rays. Which effects this could have on the risk calculations for mammography screening is unclear, since a lot of parameters will influence the repair of these radiation-induced DSB. However, in our previous study, we have shown that the DSB induced by the higher LET mammography X-rays are more difficult to repair than the DSB induced by γ -rays, and that the same number of mammography induced DSB resulted in a higher number of chromosomal aberrations (26). Thus, the low-dose hypersensitive response observed for DSB induction in the dose range representative for mammography screening together with the findings obtained with chromosomal aberration-assays at higher doses might suggest that also in the 0-20 mGy dose range more chromosomal aberrations than initially assumed by the LNT model will be induced.

These results are based on a small patient-population and a future larger study will be needed to confirm the obtained results. Furthermore, it would be interesting to include more donors with a BRCA-mutation and to compare the repair kinetics of γ HAX-foci in the group with and without an increased risk for breast cancer or investigate differences in induction and repair of other DSB repair-proteins such as rad51 between both groups. This might give a better indication about the damaging effects of mammography X-rays in donors with and without an increased risk for breast cancer.

Acknowledgements

The authors are grateful to the staff of the Plastic Surgery department for their help in recruiting volunteers and to the volunteers who donated the tissue samples. We would also like to thank Leen Pieters, who was very helpful with the preparation of the samples and the counting of the foci.

Declaration of interest

The authors report no conflicts of interest.

References

1. Ferlay J, Autier P, Boniol M, Heanue M, Colombet M, Boyle P, Estimates of the cancer incidence and mortality in Europe in 2006. *Annals of Oncology* 2007; 18, 581-92.
2. Jemal A, Bray F, Center MM, Ferlay J, Ward E, Forman D, Global Cancer Statistics. *Ca-a Cancer Journal for Clinicians* 2011; 61, 69-90.
3. Althuis MD, Dozier JM, Anderson WF, Devesa SS, Brinton LA, Global trends in breast cancer incidence and mortality 1973-1997. *International Journal of Epidemiology* 2005; 34, 405-12.
4. Parkin DM, Fernandez LMG, Use of statistics to assess the global burden of breast cancer. *Breast Journal* 2006; 12, S70-S80.
5. Jemal A, Center MM, DeSantis C, Ward EM, Global Patterns of Cancer Incidence and Mortality Rates and Trends. *Cancer Epidemiology Biomarkers & Prevention* 2010; 19, 1893-907.
6. Altobelli E, Lattanzi A, Breast cancer in European Union: An update of screening programmes as of March 2014 (Review). *International Journal of Oncology* 2014; 45, 1785-92.
7. Klein R, Aichinger H, Dierker J, Jansen JTM, JoiteBarfuss S, Sabel M, et al., Determination of average glandular dose with modern mammography units for two large groups of patients. *Physics in Medicine and Biology* 1997; 42, 651-71.
8. Brenner DJ, Doll R, Goodhead DT, Hall EJ, Land CE, Little JB, et al., Cancer risks attributable to low doses of ionizing radiation: Assessing what we really know. *Proceedings of the National Academy of Sciences of the United States of America* 2003; 100, 13761-66.
9. Hendrick RE, Pisano ED, Averbukh A, Moran C, Berns EA, Yaffe MJ, et al., Comparison of Acquisition Parameters and Breast Dose in Digital Mammography and Screen-Film Mammography in the American College of Radiology Imaging Network Digital Mammographic Imaging Screening Trial. *American Journal of Roentgenology* 2010; 194, 362-69.
10. ICRP, The 2007 recommendations of the International Commission on Radiological Protection. ICRP Publication 103. *Annals of the ICRP* 2007; 37.
11. Averbek D, Does scientific evidence support a change from the LNT model for low-dose radiation risk extrapolation? *Health Phys* 2009; 97, 493-504.
12. Rothkamm K, Lobrich M, Evidence for a lack of DNA double-strand break repair in human cells exposed to very low x-ray doses. *Proceedings of the National Academy of Sciences of the United States of America* 2003; 100, 5057-62.
13. Bakkenist CJ, Kastan MB, Initiating cellular stress responses. *Cell* 2004; 118, 9-17.
14. Grudzinski S, Raths A, Conrad S, Rube CE, Lobrich M, Inducible response required for repair of low-dose radiation

- damage in human fibroblasts. *Proceedings of the National Academy of Sciences of the United States of America* 2010; 107, 14205-10.
15. Colin C, Devic C, Noel A, Rabilloud M, Zabot MT, Pinet-Isaac S, et al., DNA double-strand breaks induced by mammographic screening procedures in human mammary epithelial cells. *International Journal of Radiation Biology* 2011; 87, 1103-12.
 16. Amundson SA, Lee RA, Koch-Paiz CA, Bittner ML, Meltzer P, Trent JM, et al., Differential responses of stress genes to low dose-rate gamma irradiation. *Molecular Cancer Research* 2003; 1, 445-52.
 17. Franco N, Lamartine J, Frouin V, Le Minter P, Petal C, Leplat JJ, et al., Low-dose exposure to gamma rays induces specific gene regulations in normal human keratinocytes. *Radiation Research* 2005; 163, 623-35.
 18. Yang F, Stenoien DL, Strittmatter EF, Wang JH, Ding LH, Lipton MS, et al., Phosphoproteome profiling of human skin fibroblast cells in response to low- and high-dose irradiation. *Journal of Proteome Research* 2006; 5, 1252-60.
 19. El-Saghire H, Thierens H, Monsieurs P, Michaux A, Vandevoorde C, Baatout S, Gene set enrichment analysis highlights different gene expression profiles in whole blood samples X-irradiated with low and high doses. *International Journal of Radiation Biology* 2013; 89, 628-38.
 20. Fucic A, Gamulin M, Interaction between ionizing radiation and estrogen: What we are missing? *Medical Hypotheses* 2011; 77, 966-69.
 21. Shao CL, Folkard M, Held KD, Prise KM, Estrogen enhanced cell-cell signalling in breast cancer cells exposed to targeted irradiation. *BMC Cancer* 2008; 8, 9.
 22. Liehler JG, Genotoxicity of the steroidal oestrogens oestrone and oestradiol: possible mechanism of uterine and mammary cancer development. *Human Reproduction Update* 2001; 7, 273-81.
 23. Cavalieri E, Chakravarti D, Guttenplan J, Hart E, Ingle J, Jankowiak R, et al., Catechol estrogen quinones as initiators of breast and other human cancers: Implications for biomarkers of susceptibility and cancer prevention. *Biochimica Et Biophysica Acta-Reviews on Cancer* 2006; 1766, 63-78.
 24. Rogakou EP, Pilch DR, Orr AH, Ivanova VS, Bonner WM, DNA double-stranded breaks induce histone H2AX phosphorylation on serine 139. *Journal of Biological Chemistry* 1998; 273, 5858-68.
 25. Averbek D, Non-targeted effects as a paradigm breaking evidence. *Mutation Research-Fundamental and Molecular Mechanisms of Mutagenesis* 2010; 687, 7-12.
 26. Depuydt J, Baert A, Vandersickel V, Thierens H, Vral A, Relative biological effectiveness of mammography X-rays at the level of DNA and chromosomes in lymphocytes. *International Journal of Radiation Biology* 2013; 89, 532-38.
 27. Mills CE, Thome C, Koff D, Andrews DW, Boreham DR, The Relative Biological Effectiveness of Low-Dose Mammography Quality X Rays in the Human Breast MCF-10A Cell Line. *Radiation Research* 2015; 183, 42-51.
 28. Beels L, Bacher K, De Wolf D, Werbrout J, Thierens H, gamma-H2AX Foci as a Biomarker for Patient X-Ray Exposure in Pediatric Cardiac Catheterization Are We Underestimating Radiation Risks? *Circulation* 2009; 120, 1903-09.
 29. Beels L, Werbrout J, Thierens H, Dose response and repair kinetics of gamma-H2AX foci induced by in vitro irradiation of whole blood and T-lymphocytes with X- and gamma-radiation. *International Journal of Radiation Biology* 2010;

- 86, 760-68.
30. Groesser T, Cooper B, Rydberg B, Lack of bystander effects from high-LET radiation for early cytogenetic end points. *Radiat Res* 2008; 170, 794-802.
 31. Azzam EI, de Toledo SM, Little JB, Stress signaling from irradiated to non-irradiated cells. *Curr Cancer Drug Targets* 2004; 4, 53-64.
 32. Azzam EI, de Toledo SM, Little JB, Direct evidence for the participation of gap junction-mediated intercellular communication in the transmission of damage signals from alpha-particle irradiated to nonirradiated cells. *Proceedings of the National Academy of Sciences of the United States of America* 2001; 98, 473-78.
 33. Hanot M, Hoarau J, Carriere M, Angulo JF, Khodja H, Membrane-dependent bystander effect contributes to amplification of the response to alpha-particle irradiation in targeted and nontargeted cells. *International Journal of Radiation Oncology Biology Physics* 2009; 75, 1247-53.
 34. Mothersill C, Seymour C, Radiation-induced bystander effects: Past history and future directions. *Radiation Research* 2001; 155, 759-67.
 35. Zhou HN, Suzuki M, Geard CR, Hei TK, Effects of irradiated medium with or without cells on bystander cell responses. *Mutation Research-Fundamental and Molecular Mechanisms of Mutagenesis* 2002; 499, 135-41.
 36. Lisowska H, Wegierek-Ciuk A, Banasik-Nowak A, Braziewicz J, Wojewodzka M, Wojcik A, et al., The dose-response relationship for dicentric chromosomes and gamma-H2AX foci in human peripheral blood lymphocytes: Influence of temperature during exposure and intra- and inter-individual variability of donors. *International Journal of Radiation Biology* 2013; 89, 191-99.
 37. Dang L, Lisowska H, Manesh SS, Sollazzo A, Deperas-Kaminska M, Staaf E, et al., Radioprotective effect of hypothermia on cells – a multiparametric approach to delineate the mechanisms. *International Journal of Radiation Biology* 2012; 88, 507-14.

Article 5

In vitro cellular radiosensitivity in relationship to late normal tissue reactions in breast cancer patients: a multi-endpoint case-control study

Charlot Vandevoorde^{a,1}, Julie Depuydt^{a,1}, Liv Veldeman^b, Wilfried De Neve^b, Natividad Sebastià^{c,d}, Greet Wiemea^e, Annelot Baert^a, Sofie De Langhe^a, Jan Philippé^f, Anne Vral^a and Hubert Thierens^a

1 These authors contributed equally to this work

a Ghent University, Department of Basic Medical Sciences, Ghent, Belgium

b Department of Radiotherapy, Ghent University Hospital, Ghent, Belgium

c Radiation Protection Service, IISLAFE, Valencia, Spain

d Grupo de Investigación Biomédica en Imagen GIBI230, IISLAFE, Valencia, Spain

e Department of Pediatrics and Medical Genetics, Ghent University, Ghent, Belgium

f Department of Clinical Chemistry, Microbiology and Immunology, Ghent University, Ghent, Belgium

Resubmitted to International Journal of Radiation Biology with minor revisions

Abstract

Purpose: A minority of patients exhibits severe late normal tissue toxicity after radiotherapy (RT), possibly related to their inherent individual radiation sensitivity. This study aimed to evaluate four different candidate *in vitro* cellular radiosensitivity assays for prediction of late normal tissue reactions, in a retrospective matched case-control set-up of breast cancer patients.

Methods: The study population consists of breast cancer patients expressing severe radiation toxicity (12 cases) and no or minimal reactions (12 controls), with a follow-up for at least 3 years. Late adverse reactions were evaluated by comparing standardized photographs pre- and post-RT resulting in an overall cosmetic score and by clinical examination using the LENT-SOMA scale. Four cellular assays on peripheral blood lymphocytes reported to be associated with normal tissue reactions were performed after *in vitro* irradiation of patient blood samples to compare case and control radiation responses: radiation-induced CD8+ late apoptosis, residual DNA double strand breaks, G0 and G2 micronucleus assay.

Results: A significant difference was observed for all cellular endpoints when matched cases and controls were compared both pairwise and grouped. However, it is important to point out that most case-control pairs showed a substantial overlap in standard deviations, which questions the predictive value of the individual assays. The apoptosis assay performed best, with less apoptosis seen in CD8+ lymphocytes of the cases (average: 14.45%) than in their matched controls (average: 30.64%) for 11 out of 12 patient pairs ($p < 0.01$). The number of residual DNA DSB was higher in cases (average: 9.92 foci/cell) compared to their matched control patients (average: 9.17 foci/cell) ($p < 0.01$). The average dose response curve of the G0 MN assay for cases lies above the average dose response curve of the controls. Finally, a pairwise comparison of the G2 MN results showed a higher MN yield for cases (average: 351 MN/1000BN) compared to controls (average: 219 MN/1000BN) in 9 out of 10 pairs ($p < 0.01$).

Conclusion: This matched case-control study in breast cancer patients, using different endpoints for *in vitro* cellular radiosensitivity related to DNA repair and apoptosis, suggests that patients' intrinsic radiosensitivity is involved in the development of late normal tissue reactions after RT. Larger prospective studies are warranted to validate the retrospective findings and to use *in vitro* cellular assays in the future to predict late normal tissue radiosensitivity and discriminate individuals with marked RT responses.

Introduction

The use of radiotherapy (RT) reduces the risk of local-regional recurrence of breast cancer and improves the overall survival of breast

cancer patients after breast-conserving surgery or mastectomy (1, 2). The evolution of RT techniques and the introduction of intensity-modulated radiotherapy (IMRT) have substantially

improved the morbidity among breast cancer patients (3-5). However, a minority of patients still suffers from severe adverse reactions, which are usually divided into acute and late reactions (6). During or shortly after the RT course, a large portion of the breast cancer patients will experience a moderate-to-severe skin reaction, leading to poor cosmetic outcomes (7-9). In contrast to acute reactions, most of the late reactions are irreversible and occur only several months or even years after RT and they significantly reduce the quality-of-life (10, 11). There exists a direct relationship between radiation dose and tumor control, but the severe normal tissue toxicity in a minority of patients limits the dose that can be safely prescribed (12). Current RT doses are generally limited such that less than 5% of the treated patients suffer from severe toxicity up to 5 years following RT. The development of a test to predict late toxicity would enable individualized radiation dose prescription and would reduce the number of survivors suffering from the consequences of treatment (13-16).

Variation in normal tissue reactions among patients has been observed since the early days of RT and the individual radiosensitivity follows approximately a Gaussian distribution (17). Despite the fact that potential side effects of RT are well described, it remains difficult to predict the extent of complications for a given individual patient. Although there is clinical evidence that acute skin reactions are sometimes associated with the development of late toxicity as telangiectasia, patients who suffer from severe acute reactions do not necessari-

ly or predictably develop significant late reactions (Lilla et al, 2007; Lopez et al, 2005). This finding may reflect differences in the underlying mechanisms involved in the development of both types of reactions. The pathology of late normal tissue reactions in breast cancer patients comprises processes such as pigmentation changes, atrophy, fibrosis and vascular damage (18).

Several factors associated with an increased risk of side effects in breast cancer patients were previously described and can be separated in two general categories. First, RT related risk factors including the total dose and additional boost, the irradiated volume, the fractionation regimen and the total treatment time (Bentzen et al, 2010; Deantonio et al, 2010). Secondly, patient-related factors may influence the risk and severity of late normal tissue toxicity after breast cancer treatment: age, concomitant chemotherapy or hormonal treatment, trauma or surgery in the irradiated site, co-morbidities involving impaired vascularity such as diabetes and hypertension, and breast size (9, 18, 19).

It has been estimated that if known extrinsic factors are controlled, 80% of the observed variation in the severity of normal tissue responses is due to inherent differences among the patients (20, 21). It has been suggested that the observed variability may be due to differences in genetic alterations in proteins participating in the radiation response. Many studies investigated the association between single nucleotide polymorphisms (SNP) in genes with radiotoxic effects, but replication of the studies remains difficult (13, 16). The association between indi-

vidual variation in clinical radiosensitivity and cellular radiosensitivity and/or genomic instability could provide a possibility to determine the individual sensitivity of patients in terms of developing severe treatment-related side effects (22). Several studies were initiated and reported to a certain extent associations between a range of cellular biomarker assays and clinical radiosensitivity (23-26). These assays use peripheral blood lymphocytes and include chromosomal radiosensitivity measured with G2 and G0 micronucleus assay, kinetics of residual DNA damage assessed by the γ -H2AX foci assay and radiation-induced apoptosis on T-lymphocyte subsets (15, 24, 27-34). Among those assays, radiation-induced apoptosis (RIA) in lymphocyte subsets after *in vitro* irradiation gives the most promising results for correlation with late toxicity after RT (15, 25, 33). Furthermore, more recent small studies suggest that the scoring of residual DNA damage by using the γ -H2AX foci assay may be useful for prediction of reactions to RT (27, 35).

Most of the work published on cellular radiosensitivity endpoints was performed on patient cohorts taking into account the clinical radiation toxicity scores while ignoring therapy and patient related risk factors. To rule out the strong influence of these risk factors on normal tissue radiation effects a strict matched case-control set-up for these variables was used in present study. Breast cancer patients manifesting clear late radiotoxic effects and control patients showing no or minimal radiation effects were selected retrospectively and different endpoints for *in vitro* cellular radiosensitivity were evalu-

ated. Based on the existing literature, protocols were selected from previous studies that could demonstrate a correlation between a specific cellular assay and late normal tissue toxicity: RIA levels in CD8+ T-lymphocytes(36), residual number of DNA double-strand breaks (DSB) by means of γ -H2AX/53BP1 foci assay (27) and the chromosomal radiosensitivity using the G2 and G0 MN assays (based on our own protocols). The study was designed as a small scale proof of principle study on a well-defined cohort of case and control breast cancer patients in order to evaluate if cellular radiosensitivity assays can be of value in the prediction of late clinical toxicity.

Material and Methods

Patient selection

The population investigated in this study consists of breast cancer patients who underwent breast conserving surgery, followed by adjuvant systemic treatment and IMRT between 2010 and 2012. The women were treated with a hypofractionated RT scheme (START B, 15 x 2.67Gy) (37), followed by an additional boost (4 x 2.5Gy). All women were selected retrospectively after a follow-up period of at least 3 years. Out of a cohort of 440 patients 12 cases with severe late radiotoxic effects were selected and for each case, a control with minimal or no reaction was recruited, matching as much as possible the case for a number of characteristics. The following therapy related factors were taken into account for the case-control matching:

boost, therapy position (supine or prone), nodal irradiation and adjuvant systemic treatment (chemotherapy, hormonal therapy and targeted therapy). Patients were also matched for cup size and BMI was also taken into account as much as possible. Treatment and demographic characteristics of the matched case-control patients are presented in Table I. A paired t-test showed that cup-size ranked numerically and BMI were not significantly different between cases and controls. Four of the patients fulfilled the criteria for BRCA1/2 analysis, but no mutation was identified. Ethical approval was obtained through the institutional review board of Ghent University Hospital and all participating patients signed an informed consent.

Assessment of late normal tissue reactions

A first triage of candidate-cases out of a cohort of 440 breast cancer patients was performed by comparing post-surgical photographs, under standardized conditions, of the patients with follow-up photographs (latest photographs: 2 years after RT). Based on the comparison of these photographs a group of patients was identified with severe radiation-induced changes. From these candidate cases, the final selection of ‘cases’ for this study was based on the monitoring and documentation of the occurrence of late normal tissue effects by the physician during follow-up examinations by using the breast module of the LENT-SOMA grading system (SOMA stands for “subjective symptoms, objective signs, management, and analytical measures” and LENT is an abbreviation for “late effects on normal tissue”) (38). The

LENT-SOMA scores of the 24 case-control patients obtained three years after RT are presented in Table I. It is a comprehensive grading system in which several toxicity items are classified: retraction and atrophy, breast oedema, ulceration, telangiectasia, post-irradiation fibrosis, arm lymph-oedema, pigmentation change and pain. Since ulceration is very rare and none of our patients expressed this late effect and pain is subjective, both endpoints were not included in Table I. Fibrosis is known to be slowly progressive and in our patient population it was fairly common. Therefore we decided to differentiate the fibrosis scoring in fibrosis of the scar area (possibly as result of surgery) and fibrosis outside the tumor bed. Patients were selected as ‘cases’ if an increase in grade of minimally 2 was observed for one of the LENT-SOMA endpoints when comparing pre-and post-RT scores. The matching ‘controls’ showed minimal late effects (increase in toxicity score of 0 or 1). In addition, an overall 4-categories cosmetic score was determined in consensus by three different observers based on the pre-therapy and follow-up photographs (1-excellent, 2-good, 3-fair, 4-poor), see Table I (39).

Sample preparation and *in vitro* irradiation

From each patient participating in the study two 10 ml blood samples were collected into sodium heparin blood collection tubes. 3 ml whole blood was used for the quantification of residual DNA DSB in T-lymphocytes, which were isolated by using RosetteSep Human T-cell Enrichment Cocktail (Stemcell Tech-

Patients case-control	Patient			Therapy				LENT-SOMA Scale										Cosmetic			Cellular tests												
	Age at start of RT	Cupsize	BMI	Follow up period (y)	Postion for irradiation	Nodal irradiation	Chemotherapy	Hormonal therapy	Retraction		Breast oedema		Telangiectasia		Fibrosis around scar		Fibrosis outside of tumor-bed		Lymph oedema		Pigmentation		Overall cosmetic score (photographs)		Apoptosis	YH2AX/53BP1 foci	GO MN (AUC)	G2 MN with caffeine					
									B	A	B	A	B	A	B	A	B	A	B	A	B	A	B	A									
1	48	B	27	5.4	supine		x		3	3	0	0	0	0	2	2	0	0	0	0	0	0	0	1	4	4			Y	Y			
2	36	C	25	3.8	supine		x		0	0	0	0	0	0	0	0	0	0	0	0	0	0	0	0	1	1			Y	Y			
3	75	E	34	4	supine			AI	1	3	0	1	0	0	0	2	0	1	0	0	0	0	0	0	2	2	3	Y	Y	Y	NA		
4	59	D	37	3	supine			AI	0	1	0	0	0	0	0	0	0	0	0	0	0	0	0	0	1	1			Y	Y	Y	Y	
5	62	C	26	3.8	supine	x		AI	1	2	1	1	0	0	0	0	0	0	0	0	0	0	0	1	1	3	4	Y	Y	Y	Y	Y	
6	62	D	22	4	supine	x		AI	0	0	0	1	0	0	0	0	0	0	0	0	0	0	0	0	1	1			Y	Y	Y	Y	
7	70	C	31	3.4	supine	x		AI	2	2	0	2	0	1	1	2	0	2	1	0	1	0	1	2	4	4	Y	Y	Y	Y	Y	Y	
8	60	C	22	3.8	supine	x		AI	0	0	0	0	0	0	0	0	0	0	0	0	0	0	0	0	1	1			Y	Y	Y	Y	
9	56	D	38	4	prone		x	T	2	3	0	1	0	0	0	2	0	2	0	0	0	0	0	0	1	4	4	Y	Y	Y	Y	Y	
10	44	F	29	4	prone			T	0	1	0	0	0	0	0	0	0	0	0	1	0	0	0	0	1	1			Y	Y	Y	Y	
11	80	C	33	3.6	supine			AI	1	2	0	1	0	0	0	1	0	1	0	0	0	0	0	0	2	2	3	Y	Y	Y	Y	Y	Y
12	64	D	25	3	supine		x	AI	0	0	0	0	0	0	0	0	0	0	0	0	0	0	0	0	0	1	1			Y	Y	Y	Y
13	78	C	31	3	supine			T	1	1	1	1	0	0	1	1	1	1	0	0	0	0	0	0	2	2	4	Y	Y	Y	Y	Y	Y
14	53	C	21	4.8	supine			T	0	0	1	0	0	1	0	0	0	0	0	0	0	0	0	0	0	1	1			Y	Y	Y	Y
15	78	C	25	3.5	supine			T	1	1	0	0	0	0	0	2	0	2	0	0	0	0	0	0	2	2	4	Y	Y	Y	Y	Y	Y
16	74	C	30	4	supine			T	1	1	0	0	0	0	0	0	0	1	0	0	0	0	0	0	0	3	2	Y	Y	Y	Y	Y	Y
17	61	D	27	3.1	supine	x		AI	0	0	0	1	0	0	1	1	0	0	0	0	0	0	0	0	2	3	3	Y	Y	Y	Y	Y	Y
18	66	C	35	3	supine	x		AI	0	3	0	0	0	0	0	1	0	0	0	0	3	0	2	2	2	4	Y	Y	Y	Y	Y	Y	Y
19	44	C	23	4.2	supine	x		T	0	0	1	0	0	0	1	1	0	0	0	0	0	0	0	0	0	1	1			Y	Y	Y	Y
20	67	H	33	4	supine	x		AI	0	1	0	1	0	0	0	2	0	2	0	0	0	0	0	2	1	2	Y	Y	Y	Y	Y	Y	Y
21	57	E	50	4	supine	x		AI	3	3	0	0	0	0	0	0	0	0	0	0	0	0	0	0	3	3	Y	Y	Y	Y	Y	Y	Y
22	67	D	24	3.8	supine			AI	1	1	1	2	0	0	2	2	0	2	0	0	0	0	1	2	3	3	Y	Y	Y	Y	Y	Y	Y
23	70	D	27	5	supine			AI	1	1	0	0	0	0	0	1	0	0	0	0	0	0	0	0	0	2	2	Y	Y	Y	Y	Y	Y

TABLE 1

For each of the patients, patient and therapy-related information, the scoring results of late radiotoxic effects according to the LENT-SOMA Scale and the overall cosmetic score deduced from standardized photographs are given. Furthermore the table summarizes whether the case' radiosensitivity assay scores are higher (YH2AX/53BP1 foci, AUC GO MN and G2 MN) or lower (apoptosis) than its matched control (marked with Y). The patients are ordered per case-control pair, the first line is the case and the second line is the matching control. B: LENT-SOMA score or overall cosmetic score before RT; A: LENT-SOMA score 3 years after RT or overall cosmetic score 2 years after RT. Grey cells in the LENT-SOMA section highlight endpoints with an increase of minimally two units between scoring before RT and three years after RT. Grey cells in the cosmetic section highlight an increase in overall cosmetic score between pre-RT and two years after RT.

nologies, France). With this isolation method, unwanted cells are targeted for removal with Tetrameric Antibody Complexes recognizing CD16, CD19, CD36, CD56, CD66b and glycoporphin A on red blood cells (RBCs), resulting in a highly enriched population of CD3+ T-lymphocytes (purity assessed by flow cytometry > 98%). After centrifugation and washing, the cells were resuspended at a concentration between 0.6 and 1 million cells per ml in cRPMI (RPMI-1640 supplemented with 1% L-glutamine and 0.5% penicillin/streptomycin; all products Life Technologies, Belgium) containing 10% Foetal Calf Serum (FCS) (Life Technologies, Belgium). For the apoptosis assay, 0.5 ml of the heparinized whole blood samples was diluted in cRPMI (1:10) containing 20% FCS. For the assessment of the number of residual DNA DSB and apoptosis scoring, the samples were irradiated with respectively 4 Gy and 8 Gy x-rays (160 kV, 4mA, 3mm Al filtration; dose rate: 1Gy/min). The irradiated samples were kept at 37°C in a humidified 5% CO₂ atmosphere incubator (Thermo Scientific, United States). A repair time of 24 h was considered to study residual DNA DSB, while apoptosis was scored after 48 h of incubation.

For the G0 MN assay 4.5 ml of the blood sample was aliquoted and irradiated with ⁶⁰Co γ-rays, with 5 doses ranging from 0.2 to 3 Gy, in order to establish a dose response curve per patient. For the G2 MN assay, blood cultures set up from 3 ml of blood in cRPMI were incubated for 72 h in the presence of the mitogen phytohaemagglutinin (PHA) (Gibco by Life Technologies, Belgium), and subsequently ir-

radiated with 4 Gy ⁶⁰Co γ-rays. The irradiations for the G0 and G2 MN assay were performed at a dose rate of 0.14 Gy/min in a water bath at 37°C. For all *in vitro* radiosensitivity endpoints sham-irradiated controls were included.

Assessment of radiation-induced apoptosis

After irradiation and incubation for 48 h, apoptosis was assessed in CD8+ lymphocytes. Apoptotic cells were determined by means of flow cytometry using the following panel of antibodies: V500-CD45, APC-CD8, Annexin V-FITC and 7-amino-actinomycin D (7-AAD) (all Becton Dickinson (BD) Biosciences, United States). Briefly, 100 μl of the concentrated cell suspension was stained with 5% V500-CD45 and APC-CD8. After 20 min incubation in dark, red blood cells were lysed (BD Pharm Lyse™, BD Biosciences), incubated and washed with Cellwash (BD Biosciences). Afterwards, the pellet was resuspended in 100 μl annexin buffer (BD Biosciences) and 5% 7-AAD and 5% FITC-annexin V were added. After incubation, 400 μl annexin buffer was added before the samples were analyzed. Data were acquired on a BD FACSCanto™ II flow cytometer (BD Biosciences) and approximately 5000 CD8+ events were analyzed.

Assessment of residual radiation-induced DNA DSB

After irradiation and incubation, T-lymphocytes were centrifuged onto poly-L-lysine slides in a concentration of 600,000 cells/ml (VWR, Belgium). The slides were fixed in PBS (Sigma-Aldrich, United States) containing 3%

paraformaldehyde (PFA) (Sigma-Aldrich) for 20 min and stored overnight in PBS containing 0.5% PFA. Slides were washed in PBS (Sigma-Aldrich) and permeabilized in PBS containing 0.2% Triton X-100 (Sigma Aldrich, Belgium) for 10 min. Thereafter, cells were blocked by washing them three times for 10 min in PBS containing 1% Bovine Serum Albumin (BSA) (Roche, Switzerland). Immunostaining was performed by incubating the cells during 1 h with anti- γ -H2AX (mouse mAb, Biolegend) and anti-53BP1 (rabbit pAb, Abcam) primary antibodies diluted 1/500 in blocking buffer. After washing the cells three times in PBS containing 1% BSA, slides were incubated with GAM-TRITC (Sigma-Aldrich) and GAR-Alexa488 (Invitrogen) secondary antibodies during 1 h diluted 1/1000 in blocking buffer. The cells were washed in D-PBS with 1% BSA (3 times 10 min), the nuclei were counterstained with 2% DAPI (Sigma Aldrich) dissolved in Fluoromount Mounting Medium (Sigma Aldrich) and a coverslip was added. Slides were scanned using a Metafer 4 scanning system (MetaSystems, Germany). This system uses a Zeiss Imager.Z2 microscope (Zeiss, Germany) and the images are captured by a CoolCube1 camera (Metasystems) in the green (TRITC, γ H2AX spots), red (Alexa488, 53BP1 spots) and blue (DAPI, nuclei) channel. Cells are scanned with a 63x/1.30 oil objective, a z-stack of 10 focal planes and a step size of 0.35 μ m between planes for both the green and the red channel. Per experimental condition at least 3 different slides were scanned. The scanned images were coded and 50 cells per

slide were analyzed manually on the screen. First, cells were selected as positives based on the nucleus morphology visible in the DAPI channel. Secondly, foci were scored by projecting TRITC and Alexa Fluor 488 sections on top of each other. Only foci with overlapping γ -H2AX- and 53BP1-spots were scored as residual DNA DSB.

G0 and G2 MN assay

For the G0 MN assay two blood cultures were set up (0.5 ml blood in 4.5 ml cRPMI complemented with 10% FCS) per dose point immediately after irradiation and T-lymphocytes were stimulated by adding 100 μ l phytohaemagglutinin (PHA) (Life Technologies, Gent, Belgium). To block cytokinesis, 24 hours later 6 μ g/ml cytochalasin B (Sigma Aldrich) was added. Cells were harvested 70 h post irradiation by a cold hypotonic shock with 0.075 M KCl, followed by overnight fixation in 4/1/5 Methanol/acetic acid/ringer solution. Subsequently, the cells were fixed three times in 4/1 methanol/acetic acid.

The G2 MN assay with the addition of caffeine was performed as described in (Claes et al, 2013). Two blood cultures were set up with the addition of PHA to stimulate the T-lymphocytes prior to irradiation. After 72 h culture time the cultures were irradiated. Immediately after irradiation cytochalasin B (6 μ g/ml) and caffeine (Sigma Aldrich, final concentration 4mM) were added to the cultures. 8 h post-irradiation the cultures were arrested and fixed as described for the G0 MN assay.

For further analysis, a suspension of cells

was dropped on clean slides and stained with DAPI Vectashield (Lab Consult). Slides were scanned with the MSearch software module of the Metafer 4 scanning system (MetaSystems) as described by Willems et al. (40), using a Zeiss Imager.Z2 microscope (Zeiss) and a CoolCube1 camera (MetaSystems). The MSearch software allows automated detection of binucleated (BN) cells and automated scoring of MN. 2 slides per culture were automatically scanned with a 10X magnification and analyzed. The scanned gallery-images were coded and all BN cells were checked manually on their MN score. Per slide approximately 1000 BN cells were scored.

Analysis

For the analysis of the γ -H2AX/53BP1 foci assay, the apoptosis assay and the G2 MN assay the radiation-induced number of foci, apoptotic cells and MN, obtained by subtraction of the data of sham-irradiated samples, were used.

For the analysis of the G0 MN assay data a dose response curve was determined for each patient assuming a linear-quadratic model:

$$Y = c + \alpha D + \beta D^2 \quad (1)$$

Based on these curves the area under the curve (AUC) up to 3 Gy was determined for each patient. To quantify inherent differences in radiosensitivity at the 95% confidence level, ellipses have been constructed that delimit the covariance between cellular dose response parameters which represent the inherent radiosensitivity (α), as well as the capacity to accu-

mulate repairable damage (β) for each donor. The average values and variances were used to calculate a set of α and β coordinates that demarcates the 95% confidence interval (Sokal and Rohlf 2012). Calculations were performed using Matlab (Matlab R2015b).

Unless otherwise mentioned a paired statistical analysis was performed using a paired t-test or Wilcoxon Signed Rank test, whichever was appropriate. When the group of cases was compared with the group of controls a t-test or Rank Sum test was used.

As only patients with severe late RT changes were selected as cases, which represent approximately 1% of non-syndromic individuals, only a relatively small study number was obtained limiting the statistical robustness of the study. In order to account for this limitation, statistical significance was set at a p-value of 0.01 (35).

Results

Apoptosis

With the combined use of Annexin V and 7-AAD only the late apoptotic cells were scored. In early stages of apoptosis, the plasma membrane excludes viable dyes such as 7-AAD (specific for double-stranded DNA) and cells will only be positive for Annexin V. During late stage apoptosis, loss of cell membrane integrity allows Annexin V binding as well as uptake of 7-AAD. A representative example of the flow cytometry analysis is presented in figure 1. The effect of radiation exposure on the propor-

tion of apoptotic cells is clearly illustrated in the data plots. For this analysis, we have first drawn gates for the selection of CD8+ T-lymphocytes (see figure 1 – c), and thereafter, a further selection was made based on the forward/side scatter (FSC and SSC) and the position in de CD45+ plot (figure 1 – a & b). A paired statistical analysis indicated significantly less apoptosis in the cases compared to their matched controls ($p < 0.001$). However, case 11 displays a higher apoptosis level than her matched control and the overlapping error bars for 4 of the matched pairs necessitate a large prospective set-up to assess the predictive value of the assay. Grouped analysis illustrates that cases (average 14.45% apoptosis) have significantly lower apoptotic responses than controls (average 30.64% apoptosis) ($p < 0.0001$) (figure 2).

Residual DNA DSB

Foci representing residual DNA DSB were only scored when γ -H2AX- and 53BP1-spots overlap (approx. 90% of the spots overlap, see (41)) as observed on the Metafer system after scanning at 63X magnification (figure 3). The scoring of γ -H2AX/53BP1 co-localized foci increases the reliability that the observed spots are indeed DNA DSB and enhances the sensitivity of foci scoring by reducing the impact of artifacts and false positives. A pairwise comparison showed a significantly higher number of foci for the cases compared to the controls ($p < 0.01$). However, case 1 scores lower than her control and 9 out of 12 matched pairs show overlap in error bars which gives this assay only a modest strength to predict normal tissue

radiosensitivity in a predictive set-up for breast cancer patients (see figure 4).

When cases and controls are compared as groups, the cases (average 9.92 foci per cell) have a significantly higher number of foci than the controls (9.17 foci per cell) ($p < 0.01$) (figure 4).

GO MN assay

The cases (average age 68y) have a significantly elevated number of background MN compared to their matched controls (average age 57y), respectively 50 and 36 MN per 1000 BN cells ($p = 0.025$). When compared to a healthy control group of 29 adult donors (the group consists of healthy donors at the laboratory since 2010; average age of 48 years; 63% female) with an average of 15 MN per 1000 BN cells, the patient group has an elevated number of background MN (Rank sum test $p < 0.0001$). The individual data of all patients showed a linear-quadratic dose response with weighted regression fits resulting in high R^2 values (range: 0.959 – 0.999). A comparison between the linear quadratic fits of the average dose response data of cases and controls, represented in figure 5, shows clearly that average MN yields are systematically higher for cases than controls for each dose point. In the insert of figure 5, the ellipses giving the 95 % confidence intervals on the α and β values of the fits to the group of cases and controls are depicted: α as well as β are higher for cases than controls. The ellipses do not overlap, indicating that the dose responses of the average case and control data are significantly different. For the individual

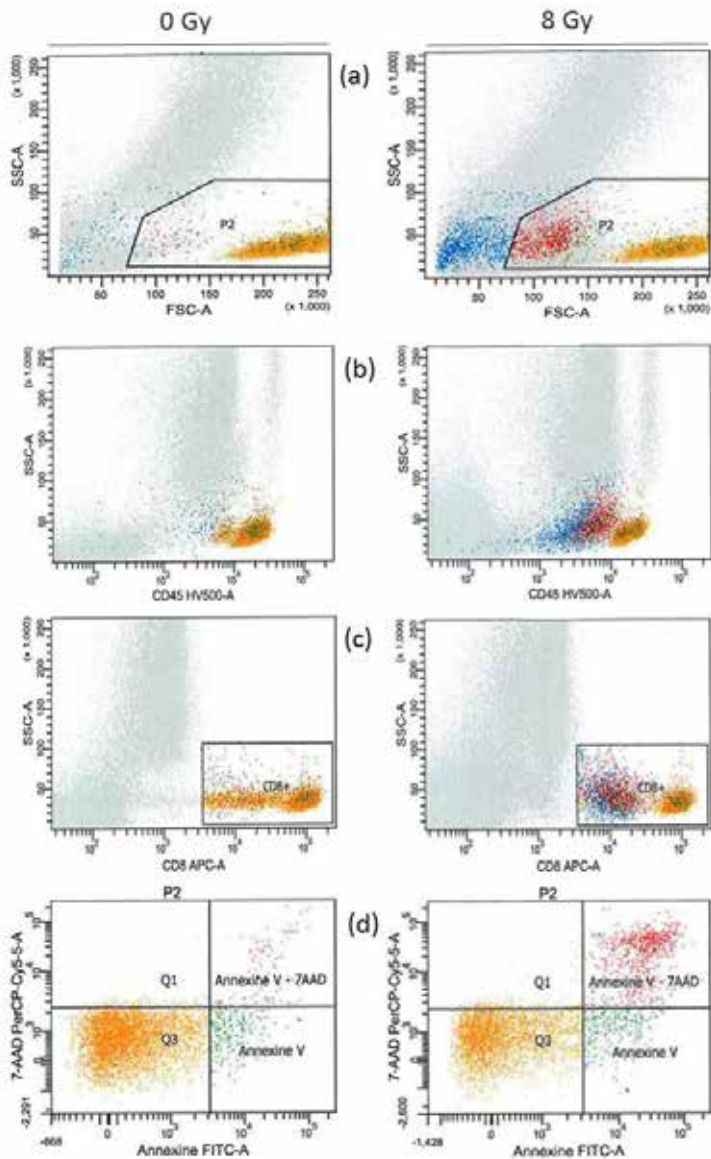


FIGURE 1

Flow cytometry data analysis of apoptosis in CD8 T-lymphocytes, 48 h post irradiation with 8 Gy x-rays. Cells were first gated on CD8+ marker expression displayed in APC (c). Thereafter cells were gated on cell size and granularity on the FSC/SSC data plot (a) and there positive staining for CD45+ displayed in HV500 was checked. Eventually Annexin V/7-AAD positive cells were selected in the upper right quadrant of data plot presented in (d). The left column illustrates the results for a non-irradiated sample with low late apoptosis levels (2.0%) versus the results for an irradiated sample with a remarkable increase in late apoptosis levels (18.9%).

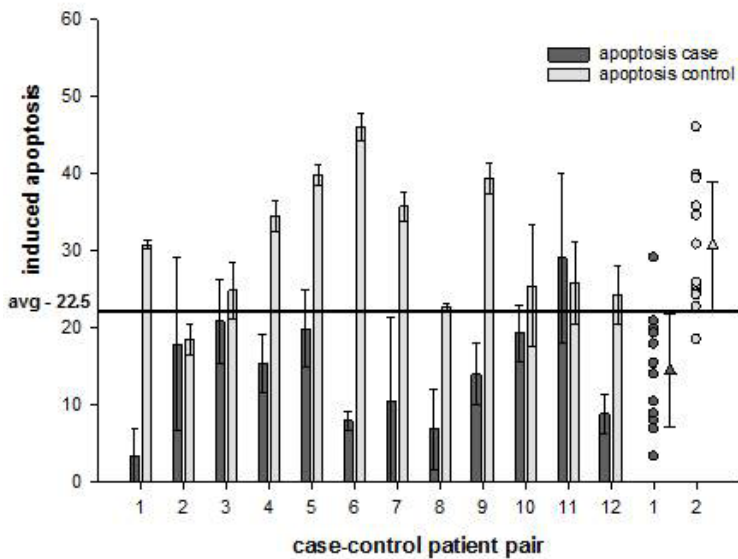


FIGURE 2

Percentage of cells with radiation-induced late apoptosis in each of the cases (dark grey bars) and controls (white bars). The average of all cases (dark grey triangle) and controls (white triangle) with the corresponding spread in data points, is represented at the right end of the graph. The horizontal line represents the average over all patients (cases and controls). The error bars represent standard deviations based on multiple replicates (generally three, but for some of the measurements only two samples were available).

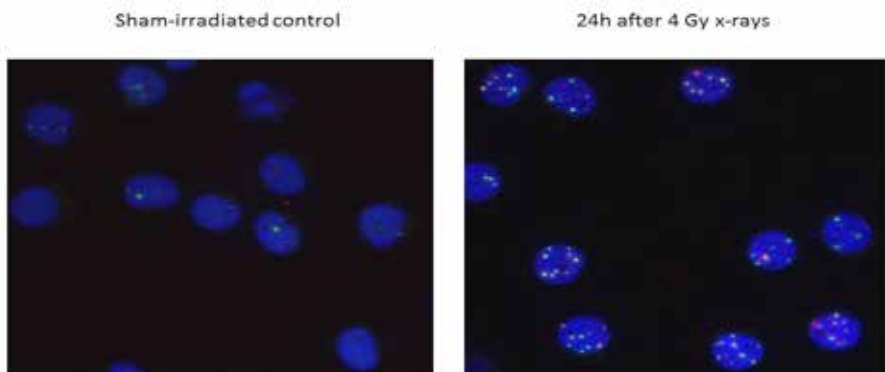


FIGURE 3

Illustration of γ -H2AX/53BP1 foci staining, with the blue DAPI stained nuclei of the T-lymphocytes and overlapping green 53BP1 and red γ -H2AX foci. The left figure represents a sham-irradiated sample, while the right figure represents the number of residual γ -H2AX/53BP1 foci 24h post irradiation at 4 Gy x-rays.

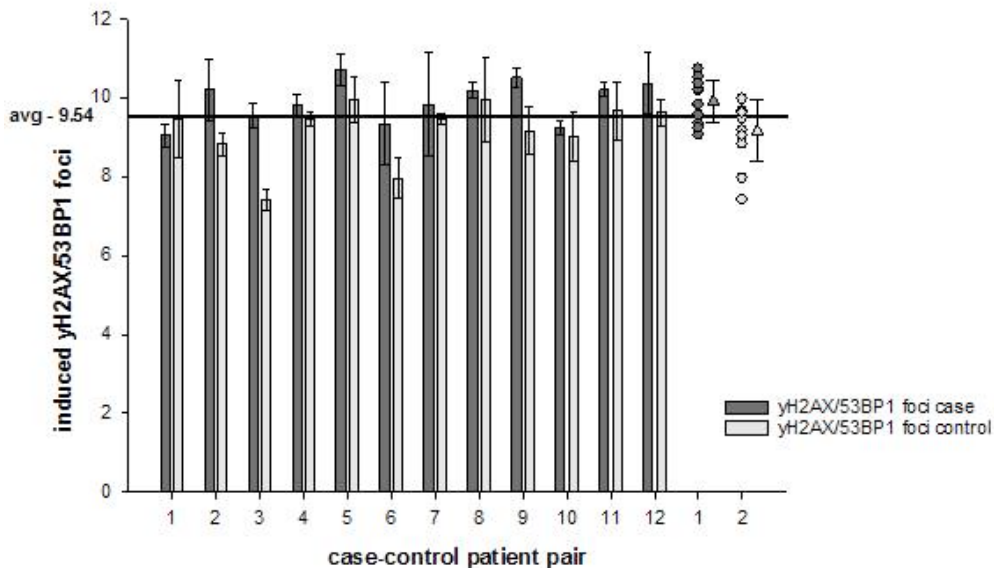


FIGURE 4

Number of radiation-induced γ H2AX/53BP1 foci per cell in cases (dark grey bars) and controls (white bars). The average of all cases (dark grey triangle) and controls (white triangle) with the corresponding spread in case and control γ H2AX/53BP1 foci values are represented at the right end part of the graph. The horizontal line represents the average over all patients. The error bars represent standard deviations based on the scoring of at least three different slides.

case-control patient data, ellipses also do not overlap in 10 out of 12 pairs. There is however no systematic shift in the location of the ellipse from case to control on an individual basis, indicating that the change in α and β values of the individual patient dose response are not directly correlated with the clinical radiotoxic effects. A Wilcoxon Signed Rank Test including all dose-points showed a significant difference between the average case and control MN data,

presented in figure 5 ($p < 0.001$).

For the interpretation of the dose response curves at the individual case-control pair level the AUC of the dose response up to 3 Gy was calculated. Using this quantity 10 out of 12 cases scored higher than their matched control ($p = 0.01$), however 6 of the 12 pairs show overlap in standard deviations (figure 6). For the MN data at a single dose-point, differences in radiation-induced number of MN between cases and

matched controls were found to be statistically different at the p 0.05 level from 1 Gy upwards ($p_{1\text{Gy}} = 0.04$; $p_{2\text{Gy}} = 0.021$; $p_{3\text{Gy}} = 0.018$).

G2 MN assay

A very low binucleated index resulted in a very low number of binucleated cells for case 10 and control 2, which were excluded from the

analysis. In a pairwise comparison, MN scores in the cases were significantly higher than the MN yields in the matched control ($p < 0.01$). In 9 out of 10 patient pairs, the cases score higher than their matching controls (figure 7). However, 4 out the 10 pairs show a substantial overlap in standard deviation.

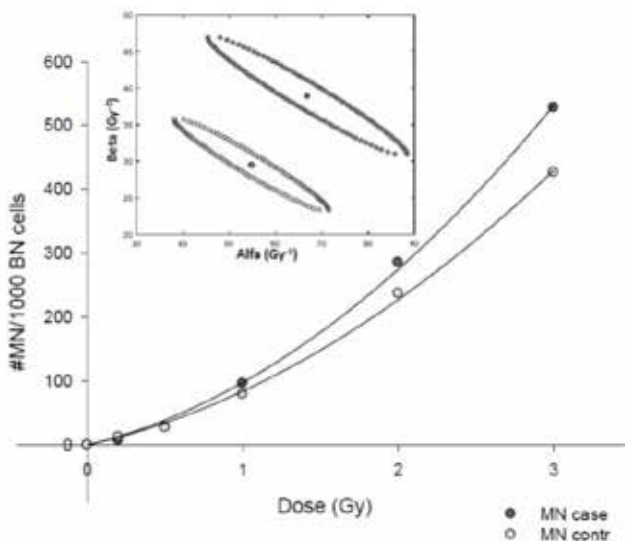


FIGURE 5

Dose-response curve for the average number of radiation-induced MN per 1000 BN cells for cases (grey circles) and controls (white circles). The dose-response curves are the result of fits using a weighted linear-quadratic regression. In the insert the 95% confidence ellipses for the α and β coefficients of the average dose-response curves for cases (grey dots) and controls (white dots) are given.

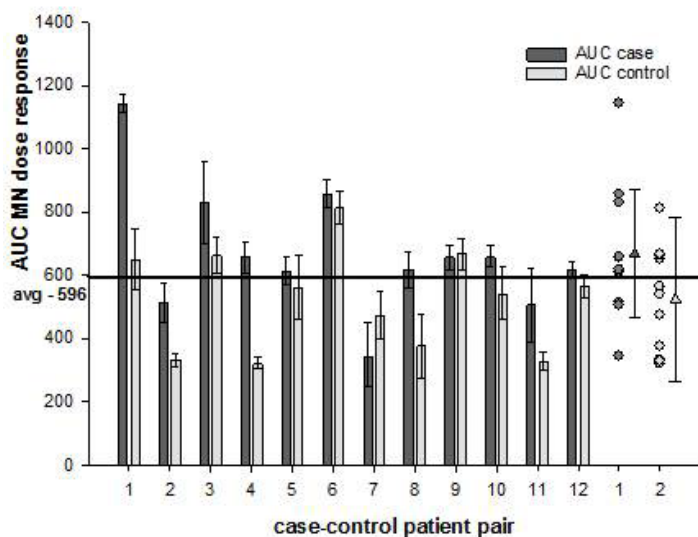


FIGURE 6

The AUC calculated from the G0-MN dose-response curve for each of the cases (dark grey bars) and controls (white bars). The average of all cases (dark grey triangle) and controls (white triangle) and the corresponding spread in case and control AUC values is represented in the right part of the graph. The horizontal line represents the average over all patients. The error bars represent standard deviations based on the scoring of four different slides per dose point.

A group analysis showed that the G2 MN yield in the group of cases (average 351 MN per 1000 BN cells) was significantly higher than in the group of controls (average 219 MN per 1000 BN cells) ($p < 0.01$).

Discussion

In present study the individual cellular radiosensitivity of breast cancer patients who expressed severe versus minimal late toxicity after RT was compared in a retrospective case-control setting using four different assays. The selection of the different cellular radiosens-

itivity assays was based on existing literature and protocols previously used by other research groups who were able to successfully show a good correlation between *in vitro* cellular radiosensitivity and late normal tissue reactions in cancer patients. An accurate selection of patients showing severe late radiotoxic effects at the follow-up examinations by the radiation oncologist is a prerequisite for the quality of this kind of studies. The latter determines the strength of the current study as patients were carefully assessed for late toxicity and matched into case-control pairs. Therefore, this study cohort of patient outliers (only no/minimal re-

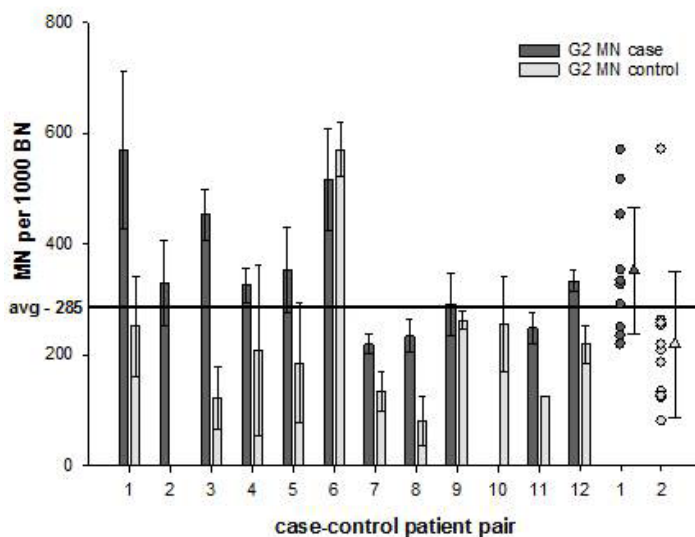


FIGURE 7

Number of radiation-induced G2 MN per 1000 BN cells in each of the cases (dark grey bars) and controls (white bars). The average of all cases (dark grey triangle) and controls (white triangle) and the corresponding spread in case and control G2 values is presented in the right part of the graph. No results were available for two patients owing to low BN yields (control 2 and case 10). The horizontal line represents the average over all patients. The error bars represent standard deviations based on the scoring of four different slides per dose point.

sponders and severe responders) could be used for this proof of principle study to evaluate and estimate the possible clinical value of four different radiosensitivity assays to predict late normal tissue toxicity following RT.

Late toxicity is a broad term that includes multiple endpoints. In present study, patient's toxicity score was based on the LENT-SOMA scale and an overall breast cosmetic score was derived from standardized photographs with a 4-categories cosmetic score as proposed by the Harvard Medical School (Table I) (38, 39, 42). Patients were selected as cases based on the criterion that the LENT-SOMA score three years

after RT was increased by 2 compared to pre-RT for at least one endpoint. This corresponded with an overall cosmetic score of 3 or 4 for all patients, except for case 11. The latter patient was included based on a grade 2 fibrosis score in LENT-SOMA. The overall cosmetic score focuses on cosmesis and unfortunately, fibrosis as such is not taken into account, resulting in a cosmetic score of only 2. Scoring of retraction in this patient population who underwent breast conserving surgery was not obvious, as this endpoint depends strongly on the volume of tissue removed during surgery. This is for example a problem in control 11, who had a

lot of tissue removed during surgery, resulting in a high cosmetic score of 3 (fair) and a high retraction score of 3 before RT, but no further RT-related changes were detected during follow-up. By matching the controls as much as possible to the cases for therapy variables, cup-size, BMI and age, we obtained a case-control with minimal impact of variables, known to be associated with radiotoxicity.

The observation that normal tissue damage can involve a combination of phenotypes suggests that their underlying cellular mechanisms may be different (43). The identification of these mechanisms could help in clinical response prediction, however current literature reports are very mixed and confusing. A first study that we have to highlight is the study of Finnon et al. who used gene expression in addition to *in vitro* cellular endpoints similar to the assays used in the current study (34). In their study on breast cancer patients, 31 cases with late normal tissue reactions were matched with 28 control patients who showed no changes in breast appearance. Matching of case-control patients was also based on RT parameters, breast size and adjuvant therapy. Significant inter-sample variation was observed for all cellular endpoints, but cases and controls could not be distinguished with the different *in vitro* radiosensitivity assays. This difference in study results compared to our study may be attributed, at least in part, to different experimental conditions. Finnon et al. used a radiation dose of 4Gy x-rays and frozen lymphocytes to assess radiation-induced apoptosis levels, the used γ -H2AX flow cytometric assay is not as

sensitive as the fluorescence microscopic scoring method, used in our study and G0 MN were scored for 3.5 Gy x-rays while we used a 5 point dose response ranging from 0.2 to 3 Gy. Of all studies on the association between cellular radiosensitivity and normal tissue reactions, the apoptosis assay gives the most impressive and promising results. The decreased intrinsic ability to recognize cell damage and subsequently initiate apoptosis, is one of the proposed mechanisms for patients experiencing late toxicity. Due to the lack of repair or removal, the damaged cells linger in the irradiated breast tissue or cause genetic damage to daughter cells, resulting in late toxicity (15). Previous studies showed altered apoptotic profiles after *in vitro* irradiation with doses up to 8 Gy in patients with increased radiotoxicity in various cancer patient cohorts (15, 32, 44, 45). In a large scale study of patients treated for miscellaneous cancers Ozsahin *et al.* could demonstrate a reduced apoptotic response in CD4+ and CD8+ lymphocytes after an *in vitro* dose of 8 Gy in patients experiencing radiation-induced toxicity (25). According to these authors the CD8+ subpopulation is more sensitive and specific than CD4+ T-lymphocytes. Based on the promising results of Ozsahin *et al.* we adopted the irradiation protocol described in this paper and we scored CD8+ T-lymphocyte apoptosis after an *in vitro* dose of 8 Gy. The results obtained in present study confirm the value of apoptosis scoring as cellular assay in the prediction of late toxic effects in breast cancer patients. However, despite the fact that 11 out of 12 cases showed lower apoptosis

scores compared to their matched control patients and the observed statistical significance for both paired and grouped analysis, there was a substantial overlap in standard deviations which may hinder the successful translation of this assay into clinical practice. In a small breast cancer cohort study of Chua et al. the average apoptotic fraction after 8 Gy was not different for the population of 8 cases with severe late radiotoxic effects compared to 8 controls and this when apoptosis was measured in both the total lymphocyte population and the CD4+ and CD8+ T-lymphocyte subsets (27). In the latter paper, radiation-induced apoptosis was assessed using an inhibitor of caspases assay (FLICA) while in our study late apoptosis was scored by means of Annexin V and 7-AAD staining. Measurement of apoptosis after *in vitro* doses lower than 8 Gy often failed to find a correlation with clinical radiation sensitivity (15, 34, 46). Furthermore, the use of T-lymphocyte subsets for apoptosis scoring is still a controversial issue in the literature. For example, Schnarr *et al.* could find a statistical significant difference between cases (38.0%) and controls (33.6%) after 8 Gy irradiation for the total lymphocyte population. However this observation could not be made for either the CD4+ or CD8+ lymphocyte subsets (15). The authors suggest that another lymphocyte population (CD4-/CD8-) could affect their findings. The detection of residual γ -H2AX/53BP1 foci 24 h post irradiation is a sensitive method to determine the number of residual DNA DSB. It is generally accepted that the disappearance of foci is representative for the repair of

DNA DSB while persistence of foci indicates impaired DNA repair (35, 47). We know from studies on ataxia telangiectasia (AT) and other chromosomal breakage syndrome patients that their underlying genetic defect in DNA DSB repair results in extreme clinical and cellular hypersensitivity to ionizing radiation (48, 49). It is anticipated that differences in residual foci levels are indicative for significant differences in DSB repair, however, the assay doesn't provide information on the underlying mechanism for this difference. Studies on the relationship between the number of residual DNA DSB in lymphocytes after *in vitro* irradiation and clinical radiotoxicity published are contradictory. In our study we could observe a positive correlation between residual γ -H2AX/53BP1 foci levels 24 h after 4 Gy x-rays and late normal tissue toxicity, both at individual case-control level ($p < 0.01$) and group level ($p < 0.01$). The results are in agreement with those reported by Chua et al. (31) using the same protocol for breast cancer patients and indicate the potential of the γ -H2AX/53BP1 foci assay for the prediction of late normal tissue reactions. In the study of Chua et al. average foci levels per cell 24 h after 4 Gy x-rays were 12.78 in cases and 10.15 in controls compared to respectively 9.92 and 9.17 in the current study. On the contrary different studies could not find an association between residual DNA damage and severe late toxicity, such as Werbrouck et al. in a cohort of gynecological cancer patients and Brzowska *et al.* in prostate cancer patients (50, 51). While significant differences were observed between cases and controls, we could not find a

correlation between apoptosis levels 48 h after 8 Gy in CD8+ T-lymphocytes and residual foci levels 24 h after 4 Gy in T-lymphocytes (Spearman's $R = 0.284$, $p = 0.178$). This confirms earlier observations made by Chua et al. (27).

Cytogenetic assays, such as the MN assay, are frequently used to evaluate the damage response of the cell to radiation-induced DNA damage and to assess radiosensitivity *in vitro*. The elevated background number of MN observed in the patient group (42 MN/1000 BN cells) compared to a healthy population (15 MN/1000 BN cells) is significant ($p < 0.0001$), even after correction for age and gender differences (males 0.31 MN/1000 BN cells/year; females 0.58 MN/1000 BN cells/year) (52-54). An elevated number of spontaneous MN or chromosomal aberrations in cancer patients has been reported by different research groups (55-58) and is considered to be a hallmark for cancer and chromosomal instability. However, in this study, the residual effect of RT can also be the cause of the higher spontaneous MN yields (59), as MN disappear from the body gradually with a half-life of approximately 1 year (60, 61). There is also a difference in background MN numbers between the case (50 MN/1000 BN cells) and control group (36 MN/1000 BN cells) ($p = 0.025$). Correcting the MN data for the age difference between cases (average age 68 years) and controls (average age 57 years) at a rate of 0.58 MN/1000 BN cells/year reduces strongly the difference and renders the difference statistically not significant.

Different studies of various cancer patient cohorts have investigated the correlation between

the number of chromosomal aberrations (dicentric or MN) induced after *in vitro* irradiation of lymphocytes and late normal tissue toxicity to RT, with varying success (29, 34, 62-65). Specifically for breast cancer patient cohorts some studies report a positive association (31, 66), while others don't (24, 34, 67). Factors as definition of the groups, the selected cellular endpoints and differences in experimental setup might account for the lack of consistency in the results. Compared to these studies we used a case-control setting with matching of the most important variables. Furthermore, instead of analyzing one dose point, we determined a dose response relationship (0 to 3 Gy) for each patient with the G0 MN assay.

Distinct differences in the average dose response curves between both groups are observed. Fitting linear-quadratic functions to the dose response data results in α and β values which are different at the 95% confidence level. This is illustrated by the 95% confidence ellipses, depicted in figure 5, which are clearly separated for both groups. For the interpretation of the individual case-control pairs, the AUC for the dose response curves up to 3 Gy was used which showed a statistically significant difference between cases and controls ($p = 0.01$).

In this study we also applied a G2 MN assay (47) to study the association with clinical radiotoxicity. Up to now application of the G2 assay with scoring of chromatid breaks in lymphocytes was unsuccessful in the prediction of radiotoxicity in breast cancer patients (34, 66, 67). In the G2 MN assay we used in this study, cells are irradiated in the G2 phase and caffeine

is added to abrogate the G2/M checkpoint (68, 69). The use of caffeine on G2-cells will allow heavily damaged and yet unrepaired cells, which would otherwise be blocked at the G2/M checkpoint, to progress through mitosis. This allows us to analyze differences in individual repair efficiency independent from differences in individual cell cycle control (70, 71). Applying the G2 MN assay on the patient groups in present study results in a significantly higher number of MN in cases compared to controls ($p < 0.01$). This could indicate that the development of late normal tissue toxicity following RT is associated with a less efficient DNA repair.

When comparing the performance of the different *in vitro* cellular radiosensitivity assays to distinguish patients with severe radiotoxic effects in present case-control setting, all assays perform relatively well and highlight most cases in the paired setting (Table I). However, it is important to note that some of the case-control pairs show substantial overlap in standard deviations, which questions the value of the assays in clinical RT practice. The results presented in this study, serve to strengthen the evidence for an association between lower levels of radiation-induced CD8+ apoptosis, increased levels of residual DNA damage and chromosomal radiosensitivity with severe normal tissue reactions following RT. However, the case-control pairs for which no correlation was found between *in vitro* and *in vivo* radiosensitivity differ for the different assays, showing that the failures are not linked to a systematic difference in intrinsic radiosensitivity. The lack of

correlation between the different *in vitro* cellular radiosensitivity assays may be linked to the different radiation doses and time points, which were based on previously published studies selected for the different assays.

In order to overcome the limitations of the current study, the different culture conditions and radiation doses used in the four assays should be further optimized and aligned with each other. It is anticipated that a number of cells will die and disappear during culturing, so it would be interesting to test the influence of the difference in radiation dose, culture condition and time point by comparing the total number of cells after irradiation with the same samples prior to irradiation. The different endpoints can be compromised by parallel processes inherent to the different methodologies and this could theoretically impact the predictive value of the used assays in identifying breast cancer patients prone to late toxicity.

In a predictive scenario with a large patient population, apoptosis seems to be the most promising assay of the four different tests used in this study. When using the average value of the endpoint over the whole patient population as threshold value only control 2 scores below the average apoptosis value of 22.5% and case 11 would erroneously be categorized as a non-radiosensitive patient (see figure 2). The current study comprised only high and low outliers with respect to expression of late normal tissue reactions of the total group of breast cancer patients, which does not allow to determine a robust cut-off value. Large scale prospective studies on RT patients are necessary to fill this gap.

In conclusion, present study of RT breast cancer patients using a matched case-control setup and different endpoints for assessing *in vitro* cellular radiosensitivity, related to DNA repair and apoptosis, suggests that patient's intrinsic radiosensitivity is involved in the development of late radiotoxic effects. As the biological mechanisms behind the different symptoms of late radiotoxicity differ, it can be expected that not all clinical manifestations of late radiotoxicity are linked in the same degree to intrinsic radiosensitivity with respect to DNA repair and apoptosis. Finally, of the four radiosensitivity tests applied, the apoptosis assay seems to be most promising in the framework of predicting radiotoxic effects in individual patients. However, the large variation in the data set as reflected in overlapping standard deviations, warrants further research to validate the findings for the different cellular radiosensitivity assay in larger patients groups and prospective studies. The results of this study can be used to demonstrate a possible association between intrinsic radiosensitivity and late normal tissue toxicity, but confounding experimental variables should be taken into account in future association studies in order to investigate a possible correlation between the different biological end points.

Acknowledgements

This work was supported by the National Cancer Plan, Action 29 project 015, financed by the Federal Office of Health and Social Affairs, Belgium. Alegria Montoro of the Radiation Protection Service and the Grupo de Investigación

Biomédica en Imagen GIBI230, IISLAFE, Valencia (Spain), is acknowledged for providing financial support to Natividad Sebastià (co-author) for her stay at Ghent University. We wish to thank all patients who donated blood and the nursing staff, especially Annick Van Greveling, for helping collecting the samples. We also like to thank Philip Beukes from iThemba LABS (South Africa) for providing the software for the analysis of the dose response curves with respect to the covariates and 95% confidence intervals.

Declaration of interest

The authors report no declarations of interest.

References

1. EBCTCG, Effect of radiotherapy after breast-conserving surgery on 10-year recurrence and 15-year breast cancer death: meta-analysis of individual patient data for 10801 women in 17 randomized trials. *Lancet* 2011; 378, 1707-60.
2. EBCTCG, Effect of radiotherapy after mastectomy and axillary surgery on 10-year recurrence and 20-year breast cancer mortality: meta-analysis of individual patient data for 8135 women in 22 randomised trials. *Lancet* 2014; 383, 2127-35.
3. Dayes I, Rumble RB, Bowen J, Dixon P, Warde P, Intensity-modulated radiotherapy in the treatment of breast cancer. *Clinical oncology (Royal College of Radiologists (Great Britain))* 2012; 24, 488-98.
4. Veldeman L, Madani I, Hulstaert F, De Meerleer G, Mareel M, De Neve W, Evidence behind use of intensity-modulated

- radiotherapy: a systematic review of comparative clinical studies. *Lancet Oncol* 2008; 9, 367-75.
5. De Neve W, De Gersem W, Madani I, Rational use of intensity-modulated radiation therapy: the importance of clinical outcome. *Seminars in radiation oncology* 2012; 22, 40-9.
 6. Alsner J, Andreassen CN, Overgaard J, Genetic markers for prediction of normal tissue toxicity after radiotherapy. *Semin Radiat Oncol* 2008; 18, 126-35.
 7. Feight D, Baney T, Bruce S, McQuestion M, Putting Evidence Into Practice: Evidence-Based Interventions for Radiation Dermatitis. *Clinical Journal of Oncology Nursing* 2011; 15, 481-92.
 8. Waljee JF, Hu ES, Ubel PA, Smith DM, Newman LA, Alderman AK, Effect of esthetic outcome after breast-conserving surgery on psychosocial functioning and quality of life. *Journal of clinical oncology : official journal of the American Society of Clinical Oncology* 2008; 26, 3331-7.
 9. De Langhe S, Mulliez T, Veldeman L, Remouchamps V, van Greveling A, Gilsoul M, et al., Factors modifying the risk for developing acute skin toxicity after whole-breast intensity modulated radiotherapy. *BMC Cancer* 2014; 14, 9.
 10. Dubray B, Delanian S, Lefaix JL, Late effects of mammary radiotherapy on skin and subcutaneous tissues. *Cancer Radiother* 1997; 1, 744-52.
 11. Barker CL, Routledge JA, Farnell DJJ, Swindell R, Davidson SE, The impact of radiotherapy late effects on quality of life in gynaecological cancer patients. *British Journal of Cancer* 2009; 100, 1558-65.
 12. Peters LJ, Radiation therapy tolerance limits. For one or for all?--Janeway Lecture. *Cancer* 1996; 77, 2379-85.
 13. West CM, Barnett GC, Genetics and genomics of radiotherapy toxicity: towards prediction. *Genome Med* 2011; 3, 52.
 14. Barnett GC, West CML, Dunning AM, Elliott RM, Coles CE, Pharoah PDP, et al., Normal tissue reactions to radiotherapy: towards tailoring treatment dose by genotype. *Nat Rev Cancer* 2009; 9, 134-42.
 15. Schnarr K, Boreham D, Sathya J, Julian J, Dayes IS, Radiation-induced lymphocyte apoptosis to predict radiation therapy late toxicity in prostate cancer patients. *Int J Radiat Oncol Biol Phys* 2009; 74, 1424-30.
 16. Barnett GC, Coles CE, Elliott RM, Baynes C, Luccarini C, Conroy D, et al., Independent validation of genes and polymorphisms reported to be associated with radiation toxicity: a prospective analysis study. *Lancet Oncology* 2012; 13, 65-77.
 17. Burnet NG, Johansen J, Turesson I, Nyman J, Peacock JH, Describing patients' normal tissue reactions: concerning the possibility of individualising radiotherapy dose prescriptions based on potential predictive assays of normal tissue radiosensitivity. Steering Committee of the BioMed2 European Union Concerted Action Programme on the Development of Predictive Tests of Normal Tissue Response to Radiation Therapy. *Int J Cancer* 1998; 79, 606-13.
 18. Stone HB, Coleman CN, Anscher MS, McBride WH, Effects of radiation on normal tissue: consequences and mechanisms. *Lancet Oncol* 2003; 4, 529-36.
 19. Barnett GC, Wilkinson JS, Moody AM, Wilson CB, Twyman N, Wishart GC, et al., The Cambridge Breast Intensity-modulated Radiotherapy Trial: Patient- and Treatment-related Factors that Influence Late Toxicity. *Clin Oncol* 2011; 23, 662-73.
 20. Tucker SL, Turesson I, Thames HD, Evidence for individual differences in the radiosensitivity of human skin. *European*

- Journal of Cancer; 28, 1783-91.
21. Turesson I, Nyman J, Holmberg E, Oden A, Prognostic factors for acute and late skin reactions in radiotherapy patients. *Int J Radiat Oncol Biol Phys* 1996; 36, 1065-75.
 22. Burnet N, Nyman J, Turesson I, Wurm R, Yarnold J, Peacock J, Prediction of normal-tissue tolerance to radiotherapy from in vitro cellular radiation sensitivity. *Lancet* 1992; 339, 1570-71.
 23. Borgmann K, Hoeller U, Nowack S, Bernhard M, Roper B, Brackrock S, et al., Individual radiosensitivity measured with lymphocytes may predict the risk of acute reaction after radiotherapy. *International Journal of Radiation Oncology Biology Physics* 2008; 71, 256-64.
 24. Hoeller U, Borgmann K, Bonacker M, Kuhlmeiy A, Bajrovic A, Jung H, et al., Individual radiosensitivity measured with lymphocytes may be used to predict the risk of fibrosis after radiotherapy for breast cancer. *Radiother Oncol* 2003; 69, 137-44.
 25. Ozsahin M, Crompton NEA, Gourgou S, Kramar A, Li L, Shi YQ, et al., CD4 and CD8 T-lymphocyte apoptosis can predict radiation-induced late toxicity: A prospective study in 399 patients. *Clinical Cancer Research* 2005; 11, 7426-33.
 26. Chua MLK, Rothkamm K, Biomarkers of Radiation Exposure: Can They Predict Normal Tissue Radiosensitivity? *Clin Oncol* 2013; 25, 610-16.
 27. Chua MLK, Horn S, Somaiah N, Davies S, Gothard L, A'Hern R, et al., DNA double-strand break repair and induction of apoptosis in ex vivo irradiated blood lymphocytes in relation to late normal tissue reactions following breast radiotherapy. *Radiation and Environmental Biophysics* 2014; 53, 355-64.
 28. Borgmann K, Haeberle D, Doerk T, Busjahn A, Stephan G, Dikomey E, Genetic determination of chromosomal radiosensitivities in G0- and G2-phase human lymphocytes. *Radiother Oncol* 2007; 83, 196-202.
 29. Widel M, Jedrus S, Lukaszczyk B, Raczek-Zwierzycka K, Swierniak A, Radiation-Induced Micronucleus Frequency in Peripheral Blood Lymphocytes is Correlated with Normal Tissue Damage in Patients with Cervical Carcinoma Undergoing Radiotherapy. *Radiation Research* 2003; 159, 713-21.
 30. Taghavi-Dehaghani M, Mohammadi S, Ziafazeli T, Sardari-Kermani M, A study on differences between radiation-induced micronuclei and apoptosis of lymphocytes in breast cancer patients after radiotherapy. *Zeitschrift Fur Naturforschung C-a Journal of Biosciences* 2005; 60, 938-42.
 31. Chua MLK, Somaiah N, A'Hern R, Davies S, Gothard L, Yarnold J, et al., Residual DNA and chromosomal damage in ex vivo irradiated blood lymphocytes correlated with late normal tissue response to breast radiotherapy. *Radiother Oncol* 2011; 99, 362-66.
 32. Crompton NE, Miralbell R, Rutz HP, Ersoy F, Sanal O, Wellmann D, et al., Altered apoptotic profiles in irradiated patients with increased toxicity. *International journal of radiation oncology, biology, physics* 1999; 45, 707-14.
 33. Ozsahin M, Azria D, Radiation-Induced Sequelae Measured by Lymphocyte Apoptosis. *International Journal of Radiation Oncology Biology Physics* 2014; 90, 470-70.
 34. Finnon P, Kabacik S, MacKay A, Raffy C, A'Hern R, Owen R, et al., Correlation of in vitro lymphocyte radiosensitivity and gene expression with late normal tissue reactions following curative radiotherapy for breast cancer. *Radiotherapy and Oncology* 2012; 105, 329-36.

35. Bourton EC, Plowman PN, Smith D, Arlett CF, Parris CN, Prolonged expression of the gamma-H2AX DNA repair biomarker correlates with excess acute and chronic toxicity from radiotherapy treatment. *Int J Cancer* 2011; 129, 2928-34.
36. Azria D, Riou O, Castan F, Nguyen TD, Peignaux K, Lemanski C, et al., Radiation-induced CD8 T-lymphocyte Apoptosis as a Predictor of Breast Fibrosis After Radiotherapy: Results of the Prospective Multicenter French Trial. *EBioMedicine* 2015; 2, 1965-73.
37. Bentzen SM, Agrawal RK, Aird EGA, Barrett JM, Barrett-Lee PJ, Bliss JM, et al., The UK Standardisation of Breast Radiotherapy (START) Trial A of radiotherapy hypofractionation for treatment of early breast cancer: A randomised trial. *Lancet Oncology* 2008; 9, 331-41.
38. LENT SOMA tables. *Radiotherapy and oncology : journal of the European Society for Therapeutic Radiology and Oncology* 1995; 35, 17-60.
39. Harris JR, Levene MB, Svensson G, Hellman S, Analysis of cosmetic results following primary radiation therapy for stages I and II carcinoma of the breast. *International journal of radiation oncology, biology, physics* 1979; 5, 257-61.
40. Willems P, August L, Slabbert J, Romm H, Oestreicher U, Thierens H, et al., Automated micronucleus (MN) scoring for population triage in case of large scale radiation events. *International Journal of Radiation Biology* 2010; 86, 2-11.
41. Vandevoorde C, Gomolka M, Roessler U, Samaga D, Lindholm C, Fernet M, et al., EPI-CT: in vitro assessment of the applicability of the gamma-H2AX-foci assay as cellular biomarker for exposure in a multicentre study of children in diagnostic radiology. *Int J Radiat Biol* 2015; 91, 653-63.
42. Pavy JJ, Denekamp J, Letschert J, Littbrand B, Mornex F, Bernier J, et al., EORTC Late Effects Working Group. Late effects toxicity scoring: the SOMA scale. *Radiotherapy and oncology : journal of the European Society for Therapeutic Radiology and Oncology* 1995; 35, 11-5.
43. Giotopoulos G, Symonds RP, Foweraker K, Griffin M, Peat I, Osman A, et al., The late radiotherapy normal tissue injury phenotypes of telangiectasia, fibrosis and atrophy in breast cancer patients have distinct genotype-dependent causes. *Br J Cancer* 2007; 96, 1001-7.
44. Bordon E, Henriquez Hernandez LA, Lara PC, Pinar B, Fontes F, Rodriguez Gallego C, et al., Prediction of clinical toxicity in localized cervical carcinoma by radio-induced apoptosis study in peripheral blood lymphocytes (PBLs). *Radiation oncology (London, England)* 2009; 4, 58.
45. Bordon E, Henriquez-Hernandez LA, Lara PC, Ruiz A, Pinar B, Rodriguez-Gallego C, et al., Prediction of clinical toxicity in locally advanced head and neck cancer patients by radio-induced apoptosis in peripheral blood lymphocytes (PBLs). *Radiation oncology (London, England)* 2010; 5, 4.
46. Barber JBP, West CML, Kiltie AE, Roberts SA, Scott D, Detection of individual differences in radiation-induced apoptosis of peripheral blood lymphocytes in normal individuals, ataxia telangiectasia homozygotes and heterozygotes, and breast cancer patients after radiotherapy. *Radiation Research* 2000; 153, 570-78.
47. Claes K, Depuydt J, Taylor AMR, Last JJ, Baert A, Schietecatte P, et al., Variant Ataxia Telangiectasia: Clinical and Molecular Findings and Evaluation of Radio-sensitive Phenotypes in a Patient and Relatives. *Neuromol Med* 2013; 15, 447-57.
48. Lavin MF, Shiloh Y, The genetic defect in ataxia-telangiectasia. Annual review of

- immunology 1997; 15, 177-202.
49. Carney JP, Chromosomal breakage syndromes. *Current opinion in immunology* 1999; 11, 443-7.
 50. Werbrouck J, De Ruyck K, Beels L, Vral A, Van Eijkeren M, De Neve W, et al., Prediction of late normal tissue complications in RT treated gynaecological cancer patients: Potential of the gamma-H2AX foci assay and association with chromosomal radiosensitivity. *Oncology Reports* 2010; 23, 571-78.
 51. Brzozowska K, Pinkawa M, Eble MJ, Muller WU, Wojcik A, Kriehuber R, et al., In vivo versus in vitro individual radiosensitivity analysed in healthy donors and in prostate cancer patients with and without severe side effects after radiotherapy. *International Journal of Radiation Biology* 2012; 88, 405-13.
 52. Thierens H, Vral A, Morthier R, Aousalah B, De Ridder L, Cytogenetic monitoring of hospital workers occupationally exposed to ionizing radiation using the micronucleus centromere assay. *Mutagenesis* 2000; 15, 245-49.
 53. Fenech M, Holland N, Chang WP, Zeiger E, Bonassi S, The HUMAN MicroNucleus Project – An international collaborative study on the use of the micronucleus technique for measuring DNA damage in humans. *Mutation Research-Fundamental and Molecular Mechanisms of Mutagenesis* 1999; 428, 271-83.
 54. Fenech M, Morley AA, Cytokinesis-block micronucleus method in human lymphocytes – Effect of in vivo aging and low-dose X-irradiation. *Mutation Research* 1986; 161, 193-98.
 55. Vodicka P, Polivkova Z, Sytarova S, Demova H, Kucerova M, Vodickova L, et al., Chromosomal damage in peripheral blood lymphocytes of newly diagnosed cancer patients and healthy controls. *Carcinogenesis* 2010; 31, 1238-41.
 56. Rached E, Schindler R, Beer KT, Vetterli D, Greiner RH, No predictive value of the micronucleus assay for patients with severe acute reaction of normal tissue after radiotherapy. *Eur J Cancer* 1998; 34, 378-83.
 57. Baeyens A, Claes K, Willems P, De Ruyck K, Thierens H, Vral A, Chromosomal radio sensitivity of breast cancer with a CHEK2 mutation. *Cancer Genet Cytogenet* 2005; 163, 106-12.
 58. Cardinale F, Bruzzi P, Bolognesi C, Role of micronucleus test in predicting breast cancer susceptibility: a systematic review and meta-analysis. *British Journal of Cancer* 2012; 106, 780-90.
 59. Wolff HA, Hennies S, Herrmann MKA, Rave-Frank M, Eickelmann D, Virsik P, et al., Comparison of the Micronucleus and Chromosome Aberration Techniques for the Documentation of Cytogenetic Damage in Radiochemotherapy-Treated Patients with Rectal Cancer. *Strahlenther Onkol* 2011; 187, 52-58.
 60. Wang ZD, Zhang XQ, Du J, Lu X, Wang Y, Tian R, et al., Continuous cytogenetic follow-up, over 5 years, of three individuals accidentally irradiated by a cobalt-60 source. *Mutation Research-Genetic Toxicology and Environmental Mutagenesis* 2015; 779, 1-4.
 61. Liu Q, Cao J, Liu Y, Lu YM, Qin B, Jiang B, et al., Follow-up study by chromosome aberration analysis and micronucleus assays in victims accidentally exposed to Co-60 radiation *Health Phys* 2010; 98, 885-88.
 62. Lee TK, Allison RR, O'Brien KF, Johnke RM, Christie KI, Naves JL, et al., Lymphocyte radiosensitivity correlated with pelvic radiotherapy morbidity. *International Journal of Radiation Oncology Biology Physics* 2003; 57, 222-29.
 63. Ban S, Konomi C, Iwakawa M, Yamada S, Ohno T, Tsuji H, et al., Radiosensitiv-

- ity of peripheral blood lymphocytes obtained from patients with cancers of the breast, head and neck or cervix as determined with a micronucleus assay. *Journal of Radiation Research* 2004; 45, 535-41.
64. Beaton LA, Ferrarotto C, Marro L, Samiee S, Malone S, Grimes S, et al., Chromosome Damage and Cell Proliferation Rates in In Vitro Irradiated Whole Blood as Markers of Late Radiation Toxicity After Radiation Therapy to the Prostate. *International Journal of Radiation Oncology Biology Physics* 2013; 85, 1346-52.
65. Borgmann K, Roper B, Abd El-Awady R, Brackrock S, Bigalke M, Dork T, et al., Indicators of late normal tissue response after radiotherapy for head and neck cancer: fibroblasts, lymphocytes, genetics, DNA repair, and chromosome aberrations. *Radiother Oncol* 2002; 64, 141-52.
66. Barber JBP, Burrill W, Spreadborough AR, Levine E, Warren C, Kiltie AE, et al., Relationship between in vitro chromosomal radiosensitivity of peripheral blood lymphocytes and the expression of normal tissue damage following radiotherapy for breast cancer. *Radiother Oncol* 2000; 55, 179-86.
67. Padjas A, Kedzierawski P, Florek A, Kukulowicz P, Kuszewski T, Gozdz S, et al., Comparative analysis of three functional predictive assays in lymphocytes of patients with breast and gynaecological cancer treated by radiotherapy. *J Contemp Brachytherapy* 2012; 4, 219-26.
68. Sarkaria JN, Busby EC, Tibbetts RS, Roos P, Taya Y, Karnitz LM, et al., Inhibition of ATM and ATR kinase activities by the radiosensitizing agent, caffeine. *Cancer Research* 1999; 59, 4375-82.
69. Busse PM, Bose SK, Jones RW, Tolmach LJ, Action of caffeine on X-irradiated HeLa-cells. 2. Synergistic lethality. *Radiation Research* 1977; 71, 666-77.
70. Pujol M, Puig R, Caballin MR, Barrios L, Barquinero JF, The use of caffeine to assess high dose exposures to ionising radiation by dicentric analysis. *Radiation Protection Dosimetry* 2012; 149, 392-98.
71. Natarajan TG, Ganesan N, Carter-Nolan P, Tucker CA, Shields PG, Adams-Campbell LL, gamma-radiation-induced chromosomal mutagen sensitivity is associated with breast cancer risk in African-American women: Caffeine modulates the outcome of mutagen sensitivity assay. *Cancer Epidemiology Biomarkers & Prevention* 2006; 15, 437-42.



Part 3

General discussion

1 Biological efficiency of different radiation qualities

Technological advances in radiotherapy such as IMRT or IPRT and the use of particle radiotherapy resulted in a maximum dose deposition to the tumor and a reduction of dose to healthy tissue. However, some degree of normal tissue injury is still inevitable. High-LET radiotherapy, using neutrons or carbon ions, provides a successful approach to treat cancer, where cell killing is the main objective. Furthermore, in space travel and airplane traffic, high-LET radiation is critical.

However, high-LET radiation-induced damage seems to induce a different cellular response than low-LET radiation. Reports show that for instance DNA repair pathways, apoptosis and gene expression are activated in a different way by high-LET radiation compared to low-LET radiation (1). This emphasizes the need for further research into the effects of high-LET radiation.

1.1 Fast neutrons

Neutrons can have different energies, ranging from 0.0-0.025 eV (cold neutrons) to more than 200 MeV (ultrafast neutrons) and the ionization density of neutrons varies extensively as a function of neutron energy, hence the RBE of neutrons is dependent on their energy.

Neutrons are used at different radiotherapy facilities around the world among which are Fermilab, Washington University and the Karmanos Cancer Center in the USA, iThemba Labs in South Africa and different centers in Germany, Japan and Russia (2, 3). Furthermore, their energy deposition pattern is comparable to that of carbon ions and as such neutrons can be used as a model system to predict the effects of carbon ion beam radiotherapy (2) (see figure 1.1). Also in space their impact is important, the interactions of charged particles and very high energy γ -rays with the fuselage of the aircraft cause a shower of neutrons of different energies.

In light of the very important issue of the astronaut radiation burden, which is at the moment one of the important restrictions for long time travel in space and the effects of radiotherapy on healthy and cancerous tissue it is important to study the biological effects of neutrons.

All neutron-experiments in this thesis were done in collaboration with iThemba Labs in South Africa. $p(66)+Be(40)$ neutrons were used, which have an energy of 29 MeV and a LET of 20 keV/ μ m. They belong to the so called 'fast neutrons', which range in energy between 15 MeV up to 200 MeV.

In all papers used for this thesis, γ -rays were used as reference radiation. Also in the literature referred to, γ -rays were used as reference radiation unless specifically stated otherwise.

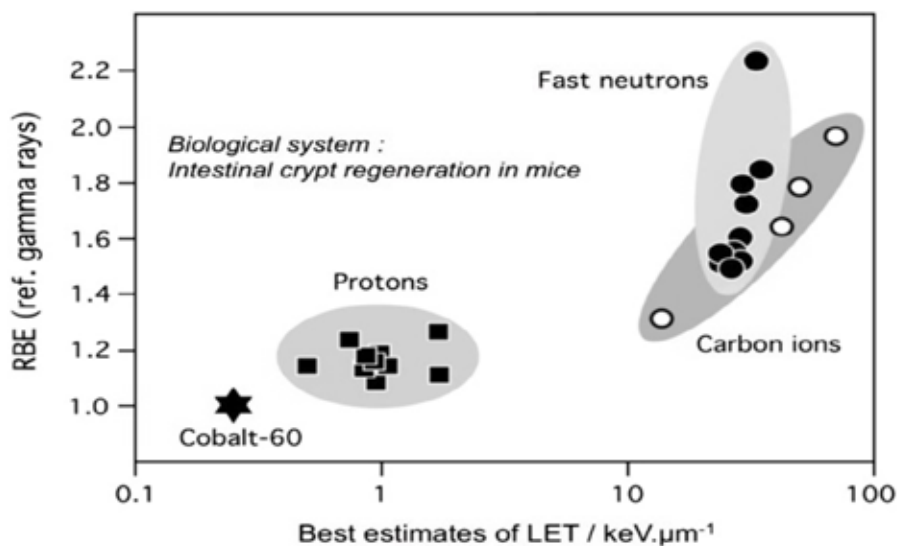


FIGURE 1.1

Variation of the RBE as a function of the LET for different types of clinical radiation beams (2).

1.1.1 Induction and repair of γ H2AX foci induced by fast neutrons

The phosphorylation and dephosphorylation of the histone H2AX is a key process in DNA DSB repair (see introduction 2.3 and 5.1) and immunostaining of γ H2AX can be used to quantify the number of DNA DSB.

In our study performed on lymphocytes (article 1), we found an RBE_M value, which is the maximal RBE and is found by extrapolation of the low-dose behavior to zero, for the induction of γ H2AX foci of 0.70 (4). No other reports on foci induction by fast neutrons have been published. Antonelli et al found a comparable RBE-value for γ H2AX induction in human foreskin fibroblasts (HFF) after irradiation with carbon ions (5). This fits well with the reports stating that carbon ions have a comparable energy deposition pattern as neutrons (see figure 1.1) (2).

Our results are in accordance with other studies that report that high-LET RBE values, based on DSB induction, are equal or lower than unity (6-12).

Studies investigating the γ H2AX foci showed that high-LET radiation-induced foci are larger and have a higher staining intensity than low-LET radiation-induced foci (5, 6, 12). Furthermore, high-LET radiation-induced foci increase in size up to 2h after induction, while low-LET radiation-induced foci remain constant in size (12).

The high ionization density of neutrons and other high-LET radiation qualities produces ‘complex damage sites’ (13), which can consist of base lesions, SSB and DSB in very close proximity (14-20). These complex damage sites can also contain multiple DSB (21). This can explain why the RBE for high-LET radiation is equal or lower than unity. Furthermore, the high-LET induced foci are larger, which can be caused by a merger of different foci into DNA repair centers (22-25), or the large foci can consist of different smaller foci, which overlap and visually form one focus (5, 12, 23). The large foci which merge or overlap can also explain the low RBE values.

In article 1 we found that the foci induced by neutrons disappeared slower than those induced by γ -rays. Less foci were induced 30 minutes following irradiation by neutrons compared to γ -rays, however, 4 hours after irradiation, the number of foci was the same irrespective of the radiation quality. At later time-points after irradiation, the number of foci remained higher after neutron irradiation compared to γ -irradiation. 24h after irradiation 25% of the neutron-induced foci were persistent compared to 12% of the γ -induced foci (4). These results are very similar to the results published for carbon ions (5), where a slower repair and higher number of resistant foci after 24h were also noted.

In literature it has been reported that high-LET radiation-induced foci disappear much slower than low-LET induced foci (4, 5, 26). 4 to 24 hours after irradiation, a higher number of repair-foci can be found after high-LET irradiation compared to lower LET radiation (7, 26-28) and the complex damage sites containing DSB, single strand breaks and base damage in very close proximity, result in the most persistent foci (29). Also other assays based on the number of DSB, such as pulsed field gel electrophoresis (PFGE) and PCC, confirm that high-LET radiation-induced DSB disappear with slower kinetics compared to low-LET induced DSB (30-34). The slower rate of disappearance and the fact that the most persistent foci contain the most complex damage sites, indicate that the large and more intensely stained foci are indicative of complex breaks rather than a visual overlap of smaller foci.

1.1.2 Chromosomal aberrations (MN-assay) and cell proliferation (CV cell proliferation assay)

Misrepaired or unrepaired DSB can lead to chromosomal aberrations, which in turn can underlie tumorigenesis and cell death. Assays based on chromosomal aberrations, like the micronucleus assay, translocation or dicentric assay, are good biomarkers for radiation exposure and cancer risk assessment (35-39).

With the MN assay we found an RBE_M of 3.9 in lymphocytes irradiated with neutrons in the G0 phase of the cell cycle (Article 1). In article 2 we used mammary epithelial cells (MCF-10A cells) which were synchronized in the G1 phase of the cell cycle and found an RBE_M value of 4.90 for

CON_{BRCA} and 6.9 for CON_{Ku70}¹. These values are in good agreement with the values of 4.8 and 5.3 found for the *in vitro* irradiation of lymphocytes reported by Slabbert et al with the same neutron beam (40, 41). Vral et al reported an RBE_M of 7.6 in G0 lymphocytes irradiated with 5 MeV neutrons (42). Our reported RBE_M-values in lymphocytes are lower, which can be due to the higher energy of the neutrons used in this study (29 MeV) and are in agreement with what is reported by the ICRP (43).

The RBE_M values obtained with the CV cell proliferation assay on MCF-10A cells synchronized in G1 (RBE_M 2.52 and 2.45; article 2) are lower than those obtained with the MN assay. This can be explained by the fact that different end-points are considered: the MN assay focuses specifically on chromosomal aberrations, while the crystal violet proliferation assay focuses on the ability of the cells to proliferate. In general, RBE_M values based on chromosomal aberration results are systematically higher than those based on cell proliferation assays.

Assays based on chromosomal aberrations, like the micronucleus assay, translocation or dicentric assay, show an incline in RBE value consistent with rising LET-values for high-LET radiation up to approximately 100 -200 keV/μm (44), at higher LET the RBE will drop again due to overkill. The value of 100-200 keV/μm is however dependent on the cell type and end point used, and can be higher for more radioresistant cells (45).

From the data above, it is clear that, compared to γ-rays, fast neutrons induce a lower number of DSB γH2AX foci (RBE <1) which result in a higher number of chromosomal aberrations (RBE_{MN} >4), due to mis- or nonrepaired DSB. The complex damage sites induced by the neutrons are more difficult for the cell to process correctly and each neutron-induced focus will give rise to more chromosomal aberrations than each γ-induced focus (see figure 1.2). Different suggestions why these clustered lesions are more difficult to repair have been put forward in the literature. The closer spatial distribution of the DSB makes it more likely for break-termini to be reattached wrongly (46, 47). Furthermore, the complexity of the damage delays the processing of the base damage and single strand breaks and leads to conformational changes in the DNA which seem to interfere with the ability of the repair proteins to bind (29, 48-50). It has been suggested that unrepaired clusters of non-DSB DNA damage may generate additional DSB, which can, if unrepaired, lead to even more mutations and chromosome abnormalities (51, 52). The slower repair might furthermore aggravate the possibility of misrepair, the longer a break-end stays open, the longer they are reactive and available for misrepair (53).

¹ CONBRCA and CONKU70 are two mock-transduced MCF-10A cell lines which are used as control cell lines. For further information, see article 2.

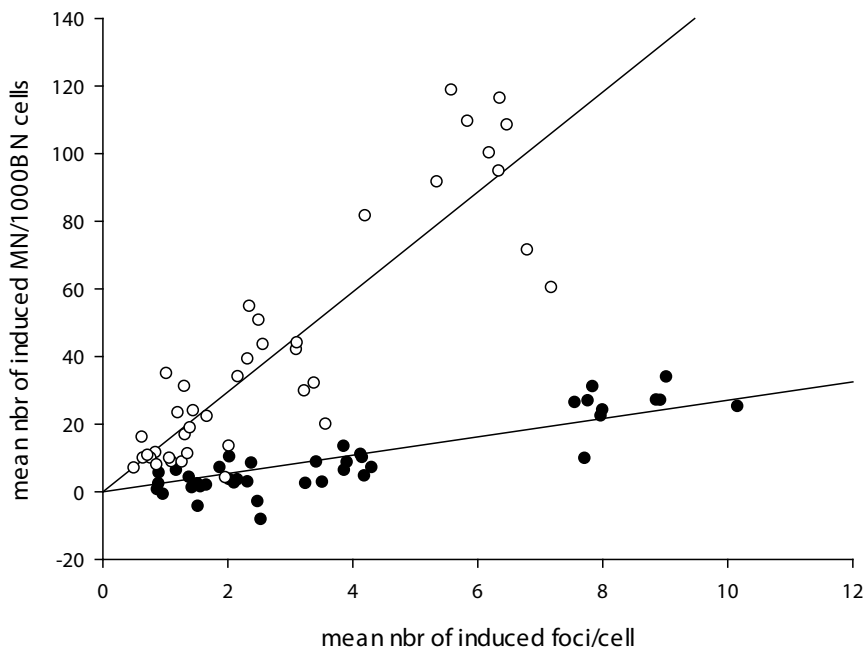


FIGURE 1.2

Radiation-induced MN as a function of radiation-induced γ H2AX-foci (30' after irradiation) for neutrons (○) and γ -rays (●).

Figure based on data obtained in article 1.

1.2 Mammography X-rays

1.2.1 RBE of mammography X-rays

30kV X-rays (mammography X-rays) are considered low-LET radiation and the International Commission on Radiological Protection (ICRP) still recommends the use of radiation weighting factor of 1 for mammography X-rays (54). However, there is general consensus that they are qualitatively different from γ -radiation. Mammography X-rays are low-energy X-rays with a peak and mean photon energy of typically 28-30 keV and 15-20 keV, compared to ^{60}Co γ -rays which have a high energy of approximately 1.25 MeV. Their low energy causes them to lose their energy rapidly, resulting in a denser ionization pattern (LET 4.34 keV/ μm) compared to ^{60}Co γ -rays (LET 0.3 keV/ μm) and to a certain extent they can be compared with high-LET radiation qualities.

In light of mammography-screening programs, in which a large group of asymptomatic women receive periodically small doses of radiation to the breast, it is important to demonstrate that the benefits, arising from reduced mortality due to early diagnosis exceeds to a large extent any potential risk arising from future radiation-induced breast cancers. Although there are several ways to assess benefit/risk ratios, a simplified approach is to calculate the breast cancer detection over induction ratio (DIR). These calculations are essentially based on performance data of breast screening programs, breast radiation doses and cancer induction risk factors (54-56). Although such calculation models are subject to a certain degree of statistical uncertainty, they can be used to assess benefit/risk taking into account that the number of breast cancers detected must exceed the number of induced cancers to a significant extent. Since DIR-values are used to justify low doses of low energy radiation exposures to a large asymptomatic population it is necessary to have a correct estimation of the RBE of 30 kV X-rays, since this is used for the calculation of the cancer induction risk.

In article 3 we studied the RBE of mammography X-rays in lymphocytes and found an RBE-value for the induction of γ H2AX foci of 1.36 (57). In our study on mammary epithelial cells present in breast tissue (article 4) we found an RBE of 1.2 (58). These RBE values are in agreement with literature, where RBE values between 1.1 and 1.4 with γ -rays as reference radiation have been published (59, 60). They are also in the same range as theoretical calculations and simulations, which point to an RBE between 1.3 and less than 2 (61-63). It seems that mammography X-rays are slightly more efficient in inducing DSB than γ -rays.

In light of differences in radiosensitivity between tissues, we studied the RBE of mammography X-rays in mammary epithelial cells present in dissected breast tissue (article 4). It is interesting to confirm that the RBE values which have been obtained in human fibroblasts, peripheral blood lymphocytes and MCF-10A's, are in line with the RBE-value of 1.2 that we found for DSB-induction in ex vivo irradiated breast tissue (58).

RBE values between 1.2 and 1.4 for foci induction by 30kV X-rays seems to be in contradiction with the $RBE_{foci} < 1$ after high-LET radiation. However, while the LET of 30 kV X-rays is higher than the LET of γ -rays (respectively 4.3 and 0.3 keV/ μ m), it is considered low-LET and its LET is considerably lower than the LET of e.g. neutrons (20keV/ μ m) (see introduction table 1.1 for more examples of high and low-LET values).

Compared to γ -rays, 30kV X-rays will produce ionization tracks which are more dense, by which the chance of one ionization track producing two or more SSB in close proximity leading to a DSB is higher compared to γ -rays (17). The density of the ionization tracks is however not high enough

to induce the complex damaged sites and related RBE values lower than unity as are obtained with high-LET radiation.

Furthermore, for a given number of DSB induced by 30 kV X-rays or γ -rays a higher number of MN was obtained after irradiation with 30 kV X-rays compared to ^{60}Co γ -rays (see figure 1.3). This implies that mammography X-rays not only induce more DSB compared to γ -rays but also that DSB arising from 30 kV X-rays are more difficult to repair, probably because of the density of the ionizations (57). This resulted in a higher RBE_M -value of 4 for MN induction in lymphocytes.

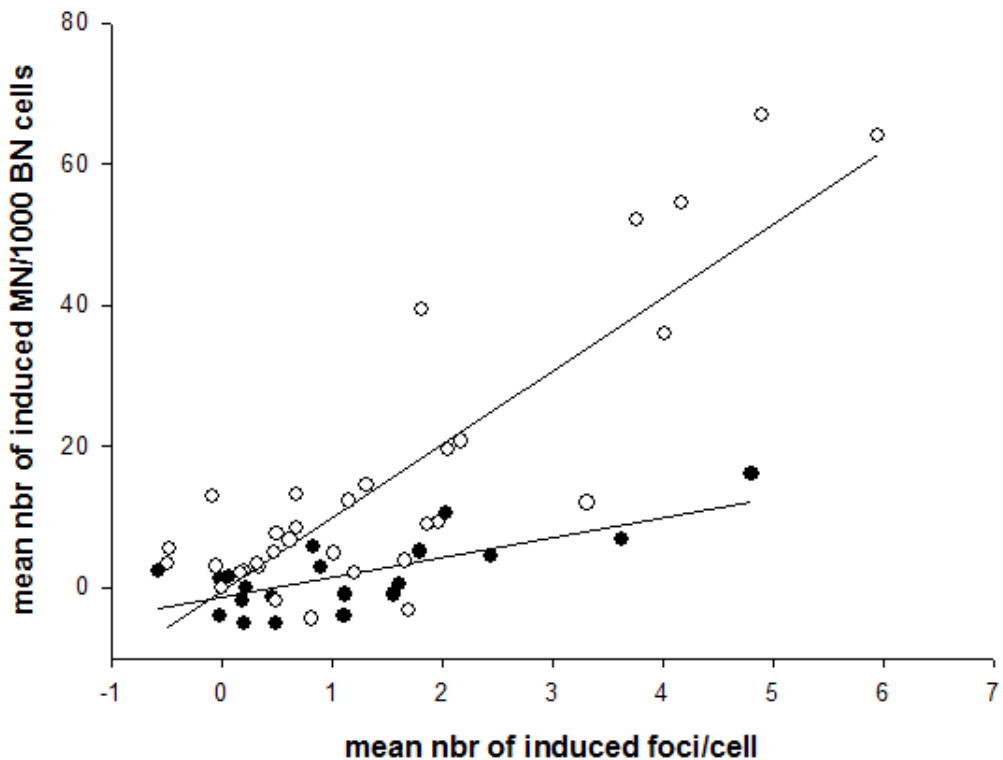


FIGURE 1.3

Radiation-induced MN as a function of radiation-induced γH2AX -foci for 30 kV X-rays (○) and γ -rays (●). Figure from article 3.

Although different studies investigating the RBE of low energy X-rays by means of cytogenetic assays and neoplastic transformation have been published, comparison is difficult due to differences in the physical characteristics and energies (25-50kV) of the X-rays, the reference radiation quality, the cell type and cytogenetic assay used. Especially the quality of the reference radiation seems to play a big role in assessing the RBE value and can explain the apparent discrepancy between sets of RBE_M values. For instance, with the dicentric assay an RBE_M value of 2.1 has been reported for 220 kV X-rays using γ -rays as reference radiation (64).

Using 200 kV X-rays as reference radiation, RBE_M values for 30kV X-rays vary from 1.2 to 1.7 with MN or dicentrics as endpoint (65-68). RBE_M values ranging between 2 and 6 were found for MN or dicentrics when ^{60}Co γ -rays were used as reference (57, 69, 70).

When neoplastic transformation in CGL1-cells (HeLa X skin fibroblast, non-tumorigenic (71)) is used as end-point for RBE calculation, the RBE values are situated between 3.6 and approximately 8 and situate mostly around 4.4 (72-75).

The above mentioned studies have been performed on CGL1 cells, lymphocytes, fibroblasts and keratinocytes and to our knowledge, no studies on the efficiency of mammography X-rays to induce chromosomal aberrations are performed using mammary epithelial cells, like MCF-10A cells, isolated and cultured mammary epithelial cells or even epithelial cells in breast tissue. Colin et al performed an adapted MN assay on isolated and cultured breast epithelial cells (76), however the MN assay used in this study contained no cytokinesis-block and cannot be compared to the classical MN assay. Furthermore, no reference radiation was used, so the results cannot be used for RBE calculation.

1.2.2 RBE of mammography X-rays after very low dose irradiation

Most of the mammography RBE-studies quoted are based on experiments in the dose-range 0.1 or 0.5 Gy to 4 or 5 Gy. However, during a mammography screening the average dose delivered to the breast tissue is typically 3-4 mGy. Mammographic screening, with a bi-annual mammogram with two projections, for women aging between 50 and 70 years, would deliver a total cumulative dose of 30-40 mGy to the breast.

While there seems to be convincing evidence for the presence of an increased $RBE_{\text{chrom ab}}$ between 3 and 4 in the 0.1-4Gy dose range, the question is if this can be extrapolated by the LNT model to the very low dose range. As the low-dose threshold for detection of chromosomal aberrations is around 0.05-0.1Gy, information can best be obtained by analyzing the induction and disappearance of DNA repair foci. The γH2AX foci assay is sensitive enough to visualize the induction of DSB following doses of a few mGy. Furthermore, as discussed above, the repair kinetics of γH2AX foci and the number of persistence foci show a clear link to the complexity of the DSB. This gives information on how difficult it will be for the cell to repair the DSB correctly.

In our study on the RBE of mammography X-rays on breast tissue (article 4) (58), we found a low-dose hypersensitive response to 30kV X-rays in the dose range 0 to 20 mGy with the γ H2AX foci-assay. Following irradiation with γ -rays, this hypersensitive response was absent and a linear regression over the complete dose range seemed the most appropriate way to describe the data. This led to an increase in RBE-value from 1.0 in the dose range 20 to 500 mGy to 3.7 in the 0-40 mGy dose range.

A very similar low-dose hypersensitive response was described by Beels et al after exposure of lymphocytes to X-rays in the 0 to 10 mGy dose range (77, 78). The hypersensitive response described by Beels et al was less pronounced when γ -rays were used instead of X-rays and when lymphocytes were isolated, pointing to the importance of radiation quality and cellular environment. A strong link between the low-dose hypersensitive response and cell culture conditions was also reported by Groesser et al (79).

Mills et al on the other hand, did not find a significant difference in number of foci after γ -irradiation or 30 kV X-ray irradiation in the 0 to 30 mGy dose range and calculated an RBE value of only 1.1 (60).

At low doses, phenomena such as bystander effect, adaptive response, threshold hypothesis and hormesis response play a role (80-82) (see introduction 1.4). The low-dose hypersensitive response observed in mammary epithelial cells in breast tissue (article 4) is probably caused by the bystander effect. The irradiated epithelial cells of the mammary glands present in the connective tissue of the breast will propagate signaling molecules to neighboring cells via GAP-junction mediated signal transduction and via the release of diffusible factors into the extracellular environment. The different cellular context and cellular environment might explain the different results found in our study on mammary epithelial cells in breast tissue and the study of Mills where a cell line of mammary epithelial cells (MCF-10A) grown in monolayer was used. Furthermore, the cells of Mills et al were irradiated at 0°C and kept at that temperature some time before and after irradiation. Hypothermia has a radioprotective effect and can have an influence on cellular communication (83).

It is interesting to note here that at higher doses the same biological effects of 30 kV X-rays were observed over a wide range of cell types. At very low doses however, tissue-effects, cellular communication and cellular environment start to play a role and the biological effects observed might differ strongly from cell-type to cell-type. This should be kept in mind when performing further studies on the very low-dose effects of 30kV X-rays.

There have been studies which report that a certain threshold of stress or damage needs to be surpassed before efficient repair takes place. DSB induced by very low doses, such as those used in mammography screening, might not trigger the repair response, repair is slower and foci persist for days after induction (84, 85). This has been contradicted by Asaithamby who did see efficient repair at a dose of 5mGy (86). However Asaithamby used γ -rays while Rothkamm and Grudzenski used 90 kV X-rays and again, differences in LET might have a significant impact on the results. Using 30kV X-rays, Mills et al found a reduction in the number of repair-foci measured 4h after irradiation compared to 1h after a dose of 30mGy, showing that repair did start. However, a significantly higher percentage of persistent foci was found in the samples irradiated with 30mGy of mammography X-rays compared to γ -rays (60). Colin et al also reported persistent foci after very low doses of 30kV X-rays (2, 4 and 2+2 mGy), however, since no results for γ irradiation are given, no comparison is possible (76).

How these very low-dose effects affect the formation of chromosomal aberrations and neoplastic transformation is difficult to assess. We found a threshold detection dose of 50mGy for the induction of centromere-negative MN after irradiating lymphocytes with 30 kV X-rays (article 3). No studies have been published on MN or dicentric formation in the region 0 to 30mGy after irradiation with mammography X-rays.

Certain characteristics found in foci induced by high doses of 30kV X-rays, such as higher intensity and slower repair of the foci, are also found in foci induced by very low doses (60). This suggests that the DSB induced by low-doses might be handled by the cell in more or less the same way as DSB induced by higher doses and a higher $RBE_{\text{chrom ab}}$ compared to $RBE_{\text{foci ind}}$ can also be expected in the low-dose region. Furthermore, we found a low-dose hypersensitivity for DSB induction in breast epithelial cells in breast tissue irradiated by very low doses of 30kV X-rays, indicating that more DSB were induced than would be assumed by the LNT model and in turn even more chromosomal aberrations can be expected.

While more research is needed to clarify all these results and solve the inconsistencies, we think that the high dose $RBE_{\text{chrom ab}}$ of 3-4 for mammography X-rays can be extrapolated to the low dose range and might even be higher in the very low-dose range due to the bystander effect.

Applying an RBE of 3 to the detection over induction ratio (DIR) of mammography screening programs as they exist today in Belgium would result in a drop of the DIR from 180 to 60 and the use of mammography as a screening tool is still justified (55, 56, 87, 88). But our results do warn for expanding those programs to younger age-groups. Younger women are more radiosensitive

with respect to cancer and need higher doses due to denser breast tissue. If the age group between 40 and 49 would be included in the current screening program of the Flemish community, the DIR for that age group would drop from 52 to 17 if we apply our RBE of 3 (personal communication Prof dr. H. Thierens).

In the case of women with an increased risk to develop breast cancer due to a mutation in a breast cancer predisposing gene the benefit /risk ratio of mammography screening is even more disputable as most of the known breast cancer genes (*BRCA1*, *BRCA2*, *ATM*, *CHEK2*, *PALB2*, etc) are all involved in the DNA damage response pathway activated by DSB. Mutations in these genes may not only contribute to genomic instability and cancer but also to a radiosensitive phenotype, increasing the carcinogenic risk of mammography screening in mutation carriers (87-90) (see discussion chapter 2.3)

1.3 Cell cycle dependence of RBE

The radiosensitivity of the cell is heavily dependent on the cell cycle, since cell cycle phase influences the DSB repair pathways which are available for the cell. Furthermore, the radiation quality plays an important role. High-LET radiation will induce more complex damage compared to low-LET. These complex damage sites are difficult to repair accurately by NHEJ, particularly when there is loss of nucleotides as NHEJ cannot restore genetic information. HR on the other hand can repair complex damage sites more efficiently, but is not active in G0/G1. As a result, high-LET radiation will be more efficient in inducing chromosomal aberrations in G0/G1.

In the MCF-10A control cell lines (CON_{BRCA}^2 and CON_{KU70}) used in article 2 we found the described pattern of changes in inherent radiosensitivity, represented by the α -value of the MN-dose response curve. The cells showed an increased radiosensitivity to high-LET radiation in G1 compared to S and G2. Irradiation of CON_{BRCA} and CON_{KU70} in the mixed cell cultures and in the cell cultures synchronized in G1 with γ -rays didn't induce any significant differences in α -value (see squares in figure 1.4). However, when they were irradiated with high-LET neutrons the sensitivity increased significantly more in the synchronized G1 cell cultures compared to the mixed cultures (see resp. open and black triangles in figure 1.4).

These differences in cellular radiosensitivity during the cell cycle affect the RBE_M . At low dose the high sensitivity of the G1 cells irradiated by neutrons translates in much higher RBE_M values ($RBE_{CONBRCA}$ 4.9 and $RBE_{CONKU70}$ 6.9) compared to the cells irradiated as mixed cultures ($RBE_{CONBRCA}$ 2.8 and $RBE_{CONKU70}$ 3.4). At higher doses (2-5Gy) the RBE values drop and are very similar for the mixed and the synchronized G1 cultures (RBE_{2Gy} is on average 1.83) (see figure 1.5). This is caused by the influence of the β -value of the dose-response curve following γ -irradiation at

high doses. This β -value, representing the repair-component in the dose-response, and makes the cells relatively more radiosensitive to low-LET radiation at higher doses compared to low doses (see figure 1.6) which is caused by an increase in complexity of the damage induced by low-LET radiation when the dose increases.

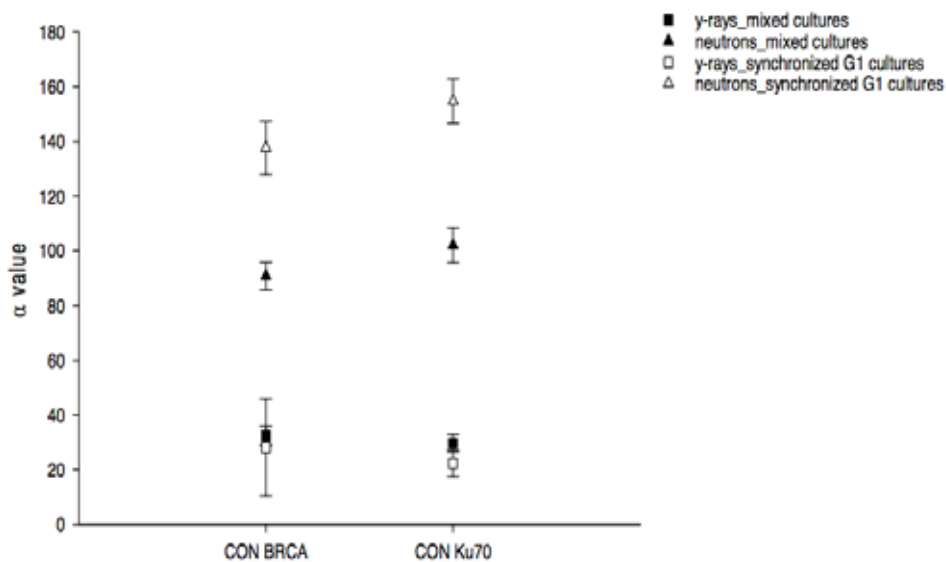


FIGURE 1.4

Changes in cellular radiosensitivity, represented by the α -value of the MN dose response, following γ -radiation and neutron radiation in cell cultures synchronized in G1 and in mixed cell cultures. Figure based on data obtained in article 2.

² CON_{BRCA} and CON_{Ku70} are two mock-transduced MCF-10A cell lines which are used as control cell lines.

³ The response curve for chromosomal aberrations is linear-quadratic. α describes the linear component and is a measure for inherent radiosensitivity of the cell. β describes the quadratic component and is a measure for the repair-capacity of the cell. More information can be found in figure 1.6 and in the introduction chapter 1

⁴ The MCF-10A cells were irradiated (i) as exponentially growing cell cultures, which contained cells from G1 (37%), G2 (25%), S (39%) (called 'mixed cultures') and (ii) as cultures synchronized in G1 (86% G1 cells) before irradiation. For further information, see article 2.

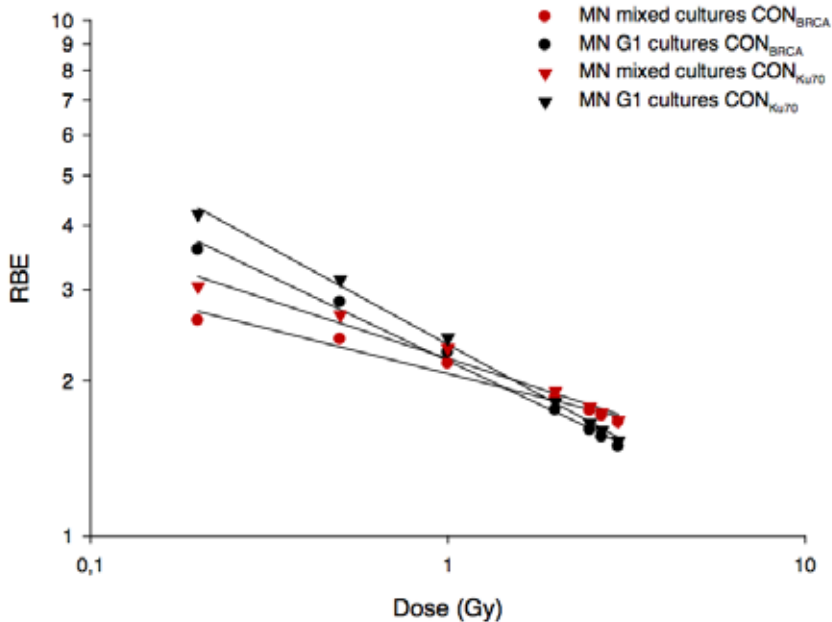


FIGURE 1.5

RBE of fast neutrons at different doses following irradiation of mixed and synchronized G1 cells. Figure based on data obtained in article 2.

1.4 Influence of LET on DSB repair pathway choice and cellular radiosensitivity

In the introduction we already discussed that DSB repair pathway choice is an interplay between different factors among which cell cycle phase is the most important. The complexity of the DSB, which will increase with increasing LET of the radiation quality, can also influence repair pathway choice and as a consequence cellular radiosensitivity.

To investigate the influence of cell cycle phase and LET on DSB repair pathway choice, we developed MCF-10A cell lines containing a knock-down for DSB repair proteins and irradiated these cell lines with γ -rays and neutrons in different phases of the cell cycle.

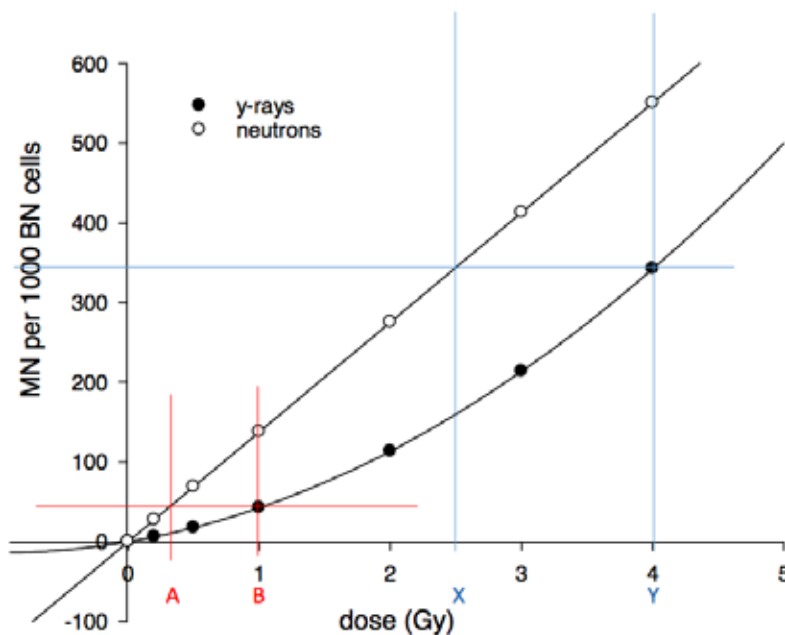


FIGURE 1.6

Dose response curve for induction of micronuclei in the CONBRCA cell line (cells synchronized in G1), following low and high-LET irradiation. The blue lines represent an RBE at high dose ($=Y/X$), the red lines at low dose ($=B/A$). For more information, see introduction chapter 1. Figure based on data obtained in article 2.

A knockdown cell line was made for:

- Ku70 (called Ku70i) a protein which is important in NHEJ
- BRCA1 (called BRCA1i) a protein which is important in NHEJ and HR
- BRCA2 (called BRCA2i) a protein which is important in HR

Furthermore, two mock-transduced cell lines (CON_{BRCA} and CON_{Ku70}) were used as control lines. All cell lines were irradiated as exponentially growing cell cultures, which contained cells from G1 (37%), G2 (25%) and S (39%) phase (called ‘mixed cultures’), and as cultures synchronized in G1 (86% G1 cells; called ‘synchronized G1 cultures’) before irradiation. For further information, see article 2.

1.4.1 Cell cycle and DNA DSB repair (see figure 1.6)

To investigate the importance of HR and NHEJ in different phases of the cell cycle, the knock-down cell lines were irradiated as mixed and synchronized G1 cultures with γ -rays. The change in radiosensitivity was analyzed by comparing the α -values, a measure of inherent cellular radiosensitivity, of the knockdown cell lines with the α -values of the control cell lines (figure 1.7 and table 1.1).

Compared to the control cell lines, **BRCA2i cells** (\blacktriangle), deficient in HR which is not active in G0/G1, showed no increased radiosensitivity in the synchronized G1 cultures and a significant increase in radiosensitivity in the mixed cell cultures compared to the control cell lines ($2.3 \times \alpha_{\text{CON}}$: 2.3 fold increase of α -value). The latter can be explained by the importance of the HR pathway in the late S and G2 stage.

The **Ku70i cells** (\blacksquare) on the other hand, showed an increase in radiosensitivity after irradiation of both the synchronized G1 cells ($1.9 \times \alpha_{\text{CON}}$) and mixed cells ($3.5 \times \alpha_{\text{CON}}$). This is consistent with the role of Ku70 in NHEJ which is active throughout the cell cycle.

BRCA1 plays a role in both HR and NHEJ. For the **BRCA1i cells** (\blacktriangledown) synchronized in G1, no MN-results could be obtained due to lack of BN-cells. The cells were probably too radiosensitive and underwent cell cycle arrest. The cells irradiated as mixed cultures showed a large increase in sensitivity ($5.8 \times \alpha_{\text{CON}}$) compared to the control cell lines.

These results are in line with the results of Hinz et al who showed that, compared to wild type cells, HR deficient CHO cells are increasingly radiosensitive as they progress through S and G2/M phase. NHEJ deficient CHO cells on the other hand, are clearly more radiosensitive than wild type (WT) cells, but they show the same pattern of radiosensitivity as WT cells as they progress through the cell cycle (91, 92).

While direct comparison of the knockdown cell lines is not possible due to differences in protein-knockdown, BRCA2i shows a tendency to be the least radiosensitive of the three knock-down cell lines and BRCA1i the most radiosensitive one. Overall our results show that both NHEJ and HR deficiency result in increased cellular radiosensitivity and that this is more pronounced after abrogation of NHEJ. A defect in a gene involved in both NHEJ and HR seems to give a cumulative effect, resulting in very sensitive cells. Furthermore, these results confirm that NHEJ plays a major role throughout the cell cycle. HR on the other hand is not involved in repair of DSB in G0/G1.

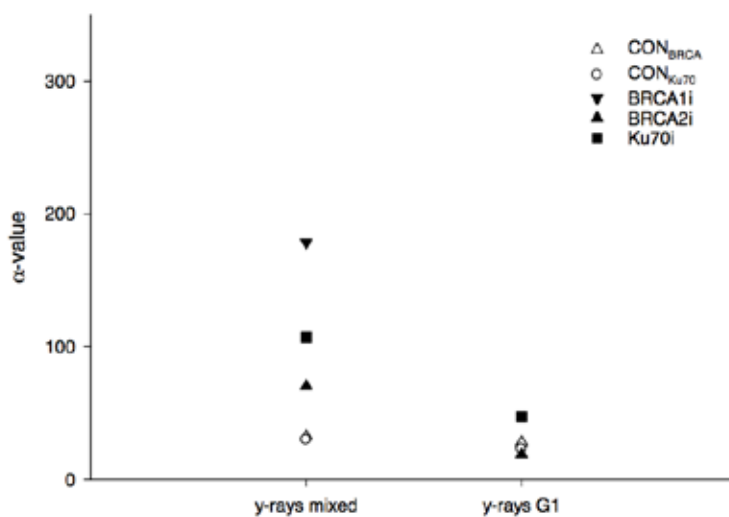


FIGURE 1.7

Changes in inherent sensitivity, represented by the α -value, of control cell lines and knockdown cell lines, following γ -radiation in cell cultures synchronized in G1 and in mixed cell cultures.

		α_{γ}	$\times \alpha_{\text{CON}}$	α_{neutr}	$\times \alpha_{\text{CON}}$	RBE_{M}	$\text{RBE}_{2\text{Gy}}$
mixed cell cultures	CON	31	1.0	96	1.0	3.1	1.9
	BRCA1i	179	5.8	309	3.2	1.7	1.7
	BRCA2i	70	2.3	221	2.3	3.1	1.8
	Ku70i	107	3.5	269	2.8	2.5	1.7
synchr. G1 cell cultures	CON	25	1.0	146	1.0	5.9	1.8
	BRCA1i						
	BRCA2i	19	0.8	136	0.9	7.2	1.5
	Ku70i	47	1.9	200	1.4	4.2	2.1

TABLE 1.1

Overview of the α -values, the fold increase compared to the control cell line ($\times \alpha_{\text{CON}}$), the RBE_{M} , and the RBE at 2 Gy ($\text{RBE}_{2\text{Gy}}$) for the control cell line (CON: average of CON_{BRCA} and CON_{KU70}) and the repair-deficient cell lines.

1.4.2 Effect of LET in DSB repair deficient cells

To investigate the importance of LET on HR and NHEJ in different phases of the cell cycle, the mixed and synchronized G1 cultures of the control cell lines and knockdown cell lines were also irradiated with fast neutrons.

Analogous to what we observed for low-LET radiation, the mixed cultures of **BRCA2i** cells showed an increased sensitivity after neutron-irradiation compared to the control cell lines. For G1 synchronized cultures no differences in sensitivity were observed between the BRCA2 repair deficient and control cell lines (figure 1.8).

The **Ku70i** cells showed an increase in α -value after neutron-irradiation of both the mixed and the synchronized G1 cultures compared to the control cell line (figure 1.8).

As mentioned previously the **BRCA1i** cells didn't divide after irradiation of the synchronized G1 cells, probably related to the highly increased radiosensitivity and no MN results were available. The mixed cultures of BRCA1i cells also showed a highly increased radiosensitivity after neutron irradiation in comparison with the control cell lines (figure 1.8).

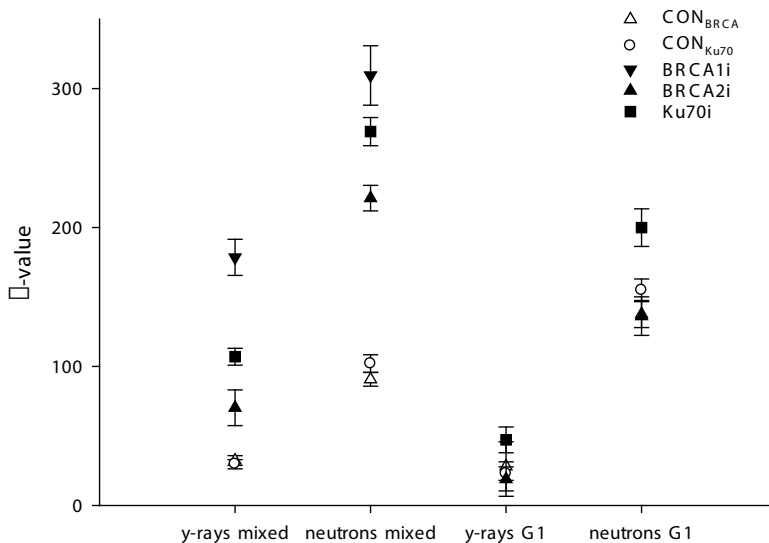


FIGURE 1.8

Changes in inherent sensitivity, represented by the α -value, of control cell lines and knockdown cells lines, following γ -radiation and neutron-irradiation in cell cultures synchronized in G1 and in mixed cell cultures. Figure based on data obtained in article 2.

From the different inherent radiosensitivities (represented by the α -values) after neutron and γ -irradiation of the synchronized G1 and mixed cells, the RBE_M values can be calculated (Table 1.1).

In the **mixed cultures** the highest RBE_M values are observed for the control cell lines and the BRCA2i cell line. The RBE_M values of the Ku70i cell line is lower and the BRCA1i cells represent the lowest RBE_M values. In literature an analogous pattern has been described for mixed cultures of CHO, DT40 and MEF cells. High-LET radiation shows an increased efficiency to induce DNA damage with increasing LET in wild type and HR-deficient cells compared to low-LET radiation (93). This causes an increase in RBE-values with increasing LET till 100-200 keV/ μ m in wild type and HR deficient cell types (see figure 1.9) (94). The efficiency to induce DNA damage in NHEJ deficient and NHEJ+HR deficient cells is highly increased after both γ and neutron irradiation and as a result RBE-values are close to unity (see figure 1.9 and table 1.1) (94-98).

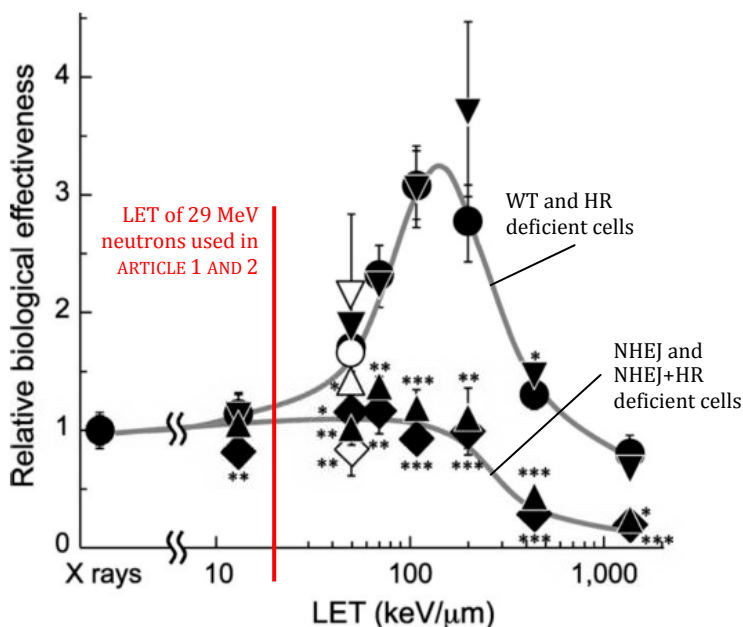


FIGURE 1.9

RBE_M values for 10% survival for different LET values in NHEJ and/or HR deficient cells. ● : wild type cells; ▲ : Lig4 knock-out cells (NHEJ deficient); ▼ : Rad54 knock-out cells (HR deficient); ◆ : double knock-out cells (deficient in NHEJ and HR). Figure adapted from (94).

Our RBE_M values for the NHEJ and NHEJ+HR knockdown cell lines on the other hand, are higher than unity. Differences in inherent radiosensitivity between the MCF-10A cells and the CHO, DT40 or MEF cells used in most studies can be an explanation. Furthermore, our cell lines have approximately a 50% knock-down of the repair-proteins, where in most studies the cell lines have a much higher knock-down. Also, the knock-downs in other papers are for different repair proteins (e.g. Lig4, Rad54, DNA-PKcs, XRCC4, XRCC3) which can lead to a stronger abrogation of the targeted repair pathway.

In the cells **synchronized in G1** RBE_M values are higher compared to the RBE_M values calculated for the mixed cultures (see table 1.1). This implies that our synchronized G1 cells are more sensitive than the mixed cultures to neutrons and confirms the general picture of HR having a more important role in the error-free repair of complex damage sites and only being available in S and G2 phase.

2 Radiosensitivity in relation to breast cancer treatment and diagnostics

The fact that there are inter-individual differences in clinical radiosensitivity was already noted shortly after the discovery of X-rays (99-101). It took however till 1956 and the introduction of the *in vitro* clonogenic assay before real research on the subject began (102, 103). Further development of molecular, cytogenetic, genomic and cellular assays confirmed the existence of a large and continuous spectrum of individual radiosensitivity (99).

On one side of the spectrum there are extremely radiosensitive patients related to genetic syndromes, such as patients with ataxia telangiectasia (AT) (104, 105), Nijmegen breakage syndrome (NBS) (106) or severe combined immunodeficiency (SCID) (107-109). A less severe form of radiosensitivity can be found in patients with e.g. a biallelic mutation in some of the genes from the FANC-group (especially *FANC-D2*) (110, 111) or patients with e.g. Cornelia de Lange syndrome (112). However, most individuals only show a slight increase or decrease in radiosensitivity when subjected to the standard radiosensitivity tests, but these marginal changes can be translated in an enhanced susceptibility to radiation-induced carcinogenesis or the development of severe radiotoxic reactions following radiation exposure.

2.1 Risks of late radiotoxic reactions following radiotherapy for breast cancer

The use of radiotherapy reduces the risk of local-regional recurrence of breast cancer and improves the overall survival of breast cancer patients after breast-conserving surgery or mastectomy (113, 114). However, some patients will develop adverse effects following radiotherapy. These effects range from acute (within 6 months after starting radiotherapy) to late (after six months of starting radiotherapy) toxic effects, with a second, radiation induced cancer considered as a very late effect (115) (see introduction chapter 3).

Severe late toxic effects occur in approximately 5 to 10% of the breast cancer patients receiving radiotherapy, mostly in the tissue surrounding the tumor which received the highest dose.

Several studies have reported an increase in risk of a secondary primary cancer of the breast, colorectal, endometrial or ovarian cancer after treatment for breast cancer (116-124). A genetic predisposition or lifestyle factors could be the cause of both primary and secondary cancer, especially in the case of contralateral breast cancer (125-127), but the increased risk for a second primary cancer could also be the consequence of the treatment of the first cancer, such as the development of leukemia after chemotherapy (128) and sarcomas (129) or lung cancer after radiotherapy (130).

Often the risk of a new primary cancer is studied by the occurrence of contralateral breast cancer five to fifteen years after treatment for breast cancer. The dose received by the contralateral breast during conventional radiotherapy treatment for breast cancer lies between 0.5 and 3Gy (131), although older studies mention doses up to 7Gy (132). The risk of contralateral breast cancer as a result of radiotherapy is small and is dependent on the dose received by the contralateral breast and the age of the patient. The EBCTCG meta-analysis estimated an absolute risk of 4.4% in 15 years, resulting in a relative risk of 1.09 in patients under 50 and 1.25 in patients older than 50 years (133). Other cohort or case-control studies estimate the risk higher and relative risks between 2 and 3 for young patients (<40) or high breast doses (>4Gy) have been reported (131, 132, 134-137).

2.2 Radiosensitivity amongst breast cancer patients

A significant proportion of cancer patients shows an enhanced chromosomal radiosensitivity. This increased sensitivity has been confirmed in several studies (138-142), with elevated sensitivities observed with both G0 MN-assay (25%) and G2 chromatid break assay (40%), but seldom both (4%) (143). This elevated *in vitro* radiosensitivity can be interesting for the risk-assessment for second primary cancers, but it could also help to adapt the course of radiotherapy in light of late toxic effects from the treatment. As stated in the introduction, dose-deposition in more recent radiotherapy techniques as IMRT has evolved in such a way that healthy tissue surrounding the tumor is spared much better than in the early days of radiotherapy, but it cannot be denied that the healthy tissue is still irradiated. On the other hand, with the new techniques the rest of the body in general also gets a low dose, which was not the case with the older techniques.

In radiotherapy the total dose received and the DNA repair capacity of both healthy and malignant tissues are important and will determine the probability of a tumor-killing effect over the risk of causing adverse effects in the healthy tissue (144).

2.2.1 Prediction of the risks of radiotoxic effects

There exists a direct relationship between radiation dose and tumor control, but the severe normal tissue toxicity in a minority of patients limits the dose that can be safely prescribed (145). Current RT doses are generally limited such that less than 5% of the treated patients suffer from severe toxicity up to 5 years following RT. The development of a test to predict late toxicity would enable individualized radiation dose prescription and would reduce the number of survivors suffering from the consequences of treatment (146-149).

A lot of cytogenetic and cell survival studies have been performed in an attempt to predict late toxic reactions following radiotherapy.

The search for a predictive assay started with fibroblast-based assays such as the colony formation assay, since a lot of the late toxic effects occur in fibroblasts (e.g. fibrosis and changes in pigmentation) and it was hypothesized that they would reflect clinical radiosensitivity. However, further attempts were abandoned since sampling of a sufficient amount of fibroblasts was problematic and results could only be obtained after 2 to 3 months, which is too late for clinical use. In more recent studies, lymphocytes were used to assess intrinsic radiosensitivity as they are easier to acquire and results of the assays can be obtained within a few days.

In our study about late radiotoxicity in breast cancer patients (Article 5), we attempted to differentiate patients showing no or very limited late effects (controls) from patients showing extreme late effects (cases). It has been estimated that if known extrinsic factors, such as dose per fraction, total dose and irradiated volume, are controlled, 80% of the observed variation in the severity of normal tissue responses is due to inherent differences among the patients (150, 151). To eliminate variables influencing radiotoxicity, in article 5 a retrospective case-control set-up was used. To each case a control was matched for therapy variables, cupsize, BMI and age. These variables are known to be associated with radiotoxicity and affect clinical radiosensitivity.

The association between individual variation in clinical radiosensitivity and cellular radiosensitivity could provide a possibility to determine the individual sensitivity of patients in terms of developing severe treatment-related side effects (152). In the study (Article 5) four different cellular assays were performed after *in vitro* irradiation of patient blood samples: G0 MN assay, G2+caffeine MN assay, residual DNA DSB (γ H2AX/53BP1; 4Gy – 24h) and radiation induced late apoptosis in lymphocytes (CD8+; 8Gy – 48h). By comparing the results of these assays we assessed the efficiency of different pathways that play a role in the DNA damage response. With all four assays we found a significant difference between the group of cases and the group of controls for both paired and grouped analysis (see figure 2.1) (153). The apoptosis assay showed the most impressive and promising results, with less apoptosis seen in CD8+ lymphocytes of the cases (average 14.5%) than in the matched controls (30.1%) However, some of the case-control pairs showed substantial overlap in standard deviations, which questions the predictive value of the assays in clinical radiotherapy practice.

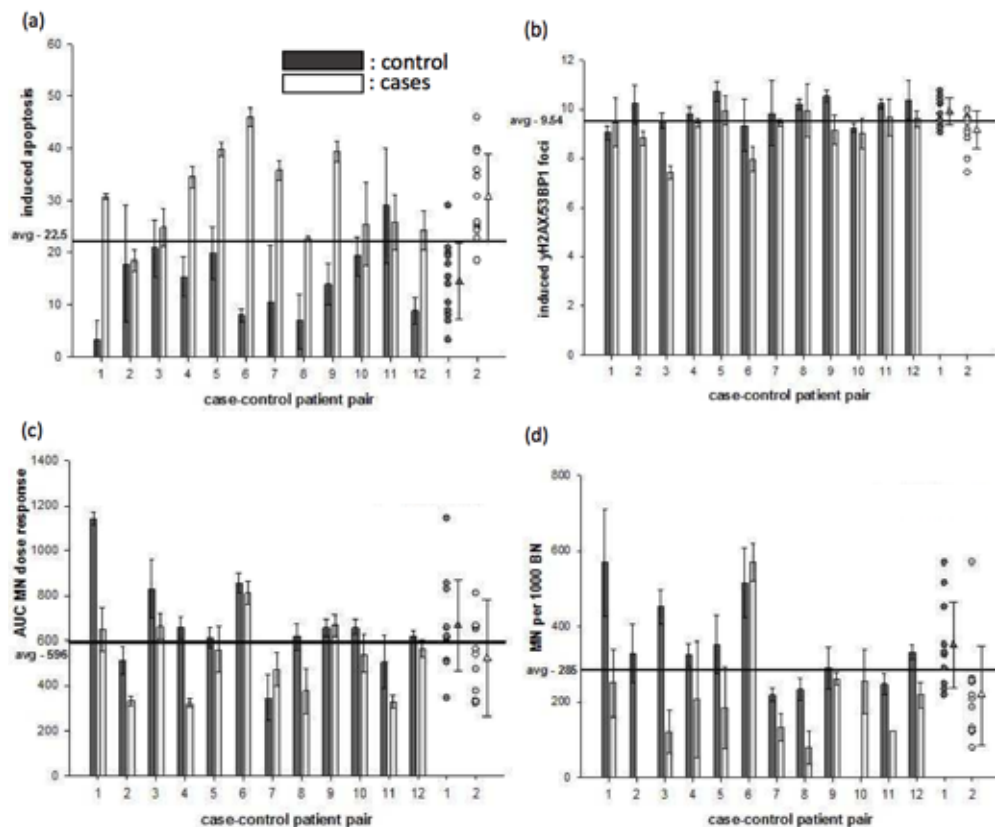


FIGURE 2.1

(a) percentage of cells with radiation induced late apoptosis, (b) number of radiation induced foci, (c) the area under the curve calculated from the GO-MN dose-response curve, (d) number of radiation induced G2 MN per 1000 BN cells in each of the cases (dark grey bars) and controls (white bars). The average of all cases (dark grey triangle) and controls (white triangle) and the corresponding spread in case and controls are presented in the right part of the graphs. The horizontal line represents the average over all patients. The error bars represent standard deviations. Figure from article 5.

Our results are in line with several other studies who also reported to a certain extent associations between a range of cellular biomarker assays and clinical radiosensitivity (154-157). These assays use peripheral blood lymphocytes and include chromosomal radiosensitivity measured with G2 chromatid break assay, dicentrics and G0 MN assay, kinetics of residual DNA damage assessed by the γ H2AX foci assay and radiation-induced apoptosis on T-lymphocyte subsets (148, 153, 155, 158-165). Among those assays, radiation-induced apoptosis in lymphocyte subsets after *in vitro* irradiation gives the most promising results for correlation with late toxicity after radiotherapy (148, 153, 156, 164). Furthermore, more recent small studies suggest that the scoring of residual DNA damage by using the γ H2AX foci assay may also be useful for prediction of reactions to RT (158, 166).

Other studies investigated the association between genetic variation and clinical radiosensitivity by analyzing single nucleotide polymorphisms (SNP) in genes involved in DNA damage response pathways (167-172). While a number of SNP have been proposed, replication of these studies remains difficult (146, 149, 173). Research in this area is now moving towards genome-wide association studies.

Studies using gene-expression profiles to predict late-toxic reactions to breast-cancer radiotherapy are emerging (165, 174-177), but at the moment there is a large variability in the results. This work is challenging and a lot of questions still exist on the study set-up and used protocols. Especially whether to determine gene-expression after irradiation or not and if cells are irradiated, which dose and post-irradiation incubation-times should be used. Gene-expression profiles change due to irradiation and as a function of time after the irradiation, but also the LET and the dose (178) of the irradiation will influence the expression profiles, hence these factors can affect the reported patterns of gene expression.

An increased radiosensitivity to ionizing radiation is linked to a deficiency in DNA DSB repair. However, there are several mechanisms by which this can occur. Genetic mutations found in radiosensitivity-syndromes, showed that most mutations occur in genes coding for proteins of the DNA repair pathways (NHEJ, HR or one of the back-up pathways) or in genes participating in the activation of the DNA damage response, the cell cycle checkpoints or apoptosis. But also genes involved in response to oxidative stress and cohesins, which function to hold chromosomes together during DNA replication and repair, have been implicated. The intrinsic variability in clinical radiosensitivity noted between different patients, might have a very different underlying genetic cause. Hence, it might be difficult to identify one screening assay to identify all the patients at high risk for developing late toxic effects to radiotherapy in the normal tissue. This can be illustrated with our radiosensitivity results in an atypical AT-patient and her parents. While the

G0 MN-assay showed only limited increased radiosensitivity for the patient (x1.8 compared to control donor) and non for the parents, the G2 MN-assay showed a marked increase for both the patient (x4) and the parents (mother: x2.8; father: x1.4) (179).

Furthermore, different radiotoxicity endpoints (fibrosis, edema, telangiectasia, etc.) have a different underlying cause and as such are linked to different genetic mutations. This can be illustrated by Barnett et al., who found in a genome wide association study with 1850 prostate and breast cancer patients the strongest associations for individual endpoints rather than to the overall measure of toxicity (180). This would again explain why we cannot expect one common test to identify all individuals who will react toxic to radiotherapy.

2.3 BRCA-radiosensitivity

2.3.1 Are BRCA mutation carriers radiosensitive?

Mutations in *BRCA1* or *BRCA2* are well-known risk factors for breast cancer, but the question remains whether mutations in these genes imply increased risk for radiation carcinogenesis. While radiosensitivity is a hallmark for cancer risk, cancer risk is not a hallmark for radiosensitivity. In light of screening and treatment of individuals with a *BRCA1/2*-mutation, it is important to know whether this group of individuals is more sensitive to ionizing radiation.

Patient studies focused mostly on the association between medical radiation burden and the occurrence or recurrence of radiation-induced breast cancer in persons with and without a *BRCA1* or *BRCA2* mutation. Results are inconclusive due to low statistical performance related to small populations and the many variables such as dose, radiation qualities, age and irradiated tissue involved. *In vivo* studies often lack the power to ultimately demonstrate a connection between the presence of *BRCA1* or *BRCA2* mutations and increased radiosensitivity (181). Some studies find an increased susceptibility to radiation carcinogenesis in *BRCA1/2* mutation carriers (182-184), often closely linked to age at the time of exposure, while other studies don't (144, 185-187).

To overcome the difficulties of *in vivo* studies, *in vitro* experiments investigating the radiosensitivity of lymphocytes, fibroblasts or EBV cell lines (Epstein Barr virus immortalized cell lines) derived from patients with and without a *BRCA1* or *BRCA2* mutation have been performed. These studies lead again to contradictory results, with some studies pointing to an increased sensitivity (188-191), and others not (190, 192).

To assess the impact of a *BRCA1* and *BRCA2* mutation on radiosensitivity, we used mammary epithelial cells (MCF-10A) in which *BRCA1* and *BRCA2* were downregulated using RNA inter-

ference transduction (called respectively BRCA1i and BRCA2i) (article 2). The cell lines had a knockdown of the targeted proteins of approximately 50%, which is comparable with the BRCA1 and BRCA2 levels in heterozygous mutation carriers and are as such very useful to assess the radiosensitivity of *BRCA*-mutation carriers.

The BRCA1i cells showed a significant increase in cellular radiosensitivity compared to the control cells and this for high-LET as well as low-LET radiation (see discussion chapter 1.4). When the G1 synchronized cells were irradiated, the sensitivity was so high that no MN-results could be obtained, due to a dose-related cell killing. When the mixed cultures, containing cells from G1 (37%), G2 (25%) and S (39%) were irradiated with neutrons, a 3.4-fold increase in sensitivity compared to the control cell line, irrespective of the dose was obtained. Irradiation with γ -rays resulted in a 3-fold increase in cellular radiosensitivity at a dose of 2Gy, rising to 5.5 at very low doses (193).

The BRCA2i cells also showed an increased radiosensitivity. But unlike the BRCA1i cells they only show a clear increased radiosensitivity in mixed cell cultures. This can be explained by the role of BRCA2 in HR, which doesn't play a role in the G1 phase of the cell cycle. After γ -irradiation, approximately a 2-fold increase in MN-yield was obtained compared to the control cell line, this increase in MN yield raised to 2.4 after neutron irradiation (193).

The increase in cellular radiosensitivity for both BRCA1 and BRCA2 we found in breast epithelial cells might have an impact on the risk assessment for the use of mammography and radiotherapy in BRCA1/2 mutation carriers.

2.3.2 BRCA and mammography

Two-view mammography gives a dose of 4 mGy to the breast of 30 kV X-rays to the glandular tissue of the breast. As previously discussed (see discussion chapter 1.2), the lower energy of mammography X-rays might increase the risk of mammography by a factor 3 to 4 compared to γ -rays (article 3). However, risk models show that mammography screening programs in healthy women with a bi-annual mammogram starting at the age of 50 still have a favorable detection-over-induction ratio.

BRCA-mutation carriers need to be screened for breast cancer from a young age. Breast tissue in younger persons is more dense and a higher dose is needed to obtain a good image for scoring. Furthermore, the risk of radiation to induce breast cancer is higher at younger age. While mammography screening comes with acceptable risks in the healthy population, it might not be optimal for BRCA1/2-mutation carriers.

Recent research showed that mammography X-rays in the very low-dose region might induce more damage than extrapolation from the higher dose region with the LNT model would suggest (see discussion chapter 1.2). In article 3 and article 4 we detected DSB, by means of the γ H2AX foci

assay, induced by doses less than 10mGy of 30kV X-rays in lymphocytes and breast epithelial cells and this was also reported by others (60, 76). This shows that 30kV X-rays induces DNA breaks at very low doses. Furthermore, in the very low dose region, we found a low dose hypersensitive response in mammary epithelial cells in breast tissue probably caused by the bystander effect. This hypersensitive response might further enhance the risks of mammography X-rays (article 4).

Our experiments in article 2 were performed at doses between 0.2 and 4 Gy, which is much higher than the doses used in mammography screening. The results show that the increased radiosensitivity for the BRCA1/2 knockdown cell lines is more pronounced in the low dose range compared to the high dose range (see figure 2.2) (193). Extrapolation to the very low-dose region, showed an increased radiosensitivity of BRCA1i and BRCA2i of respectively 5.5 and 2.2 fold after γ -radiation in comparison with the control cell line, especially for BRCA1i (193).

Some patient studies show no increased risk following exposures in *BRCA1* and *BRCA2* heterozygote mutation carriers to diagnostic X-rays (194) and mammography X-rays (185, 195). In contrast, other retrospective studies did find an association between diagnostic imaging and the risk of developing breast cancer in BRCA mutation carriers and this risk seems correlated with the age of exposure and the total dose received (183, 184, 196, 197). Remarkably, in the patient-study of Pijpe et al a positive association was even found for individuals exposed to the lowest dose (<6.6 mGy) in the younger age group (<30y) (196).

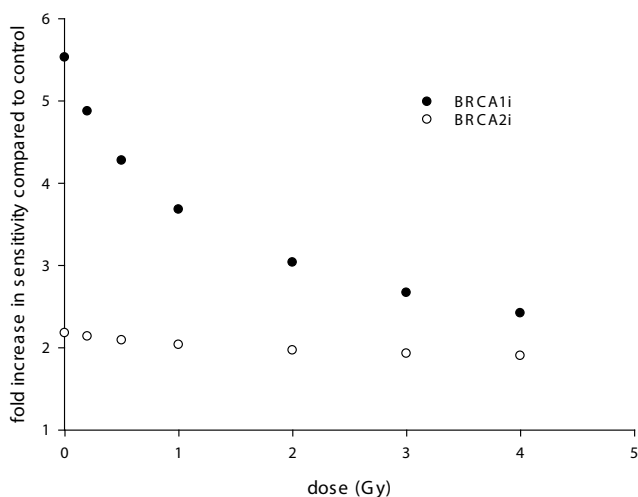


FIGURE 2.2

Overview of the fold increase of the cellular radiosensitivity of BRCA1i and BRCA2i compared to control cell line following γ -radiation of the mixed cultures.

Results aren't conclusive, but our study and other studies on BRCA1/2 related radiosensitivity provide evidence that *BRCA1* and *BRCA2* mutation carriers are likely to be more sensitive to low doses of radiation than individuals without a mutation.

BRCA-tumors are generally aggressive and hard to detect and early detection by regular screening for breast cancer from a young age in *BRCA*-mutation carriers is necessary. The risks of mammography for *BRCA* mutation carriers are not unambiguous, and national guidelines for breast cancer screening differ from country to country.

Risk models which include radiation exposure risk, advice annual MRI from the age 25 followed by alternating mammography and MRI from the age of 30. Postponing mammography to the age of 30 decreases the total dose received and expected false positives (198).

The United States National Comprehensive Cancer Network (NCCN) guidelines still advice to screen *BRCA1* and *BRCA2* mutation carriers with an annual mammogram and breast MRI starting at the age of 25 and the ACS (American Cancer Society) advises a yearly mammogram and breast MRI from the age of 30 (199, 200). These guidelines might underestimate the risk from the possible increased radiosensitivity in mutation carriers, which might be further enhanced in young individuals. Other national guidelines take the risk of radiation exposure more into account. The Dutch guidelines advice to start screening with MRI from the age of 25 and to add annual mammography from the age of 30. The NICE (United Kingdom National Institute for Health and Care Excellence) guidelines advice to start screening with an annual MRI from the age of 30 and add annual mammography from the age of 40 (144). In Belgium, very high risk patients, amongst which are *BRCA*-mutation carriers, are advised to do a yearly MRI starting the age of 30 or 5 year before the age of diagnosis of the youngest family member. Additionally a single mammography is recommended at the age of 40 and between the ages of 50 and 69 a biannual mammography (201).

2.3.3 BRCA and radiotherapy

In our study with BRCA knockdown cell lines (article 2), we also found an increased radiosensitivity in the higher dose range (see figure 2.2).

In literature, no clear evidence exists that *BRCA* mutation carriers are more sensitive to the toxic effects of normal tissue following radiotherapy. However, one should keep in mind that those studies are often unethical to set-up and it is difficult to find the appropriate study populations to investigate the correlation between increased risk for radiotherapy-induced breast cancer and the presence of a mutation in *BRCA1* or *BRCA2* (144). So far, a number of patient studies have been conducted, which showed no or a very limited increased risk (202-204). The only study where an elevated relative risk was found, is a case-only study in patients with contralateral breast cancer.

More patients with mutations in DSB repair genes were found in the group receiving radiotherapy compared to the group not receiving radiotherapy. This suggests an increased risk to develop radiation-induced contralateral breast cancer in patients with a mutation in a DSB repair gene. The relative risk was higher in younger patients (<40y) and when the time interval between radiotherapy and the second primary was higher (>5y) (205).

No conclusive evidence exists yet for an increased susceptibility to radiation carcinogenesis following radiotherapy in *BRCA* mutation carriers. However, the low doses of diagnostic irradiation, specifically mammography, seems to be carcinogenic in *BRCA1* and *BRCA2* mutation carriers, especially at young age. Hence, it is unlikely that the much higher doses received in radiotherapy don't increase the risk for a second primary cancer in *BRCA* mutation carriers (144).

3 Conclusion

Our results obtained with fast neutrons in human peripheral lymphocytes and MCF-10A cells are conform to literature reports regarding the effects of high-LET radiation. While a lower number of radiation-induced DNA DSB was observed for neutron radiation compared to γ -rays until about 4h post-IR, foci repair was slower and more residual foci were present at later time points. Furthermore, neutrons seem to be more effective in inducing micronuclei and inhibiting cell proliferation. These results are important in the frame of high-LET radiotherapy and space radiation risk assessment.

Irradiation of human lymphocytes with 30kV X-rays, which are low-LET radiation, resulted in a modest increase in the number of DNA DSB compared to γ -rays, but these DSB were more difficult to repair correctly by the cell and resulted in a more pronounced increase in micronuclei compared to γ -rays. Furthermore, in the 0 to 20 mGy dose-range a low-dose hypersensitive response for DSB induction was observed in mammary glandular epithelial cells present in resected breast tissue, probably caused by the bystander effect. This hypersensitive response in the dose range representative for mammography screening, together with the findings obtained with chromosomal aberrations at higher doses might suggest that also in the 0-20mGy dose range more chromosomal aberrations than initially assumed by the LNT model will be induced. These findings may have important implications for risk assessment of mammography screening.

Analysis of the relationship between cell cycle phase, LET and radiosensitivity using DSB repair deficient cell lines (MCF-10A cell lines with a knockdown in BRCA1, BRCA2 and Ku70) confirmed that NHEJ plays a role throughout the whole cell cycle, while HR only functions in late S and G2 phase of the cell cycle. Furthermore, the importance of HR in S or G2 phase rises as the complexity of the break increases. This results in RBE values for MN-induction which are much higher when cells are irradiated in G1 compared to the S and G2 phase of the cell cycle.

As BRCA1 and BRCA2 are important proteins in the DNA DSB repair pathways, mutations in the *BRCA* genes could lead to an increased susceptibility to radiation-induced carcinogenesis. The knockdown of BRCA1 and BRCA2 proteins in mammary epithelial cells of about 50%, a condition which is representative for heterozygous mutation carriers, led to a significantly increased radiosensitivity based on MN formation and cell proliferation, which was most pronounced at low doses. The results imply that caution should be taken when administering ionizing radiation to heterozygous *BRCA1* or *BRCA2* mutation carriers.

We further attempted to identify breast-cancer patients who showed severe late toxic reactions to radiotherapy. In a matched case-control study using human lymphocytes, the *in vitro* clinical radiosensitivity of cases and controls was assessed with four different endpoints related to DNA repair and apoptosis. The results suggest that a patient's intrinsic radiosensitivity is involved in the development of late radiotoxic effects. As the biological mechanisms behind the different symptoms of late toxicity differ, it can be expected that not all clinical manifestations of late radiotoxicity are linked to the same degree to intrinsic radiosensitivity with respect to DNA repair and apoptosis. Of the four radiosensitivity tests applied, the apoptosis assay seems to be most promising in the framework of predicting radiotoxic effects in individual patients.

References

1. Niemantsverdriet M, van Goethem MJ, Bron R, Hogewerf W, Brandenburg S, Langendijk JA, et al., High and Low LET Radiation Differentially Induce Normal Tissue Damage Signals. *International Journal of Radiation Oncology Biology Physics* 2012; 83, 1291-97.
2. Gueulette J, Slabbert JP, Bischoff P, Denis JM, Wambersie A, Jones D, Fast neutrons: Inexpensive and reliable tool to investigate high-LET particle radiobiology. *Radiation Measurements* 2010; 45, 1414-16.
3. neutron therapy, <http://www.neutrontherapy.com/Worldwidecentres.asp>.
4. Vandersickel V, Beukes P, Van Bockstaele B, Depuydt J, Vral A, Slabbert J, Induction and disappearance of gamma H2AX foci and formation of micronuclei after exposure of human lymphocytes to Co-60 gamma-rays and p(66) + Be(40) neutrons. *International Journal of Radiation Biology* 2014; 90, 149-58.
5. Antonelli F, Campa A, Esposito G, Giardullo P, Belli M, Dini V, et al., Induction and Repair of DNA DSB as Revealed by H2AX Phosphorylation Foci in Human Fibroblasts Exposed to Low- and High-LET Radiation: Relationship with Early and Delayed Reproductive Cell Death. *Radiation Research* 2015; 183, 417-31.
6. Leatherbarrow EL, Harper JV, Cucinotta FA, O'Neill P, Induction and quantification of gamma-H2AX foci following low and high LET-irradiation. *International Journal of Radiation Biology* 2006; 82, 111-18.
7. Asaithamby A, Uematsu N, Chatterjee A, Story MD, Burma S, Chen DJ, Repair of HZE-Particle-induced DNA double-strand breaks in normal human fibroblasts. *Radiation Research* 2008; 169, 437-46.
8. Olive PL, Banath JP, Phosphorylation of histone H2AX as a measure of radiosensitivity. *International Journal of Radiation Oncology Biology Physics* 2004; 58, 331-35.
9. Vandersickel V, Depuydt J, Van Bockstaele B, Perletti G, Philippe J, Thierens H, et al., Early Increase of Radiation-induced gamma H2AX Foci in a Human Ku70/80 Knockdown Cell Line Characterized by an Enhanced Radiosensitivity. *Journal of Radiation Research* 2010; 51, 633-41.
10. Antonelli F, Belli M, Cuttone G, Dini V, Esposito G, Simone G, et al., Induction and repair of DNA double-strand breaks in human cells: Dephosphorylation of histone H2AX and its inhibition by calyculin A. *Radiation Research* 2005; 164, 514-17.
11. Franken NAP, ten Cate R, Krawczyk PM, Stap J, Haveman J, Aten J, et al., Comparison of RBE values of high- LET alpha-particles for the induction of DNA-DSBs, chromosome aberrations and cell reproductive death. *Radiation Oncology* 2011; 6, 8.
12. Costes SV, Boissiere A, Ravani S, Romano R, Parvin B, Barcellos-Hoff MH, Imaging features that discriminate between foci induced by high- and low-LET radiation in human fibroblasts. *Radiation Research* 2006; 165, 505-15.
13. Prise KM, Use of radiation quality as a probe for DNA lesion complexity. *International Journal of Radiation Biology* 1994; 65, 43-48.
14. Goodhead DT, Thacker J, Cox R, Effects of radiations of different qualities on cells – Molecular mechanisms of damage and repair. *International Journal of Radiation Biology* 1993; 63, 543-56.
15. Prise KM, Pinto M, Newman HC, Michael BD, A review of studies of ionizing radiation-induced double-strand break clustering. *Radiation Research* 2001; 156, 572-76.
16. Goodhead DT, Initial events in the cellular effects of ionizing-radiations – clustered damage in DNA. *International Journal of Radiation Biology* 1994; 65, 7-17.
17. Charlton DE, Nikjoo H, Humm JL, Calculation of initial yields of single-strand and double-strand breaks in cell-nuclei from electrons, protons and alpha-particles. *International*

- Journal of Radiation Biology 1989; 56, 1-19.
18. Goodhead DT, Saturable repair models of radiation action in mammalian cells. *Radiation Research* 1985; 104, S58-S67.
 19. Sutherland BM, Bennett PV, Schenk H, Sidorkina O, Laval J, Trunk J, et al., Clustered DNA damages induced by high and low LET radiation, including heavy ions. *Physica Medica* 2001; 17, 202-04.
 20. Urushibara A, Shikazono N, O'Neill P, Fujii K, Wada S, Yokoya A, LET dependence of the yield of single-, double-strand breaks and base lesions in fully hydrated plasmid DNA films by He-4(2+) ion irradiation. *International Journal of Radiation Biology* 2008; 84, 23-33.
 21. Du GH, Drexler GA, Friedland W, Greubel C, Hable V, Krucken R, et al., Spatial Dynamics of DNA Damage Response Protein Foci along the Ion Trajectory of High-LET Particles. *Radiation Research* 2011; 176, 706-15.
 22. Aten JA, Stap J, Krawczyk PM, van Oven CH, Hoebe RA, Essers J, et al., Dynamics of DNA double-strand breaks revealed by clustering of damaged chromosome domains. *Science* 2004; 303, 92-95.
 23. Tommasino F, Friedrich T, Jakob B, Meyer B, Durante M, Scholz M, Induction and Processing of the Radiation-Induced Gamma-H2AX Signal and Its Link to the Underlying Pattern of DSB: A Combined Experimental and Modelling Study. *Plos One* 2015; 10, 25.
 24. Vadhavkar N, Pham C, Georgescu W, Deschamps T, Heuskin AC, Tang J, et al., Combinatorial DNA Damage Pairing Model Based on X-Ray-Induced Foci Predicts the Dose and LET Dependence of Cell Death in Human Breast Cells. *Radiation Research* 2014; 182, 273-81.
 25. Neumaier T, Swenson J, Pham C, Polyzos A, Lo AT, Yang PA, et al., Evidence for formation of DNA repair centers and dose-response nonlinearity in human cells. *Proceedings of the National Academy of Sciences of the United States of America* 2012; 109, 443-48.
 26. Groesser T, Chang H, Fontenay G, Chen J, Costes SV, Barcellos-Hoff MH, et al., Persistence of gamma-H2AX and 53BP1 foci in proliferating and non-proliferating human mammary epithelial cells after exposure to gamma-rays or iron ions. *International Journal of Radiation Biology* 2011; 87, 696-710.
 27. Desai N, Davis E, O'Neill P, Durante M, Cucinotta EA, Wu H, Immunofluorescence detection of clustered gamma-H2AX foci induced by HZE-particle radiation. *Radiation Research* 2005; 164, 518-22.
 28. Takahashi A, Yamakawa N, Kirita T, Omori K, Ishioka N, Furusawa Y, et al., DNA Damage Recognition Proteins Localize along Heavy Ion Induced Tracks in the Cell Nucleus. *Journal of Radiation Research* 2008; 49, 645-52.
 29. Asaithamby A, Hu BR, Chen DJ, Unrepaired clustered DNA lesions induce chromosome breakage in human cells. *Proceedings of the National Academy of Sciences of the United States of America* 2011; 108, 8293-98.
 30. Pinto M, Prise KM, Michael BD, Double strand break rejoining after irradiation of human fibroblasts with X rays or alpha particles: PFGE studies and numerical models. *Radiation Protection Dosimetry* 2002; 99, 133-36.
 31. Sekine E, Okada M, Matsufuji N, Yu D, Furusawa Y, Okayasu R, High LET heavy ion radiation induces lower numbers of initial chromosome breaks with minimal repair than low LET radiation in normal human cells. *Mutation Research-Genetic Toxicology and Environmental Mutagenesis* 2008; 652, 95-101.
 32. Jenner TJ, Delara CM, Oneill P, Stevens DL, Induction and rejoining of DNA double-strand breaks in V79-4 mammalian-cells following gamma-irradiation and alpha-irradiation. *International Journal of Radiation Biology* 1993; 64, 265-73.
 33. Stenerlow B, Høglund E, Carlsson J, Blomquist E, Rejoining of DNA fragments produced by radiations of different linear energy transfer. *International Journal of Radiation Biology* 2000; 76, 549-57.

34. Lobrich M, Cooper PK, Rydberg B, Non-random distribution of DNA double-strand breaks induced by particle irradiation. *International Journal of Radiation Biology* 1996; 70, 493-503.
35. Bonassi S, El-Zein R, Bolognesi C, Fenech M, Micronuclei frequency in peripheral blood lymphocytes and cancer risk: evidence from human studies. *Mutagenesis* 2011; 26, 93-100.
36. Bonassi S, Norppa H, Ceppi M, Stromberg U, Vermeulen R, Znaor A, et al., Chromosomal aberration frequency in lymphocytes predicts the risk of cancer: results from a pooled cohort study of 22 358 subjects in 11 countries. *Carcinogenesis* 2008; 29, 1178-83.
37. Bonassi S, Znaor A, Ceppi M, Lando C, Chang WP, Holland N, et al., An increased micronucleus frequency in peripheral blood lymphocytes predicts the risk of cancer in humans. *Carcinogenesis* 2007; 28, 625-31.
38. El-Zein R, Vral A, Etzel CJ, Cytokinesis-blocked micronucleus assay and cancer risk assessment. *Mutagenesis* 2011; 26, 101-06.
39. Khanna KK, Jackson SP, DNA double-strand breaks: signaling, repair and the cancer connection. *Nature Genet* 2001; 27, 247-54.
40. Slabbert JP, August L, Vral A, Symons J, The relative biological effectiveness of a high energy neutron beam for micronuclei induction in T-lymphocytes of different individuals. *Radiation Measurements* 2010; 45, 1455-57.
41. Beukes PR, Personal communication. 2016.
42. Vral A, Verhaegen F, Thierens H, Deridder L, Micronuclei induced by fast-neutrons versus Co-60 gamma-rays in human peripheral-blood lymphocytes. *International Journal of Radiation Biology* 1994; 65, 321-28.
43. ICRP, Relative Biological Effectiveness, Radiation Weighting and Quality Factor. ICRP Publication 92. *Annals of the ICRP* 2003; 33.
44. Sorensen BS, Overgaard J, Bassler N, In vitro RBE-LET dependence for multiple particle types. *Acta Oncologica* 2011; 50, 757-U268.
45. Groesser T, Chun E, Rydberg B, Relative biological effectiveness of high-energy iron ions for micronucleus formation at low doses. *Radiation Research* 2007; 168, 675-82.
46. Loucas BD, Cornforth MN, The LET Dependence of Unrepaired Chromosome Damage in Human Cells: A Break Too Far? *Radiation Research* 2013; 179, 393-405.
47. Rydberg B, Cooper B, Cooper PK, Holley WR, Chatterjee A, Dose-dependent misrejoining of radiation-induced DNA double-strand breaks in human fibroblasts: Experimental and theoretical study for high- and low-LET radiation. *Radiation Research* 2005; 163, 526-34.
48. Asaithamby A, Chen DJ, Mechanism of cluster DNA damage repair in response to high-atomic number and energy particles radiation. *Mutation Research-Fundamental and Molecular Mechanisms of Mutagenesis* 2011; 711, 87-99.
49. Lomax ME, Salje H, Cunniffe S, O'Neill P, 8-OxoA inhibits the incision of an AP site by the DNA glycosylases Fpg, Nth and the AP endonuclease HAP1. *Radiation Research* 2005; 163, 79-84.
50. Fujimoto H, Pinak M, Nemoto T, O'Neill P, Kume E, Saito K, et al., Molecular dynamics simulation of clustered DNA damage sites containing 8-oxoguanine and abasic site. *Journal of Computational Chemistry* 2005; 26, 788-98.
51. Gulston M, de Lara C, Jenner T, Davis E, O'Neill P, Processing of clustered DNA damage generates additional double-strand breaks in mammalian cells post-irradiation. *Nucleic Acids Research* 2004; 32, 1602-09.
52. Eccles LJ, Lomax ME, O'Neill P, Hierarchy of lesion processing governs the repair, double-strand break formation and mutability of three-lesion clustered DNA damage. *Nucleic Acids Research* 2010; 38, 1123-34.
53. Eccles LJ, O'Neill P, Lomax ME, Delayed repair of radiation induced clustered DNA damage: Friend or foe? *Mutation Research-Fundamental and Molecular Mechanisms of Mu-*

- togenesis 2011; 711, 134-41.
54. ICRP, The 2007 recommendations of the International Commission on Radiological Protection. ICRP Publication 103. . *Annals of the ICRP* 2007; 37.
 55. Law J, Faulkner K, Cancers detected and induced, and associated risk and benefit, in a breast screening programme. *British Journal of Radiology* 2001; 74, 1121-27.
 56. Law J, Faulkner K, Concerning the relationship between benefit and radiation risk, and cancers detected and induced, in a breast screening programme. *British Journal of Radiology* 2002; 75, 678-84.
 57. Depuydt J, Baert A, Vandersickel V, Thierens H, Vral A, Relative biological effectiveness of mammography X-rays at the level of DNA and chromosomes in lymphocytes. *International Journal of Radiation Biology* 2013; 89, 532-38.
 58. Depuydt J, Viaene T, Blondeel P, Roche N, Vral A, Relative biological effectiveness of mammography X-rays in breast tissue. . article in preparation.
 59. Kuhne M, Urban G, Frankenberg D, Lobrich M, DNA double-strand break misrejoining after exposure of primary human fibroblasts to C-K characteristic X rays, 29 kVp X rays and Co-60 gamma rays. *Radiation Research* 2005; 164, 669-76.
 60. Mills CE, Thome C, Koff D, Andrews DW, Boreham DR, The Relative Biological Effectiveness of Low-Dose Mammography Quality X Rays in the Human Breast MCF-10A Cell Line. *Radiation Research* 2015; 183, 42-51.
 61. Kellerer AM, Electron spectra and the RBE of X rays. *Radiation Research* 2002; 158, 13-22.
 62. Bernal MA, de Almeida CE, David M, Pires E, Estimation of the RBE of mammography-quality beams using a combination of a Monte Carlo code with a B-DNA geometrical model. *Physics in Medicine and Biology* 2011; 56, 7393-403.
 63. Verhaegen F, Reniers B, Microdosimetric analysis of various mammography spectra: Lineal energy distributions and ionization cluster analysis. *Radiation Research* 2004; 162, 592-99.
 64. Schmid E, Bauchinger M, Streng S, Nahrstedt U, The effect of 220 kVp X-rays with different spectra on the dose-response of chromosome-aberrations in human-lymphocytes. . *Radiation and Environmental Biophysics* 1984; 23, 305-09.
 65. Slonina D, Spekl K, Panteleeva A, Brankovic K, Hoinkis C, Dorr W, Induction of micronuclei in human fibroblasts and keratinocytes by 25 kV x-rays. *Radiation and Environmental Biophysics* 2003; 42, 55-61.
 66. Lehnert A, Lessmann E, Pawelke J, Dorr W, RBE of 25 kV X-rays for the survival and induction of micronuclei in the human mammary epithelial cell line MCF-12A. *Radiation and Environmental Biophysics* 2006; 45, 253-60.
 67. Mestres M, Caballin MR, Barrios L, Ribas M, Barquinero JE, RBE of X rays of different energies: A cytogenetic evaluation by FISH. *Radiation Research* 2008; 170, 93-100.
 68. Virsik RP, Harder D, Hansmann I, RBE of 30 kV X-rays for induction of dicentric chromosomes in human lymphocytes. *Radiation and Environmental Biophysics* 1977; 14, 109-21.
 69. Schmid E, Regulla D, Kramer HM, Harder D, The effect of 29 W X rays on the dose response of chromosome aberrations in human lymphocytes. *Radiation Research* 2002; 158, 771-77.
 70. Verhaegen F, Vral A, Sensitivity of micronucleus induction in human-lymphocytes to low-LET radiation qualities – RBE and correlation of RBE and LET. *Radiation Research* 1994; 139, 208-13.
 71. Stanbridge EJ, Flandermeyer RR, Daniels DW, Nelsonrees WA, Specific chromosome loss associated with the expression of tumorigenicity in human cell hybrids. *Somatic Cell Genetics* 1981; 7, 699-712.
 72. Heyes GJ, Mill AJ, The neoplastic transformation potential of mammography X rays and atomic bomb spectrum radiation. *Radiation Research* 2004; 162, 120-27.
 73. Frankenberg D, Kelnhofer K, Bar K, Frankenberg-Schwager M, Enhanced neoplastic trans-

- formation by mammography X rays relative to 200 kVp X rays: Indication for a strong dependence on photon energy of the RBE_M for various end points. *Radiation Research* 2002; 158, 126-26.
74. Frankenberg D, Kelnhofer K, Garg I, Bar K, Frankenberg-Schwager M, Enhanced mutation and neoplastic transformation in human cells by 29 kV(P) relative to 200 kV(P) X rays indicating a strong dependence of RBE on photon energy. *Radiation Protection Dosimetry* 2002; 99, 261-64.
 75. Goggelmann W, Jacobsen C, Panzer W, Walsh L, Roos H, Schmid E, Re-evaluation of the RBE of 29 kV x-rays (mammography x-rays) relative to 220 kV x-rays using neoplastic transformation of human CGL1-hybrid cells. *Radiation and Environmental Biophysics* 2003; 42, 175-82.
 76. Colin C, Devic C, Noel A, Rabilloud M, Zobot MT, Pinet-Isaac S, et al., DNA double-strand breaks induced by mammographic screening procedures in human mammary epithelial cells. *International Journal of Radiation Biology* 2011; 87, 1103-12.
 77. Beels L, Bacher K, De Wolf D, Werbrouck J, Thierens H, gamma-H2AX Foci as a Biomarker for Patient X-Ray Exposure in Pediatric Cardiac Catheterization Are We Underestimating Radiation Risks? *Circulation* 2009; 120, 1903-09.
 78. Beels L, Werbrouck J, Thierens H, Dose response and repair kinetics of gamma-H2AX foci induced by in vitro irradiation of whole blood and T-lymphocytes with X- and gamma-radiation. *International Journal of Radiation Biology* 2010; 86, 760-68.
 79. Groesser T, Cooper B, Rydberg B, Lack of bystander effects from high-LET radiation for early cytogenetic end points. *Radiat Res* 2008; 170, 794-802.
 80. Brenner DJ, Doll R, Goodhead DT, Hall EJ, Land CE, Little JB, et al., Cancer risks attributable to low doses of ionizing radiation: Assessing what we really know. *Proceedings of the National Academy of Sciences of the United States of America* 2003; 100, 13761-66.
 81. Averbeck D, Does scientific evidence support a change from the LNT model for low-dose radiation risk extrapolation? *Health Phys* 2009; 97, 493-504.
 82. Averbeck D, Non-targeted effects as a paradigm breaking evidence. *Mutation Research-Fundamental and Molecular Mechanisms of Mutagenesis* 2010; 687, 7-12.
 83. Lisowska H, Wegierek-Ciuk A, Banasik-Nowak A, Braziewicz J, Wojewodzka M, Wojcik A, et al., The dose-response relationship for dicentric chromosomes and gamma-H2AX foci in human peripheral blood lymphocytes: Influence of temperature during exposure and intra- and inter-individual variability of donors. *International Journal of Radiation Biology* 2013; 89, 191-99.
 84. Rothkamm K, Lobrich M, Evidence for a lack of DNA double-strand break repair in human cells exposed to very low x-ray doses. *Proceedings of the National Academy of Sciences of the United States of America* 2003; 100, 5057-62.
 85. Grudzenski S, Raths A, Conrad S, Rube CE, Lobrich M, Inducible response required for repair of low-dose radiation damage in human fibroblasts. *Proceedings of the National Academy of Sciences of the United States of America* 2010; 107, 14205-10.
 86. Asaithamby A, Chen DJ, Cellular responses to DNA double-strand breaks after low-dose gamma-irradiation. *Nucleic Acids Research* 2009; 37, 3912-23.
 87. Law J, Faulkner K, Two-view screening and extending the age range: the balance of benefit and risk. *British Journal of Radiology* 2002; 75, 889-94.
 88. Law J, Faulkner K, Young KC, Risk factors for induction of breast cancer by X-rays and their implications for breast screening. *British Journal of Radiology* 2007; 80, 261-66.
 89. Heyes GJ, Mill AJ, Charles MW, Enhanced biological effectiveness of low energy X-rays and implications for the UK breast screening programme. *British Journal of Radiology* 2006; 79, 195-200.
 90. Jeggo P, Lavin MF, Cellular radiosensitivity: How much better do we understand it? Interna-

- tional Journal of Radiation Biology 2009; 85, 1061-81.
91. Hinz JM, Yamada NA, Salazar EP, Tebbs RS, Thompson LH, Influence of double-strand-break repair pathways on radiosensitivity throughout the cell cycle in CHO cells. *DNA Repair* 2005; 4, 782-92.
 92. Wilson PF, Hinz JM, Urbin SS, Nham PB, Thompson LH, Influence of homologous recombination on cell survival and chromosomal aberration induction during the cell cycle in gamma-irradiated CHO cells. *DNA Repair* 2010; 9, 737-44.
 93. Britten RA, Peters LJ, Murray D, Biological factors influencing the RBE of neutrons: Implications for their past, present and future use in radiotherapy. *Radiation Research* 2001; 156, 125-35.
 94. Takahashi A, Kubo M, Ma HY, Nakagawa A, Yoshida Y, Isono M, et al., Nonhomologous End-Joining Repair Plays a More Important Role than Homologous Recombination Repair in Defining Radiosensitivity after Exposure to High-LET Radiation. *Radiation Research* 2014; 182, 338-44.
 95. Wang HY, Wang X, Zhang PY, Wang Y, The Ku-dependent non-homologous end-joining but not other repair pathway is inhibited by high linear energy transfer ionizing radiation. *DNA Repair* 2008; 7, 725-33.
 96. Wang HY, Zhang XM, Wang P, Yu XY, Essers J, Chen D, et al., Characteristics of DNA-binding proteins determine the biological sensitivity to high-linear energy transfer radiation. *Nucleic Acids Research* 2010; 38, 3245-51.
 97. Weyrather WK, Ritter S, Scholz M, Kraft G, RBE for carbon track-segment irradiation in cell lines of differing repair capacity. *International Journal of Radiation Biology* 1999; 75, 1357-64.
 98. Okayasu R, Okada M, Okabe A, Noguchi M, Takakura K, Takahashi S, Repair of DNA damage induced by accelerated heavy ions in mammalian cells proficient and deficient in the non-homologous end-joining pathway. *Radiation Research* 2006; 165, 59-67.
 99. Foray N, Colin C, Bourguignon M, 100 Years of Individual Radiosensitivity: How We Have Forgotten the Evidence. *Radiology* 2012; 264, 627-31.
 100. Bergonié J, Tribondeau L, Interprétation de quelques résultats de la radiothérapie et essai de fixation d'une technique rationnelle. *CR Acad Sci* 1906; 143, 983-84.
 101. Bordier G, Une nouvelle unité de quantité de rayons X: l'unité I. *Discussions*. Paris; 1906.
 102. Puck TT, Marcus PI, Action of X-rays on mammalian cells *Journal of Experimental Medicine* 1956; 103, 653-&.
 103. Fertil B, Malaise EP, Inherent cellular radiosensitivity as a basic concept for human-tumor radiotherapy. *International Journal of Radiation Oncology Biology Physics* 1981; 7, 621-29.
 104. Badie C, Iliakis G, Foray N, Alsbeih G, Cedervall B, Chavaudra N, et al., Induction and rejoining of DNA double-strand breaks and interphase chromosome breaks after exposure to X-rays in one normal and 2 hypersensitive human fibroblast cell-lines. *Radiation Research* 1995; 144, 26-35.
 105. Foray N, Priestley A, Arlett CF, Malaise EP, Hypersensitivity of ataxia telangiectasia fibroblasts to ionizing radiation is associated with a repair deficiency of DNA double-strand breaks. *International Journal of Radiation Biology* 1997; 72, 271-83.
 106. Taalman R, Jaspers NGJ, Scheres J, Dewit J, Hustinx TWJ, Hypersensitivity to ionizing-radiation, invitro, in a new chromosomal breakage disorder, the nijmegen breakage syndrome. *Mutation Research* 1983; 112, 23-32.
 107. O'Driscoll M, Cerosaletti KM, Girard PM, Dai Y, Stumm M, Kysela B, et al., DNA ligase IV mutations identified in patients exhibiting developmental delay and immunodeficiency. *Mol Cell* 2001; 8, 1175-85.
 108. Plowman PN, Bridges BA, Arlett CF, Hinney A, Kingston JE, An instance of clinical radiation morbidity and cellular radiosensitivity, not associated with ataxia-telangiectasia. *British*

- Journal of Radiology 1990; 63, 624-28.
109. Riballo E, Critchlow SE, Teo SH, Doherty AJ, Priestley A, Broughton B, et al., Identification of a defect in DNA ligase IV in a radiosensitive leukaemia patient. *Current Biology* 1999; 9, 699-702.
 110. Godthelp BC, van Buul PPW, Jaspers NGJ, Elghalbzouri-Maghrani E, van Duijn-Goedhart A, Arwert F, et al., Cellular characterization of cells from the Fanconi anemia complementation group, FA-D1/BRCA2. *Mutation Research-Fundamental and Molecular Mechanisms of Mutagenesis* 2006; 601, 191-201.
 111. Godthelp BC, Wiegant WW, Waisfisz Q, Medhurst AL, Arwert F, Joenje H, et al., Inducibility of nuclear Rad51 foci after DNA damage distinguishes all Fanconi anemia complementation groups from D1/BRCA2. *Mutation Research-Fundamental and Molecular Mechanisms of Mutagenesis* 2006; 594, 39-48.
 112. Vrouwe MG, Elghalbzouri-Maghrani E, Meijers M, Schouten P, Godthelp BC, Bhuiyan ZA, et al., Increased DNA damage sensitivity of Cornelia de Lange syndrome cells: evidence for impaired recombinational repair. *Human Molecular Genetics* 2007; 16, 1478-87.
 113. EBCTCG, Effect of radiotherapy after breast-conserving surgery on 10-year recurrence and 15-year breast cancer death: meta-analysis of individual patient data for 10801 women in 17 randomized trials. *Lancet* 2011; 378, 1707-60.
 114. EBCTCG, Effect of radiotherapy after mastectomy and axillary surgery on 10-year recurrence and 20-year breast cancer mortality: meta-analysis of individual patient data for 8135 women in 22 randomised trials. *Lancet* 2014; 383, 2127-35.
 115. Alsner J, Andreassen CN, Overgaard J, Genetic markers for prediction of normal tissue toxicity after radiotherapy. *Seminars in radiation oncology* 2008; 18, 126-35.
 116. Mellekjær L, Friis S, Olsen JH, Scelo G, Hemminki K, Tracey E, et al., Risk of second cancer among women with breast cancer. *Int J Cancer* 2006; 118, 2285-92.
 117. Volk N, PompeKirn V, Second primary cancers in breast cancer patients in Slovenia. *Cancer Causes & Control* 1997; 8, 764-70.
 118. Soerjomataram I, Louwman WJ, de Vries E, Lemmens V, Klokman WJ, Coebergh JWW, Primary malignancy after primary female breast cancer in the south of the Netherlands, 1972-2001. *Breast Cancer Research and Treatment* 2005; 93, 91-95.
 119. Soerjomataram I, Louwman WJ, Lemmens V, de Vries E, Klokman WJ, Coebergh JWW, Risks of second primary breast and urogenital cancer following female breast cancer in the south of The Netherlands, 1972-2001. *Eur J Cancer* 2005; 41, 2331-37.
 120. Trentham-Dietz A, Newcomb PA, Nichols HB, Hampton JM, Breast cancer risk factors and second primary malignancies among women with breast cancer. *Breast Cancer Research and Treatment* 2007; 105, 195-207.
 121. Escobar PF, Patrick R, Rybicki L, Al-Husaini N, Michener CM, Crowe JP, Primary gynecological neoplasms and clinical outcomes in patients diagnosed with breast carcinoma. *International Journal of Gynecological Cancer* 2006; 16, 118-22.
 122. Raymond JS, Hogue CJR, Multiple primary tumours in women following breast cancer, 1973-2000. *British Journal of Cancer* 2006; 94, 1745-50.
 123. Strom BL, Schinnar R, Weber AL, Bunin G, Berlin JA, Baumgarten M, et al., Case-control study of postmenopausal hormone replacement therapy and endometrial cancer. *American Journal of Epidemiology* 2006; 164, 775-86.
 124. Kirova YM, De Rycke Y, Gambotti L, Pierga JY, Asselain B, Fourquet A, et al., Second malignancies after breast cancer: the impact of different treatment modalities. *British Journal of Cancer* 2008; 98, 870-74.
 125. Chen Y, Thompson W, Semenciw R, Mao Y, Epidemiology of contralateral breast cancer. *Cancer Epidemiology Biomarkers & Prevention* 1999; 8, 855-61.
 126. Bernstein JL, Thompson WD, Risch N, Holford TR, Risk-factors predicting the incidence

- of 2nd primary breast-cancer among women diagnosed with a 1st primary breast-cancer. *American Journal of Epidemiology* 1992; 136, 925-36.
127. Bernstein JL, Thompson WD, Risch N, Holford TR, The genetic epidemiology of 2nd primary breast-cancer. *American Journal of Epidemiology* 1992; 136, 937-48.
 128. Matesich SMA, Shapiro CL, Second cancers after breast cancer treatment. *Seminars in Oncology* 2003; 30, 740-48.
 129. Kirova YM, Vilcoq JR, Asselain B, Fourquet A, Radiation-induced sarcomas (RIS) following radiotherapy for breast cancer. *Radiother Oncol* 2004; 73, S36-S36.
 130. Kirova YM, Gambotti L, De Rycke Y, Vilcoq JR, Asselain B, Fourquet A, Risk of second malignancies after adjuvant radiotherapy for breast cancer: A large-scale, single-institution review. *International Journal of Radiation Oncology Biology Physics* 2007; 68, 359-63.
 131. Stovall M, Smith SA, Langholz BM, Boice JD, Shore RE, Andersson M, et al., Dose to the controlateral breast from radiotherapy and risk of second primary breast cancer in the WE-CARE study. *International Journal of Radiation Oncology Biology Physics* 2008; 72, 1021-30.
 132. Boice JD, Harvey EB, Blettner M, Stovall M, Flannery JT, Cancer in the controlateral breast after radiotherapy for breast-cancer. *New England Journal of Medicine* 1992; 326, 781-85.
 133. EBCTCG, Effects of radiotherapy and of differences in the extent of surgery for early breast cancer on local recurrence and 15-year survival: an overview of the randomised trials. *Lancet* 2005; 366, 2087-106.
 134. Storm HH, Andersson M, Boice JD, Blettner M, Stovall M, Mouridsen HT, et al., Adjuvant radiotherapy and risk of controlateral breast-cancer. *Journal of the National Cancer Institute* 1992; 84, 1245-50.
 135. Gao X, Fisher SG, Emami B, Risk of second primary cancer in the contralateral breast in women treated for early-stage breast cancer: A population-based study. *International Journal of Radiation Oncology Biology Physics* 2003; 56, 1038-45.
 136. Hooning MJ, Aleman BMP, Hauptmann M, Baaijens MHA, Klijn JGM, Noyon R, et al., Roles of Radiotherapy and Chemotherapy in the Development of Contralateral Breast Cancer. *Journal of Clinical Oncology* 2008; 26, 5561-68.
 137. Viani GA, Stefano EJ, Afonso SL, De Fendi LI, Soares FV, Leon PG, et al., Breast-conserving surgery with or without radiotherapy in women with ductal carcinoma in situ: a meta-analysis of randomized trials. *Radiation Oncology* 2007; 2, 12.
 138. Baeyens A, Thierens H, Claes K, Poppe B, Messiaen L, De Ridder L, et al., Chromosomal radiosensitivity in breast cancer patients with a known or putative genetic predisposition. *British Journal of Cancer* 2002; 87, 1379-85.
 139. Scott D, Barber JBP, Levine EL, Burrill W, Roberts SA, Radiation-induced micronucleus induction in lymphocytes identifies a high frequency of radiosensitive cases among breast cancer patients: a test for predisposition? *British Journal of Cancer* 1998; 77, 614-20.
 140. Scott D, Spreadborough A, Levine E, Roberts SA, Genetic predisposition in breast-cancer *Lancet* 1994; 344, 1444-44.
 141. Baria K, Warren C, Roberts SA, West CM, Scott D, Chromosomal radiosensitivity as a marker of predisposition to common cancers? *British Journal of Cancer* 2001; 84, 892-96.
 142. Jones LA, Scott D, Cowan R, Roberts SA, Abnormal radiosensitivity of lymphocytes from breast-cancer patients with excessive normal tissue-damage after radiotherapy – chromosome-aberrations after low dose-rate irradiation. *International Journal of Radiation Biology* 1995; 67, 519-28.
 143. Scott D, Barber JBP, Spreadborough AR, Burrill W, Roberts SA, Increased chromosomal radiosensitivity in breast cancer patients: a comparison of two assays. *International Journal of Radiation Biology* 1999; 75, 1-10.
 144. Drooger JC, Hooning MJ, Seynaeve CM, Baaijens MHA, Obdeijn IM, Sleijfer S, et al., Di-

- agnostic and therapeutic ionizing radiation and the risk of a first and second primary breast cancer, with special attention for BRCA1 and BRCA2 mutation carriers: A critical review of the literature. *Cancer Treatment Reviews* 2015; 41, 187-96.
145. Peters LJ, Radiation therapy tolerance limits. For one or for all?--Janeway Lecture. *Cancer* 1996; 77, 2379-85.
 146. West CM, Barnett GC, Genetics and genomics of radiotherapy toxicity: towards prediction. *Genome medicine* 2011; 3, 52.
 147. Barnett GC, West CML, Dunning AM, Elliott RM, Coles CE, Pharoah PDP, et al., Normal tissue reactions to radiotherapy: towards tailoring treatment dose by genotype. *Nat Rev Cancer* 2009; 9, 134-42.
 148. Schnarr K, Boreham D, Sathya J, Julian J, Dayes IS, Radiation-induced lymphocyte apoptosis to predict radiation therapy late toxicity in prostate cancer patients. *International journal of radiation oncology, biology, physics* 2009; 74, 1424-30.
 149. Barnett GC, Coles CE, Elliott RM, Baynes C, Luccarini C, Conroy D, et al., Independent validation of genes and polymorphisms reported to be associated with radiation toxicity: a prospective analysis study. *Lancet Oncology* 2012; 13, 65-77.
 150. Tucker SL, Turesson I, Thames HD, Evidence for individual differences in the radiosensitivity of human skin. *Eur J Cancer* 1992; 28A, 1783-91.
 151. Turesson I, Nyman J, Holmberg E, Oden A, Prognostic factors for acute and late skin reactions in radiotherapy patients. *International Journal of Radiation Oncology Biology Physics* 1996; 36, 1065-75.
 152. Burnet N, Nyman J, Turesson I, Wurm R, Yarnold J, Peacock J, Prediction of normal-tissue tolerance to radiotherapy from invitro cellular radiation sensitivity. *Lancet* 1992; 339, 1570-71.
 153. Vandevoorde C, Depuydt J, Veldeman L, De Neve W, Sebastia N, Wieme G, et al., In vitro cellular radiosensitivity in relationship to late normal tissue reactions in breast cancer patients: a multi-endpoint case-control study. *International Journal of Radiation Biology* article submitted.
 154. Borgmann K, Hoeller U, Nowack S, Bernhard M, Roper B, Brackrock S, et al., Individual radiosensitivity measured with lymphocytes may predict the risk of acute reaction after radiotherapy. *International Journal of Radiation Oncology Biology Physics* 2008; 71, 256-64.
 155. Hoeller U, Borgmann K, Bonacker M, Kuhlmeier A, Bajrovic A, Jung H, et al., Individual radiosensitivity measured with lymphocytes may be used to predict the risk of fibrosis after radiotherapy for breast cancer. *Radiother Oncol* 2003; 69, 137-44.
 156. Ozsahin M, Crompton NEA, Gourgou S, Kramar A, Li L, Shi YQ, et al., CD4 and CD8 T-lymphocyte apoptosis can predict radiation-induced late toxicity: A prospective study in 399 patients. *Clinical Cancer Research* 2005; 11, 7426-33.
 157. Chua MLK, Rothkamm K, Biomarkers of Radiation Exposure: Can They Predict Normal Tissue Radiosensitivity? *Clin Oncol* 2013; 25, 610-16.
 158. Chua MLK, Horn S, Somaiah N, Davies S, Gothard L, A'Hern R, et al., DNA double-strand break repair and induction of apoptosis in ex vivo irradiated blood lymphocytes in relation to late normal tissue reactions following breast radiotherapy. *Radiation and Environmental Biophysics* 2014; 53, 355-64.
 159. Borgmann K, Haerberle D, Doerk T, Busjahn A, Stephan G, Dikomey E, Genetic determination of chromosomal radiosensitivities in G0- and G2-phase human lymphocytes. *Radiother Oncol* 2007; 83, 196-202.
 160. Widel M, Jedrus S, Lukaszczyk B, Raczek-Zwierzycka K, Swierniak A, Radiation-Induced Micronucleus Frequency in Peripheral Blood Lymphocytes is Correlated with Normal Tissue Damage in Patients with Cervical Carcinoma Undergoing Radiotherapy. *Radiation Research* 2003; 159, 713-21.

161. Taghavi-Dehaghani M, Mohammadi S, Ziafazeli T, Sardari-Kermani M, A study on differences between radiation-induced micronuclei and apoptosis of lymphocytes in breast cancer patients after radiotherapy. *Zeitschrift Fur Naturforschung C-a Journal of Biosciences* 2005; 60, 938-42.
162. Chua MLK, Somaiah N, A'Hern R, Davies S, Gothard L, Yarnold J, et al., Residual DNA and chromosomal damage in ex vivo irradiated blood lymphocytes correlated with late normal tissue response to breast radiotherapy. *Radiother Oncol* 2011; 99, 362-66.
163. Crompton NE, Miralbell R, Rutz HP, Ersoy F, Sanal O, Wellmann D, et al., Altered apoptotic profiles in irradiated patients with increased toxicity. *International journal of radiation oncology, biology, physics* 1999; 45, 707-14.
164. Ozsahin M, Azria D, Radiation-Induced Sequelae Measured by Lymphocyte Apoptosis. *International Journal of Radiation Oncology Biology Physics* 2014; 90, 470-70.
165. Finnon P, Kabacik S, MacKay A, Raffy C, A'Hern R, Owen R, et al., Correlation of in vitro lymphocyte radiosensitivity and gene expression with late normal tissue reactions following curative radiotherapy for breast cancer. *Radiother Oncol* 2012; 105, 329-36.
166. Bourton EC, Plowman PN, Smith D, Arlett CF, Parris CN, Prolonged expression of the gamma-H2AX DNA repair biomarker correlates with excess acute and chronic toxicity from radiotherapy treatment. *Int J Cancer* 2011; 129, 2928-34.
167. Andreassen CN, Alsner J, Overgaard M, Overgaard J, Prediction of normal tissue radiosensitivity from polymorphisms in candidate genes. *Radiother Oncol* 2003; 69, 127-35.
168. Alsbeih G, El-Sebaie M, Al-Harbi N, Al-Buhairi M, Al-Hadyan K, Al-Rajhi N, Radiosensitivity of human fibroblasts is associated with amino acid substitution variants in susceptible genes and correlates with the number of risk alleles. *International Journal of Radiation Oncology Biology Physics* 2007; 68, 229-35.
169. De Ruyck K, Van Eijkeren M, Claes K, Morthier R, De Paepe A, Vral A, et al., Radiation-induced damage to normal tissues after radiotherapy in patients treated for gynecologic tumors: Association with single nucleotide polymorphisms in XRCC1, XRCC3, and OGG1 genes and in vitro chromosomal radiosensitivity in lymphocytes. *International Journal of Radiation Oncology Biology Physics* 2005; 62, 1140-49.
170. Azria D, Ozsahin M, Kramar A, Peters S, Atencio DP, Crompton NEA, et al., Single Nucleotide Polymorphisms, Apoptosis, and the Development of Severe Late Adverse Effects After Radiotherapy. *Clinical Cancer Research* 2008; 14, 6284-88.
171. Suga T, Iwakawa M, Tsuji H, Ishikawa H, Oda E, Noda S, et al., Influence of multiple genetic polymorphisms on genitourinary morbidity after carbon ion radiotherapy for prostate cancer. *International Journal of Radiation Oncology Biology Physics* 2008; 72, 808-13.
172. Isomura M, Oya N, Tachiiri S, Kaneyasu Y, Nishimura Y, Akimoto T, et al., IL12RB2 and ABCA1 Genes Are Associated with Susceptibility to Radiation Dermatitis. *Clinical Cancer Research* 2008; 14, 6683-89.
173. Barnett GC, Elliott RM, Alsner J, Andreassen CN, Abdelhay O, Burnet NG, et al., Individual patient data meta-analysis shows no association between the SNP rs1800469 in TGFB and late radiotherapy toxicity. *Radiother Oncol* 2012; 105, 289-95.
174. Hernandez LAH, Lara PC, Pinar B, Bordon E, Gallego CR, Bilbao C, et al., Constitutive gene expression profile segregates toxicity in locally advanced breast cancer patients treated with high-dose hyperfractionated radical radiotherapy. *Radiation Oncology* 2009; 4, 7.
175. Mayer C, Popanda O, Greve B, Fritz E, Illig T, Eckardt-Schupp F, et al., A radiation-induced gene expression signature as a tool to predict acute radiotherapy-induced adverse side effects. *Cancer Letters* 2011; 302, 20-28.
176. Quarmby S, West C, Magee B, Stewart A, Hunter R, Kumar S, Differential expression of cytokine genes in fibroblasts derived from skin biopsies of patients who developed minimal or severe normal tissue damage after radiotherapy. *Radiation Research* 2002; 157, 243-48.

177. Rodningen AK, Borresen-Dale AL, Alsner J, Hastie T, Overgaard J, Radiation-induced gene expression in human subcutaneous fibroblasts is predictive of radiation-induced fibrosis. *Radiother Oncol* 2008; 86, 314-20.
178. El-Saghire H, Thierens H, Monsieurs P, Michaux A, Vandevoorde C, Baatout S, Gene set enrichment analysis highlights different gene expression profiles in whole blood samples X-irradiated with low and high doses. *International Journal of Radiation Biology* 2013; 89, 628-38.
179. Claes K, Depuydt J, Taylor AMR, Last JI, Baert A, Schietecatte P, et al., Variant Ataxia Telangiectasia: Clinical and Molecular Findings and Evaluation of Radiosensitive Phenotypes in a Patient and Relatives. *Neuromol Med* 2013; 15, 447-57.
180. Barnett GC, Thompson D, Fachal L, Kerns S, Talbot C, Elliott RM, et al., A genome wide association study (GWAS) providing evidence of an association between common genetic variants and late radiotherapy toxicity. *Radiother Oncol* 2014; 111, 178-85.
181. Kan C, Zhang JR, BRCA1 Mutation: A Predictive Marker for Radiation Therapy? *International Journal of Radiation Oncology Biology Physics* 2015; 93, 281-93.
182. Pijpe A, Andrieu N, Easton DF, Kesminiene A, Cardis E, Nogues C, et al., Exposure to diagnostic radiation and risk of breast cancer among carriers of BRCA1/2 mutations: retrospective cohort study (GENE-RAD-RISK). *British Medical Journal* 2012; 345.
183. Andrieu N, Easton DF, Chang-Claude J, Rookus MA, Brohet R, Cardis E, et al., Effect of chest x-rays on the risk of breast cancer among BRCA1/2 mutation carriers in the International BRCA1/2 Carrier Cohort Study: A report from the EMBRACE, GENEPSO, GEO-HEBON, and IBCCS Collaborators' Group. *Journal of Clinical Oncology* 2006; 24, 3361-66.
184. Gronwald J, Pijpe A, Byrski T, Huzarski T, Stawicka M, Cybulski C, et al., Early radiation exposures and BRCA1-associated breast cancer in young women from Poland. *Breast Cancer Research and Treatment* 2008; 112, 581-84.
185. Goldfrank D, Chuai S, Bernstein JL, Cajal TR, Lee JB, Alonso MC, et al., Effect of mammography on breast cancer risk in women with mutations in BRCA1 or BRCA2. *Cancer Epidemiology Biomarkers & Prevention* 2006; 15, 2311-13.
186. Narod SA, Lubinski J, Ghadirian P, Screening mammography and risk of breast cancer in BRCA1 and BRCA2 mutation carriers: a case-control study (vol 7, pg 402, 2006). *Lancet Oncology* 2006; 7, 453-53.
187. Bernier J, Poortmans P, Clinical relevance of normal and tumour cell radiosensitivity in BRCA1/BRCA2 mutation carriers: A review. *The breast* 2015; 24, 100-06.
188. Buchholz TA, Wu XF, Hussain A, Tucker SL, Mills GB, Haffty B, et al., Evidence of haplotype insufficiency in human cells containing a germline mutation in BRCA1 or BRCA2. *Int J Cancer* 2002; 97, 557-61.
189. Foray N, Randrianarison V, Marot D, Perricaudet M, Lenoir G, Feunteun J, Gamma-rays-induced death of human cells carrying mutations of BRCA1 or BRCA2. *Oncogene* 1999; 18, 7334-42.
190. Frankenberg-Schwager M, Gregus A, Chromosomal instability induced by mammography X-rays in primary human fibroblasts from BRCA1 and BRCA2 mutation carriers. *International Journal of Radiation Biology* 2012; 88, 846-57.
191. Baert A, Depuydt J, Van Maerken T, Poppe B, Malfait F, Storm K, et al., Increased chromosomal radiosensitivity in asymptomatic carriers of a heterozygous BRCA1 mutation. *breast Cancer Research*; submitted.
192. Baeyens A, Thierens H, Claes K, Poppe B, De Ridder L, Vral A, Chromosomal radiosensitivity in BRCA1 and BRCA2 mutation carriers. *International Journal of Radiation Biology* 2004; 80, 745-56.
193. Depuydt J, Beukes PR, Baert A, Verstraete B, Van Heetvelde M, Vandersickel V, et al., The

- impact of a BRCA1 and BRCA2-mutation on the radiation response induced by gamma rays and neutrons in MCF10-A cells. article submitted.
194. John EM, McGuire V, Thomas D, Haile R, Ozcelik H, Milne RL, et al., Diagnostic Chest X-Rays and Breast Cancer Risk before Age 50 Years for BRCA1 and BRCA2 Mutation Carriers. *Cancer Epidemiology Biomarkers & Prevention* 2013; 22, 1547-56.
 195. Narod SA, Age of diagnosis, tumor size, and survival after breast cancer: implications for mammographic screening. *Breast Cancer Research and Treatment* 2011; 128, 259-66.
 196. Pijpe A, Andrieu N, Easton DF, Kesminiene A, Cardis E, Nogues C, et al., Exposure to diagnostic radiation and risk of breast cancer among carriers of BRCA1/2 mutations: retrospective cohort study (GENE-RAD-RISK). *Bmj-British Medical Journal* 2012; 345, 15.
 197. Lecarpentier J, Nogues C, Mouret-Fourme E, Stoppa-Lyonnet D, Lasset C, Caron O, et al., Variation in breast cancer risk with mutation position, smoking, alcohol, and chest X-ray history, in the French National BRCA1/2 carrier cohort (GENEPSO). *Breast Cancer Research and Treatment* 2011; 130, 927-38.
 198. Lowry KP, Lee JM, Kong CY, McMahon PM, Gilmore ME, Chubiz JEC, et al., Annual screening strategies in BRCA1 and BRCA2 gene mutation carriers. *Cancer* 2012; 118, 2021-30.
 199. Saslow D, Boetes C, Burke W, Harms S, Leach MO, Lehman CD, et al., American Cancer Society guidelines for breast screening with MRI as an adjunct to mammography. *Ca-a Cancer Journal for Clinicians* 2007; 57, 75-89.
 200. Smith RA, Andrews K, Brooks D, DeSantis CE, Fedewa SA, Lortet-Tieulent J, et al., Cancer Screening in the United States, 2016: A Review of Current American Cancer Society Guidelines and Current Issues in Cancer Screening. *Ca-a Cancer Journal for Clinicians* 2016; 66, 96-114.
 201. KCE, rapport 172A. Federaal kenniscentrum voor de gezondheid 2012.
 202. Bernstein JL, Thomas DC, Shore RE, Robson M, Boice JD, Stovall M, et al., Contralateral breast cancer after radiotherapy among BRCA1 and BRCA2 mutation carriers: A WECARE Study Report. *Eur J Cancer* 2013; 49, 2979-85.
 203. Metcalfe K, Lynch HT, Ghadirian P, Tung N, Kim-Sing C, Olopade OI, et al., Risk of ipsilateral breast cancer in BRCA1 and BRCA2 mutation carriers. *Breast Cancer Research and Treatment* 2011; 127, 287-96.
 204. Pierce LJ, Phillips KA, Griffith KA, Buys S, Gaffney DK, Moran MS, et al., Local therapy in BRCA1 and BRCA2 mutation carriers with operable breast cancer: comparison of breast conservation and mastectomy. *Breast Cancer Research and Treatment* 2010; 121, 389-98.
 205. Broeks A, Braaf LM, Huseinovic A, Nooijen A, Urbanus J, Hogervorst FBL, et al., Identification of women with an increased risk of developing radiation-induced breast cancer: a case only study. *Breast Cancer Research* 2007; 9, 9.

Curriculum

Personal information

Name: Julie Depuydt
Date of birth: 14/04/1980
Place of birth: Oostende
Adres: Puinstraat 26, 9000 Gent
Mobile: +32 477 59 50 42
Emailadres: julie.depuydt@ugent.be

Education

2004 – 2005 Master in **Economy and business-economy** at the UGent
Graduated with honors
1999 – 2004 **Bio-engineering in cellular and gene biotechnology** at the UGent
Graduated with honors
Thesis: Breukpuntonderzoek van een schijnbaar gebalanceerde translocatie in een patiënte met mentale retardatie en overgroei. (Analysis of the breakpoint of a seemingly balanced translocation in a patient with mental retardation and overgrowth)

Work experience

2009 – 2016 **Assistant at the UGent**, department of medical sciences
2007 – 2009 **Project manager at DELTAreference** in Ghent.
2005 – 2007 **Consultant at SGV management consultants** in Sint Denijs Westrem

Publications

- 1 Depuydt J, Beukes PR, Baert A, Verstraete B, Van Heetvelde M, Vandersickel V, et al., The impact of a BRCA1 and BRCA2-mutation on the radiation response induced by gamma rays and neutrons in MCF10-A cells. International Journal of Radiation Biology, article submitted (TRAB-2016-IJRB-0075).
- 2 Vandevoorde C*, Depuydt J*, Veldeman L, De Neve W, Sebastia N, Wieme G, et al., In vitro cellular radiosensitivity in relationship to late normal tissue reactions in breast cancer patients: a multi-endpoint case-control study. International Journal of Radiation Biology article submitted (TRAB-2016-IJRB-0074).
** These authors contributed equally to this work*
- 3 Vandersickel V, Beukes P, Van Bockstaele B, Depuydt J, Vral A, Slabbert J, Induction and disappearance of gamma H2AX foci and formation of micronuclei after exposure of human lymphocytes to Co-60 gamma-rays and p(66) + Be(40) neutrons. International Journal of Radiation Biology 2014; 90, 149-58.
- 4 Claes K*, Depuydt J*, Taylor AMR, Last JI, Baert A, Schietecatte P, et al., Variant Ataxia Telangiectasia: Clinical and Molecular Findings and Evaluation of Radiosensitive Phenotypes in a Patient and Relatives. Neuromol Med 2013; 15, 447-57.
** These authors contributed equally to this work*
- 5 Depuydt J, Baert A, Vandersickel V, Thierens H, Vral A, Relative biological effectiveness of mammography X-rays at the level of DNA and chromosomes in lymphocytes. International Journal of Radiation Biology 2013; 89, 532-38.
- 6 Vandersickel V, Depuydt J, Van Bockstaele B, Perletti G, Philippe J, Thierens H, et al., Early Increase of Radiation-induced gamma H2AX Foci in a Human Ku70/80 Knockdown Cell Line Characterized by an Enhanced Radiosensitivity. Journal of Radiation Research 2010; 51, 633-41.

-
- 7** Georgia I. Terzoudi, Gabriel Pantelias, Katarzyna Barszczewska, Firouz Darroudi, Julie Depuydt, Dimka Georgieva, Valeria Hadjidekova, Vasiliki I. Hatzi, Ioanna Karachristou, Maria Karakosta, Roberta Meschini, Radhia M'Kacher, Alegria Montoro, Fabrizio Palitti, Antonio Pantelias Garces, Michelle Ricoul, Laure Sabatier, Natividad Sebastià, Sylwester Sommer, Iwona Buraczewska, Anne Vral, Demetre Zafiropoulos, Andrzej Wojcik, Dose assessment inter-comparisons within the RENEB network using GO-lymphocyte prematurely condensed chromosomes (PCC assay). *International Journal of Radiation Biology*, article submitted.
- 8** Julie Depuydt, Ans Baeyens, Stephen Barnard, Christina Beinke, Anett Benedek, Philip Beukes, Iwona Buraczewska, Firouz Darroudi, Stefania De Sanctis, Inmaculada Dominguez, Dimka Georgieva, Octavia Monteiro Gil, Valeria Hadjidekova, Enikő Kis, Ulrike Kulka, Florigio Lista, Katalin Lumniczky, Radhia Mkacher, Jayne Moquet, Doina Obreja, Ursula Oestreicher, Jelena Pajic, Nuria Pastor, Ljubomira Popova, Elisa Regalbuto, Michelle Ricoul, Laure Sabatier, Jacobus Slabbert, Sylwester Sommer, Antonella Testa, Hubert Thierens, Andrzej Wojcik, Anne Vral, RENEB Intercomparison exercises analysing micronuclei (Cytokinesisblock Micronucleus Assay). *International Journal of Radiation Biology* (TRAB-2016-IJRB-0099).
- 9** Beata Brzozowska, Elizabeth Ainsbury, Annelot Baert, Lindsay Beaton-Green, Leonard Barrios, Joan Francesc Barquiner, Celine Bassinet, Christina Beinke, Anett Benedek, Philip Beukes, Emanuela Bortolin, Iwona Buraczewska, Christopher Burbidge, Andrea De Amicis, Cinzia De Angelis, Sara Della Monaca, Julie Depuydt, Stefania De Sanctis, Katalin Dobos, Mercedes Moreno Domene, Inmaculada Domínguez, Eva Facco, Paola Fattibene, Monika Frenzel, Octávia Monteiro Gil, Géraldine Gonon, Eric Gregoire, Gaëtan Gruel, Valeria Hadjidekova, Rositsa Hristova, Alicja Jaworska, Enikő Kis, Maria Kowalska, Ulrike Kulka, Florigio Lista, Katalin Lumniczky, Wilner Martinez-Lopez, Roberta Meschini, Simone Moertl, Mihaela Noditi, Ursula Oestreicher, Valentina Palma, Gabriel Pantelias, Alegria Montoro Pastor, Clarice Patrono, Laure Piqueret-Stephan, Maria Cristina Quattrini, Elisa Regalbuto, Michelle Ricoul, Sandrine Roch-Lefevre, Laurence Roy, Laure Sabatier, Lucia Sarchiapone, Natividad Sebastià, Sylwester Sommer, Yumiko Suto, Georgia Terzoudi, Francois Trompier, Vasiliki Hatzi, Anne Vral, Ruth Wilkins, Dimitros Zafiropoulos, Albrecht Wieser, Clemens Woda, Andrzej Wojcik, Reneb accident simulation exercise. *International Journal of Radiation Biology*, article submitted (TRAB-2016-IJRB-0098).

- 10** Oestreicher, Ursula; Samaga, Daniel; Ainsbury, Elizabeth; Antunes, Ana Catarina; Baeyens, Ans; Barrrios, Leonardo; Beinke, Christina; Beukes, Philip; Blakely, William F.; Cucu, Alexandra; DeAmicis, Andrea; Depuydt, Julie; DeSanctis, Stefania; DiGiorgio, Marina; Dobos, Katalin; Dominguez, Inmaculada; Duy, Pham Ngoc; Espinoza, Marco E.; Flegal, Farrah N; Figel, Markus; Garcia, O.; Monteiro Gil, Octavia; GREGOIRE, ERIC; Güçlü, İnci; Hadjidekova, Valeria; Hande, M Prakash; Kulka, Ulrike Marianne; Lemon, Jennifer; Lindholm, Carita; Lista, Florigio; Lumniczky, Katalin; Martinez-Lopez, Wilner; Maznyk, Nataliya Alexandrovna; Meschini, Roberta; M´kacher, Radia; Montoro, Alegria; Moquet, Jayne; Moreno, Mercedes; Noditi, Mihaela; Pajic, Jelena; Ricoul, Michelle; Romm, Horst; Roy, L; Sabatier, L.; Sebastià, Natividad; Slabbert, Jacobus; Sommer, Sylwester; Suto, Yumiko; Tran, Que; Testa, Antonella; Terzoudi, Georgia; Vral, Anne; Wilkins, R. C.; Yanti, LusiYanti; Zafiroopoulos, Demetre; Wojcik, Andrzej, RENEB intercomparisons applying the conventional Dicentric Chromosome Assay (DCA) International Journal of Radiation Biology, article submitted (TRAB-2016-IJRB-0087)
- 11** Baert A., Depuydt J., Van Maerken T., Poppe B., Malfait F., Storm K., van den Ende J., Van Damme T., De Nobele S., Perletti G., De Leeneer K., Claes K., Vral A., Increased chromosomal radiosensitivity in asymptomatic carriers of a heterzogenous BRCA1 mutation, breast cancer research, 2016, 18:52.
- 12** Vral A., Decorte V., Depuydt J., Wambersie A., Thierens H., The semi-automated FISH-based micronucleus-centromere assay for biomonitoring of hospital workers exposed to low doses of ionizing radiation, Molecular Medicine Reports, article accepted (MMR-8070-155222).

Conferences

Closing meeting RENE B

Lissabon, Portugal, 2-4/12/2015

Attendance

EPR biodose

Hanover, USA, 4-8/10/2015

Oral presentation: Lessons learned from the Inter-laboratory comparisons for the Micronucleus assay in the frame of the European Network of Biodosimetry – RENE B

RENE B at EPR biodose

Hanover, USA, 4/10/2015

Oral presentation: 2nd intercomparison on BCMN assay: results and lessons learned

15th International Conference of Radiation Research (ICRR)

Kyoto, 25-29/05/2015

Poster presentation: Inter-laboratory comparison for the Micronucleus assay in the frame of the European Network of Biodosimetry (RENE B)

Young investigators award

4th annual RENE B meeting

Rome, Italy, 4-6/03/2015

Attendance

41st Annual Meeting of the European Radiation Research Society (ERRS)

Rhodes, Greece, 14-19/09/2014

Oral presentation: Micronucleus formation and cell proliferation in a BRCA1 and BRCA2 knockdown breast epithelial cell line after exposure to gamma rays and neutrons

40th Annual Meeting of the European Radiation Research Society (ERRS)

Dublin, Ireland, 1-5/09/2013

Poster presentation: The role of DNA double-strand break repair proteins after low- and high-LET radiation exposure

VLIR workshop

Cape town, South Africa, 12-13/08/2013

Oral presentation: The impact of BRCA1 and BRCA2 mutations on radiosensitivity

Science day UGENT

Ghent, Belgium, 07/03/2013

Poster presentation: RBE of mammography X-rays at the level of DNA dsb and chromosomal damage

PhD Day of the Department of Basic Medical Sciences

Ghent, Belgium, 08/05/2012

Oral presentation: The efficiency of mammography X-rays in inducing DNA double strand breaks and chromosomal damage

14th International Conference of Radiation Research (ICRR) (not attended)

Warsaw, Poland, 28/08-01/09/2011

Poster presented by Prof. dr. H. Thierens: RBE of mammography X-rays at the level of DNA dsb and chromosomal damage

International training and research

14/11/2012 – 03/12/2012

iThemba Labs, Cape Town, South Africa

VLIR own initiatives program between Belgium and South Africa.

Research into the role of DNA DSB break repair proteins in MCF-10A breast epithelial cells after irradiation with fast neutrons and γ -rays.

20/05/2013 – 11/06/2013

iThemba Labs, Cape Town, South Africa

VLIR own initiatives program between Belgium and South Africa.

Continuation of research into the role of DNA DSB break repair proteins in MCF-10A breast epithelial cells after irradiation with fast neutrons and γ -rays.

